Synthesis of benzo-fused heterocycles using isomerization and ring-closing metathesis reactions

Lee Gavin Madeley

Supervised by Prof. W.A.L. van Otterlo

A dissertation submitted in the School of Chemistry
to the Faculty of Science,
University of the Witwatersrand,
in fulfilment of the requirements for the
Degree of Master of Science

March 2010

Declaration

I declare that the work presented in this dissertation is my own, unaided work and was carried out under the supervision of Prof. W.A.L. van Otterlo. It is being submitted for the Degree of Master of Science in the University of the Witwatersrand, Johannesburg. It has not been submitted before for any degree or examination in any other University.

_____

Lee Gavin Madeley

March 2010

Abstract

The first part of the dissertation involves the use of ruthenium mediated isomerization (RMI) followed by ring-closing metathesis (RCM) on a selection of phenols and naphthol-1-ol precursors – that had been subjected to allylation; followed by a heat initiated Claisen rearrangement; followed by re-allylation – to form a selection of benzofurans. This procedure, to the best of our knowledge, represents a novel method for the synthesis of benzofurans, with very good average yields of around 90% overall for the RMI/RCM and allylation steps. The lowest yield of the five synthetic steps, were for the Claisen rearrangements with a range of yields between 50% and 86%, indicating the potential to optimise the yields of these reactions, which were carried out using both conventional and microwave heating. The following five-membered oxygen-containing heterocycles were thus obtained: 4,7-dimethoxybenzofuran**,** 5-bromobenzofuran, 5-*tert*-butyl-benzofuran, 7-phenyl-1-benzofuran and naphtho[1,2-*b*]furan.

The second part of the dissertation involves the use of RMI and RCM on di-allylated; di-allylated di-isomerised; and di-allylated mono-isomerized *O,N*- (aminophenol) and *N,N*-(benzene-1,2-diamine) protected precursors. This resulted in the formation of six-, seven- and eight-membered benzo-fused heterocycles respectively. Except in the case of the mono- and di-isomerised *N,N*-precursor, which failed to undergo RCM, despite several attempts. This failure, which is not unprecedented, is most likely due to the interaction of nitrogen's lone pairs and the adjacent saturated bonds of the precursor with the GII catalyst, resulting in de-allylation. Of those reactions that were successful, the average yields for the RMI/RCM steps were in the region of 82% for the *N,N*-precursors and 95% for the *O,N*-precursors. All precursors readily submitted to allylation and isomerization, with an average yield of 94%. The following benzo-fused heterocycles were thus obtained: six-membered: 4H-1,4-benzoxazin-4-yl(phenyl) methanone; seven-membered: 1,5-benzoxazepin-5(4H)-yl(phenyl)methanone; eight-membered: 2,5-dihydro-6H-1,6-benzoxazocin-6-yl(phenyl) methanone and 1,1'-[(3Z)-2,5-dihydro-1,6-benzodiazocine-1,6-diyl]diethanone.

Acknowledgements

I would like to thank my supervisor Willem van Otterlo and the Head of School Jo Michael; my family; and my friends – especially Shaun and Warren. All your indulgences are appreciated.

After much consideration, I have included a quote which follows, it may be wasted next to such a lean work, but my intentions are most humble and I'm sure that this was the spirit in which it was intended:

"We are nothing without the work of others our predecessors, others our teachers, others our contemporaries. Even when, in the measure of our inadequacy and our fullness, new insight and new order are created, we are still nothing without others. Yet we are more."

J. Robert Oppenheimer,
Reith Lecture, 20 December 1953

Table of Contents

List of Abbreviations

Ac	*Acetyl*
ADMET	*Acyclic Diene Metathesis Polymerisation*
Boc	*tert-Butyloxy carbonyl*
Bz	*Benzoyl*
CM	*Cross Metathesis*
CPBA	*Chloro-peroxybenzoic acid*
DEAD	*Diethylazodicarboxylate*
DCN	*Dichloronitrile*
DMF	*N,N-dimethylformamide*
FTIR	*Fourier Transform Infrared*
GI	*Grubbs catalyst 1st generation*
GII	*Grubbs catalyst 2nd generation*
HRMS	*High-resolution Mass Spectrometry*
IBX	*2-Iodobenzoic acid*
Mes	*Mesitylene*
(m)mol	*(milli)Mole*
NBS	*N-Bromosuccinimide*
NMR	*Nuclear Magnetic Resonance*
RCM	*Ring Closing Metathesis*
RMI	*Ruthenium Mediated Isomerization*
ROM	*Ring Opening Metatheis*
ROMP	*Ring Opening Metathesis Polymerization*
PCy_3	*Tri-cyclophospine Ligand*
PBOX	*Pyrorolo-1,5-benzoxazepine*
PPAR	*Peroxisome proliferator-activated receptor*
TBAF	*tetra-N-butylammonium flouride*
THF	*tetrahydrofuran*
TLC	*Thin Layer Chromatography*
TMG	*Trimethyl glycine*
Ts	*Tosyl*

CHAPTER ONE

GENERAL INTRODUCTION

THEORETICAL BACKGROUND

Chapter 1: Introduction

1.1 Project overview

Benzo-fused heteroaromatic structures are common motifs in many naturally-occurring compounds, with potentially wide-ranging pharmaceutical applications such as antibiotics and anti-microbial agents.[1] This makes the synthesis of such components of interest to organic synthetic chemists.

Of the numerous methods available for their synthesis, a modern methodology involving transition metal catalysts is presented in this dissertation. Two of the key catalysts used in this project are the Grubbs' second generation (GII) ring-closing metathesis (RCM) catalyst and the ruthenium mediated allyl isomerization (RMI) catalyst. The use of these catalysts has allowed access to many synthetic products and intermediaries with increased ease, cost effectiveness and yield – not before achievable using previous synthetic methodologies.[2]

In addition, the tandem use of these catalysts has allowed access to a variety of five-, six-, seven- and eight-membered ring structures – fused to benzene sub-structures – with relative ease. In this dissertation ring structures containing oxygen, oxygen and nitrogen, and nitrogen, are presented.

Previous work in our laboratories[3] has shown that the tandem use of these catalysts have wide ranging scalability, in so far as the same allylated precursors can be used to achieve variable ring sizes, depending on at which stage and sequence of the synthesis the catalysts are deployed.

1.2 Metathesis reactions (RCM)

1.2.1 Metathesis catalysts

The formation of carbon-carbon double bonds is of key importance in the synthesis of molecular targets. The use of transition metal catalysts in this endeavour was first discovered in studies on the attempted addition polymerization of olefins using Ziegler-type catalysts. These metatheses (a term first coined by Calderon in 1967) catalysts comprised of a transition metal halide such as $MoCl_5$ and WCl_6, mixed with an alkylating reagent such as Et_3Al or $EtAlCl_2$. A selection of these first generation heterogeneous catalysts is shown in **Figure 1**.[4]

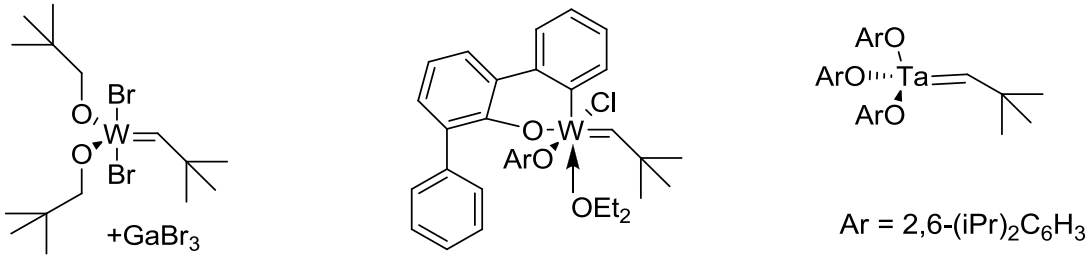

1 **2** **3**

Figure 1: First generation metal carbene catalysts

The first 'true' alkene metathesis catalysts were developed by Schrock and Grubbs in the early 90's (**Figure 2**). The Schrock catalyst **4** is still one of the most active single catalysts to date, but is highly sensitive to oxygen and water.[5] The Grubbs' first generation catalyst **5** is less reactive, but much more tolerant to oxygen and water.[6]

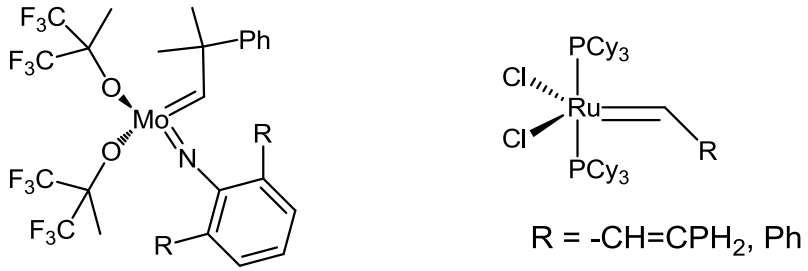

4 **5**

Figure 2: Schrock **4** and Grubbs' first generation catalyst **5**

1.2.2 Metathesis mechanism[7]

The mechanism by which metathesis proceeds was first proposed by Chauvin in 1970.[7] According to this mechanism, shown in **Scheme 1**, the activated metal carbene complex first undergoes a [2+2] cycloaddition reaction with the olefin, forming a metalocyclobutane. This complex then undergoes a [2+2] cycloreversion reaction, releasing a molecule of ethene, whilst leaving the metal complex attached to the olefin. This process can then be repeated. If another olefinic substrate is present in the same molecule, RCM can occur (as per **c** in **Scheme1**); or the process can occur on another olefinic substrate of another molecule (as per **d** in **Scheme 1**) leading to chain formation.

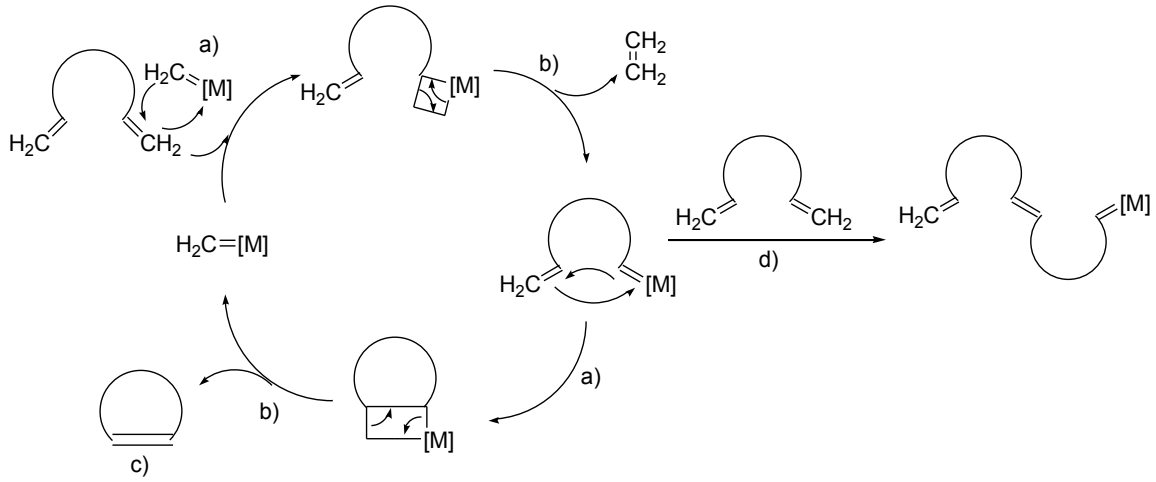

Scheme 1: The Chauvin mechanism
a) [2+2] cycloaddition
b) [2+2] cycloreversion
c) metathesis occurs within the molecule
d) metathesis occurs with another molecule

In all, five basic alkene-alkene metathesis reaction outcomes are possible, summarised in **Scheme 2**.

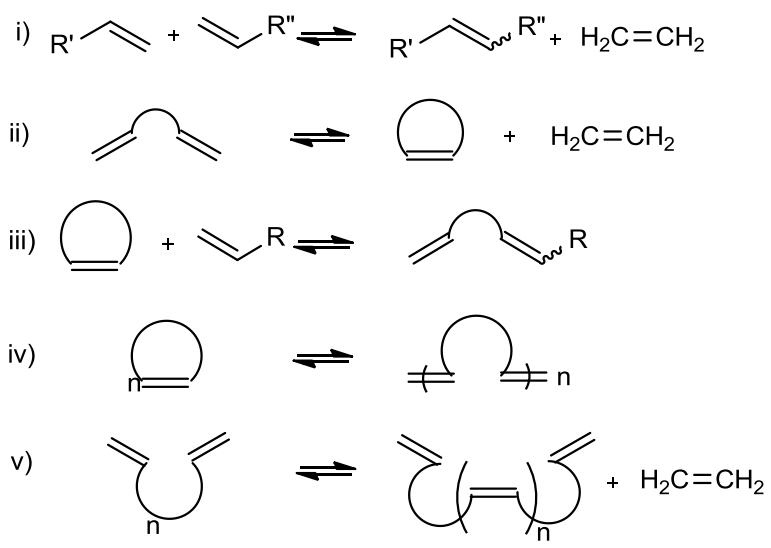

Scheme 2: Fundamental metathesis transformations
i) Cross metathesis (CM)
ii) Ring-closing metathesis (RCM)
iii) Ring-opening metathesis (ROM)
iv) Ring-opening metathesis polymerization (ROMP)
v) Acyclic Diene metathesis polymerization (ADMET)

Cross metathesis (CM), ring-closing metathesis (RCM) and acyclic diene metathesis polymerization (ADMET) reactions are all entropically driven, because the evolution of ethene gas as a by-product, greatly increases the disorder of the system and makes the reaction irreversible at this step.

On the other hand, ring opening metathesis (ROM) and ring opening metathesis polymerization (ROMP) are both enthalpically driven because of the energy released in breaking the ring. No ethene gas is released in these reactions, with irreversibility achieved because the equilibrium lies far to the right and because the products have a significantly lower enthalpy on the release of ring strain – ring reformation is thus highly unfavourable. As with all catalysts, alkene metathesis catalysts are highly reversible in the initiation phase of the reaction. This can be demonstrated using the mechanism proposed for the Grubbs' first generation catalyst (GI).[8-9] The proposed initiation phase is shown in **Scheme 3**.

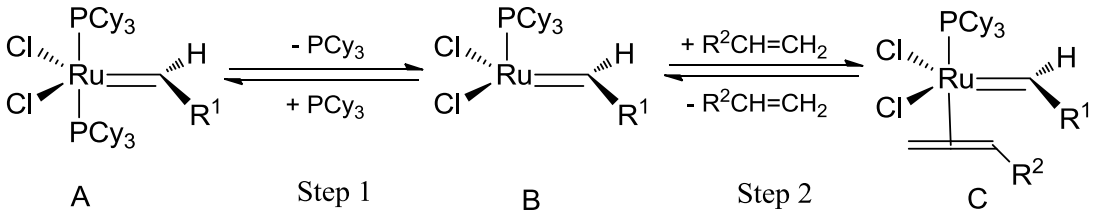

Scheme 3: Proposed initiation phase of the Grubbs' first generation catalyst (**GI**)

Step 1:

The pre-catalyst **A** has a stable 16 electron configuration around the central Ru atom. In Step 1 the bulky PCy_3 ligand is lost, causing the electron distribution around the Ru atom to drop to an unstable 14, producing the highly reactive intermediate **B**. Step 1 is highly reversible, with the forward reaction entropically driven because of the loss of the PCy_3 ligand, and the reverse reaction favoured by the increased stability around the central atom. To help prevent recombination of the ligand through steric hindrance, very bulky ligands are used.

Step 2:

In the presence of an olefinic substrate Step 2 may occur, bringing the electron count around the Ru atom in intermediate **C** back to a stable 16. The groups R^1 and R^2 have the potential for steric and electronic hindrance and it is their identity that will determine whether the intermediate **C** will form, or fall back to intermediate **B**.

It is the [2+2] cycloaddition phase (**Scheme 4**) that is the rate-determining step in the metathesis cascade. The amount of steric and electronic hindrance caused by the R^1 and R^2 groups will ultimately determine the speed and success of the reaction. Again, the reaction is driven forward entropically to intermediate **E**, with the release of ethene gas, which is then irreversible after the [2+2] cycloreversion of intermediate **D**.

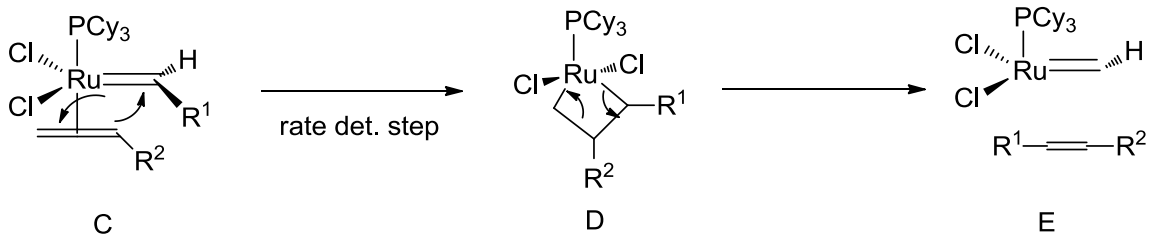

Scheme 4: [2+2] Cycloaddition phase
The rate determining step in alkene metathesis

1.2.3 Metathesis catalysts used in this project

The problem of reversibility in the initiation phase of the Grubbs' first generation catalyst has largely been overcome with the advent of the Grubbs' second generation catalyst (GII) **6**, shown in **Figure 3**.[10-11]

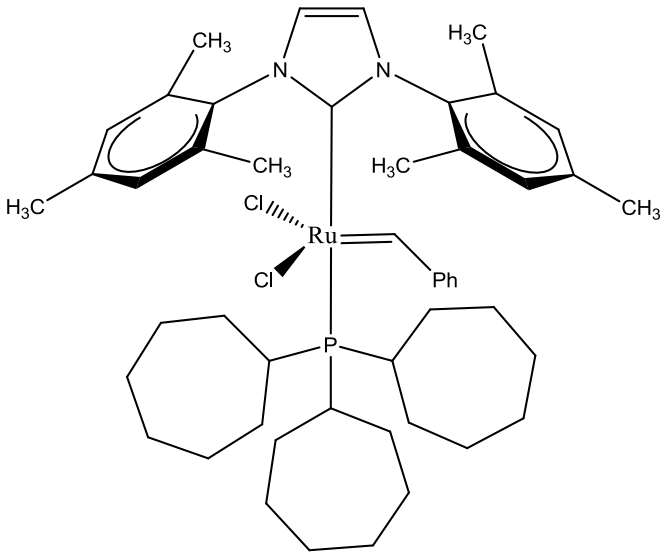

6

Figure 3: Grubbs' second generation catalyst (GII).

GII **6** was used exclusively in this project. It differs from GI **5** in that one of the PCy_3 ligands have been replaced by a nitrogen-containing carbene, which has both nucleophilic and electrophilic capabilities. This *N*-heterocycle carbene is kinetically inert, electron rich and bulky.[9]

The GII **6** has the following improvements over GI **5**:[12]

1) The nitrogen-containing carbene pushes electron density into the Ru centre, thereby lengthening – and thus weakening – the Ru-P bonds, making substrate bonding more facile.

2) PCy_3 dissociation is relatively inefficient, but due to the presence of the very bulky nitrogen carbene, PCy_3 re-association to the Ru is much less likely – because the nitrogen carbene stabilizes the 14 electron intermediate, and its large steric bulk hinders re-association.

These two factors act together to ensure the catalyst's coordination to the olefin is far more facile.

The advent of the metathesis methodology has been a dramatic improvement in carbon-carbon bond formation, as it requires a small amount of the catalyst and has the potential to remove several additional reaction steps that may otherwise have been necessary using previous methodologies. This potentially improves the cost effectiveness of the methodology and makes it more environmentally friendly, because the only significant waste product of the metathesis step is ethene gas.

1.3 Ruthenium mediated isomerization (RMI)

1.3.1 Isomerization reaction

An independent method for the displacement of saturated bonds within a molecular system can be important in synthesis, not only in the creation of a final product, but also because a saturated bond can act as a useful focal point for subsequent molecular moieties. As an example, a simple isomerization reaction involving olefins is expected to proceed according to **Scheme 5**, where two possible isomers can be produced.

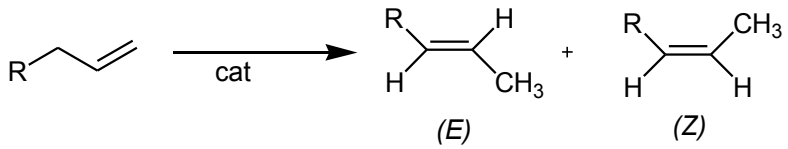

Scheme 5: Basic isomerization outcome on an allylic substrate

The action of certain transition metal metathesis compounds to facilitate such transformations were first noted by Maynard and Grubbs,[13] when isomerization occurred on the expected RCM product **8a** (**Scheme 6**), whilst being distilled in the presence of the decomposition products of a Ru RCM catalyst, resulting in the formation of **8b**. It was suspected by the researchers that Ru by-products in the distillate were responsible for the isomerization.

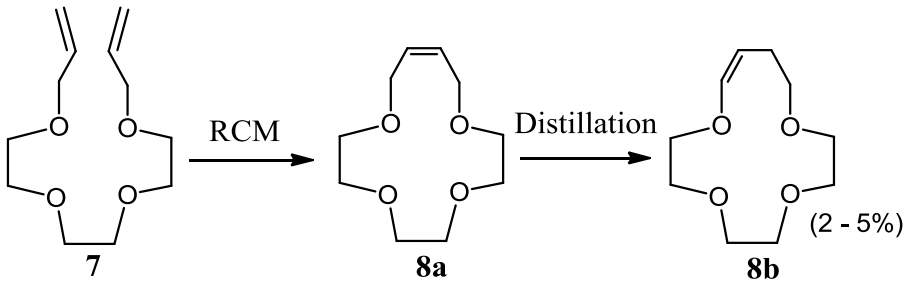

Scheme 6: Unexpected isomerization in the presence of Ru residues

Prunet and co-workers[14] also found that isomerization had occurred *subsequent* to RCM in an investigation on a diene precursor **9** as part of a total synthesis towards Taxol (**Scheme 7**). In both products, ring-closure has been affected, but compound **11** has the double bond in an unexpected position.

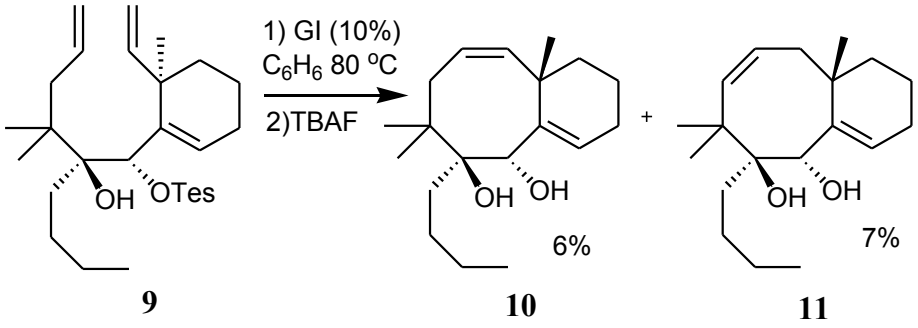

Scheme 7: Two isomeric products produced after RCM

Furstner and co-workers,[15] while attempting the RCM of **12** (**Scheme 8**) found not only the expected 21-membered macro cycle **13**, but also a 20-membered macro cycle **14**, indicating that isomerization had occurred *prior* to ring-closure. Again, only ruthenium RCM catalysts and their potential by-products were present.

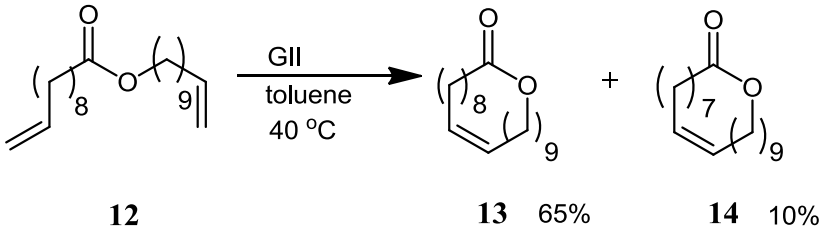

Scheme 8: Isomerization occurring prior to RCM

1.3.2 Isomerization mechanism

The first mechanistic proposals regarding Ru RCM-mediated isomerizations were made by Nolan, Prunet and co-workers[15] based on the model study of the Taxol isomerization problem. The mechanism they proposed is based on a π-allyl hydride mechanism (used to describe olefin isomerization) as shown in **Scheme 9**.

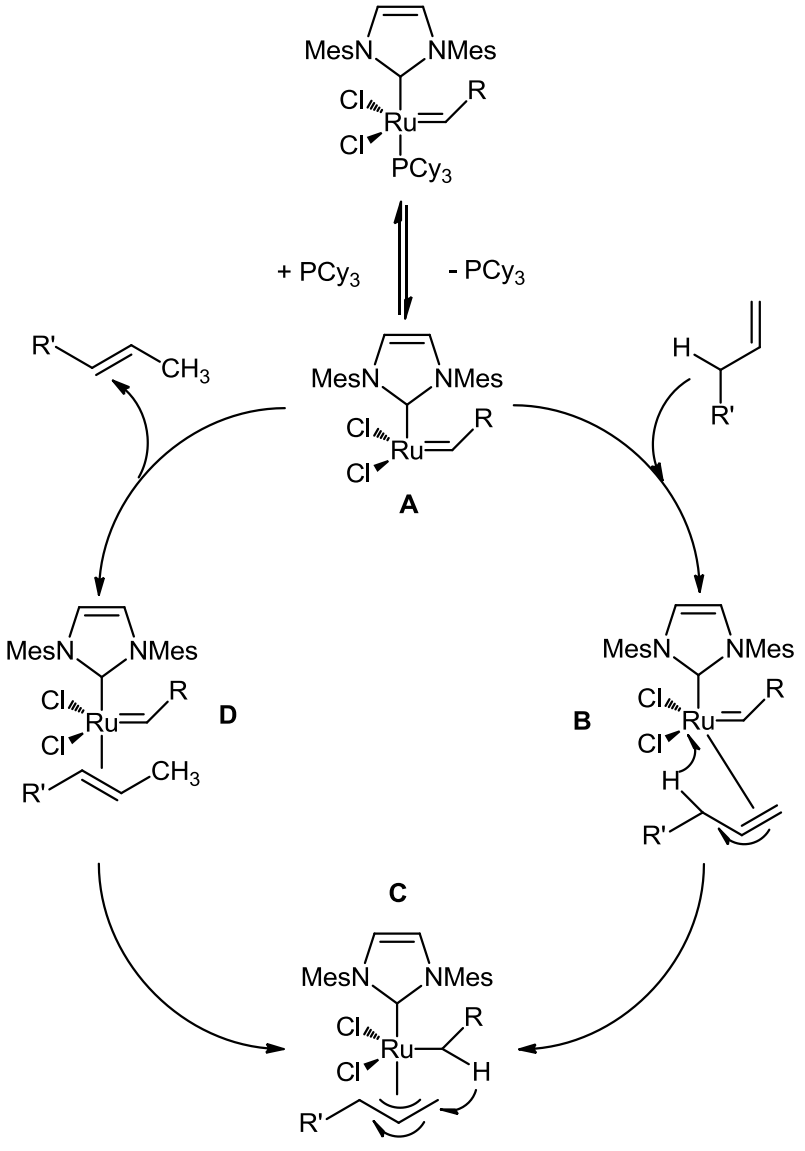

Scheme 9: Proposed catalytic cycle for isomerization
(A modification of the π-allyl hydride mechanism)

It was found that, apart from the role that the solvent plays in reaction outcome, the addition of small amounts of tricyclohexylphosphane (PCy_3), a ligand present on the **GII** catalyst **6**, resulted in the complete suppression of isomerization.

The mechanistic proposal is thus based on the idea that an unstable 14 electron fragment **A** resulting from the loss of the PCy_3 ligand is responsible for isomerization. This was inferred because the excess PCy_3 would prevent the formation of **A** thermodynamically – by driving the equilibrium towards the original catalyst; and also kinetically – by competing with any allylic substrates that would otherwise interact with **A**, re-stabilising the 16 electron count.

Without excess PCy_3, substrates with allylic groups may, depending on steric hindrance, more easily interact with the 14 electron fragment, resulting in the formation of a π-complex **B**. Then, in an agostic interaction, deprotonation of the allylic position would lead to an σ-alkyl/π-allyl complex **C**, which would react to produce the carbene complex **D**. Entropically driven dissociation of the isomerized alkene finally regenerates the catalytically active species **A**.

1.3.3 Isomerization catalyst used in this project

Numerous catalysts have been produced to facilitate isomerization. The catalyst **15** was used exclusively in this project and is shown in **Figure 4**. It is used based on the excellent results achieved by Krompiec and co-workers.[16]

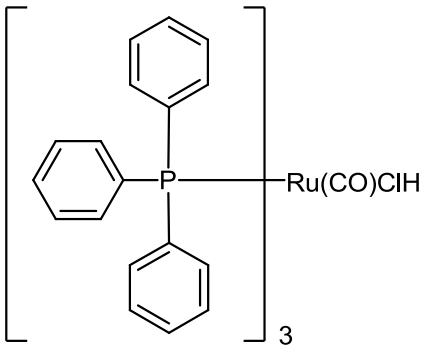

15

Figure 4: Ruthenium isomerization catalyst used in this project

The work by Krompiec and co-workers[16-17] on *N*-allylamides, *N*-allylamines and *N*-allyl ethanamide – which gave isomerised products with high stereoselectivity when using catalyst **15** – may also shine light on the mechanism of the catalyst. The researchers claim that the observed stereoselectivity of the products (almost exclusively *E*-isomers) occurs because of the coordination of aryl groups on the substrate with the Ru atom of the catalyst (**Figure 5**); and not because of the higher thermodynamic stability of the *E*-isomer, as quantum calculations using AM1 methods showed that the *E*- and *Z*-isomers differ in their heat of formation by only 10.52 kJ/Mol.

Thus, if back-bonding can occur between the Ru atom and the arene ring in the course of the reaction – (*E*)-isomers will form. This analysis is consistent with the π-allyl hydride mechanism (**Scheme 9**) and helps to explain the observed high selectivity of the Ar-allyl isomerizations insofar as they stem from the *coordination* to the Ru of the catalyst and not because of steric effects.

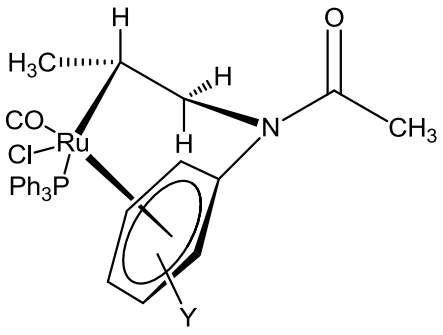

16

Figure 5: AM1 quantum calculation analysis of (*E*)-*N*-phenyl-*N*-(1-propenyl)ethanamide (in the optimal conformation) showing the possibility of interaction between the Ru atom and the arene ring during the reaction.[17]

1.4 Claisen rearrangements[18]

This useful, heat initiated reaction is classified as a [3.3]-sigmatrophic rearrangement. In its most general sense it is a transformation as outlined in **Scheme 10**.

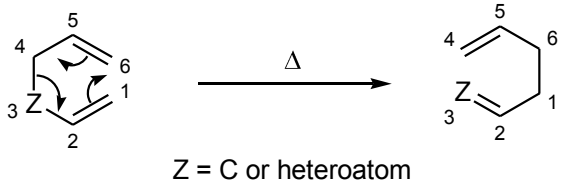

Scheme 10: Claisen rearrangement

Because this process is regulated by orbital symmetry – there will be a preferred chair transition state for the reaction, and reactions are accelerated by charged intermediates. The Claisen rearrangement related to this project involved substituted allylic phenols and follows the general reaction mechanism outlined in **Scheme 11.**

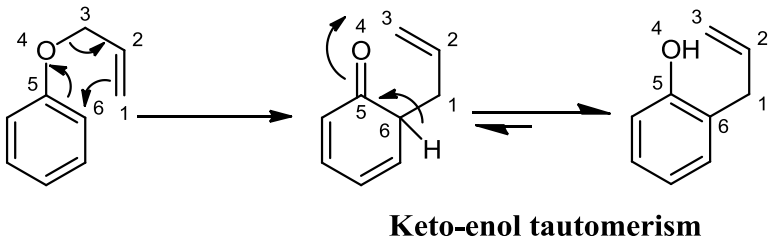

Scheme 11: Reaction mechanism related to allylic phenols[18a]

In the case of aromatic ring systems, if the both positions *ortho* to the oxygen are blocked, rearrangement can continue until a free (hydrogen) position is found, as shown in **Scheme 12**. The addition of substituent groups to the phenol can thus be used to regulate the final position of the allylic group.

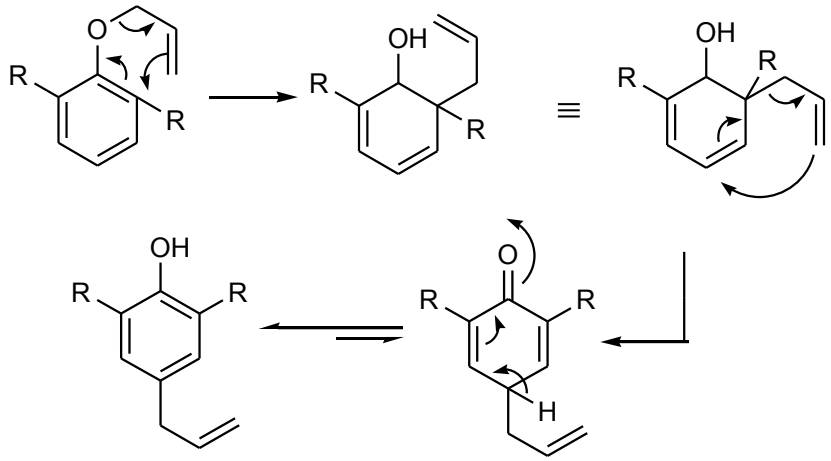

Scheme 12: Showing how substituents on the ring can affect outcome[18b]

1.5 Conclusion

The RCM and RMI catalysts and reactions outlined above were all put to use in synthetic strategies, as an alternative to previous synthetic strategies found in the literature, for the synthesis of benzo-fused ring compounds. In doing so, the suitability of such alternate reactions, to those in the literature, was investigated.

CHAPTER TWO

RELEVANCE OF THE RESEARCH

PREVIOUS SYNTHETIC STRATEGIES

Chapter 2: Relevance of the research

Numerous synthetic methodologies have been utilized in the formation of 5-, 6-, 7- and 8-membered benzo-fused heterocycles. All of these structures occur in a variety of compounds with wide-ranging medicinal applications, as they have the ability to bind to multiple receptors with high affinity, and well as other applications. They have thus been termed 'bicyclic privileged structures', a term first coined by Evans *et al.* in 1988 and is defined as a 'single molecular framework able to provide ligands for diverse receptors'.[19] There is thus an obvious interest in these structures and this chapter will briefly introduce relevant examples of molecules containing them and will also give a brief overview of previous synthetic methodologies used in their synthesis. This will allow for a more comparative discussion of the Wits RMI-RCM methodology.

2.1 5-Membered oxygen containing benzo-fused heterocycles: the benzofurans

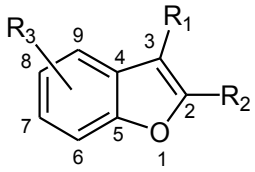

17

Figure 6: The basic benzofuran motif

The benzofuran skeleton (**Figure 6**) is a common motif in many naturally occurring bioactive compounds. A number of natural and synthetic examples are shown in **Figure 7**. Compound **18**[20] is a selective dopamine D-2 antagonist and compound **19**[21] is a κ-selective agonist with a potency 25 times greater than morphine. The analogues of Furochromonone **20**[22] inhibit platelet aggregation by inhibiting cyclic AMP phosphodiesterase; and specifically its analogue Khellin **21**[23], acts as a potent coronary vasodilator (isolated from the seeds of *Ammi visnaga*). Other examples include the furocoumarin Heraclenol **22**[24] isolated from *Cymopterus watsonii* and the benzo[*b*]-

furo[3,4-*d*]furan-1one scaffold **23**[25] found in many naturally occurring products, which have a wide range of biological effects.

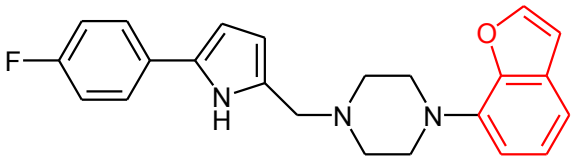

18

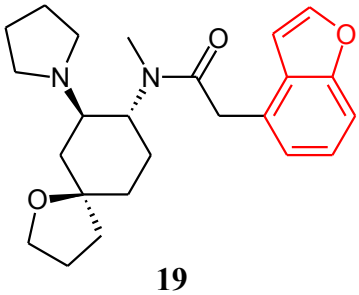

19

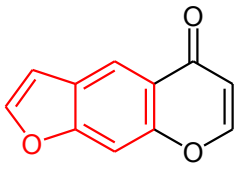

20

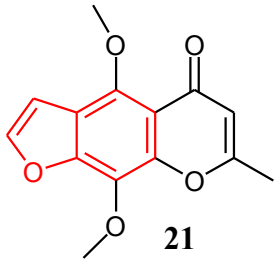

21

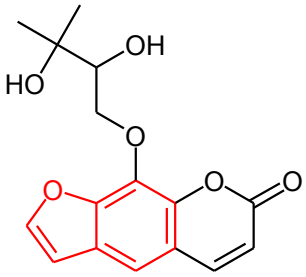

22

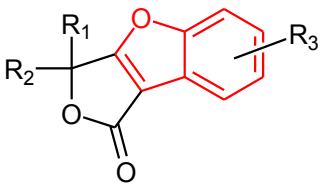

23

Figure 7: Molecules containing the benzofuran motif

(R_1, R_2 and R_3 = variety of substituents)

2.1.1 Previous synthetic strategies towards benzofurans

Outlined below, are a selection of the most prominent synthetic strategies, extracted from literature sources, employed toward the synthesis of the benzofuran motif **17** – that do not employ a RMI-RCM approach.

2.1.1.1 Non-metathetic ring-closure reactions

A review of the literature[26] shows that four main synthetic strategies have been employed prior to 1995. Only a brief description and representative example of each, in its most general form, will be given. All of the benzofuran skeletons are produced by direct ring-closure – sometimes with the use of catalysts.

2.1.1.1.1 Ring closure by the formation of the O-C(2) bond

The *o*-iodobenzoic acid **24** was refluxed with a suitably prepared cuprous acetylide **25** under a nitrogen atmosphere, with pyridine acting as both solvent and base. (**Scheme 13**.) This resulted in the formation of the benzofuran **26** with a 91% yield.

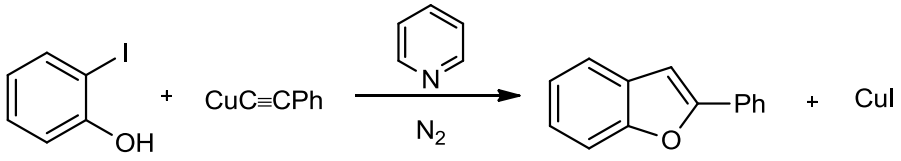

24 **25** **26**

Scheme 13: The methodology of Stephans and Castro[27]

2.1.1.1.2 Ring closure by the formation of the Ar-C(3) bond

If aryloxyalkanones (R_1 and R_2 = benzene) **27** are treated with *p*-bromobenzenesulfonyl chloride, the corresponding vinyl ester **28** is obtained. (**Scheme 14**.)
These compounds can then be cyclized to 2,3-diarylbenzofurans **29** under the action of BF_3 (65% overall yield).

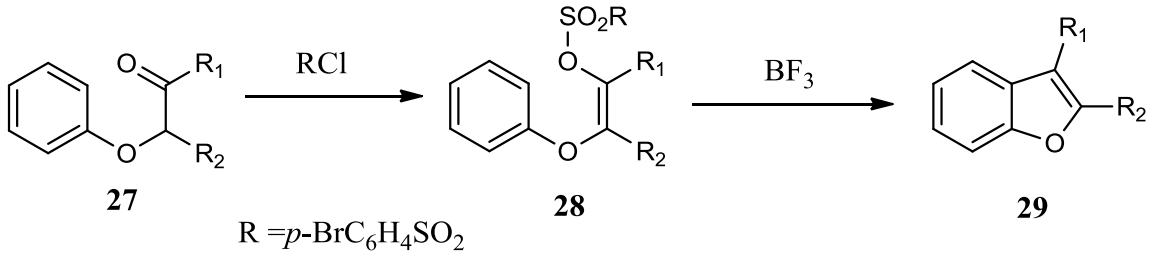

Scheme 14: The methodology of Cappozzi and Modena[28]

2.1.1.1.3 Ring closure by the formation of the C(2)-C(3) bond

Ethyl *o*-carbethoxymethylenesalicylkates **30** (which can be prepared from corresponding halogenated arenes or etherified phenols) underwent Dieckmann condensation to produce the resultant substituted benzofuran **32**, under the action of $NaOC_2H_5$ and NaOH as base. (**Scheme 15**.) Compound **33** was produced after reaction with 5% H_2SO_4. Overall yields are as follows: when R = H: yield = 65%, when R = Cl: yield = 27% and when R = I: yield = 27%.

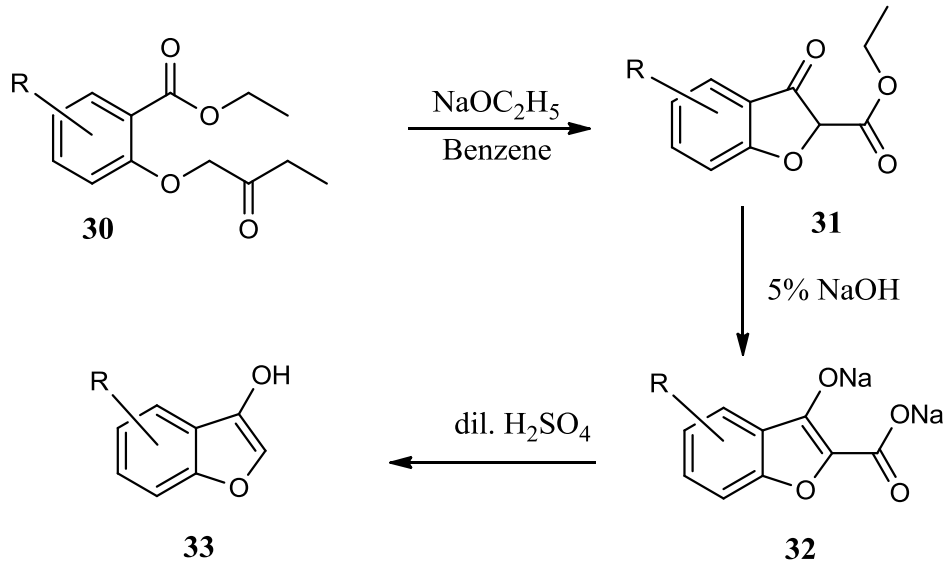

Scheme 15: The methodology of Schroeder *et al.*[29]

2.1.1.1.4 Ring closure by the formation of the Ar-O bond

The enolates of 2-aryl-1-substituted ethane-1-ones **34** can undergo photo-induced intramolecular cyclization to form 2-substituted benzofurans **35**. The general reaction procedure involved using a 125 W mercury lamp to irradiate a mixture of **34** and 1,4-dicyanonaphthalene (DCN) in a molar ratio of approximately 10:1, at > 230 nm in a Pyrex filter. A mixture of acetonitrile and water (8:2), with sodium hydroxide added to bring the pH to ~ 10, was used as solvent. (**Scheme 16**.)

The overall yield of this one pot synthesis were between 50 – 60% (R_1 = methyl and R_2 = 4'methoxy, 2'5'-dimethoxy or 3'4'-dimethoxy).

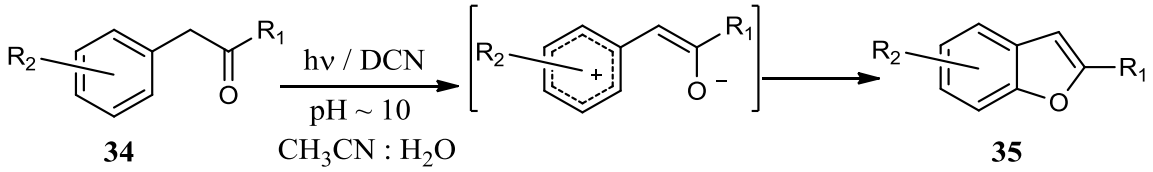

Scheme 16: The photo-induction methodology of Pandy *et al.*[30]

2.1.1.2 Synthesis from furans and dihydrofurans[31]

4-Chloro-2-cyclobutanone **36** can undergo Pd-catalysed cross-coupling with 2-stannylated furans **37**, followed by heating, to give 4-hydroxybenzo[*b*]furans **38**. (**Scheme 17**.) **37** was easily prepared in good yield by reacting benzofuran with *n*-butyl lithium and TMEDA in an ether solution at -78 °C, followed by quenching with *n*-Bu_3SnCl. 5 mol% $Cl_2Pd(PhCN)_2$ and 10 mol% *tris*-2-furylphosphine acted as the Stille cross-coupling catalyst in the first step of the reaction, which proceeded at 50 °C for 4 hours and at 100 °C for another 4 hours. (Dioxane was used as solvent). The overall yield of this reaction was 94%.

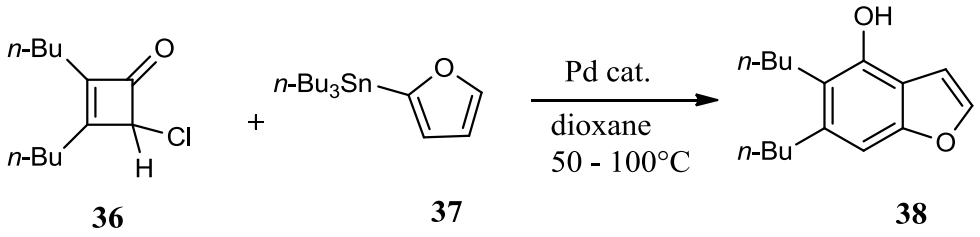

36 **37** **38**

Scheme 17: The methodology of Liebeskind and Wang[31]

2.1.1.3 Use of the Perkin rearrangement[32]

Under the action of a strong hydroxide and a halogen salt, a suitably substituted 3-halo-4-allyl-Chromenone **39** (X = Cl or Br) can undergo a Coumarin benzofuran ring contraction to produce the benzofuran **40**. (**Scheme 18**.)

The reaction process has been shown to occur in two steps by Bowden and Battah: a relatively rapid base-catalysed ring fission to give the acrylic acid intermediate, which then undergoes a relatively slow cyclization process, followed by heat-initiated de-carboxylation to form **40**. Yields for this reaction are in the region of 20% (R = NHOPh) to 90% (R= CH_3).

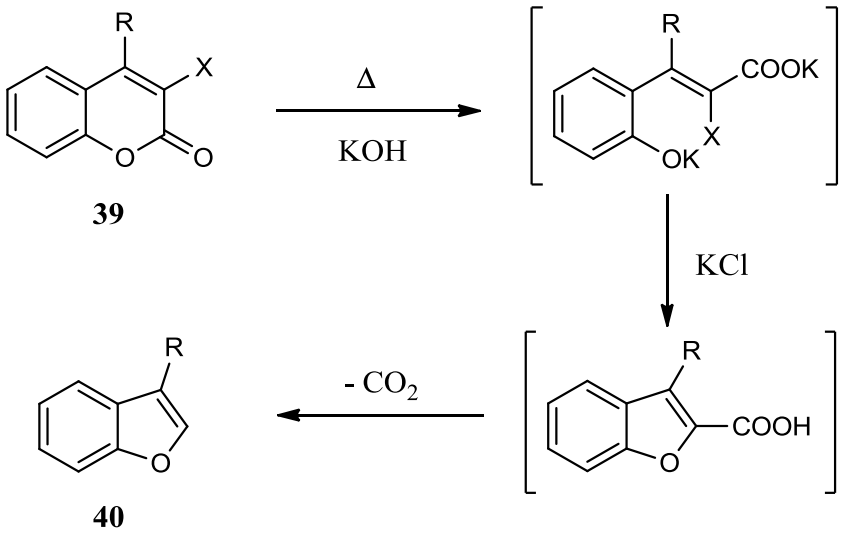

Scheme 18: The methodology of Bowden and Battah[33]

2.1.1.4 Resin-based benzofuran combinatorial approaches

2.1.1.4.1 The Habermann benzofuran combinatorial approach[34]

The synthesis utilizes solid supported reagents, the first of which – a bromine pyridine complex (**A**) – acts as a bromination agent on the commercially available acetophenols **41** to produce **42**. The second – 1,5,7-triazabicyclo[4.4.0]dec-5-ene (**B**) – acts as a base to deprotonate phenols **43** resulting in its attachment to the precursor **42** in yields > 30%. The third – Amberlyst 15 (**C**) – results in a cyclodehydration of **44** forming the benzofuran product **45** in yields > 57%. (**Scheme 19**.)

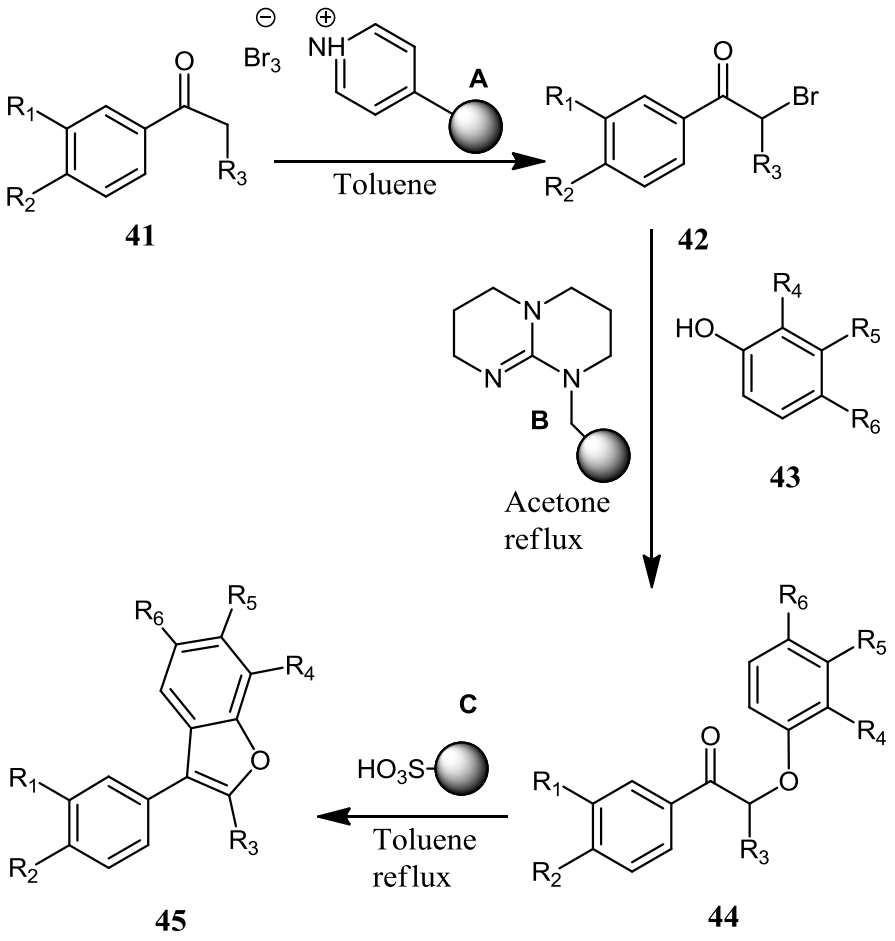

Scheme 19: The Habermann benzofuran combinatorial approach

2.1.1.4.2 The Fancelli benzofuran combinatorial approach[35]

The first stage of the reaction begins with a Mitsunobu reaction between a starting carboxylic acid **46** and Tentagel®, after which the acetate group of **47** is deprotected *via* reaction with a dilute ammonia solution. The key step in the synthesis is a palladium-catalyzed heteroannulation of **48** utilizing terminal acetylenes, which results in the benzofuran motif **49**. This product is then cleaved from the resin using a strong base to yield the product **50** in yields > 60%, depending on the identity of the acetylenes used. (**Scheme 20**.)

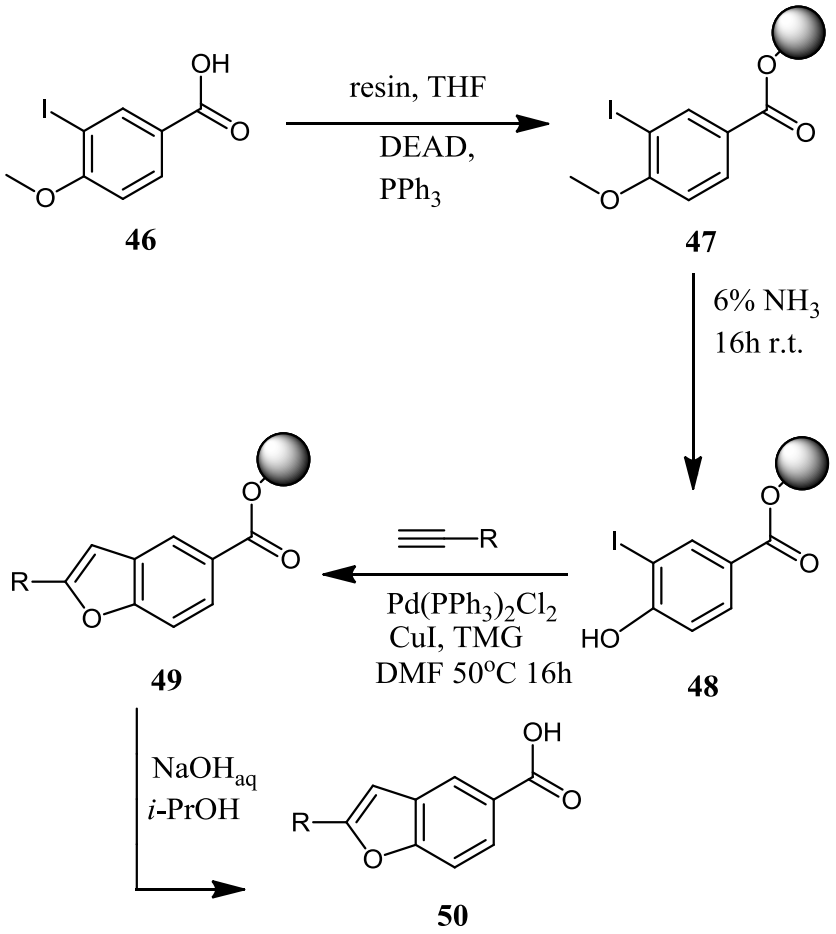

Scheme 20: The Fancelli benzofuran combinatorial approach

2.1.1.4.3 The Nicolaou benzofuran combinatorial approach[36]

Previously synthesized chloromethylsulfide resin **51** was treated with salicylaldehydes **52** to produce the resin supported aldehyde **53** under the action of $CsCO_3$. **53** was then treated with arylmagnesium bromide **54** (as Grignard reagent) to produce **55**, which was then selectively oxidized with IBX to produce the benzophenone **56**. Sulfur ylide epoxidation, followed by *m*CPBA oxidation resulted in the sulphone **57**, which was then treated with potassium *tert*-butyl alcohol to deprotonate the methylene groups adjacent to the sulphone, resulting in the a 5-*exo*-trig cyclization, forming the final 3-aryl-benzofuran

compound **58**. Yields for this procedure were in the region of 30 – 48% depending on the identity of the R groups. (**Scheme 21**.)

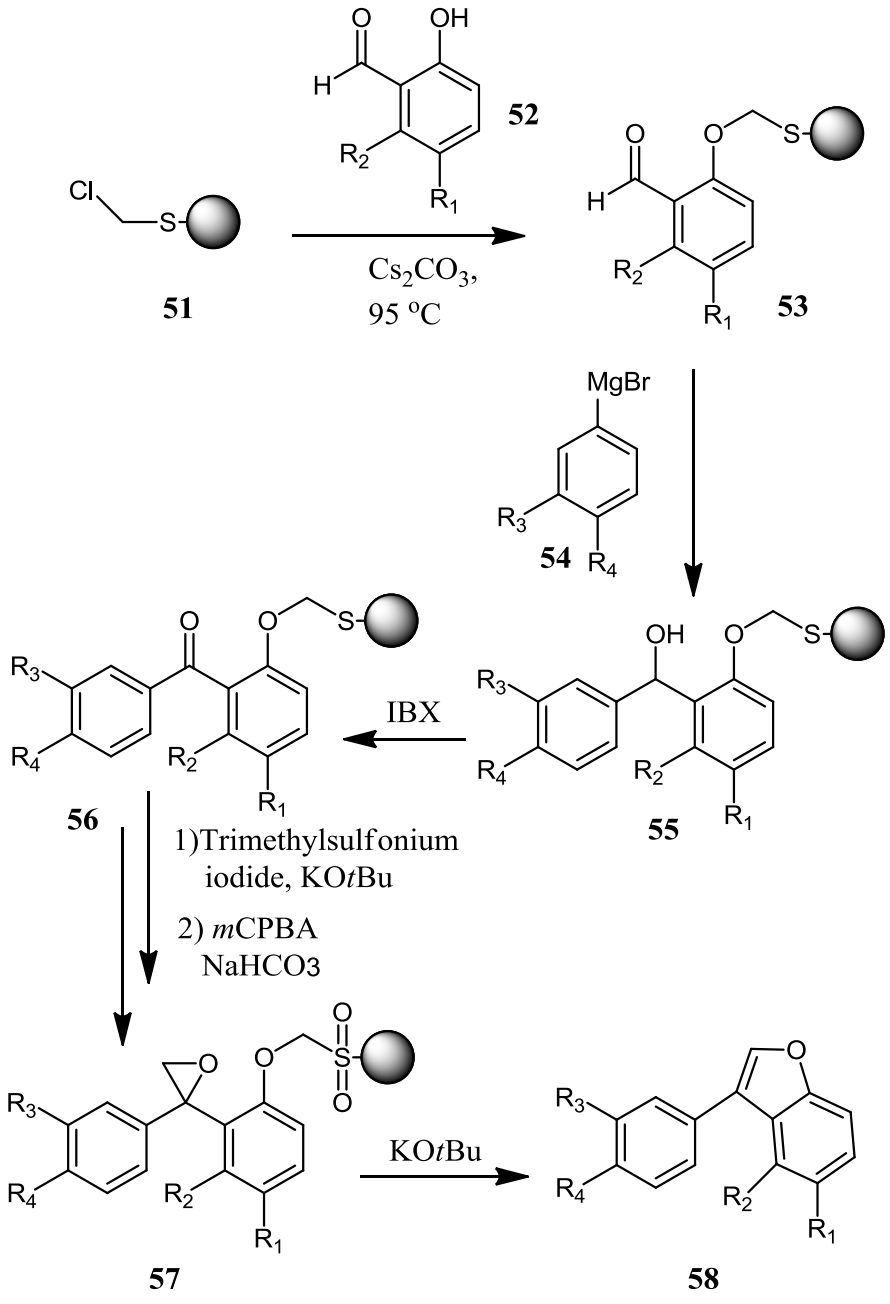

Scheme 21: The Nicolaou benzofuran combinatorial approach

2.2 6-, 7- and 8-Membered *O,N*-benzo-fused heterocycles

Outlined below, is a brief introduction to the 6-, 7- and 8-membered *O,N*-benzo-fused heterocyclic motifs, listed according to ring size, as well as the most prominent synthetic strategies, extracted from literature sources, that do not employ the RMI-RCM approach adopted in this project.

2.2.1 6-Membered *O,N*-benzo-fused heterocycles: the benzoxazines

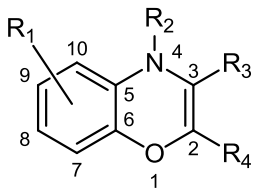

59

Figure 8: The basic 1,4-benzoxazine motif

The 1,4-benzoxazine skeleton **59** (**Figure 8**) is a rare constituent in biologically active and naturally occurring compounds. Examples (**Figure 9**) include Cappamensin A **60,**[37] isolated from *Capparsis sikkimensis* – a Taiwanese shrub with overhanging, climbing branches. The roots and seeds of this genus have been used in traditional medicine since antiquity as antirheumatic, expectorant, antispasmodic and analgesic agents. In a paper by Wu *et al.*,[37] **60** – as well as its methylated derivative **61** – have been found to exhibit significant *in vitro* anti-tumour activity against a wide variety of cancers. There is thus hope that its analogues may also exhibit anti-tumour activity. Other examples include compound **62**, which has been studied by Rybczynski *et al.*[38] as a potential Peroxisome Proliferator-Activated Receptor (PPAR) γ agonist, and (+)-PHNO **63** studied by Bergman *et al.*,[39] which is a dopamine D_2 agonist. More common, however, is the related hydrogenated analogue **64**, which can easily be achieved from **59** by way of a variety of hydrogenation reactions and by reaction at the saturated bond positions to achieve attachment of useful moieties. Examples of hydrogenated analogues include: compound **65**,[40] which possesses PPARα and PPARγ agonist activity and could be used

in treating diabetes, hyperlipidemia and other diabetic complications, and compound **66**[41] which possesses neuro-protectant properties.

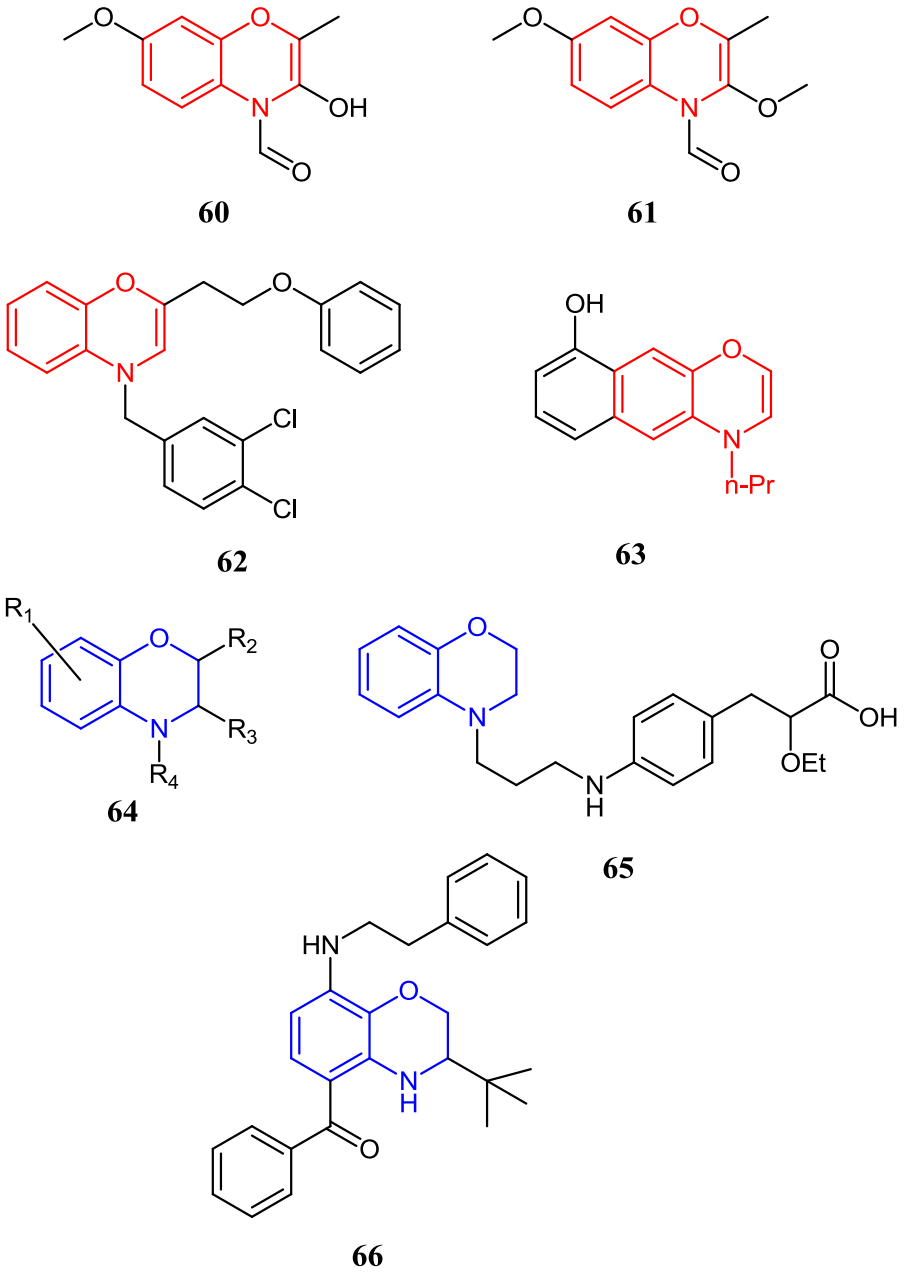

Figure 9: Molecules containing the 1,4-benzoxazine motif

2.2.1.1 Previous synthetic strategies for the 1,4-benzoxazines

A review of the literature, supported by Buon *et al.*,[42] shows that there are few published synthetic routes allowing for access to the 1,4-benzoxazine structural unit. In fact, prior to 2000, only one such system had been reported[43]. Previous strategies are those of Bartch *et al.*[44] for the formation of a 3-substituted 4*H*-1,4-benzoxazine and McKillop *et al.*[45] for the formation of 2,3-disubstituted derivatives. These systems have been prepared primarily *via* cycloaddition reactions which are less generally applicable and as such will not be discussed. Thus, only the synthetic strategy of Buon is presented (**Scheme 22**).

2.2.1.1.1 The synthetic strategy of Buon *et al.*

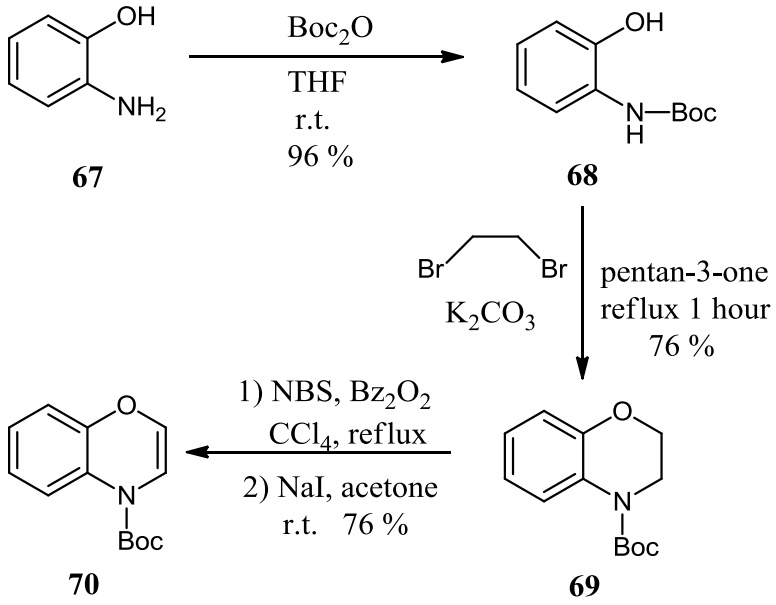

Scheme 22: The synthetic strategy of Buon *et al.*[42]

2-Aminophenol **67** is reacted with di-*tert*-butyl dicarbonate in dry tetrahydrofuran at room temperature leading to the protected *N*-Boc phenolic compound **68** in 96% yield. The 2,3-dihydrobenzoxazine **69** was then obtained in 76% yield by heating **68** and 1,2-dibromoethane under microwave conditions in pentan-3-one for one hour in the presence of an excess of K_2CO_3. The unsaturated carbamate **70** was finally obtained in 76% yield by using a bromination–debromination sequence involving NBS followed by treatment with NaI. (**Scheme 22.)**

2.2.2 7-Membered *O*,*N*-benzo-fused heterocycles: the benzoxazepines

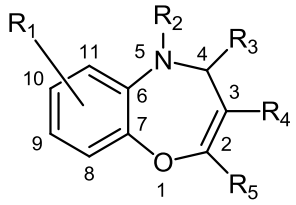

71

Figure 10: The basic 1,5-benzoxazepine motif

The 1,5-benzoxazepine skeleton **71** (**Figure 10**) is a far more common biologically active constituent than its six-membered counterpart. Just like the benzofurans, the 1,5-benzoxazapine sub-structure has fallen into the category of a 'privileged structure', with compounds containing this motif displaying the ability to bind to several diverse biological receptors with high affinity.[46] Examples of the inclusion in bioactive compounds (**Figure 11**) include: compound **72**,[47] which has been tested as a novel potassium channel opener, and compound **73**,[48] a conduction anesthetic with Curare-like nerve ganglion blocking activity. The skeleton also appears as part of testing libraries developed towards the elucidation of its status as a privileged structure, such as compound **74**.[46] In addition the motif has been added to penicillin as a modifying group, with some success, such as compound **75**,[49] which has been shown to be effective against *S. Aureus*. Finally, it also forms the basis of pyrrolo-1,5-benzoxaepines, such as

PBOX-21 **76**, which inhibits GI cyclase activity in human astrocyctoma cells, and PBOX-6 **77**, which exhibits pro-apoptic ability by binding to tubulin and acting as a microtubule targeting agent.[50]

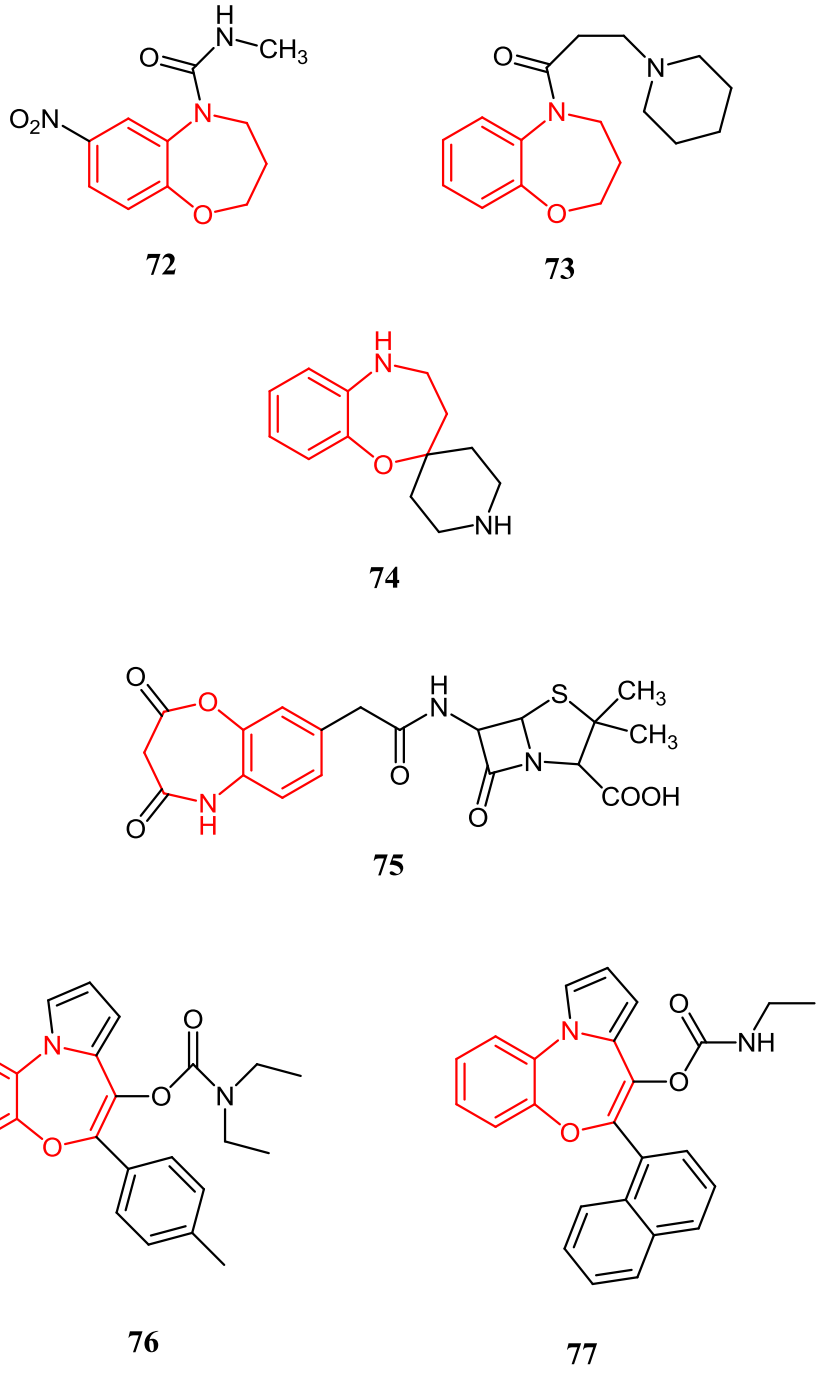

Figure 11: Molecules containing the 1,5-benzoxazepine motif

2.2.2.1 Previous synthetic strategies for the 1,5-benzoxapines

2.2.2.1.1 Sequential *N*-acylamide methylenation-enamide RCM

Similar to the RCM strategy employed in our laboratories, the methodology of Bennasar *et al.*[51] used a 2-aminophenol precursor which underwent a double protection step: first using benzoyl chloride followed by acetyl chloride. (In both cases NaH was used as base to selectively deprotonate the amino group.) The compound was then allylated using allyl bromide under the action of K_2CO_3 to form the mono-allylated and double protected precursor **78**. This compound was then subjected to RCM using a 30 mol% GII catalyst loading. Both the 6-membered **68** and 7-membered **79** ring products were produced – in a ratio of 3:1. (**Scheme 23**.)

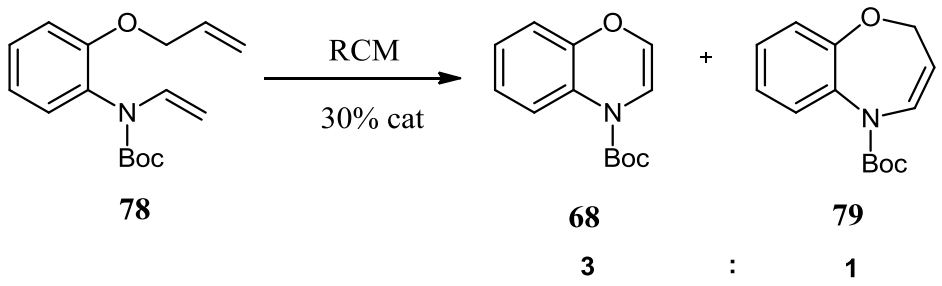

Scheme 23: The RCM strategy of Bennasar *et al.*[51]

2.2.2.1.2 Substituted 1,5-benzoxazepines from the reduction of chromanone oximes

During investigations into the reducing ability of $LiAlH_4$, the reduction of the oximes of the chroman-4-ones were studied. A 3,3,7-trimethyl-3,4-dihydronaphthalen-1(2H)-one oxime **80** was subjected to such reduction in refluxing ether containing 300 mol% LiAlH4. (**Scheme 24**.) This resulted in two products. The first – a corresponding 4-amino derivative **81** (42% yield), the second – a ring opening product – a 1,5-benzoxazepine **82** (17% yield).

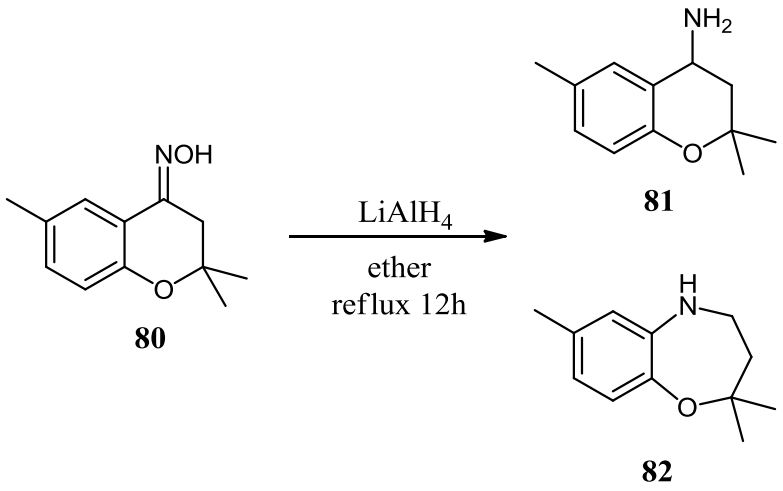

Scheme 24: The reduction strategy of Dudykina *et al.* [48]

.

2.2.3 8-Membered *O*,*N*-benzo-fused heterocycles: the benzoxazocines

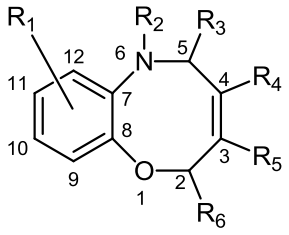

83

Figure 12: The basic 1,6-benzoxazocine motif

Medium ring sizes, such as the 1,6-benzoxazocines **83**, are more scarce in naturally occurring compounds. One of the few examples with the O and N atoms in the 1 and 6 positions is compound **84**[52] – a highly selective human β-3-adrenergic receptor agonist with high cell permeability (**Figure 13**). Other examples, indicating the importance placed on medium ringed heterocycles, include compound **85**, produced by natural enzymatic pathways.[53] More common are their 2,5-counterparts such as Nefopam **86** – a potent non-sedative analgesic that possesses a profile distinct from that of other anti-inflammatory drugs,[54] and the compound porritoxin **87**, extracted from *Alternaria porri*,

which inhibits the growth of seedlings[55]. Furthermore, molecules such as **88** are being used as precursors in new types of transannular reactions involving selective transformations into useful oxazine and oxazole derivatives.[56]

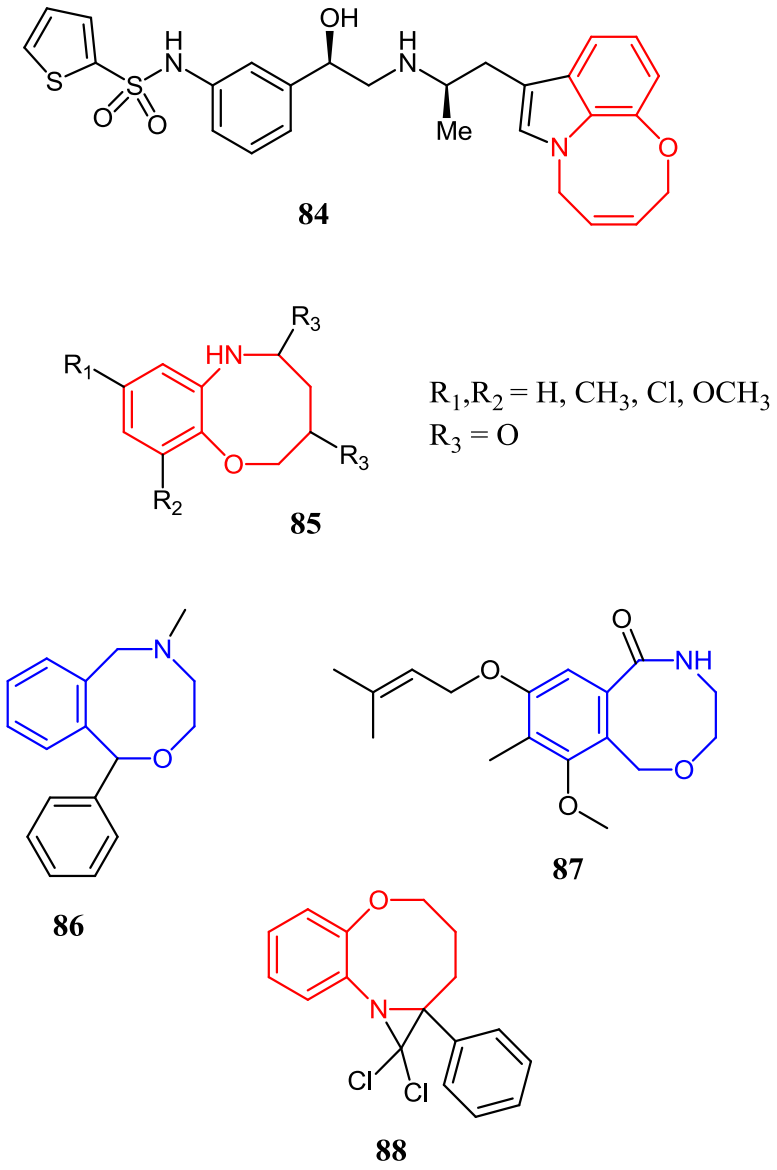

Figure 13: Molecules containing the 1,6-benzoxazacine motif

2.2.3.1 Previous synthetic strategies for the 1,6-benzoxacines

The most common synthetic strategies for medium to large membered ring cycles, particularly those fused to benzene, involve RCM similar to the method used in this project and thus only a representative example will be given here. References citing these methods include Ibrahim *et al.*,[57] Mamouni *et al.*[58] and van Otterlo *et al.*[59]

2.2.3.1.1 The RCM enyne metathesis strategy of Mori *et al.*[60]

A suitably tosylated 1-aminophenol **89** was subjected to allylation (allyl bromide, K_2CO_3) and enylation (1-bromobut-2-yne; NaH) to produce compound **90**. This was then subjected to RCM using a 10 mol% solution of the GI catalyst **5** in CH_2Cl_2. The reaction was left to run at room temperature for 7 hours, resulting in a 99% yield of the 8-membered ring product **91**. (**Scheme 25**.)

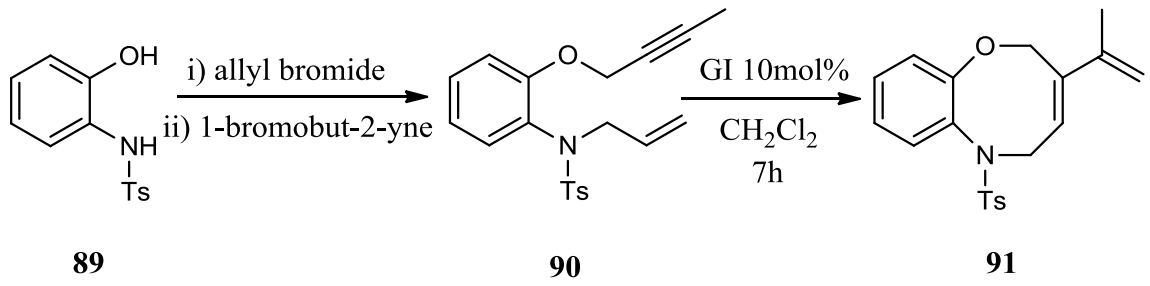

89 **90** **91**

Scheme 25: The enyne RCM strategy of Mori *et al.* [60]

2.3 6-, 7- and 8-Membered *N,N*-benzo-fused heterocycles

Outlined below, is a brief introduction to the 6-, 7- and 8-membered *N,N*-benzo-fused heterocyclic motifs, listed according to ring size, as well as the most prominent synthetic strategies, extracted from literature sources, that do not employ the RMI-RCM approach adopted in this project.

2.3.1 6-Membered *N,N*-benzo-fused heterocycles: the quinoxalines

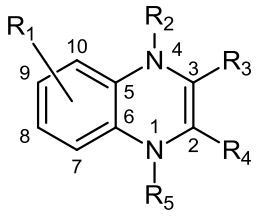

92

Figure 14: The 1,4-quinoxaline motif

As with its 6-membered 'O,N' counterpart, the 1,4-quinoxaline motif **92** (**Figure 14**) is relatively rare in naturally occurring compounds and as of yet has seen little application in medicinal formulations. Some medicinal examples that contain the motif exist, albeit with variations on the level of oxidation. With reference to **Figure 15**, these include: the quinoxaline HBY (097) **93**,[61] a non-nucleoside reverse transcriptase inhibitor; the isothiazole compound **94**,[62] which is a powerful analgesic and compound **95**,[63] (NBQX) a potent AMPA receptor antagonist. More common is its analogue **96**, which shows one of the types of electronic conjugation that 6-membered di-nitrogen ring system can support due to the presence of 8π electrons,[64] examples of the tautomeric forms that can be adopted by this system are shown in **Scheme 26**[65]. In these forms, its applications are far more numerous and include antituberculosis, antibacterial and anticancer agents.[66] Examples include: olaquindox **97**,[67] which is a powerful antibacterial mutagenic agent and compound **98,**[68] a hypoxia-cell selective anticancer agent, fifteen times more potent than currently used agents.

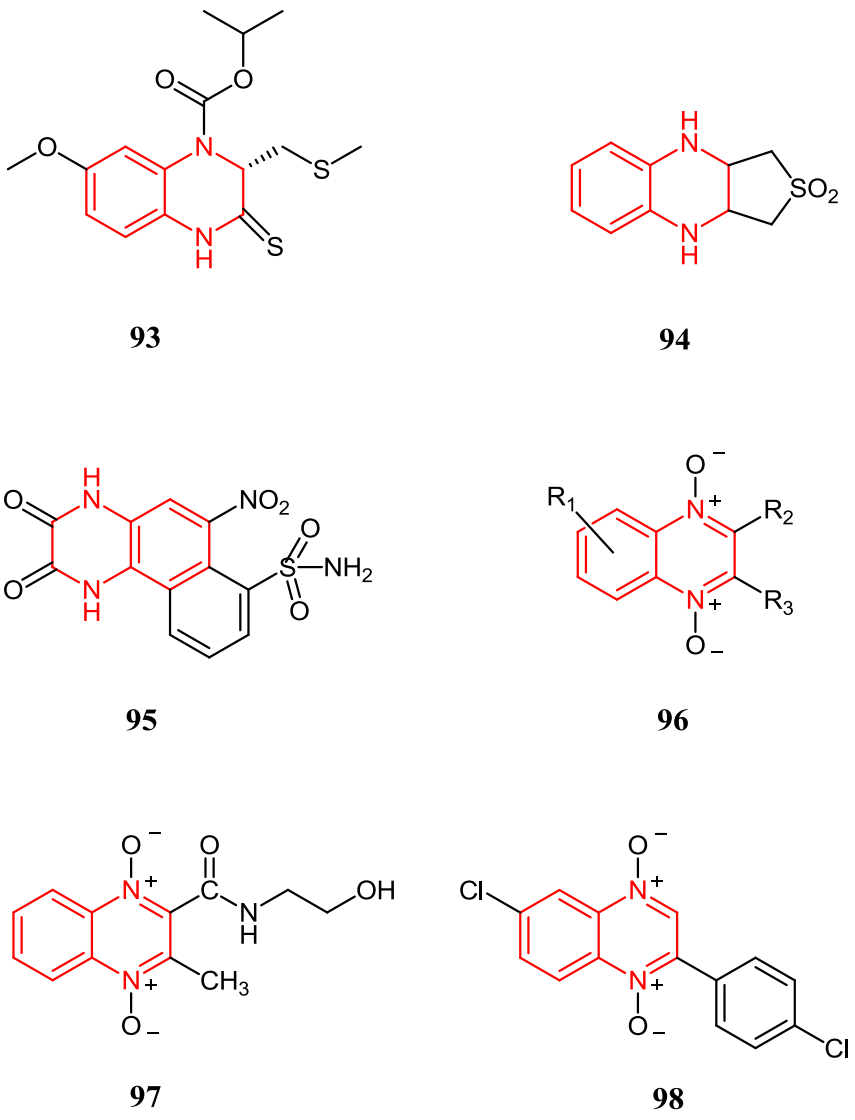

Figure 15: Molecules containing the 1,4-quinoxaline motif

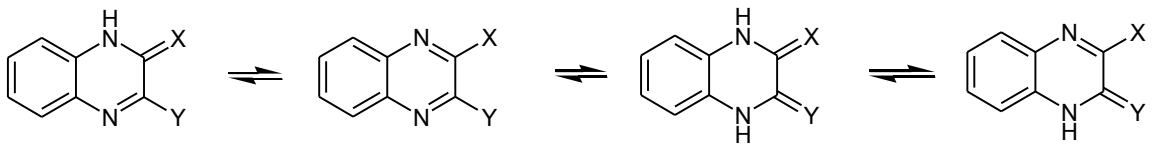

Scheme 26: Possible tautomeric forms of 8π 1,4-quinoxaline

2.3.1.1 Previous synthetic strategies for the 1,4-quinoxalines

2.3.1.1.1 Reduction methodologies involving quinoxalines

Sheinkman *et al.*[69] utilizes the quinoxaline **99,** which is reduced in the presence of zinc dust to the radical anion intermediate, followed by acylation utilizing acetic anhydride, to form 1,1-quinoxaline-1,4-diyldiethanone **100** in a relatively poor yield of 10%. In the synthetic strategy of Hamer *et al.*[70] direct reduction of **99,** employing sodium in boiling ethanol produces tetrahydroquinoxaline **101** in a yield of 43%. (**Scheme 27**.)

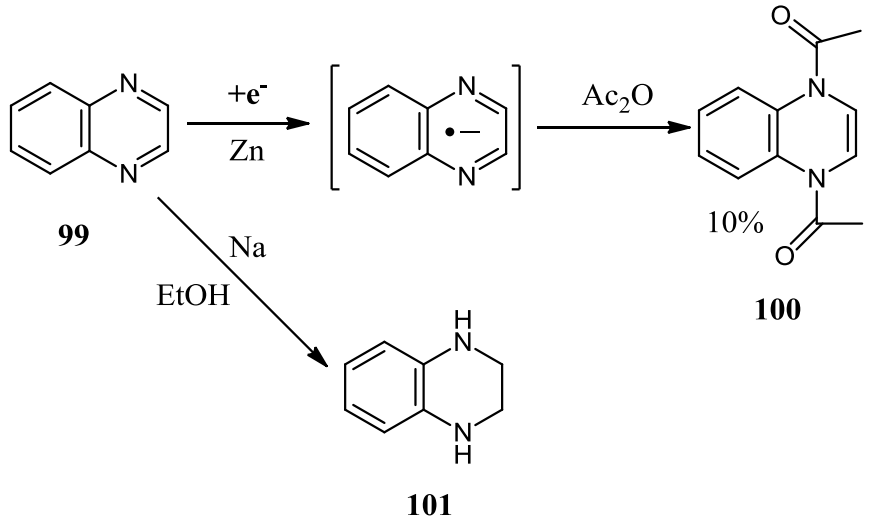

Scheme 27: Reduction strategies of Sheinkman *et al.*[69] and Hamer *et al.*[70]

2.3.1.1.2 Oxalate addition methodologies involving di-amines

The methodology of Gomtsyan *et al.*[71] involved the use of 3-nitrobenzene-1,2-diamine **102** and glyoxal as a 40% solution in water, with ethanol as solvent. The reaction was heated to reflux for 2 hours and allowed to react at room temperature for a further 16 hours resulting in **103** with a yield of 32%. (**Scheme 28**.)

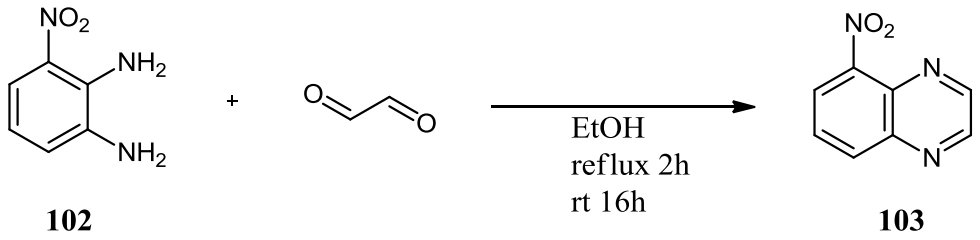

Scheme 28: Oxolate addition methodology of Gomtsyan *et al.*[71]

The methodology of Tene Ghomsi *et al.*[72] – **A** – used a protected diamine **104** (R_1 = 3-phenyl-1*H*-pyrazole) which was reacted with the substituted oxalate **105** (R_2,R_3 = OEt), acting as both reactant and solvent. After concentration of the reaction mixture compound **106** was re-crystallized from ethanol with a 90% yield. (**Scheme 29: route A**)

The 'green chemistry' methodology of Hazarika *et al.*[73] – **B** – used the un-protected diamine **104** (R_1 = H) which was reacted with the substituted oxalate **105** (R_2,R_3 = alkyl/aryl)), using $InCl_3$ (10 mol%) as catalyst, at room temperature with water as solvent. This led to the formation of **107** with yields between 88% (R_2,R_3 = alkyl) and 98% (R_2,R_3 = aryl). (**Scheme 29: route B**)

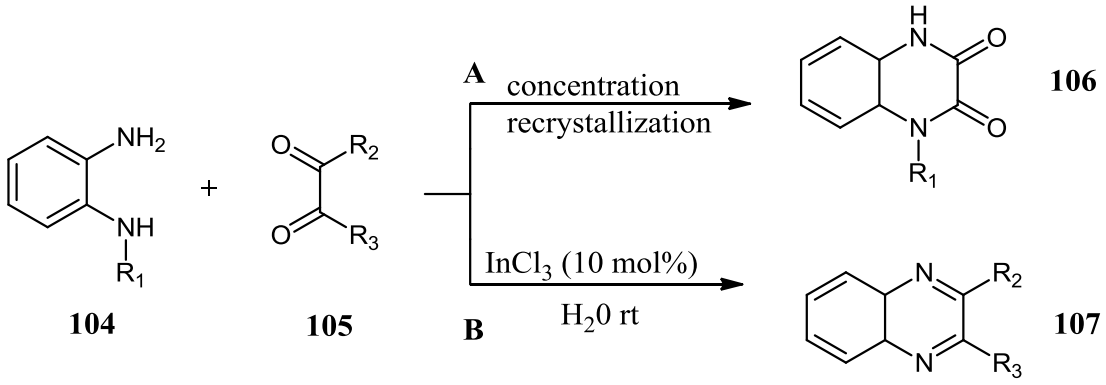

Scheme 29: Addition strategies of Tene Ghomsi *et al.*[72] (**A**) and Hazarika *et al.*[73] (**B**)

2.3.1.1.3 Beirut methodologies involving benzofuroxans

Numerous syntheses towards 6-membered di-nitrogen rings are possible utilizing variations of the well-known Beirut reaction.[77] The required substituted benzofuroxans **109**, were readily producible from variously substituted 2-nitrobenzenamines **108**, produced under the action of strong bases. The resultant benzofuroxans were then reacted with various β-ketoesters **110**, and triethylamine which was added dropwise at 0 °C and ethanol as solvent. The reaction mixtures were then left at room temperature for 1 – 3 days. After evaporation to dryness the required quinoxaline-2-carboxylate 1,4-dioxide derivatives **111** were obtained, with yields for the reactions varying between 2 – 44%, depending on the identity of the R groups. (**Scheme 30**.)

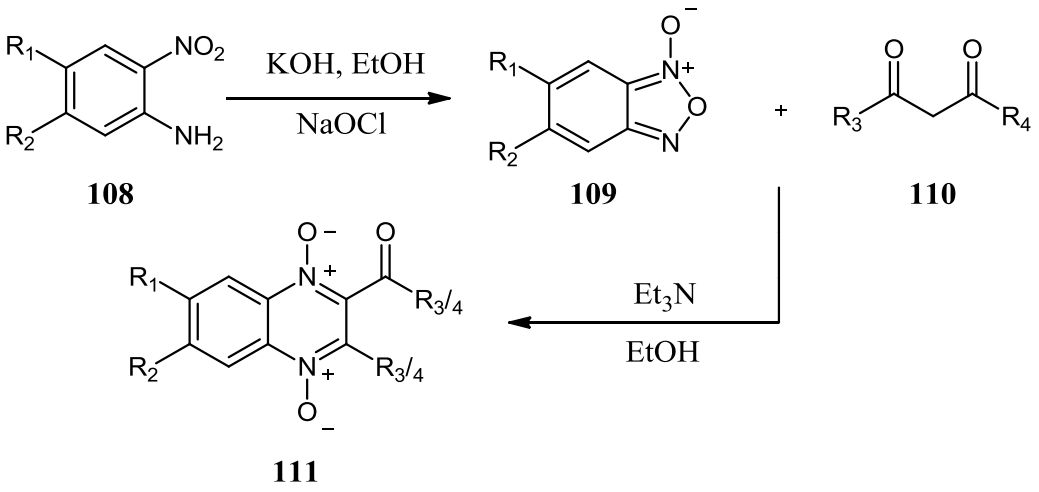

Scheme 30: Generalized methodologies of Jaso *et al.*,[74] Carta *et al.*[75] and Marin *et al.*[76]

2.3.2 7-Membered *N,N*-benzo-fused heterocycles: the benzodiazepines

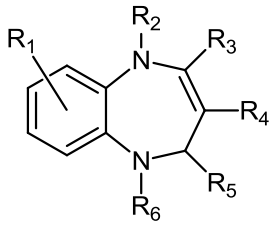

112

Figure 16: The 1,5-benzodiazepine motif

One of the most common structural motifs in biologically active and medicinal compounds is the 1,5-benzodiazepine motif **112** (**Figure 16**). Even its simplest analogues (**Figure 17**) have long been known to have potent medicinal effects. Examples include: compound **113**, which significantly lowers blood pressure; compound **114**, a powerful analgesic; and compound **115**, a well known tranquilizer.[78] Its analogues are also known to exhibit antiviral activity, such as the HIV-1 reverse transcriptase inhibitor Nivirapine **116**.[79] Compound **117**[80] has significant aldose-redutase ability and is currently being investigated for medicinal applications. The motif has been added to glycosides to investigate the behaviour of *C*-nucleocides, such as compound **118**.[81] The motif also occurs as part of larger compounds, such as the pyridobenzodiazepines: these include compound **119**,[82] (VNA-932) a potent, orally active, non-peptidic vasopressin V2 receptor selective agonist; and compound **120**,[83] a powerful inhibitor of the Hepatitis C virus (*via* NS5B polymerase inhibition).

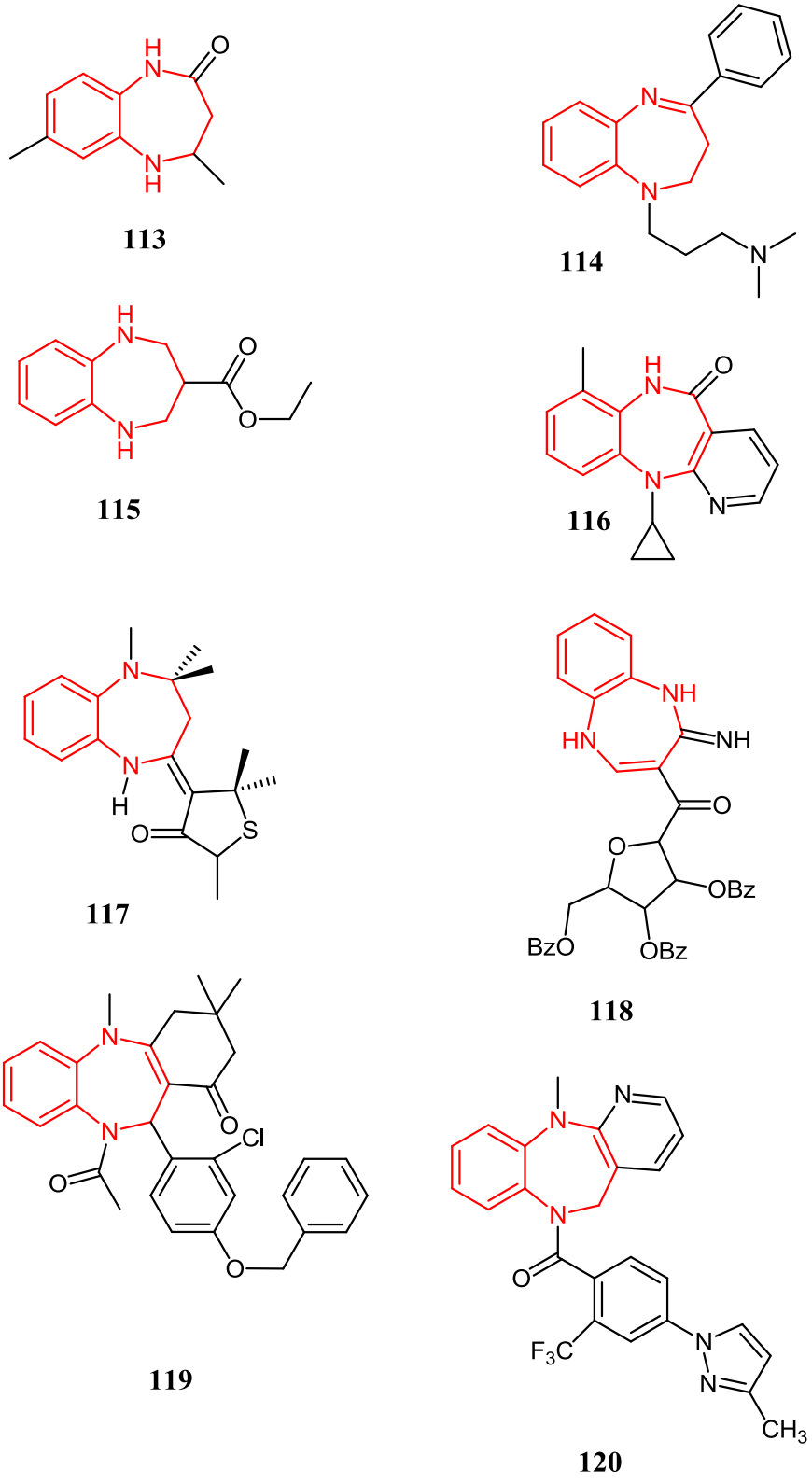

Figure 17: Molecules containing the 1,5-benzodiazapine motif

2.3.2.1 Previous synthetic strategies for the 1,5-benzodiazapines

Generally, 1,5-benzodiazepines are synthesized by the condensation reaction of *o*-phenylenediamines with *α,β*-unsaturated compounds,[84] *β*-haloketones,[85] and ketones.[86] Among these methods, the acid catalyzed condensation of *o*-phenylendiamines with ketones is one of the simplest and most applicable approaches for the synthesis of 1,5-benzodiazepines. A number of these methodologies will be described in the next section.

2.3.2.1.1 The reaction of *o*-phenylenediamines with unsaturated carbonyls

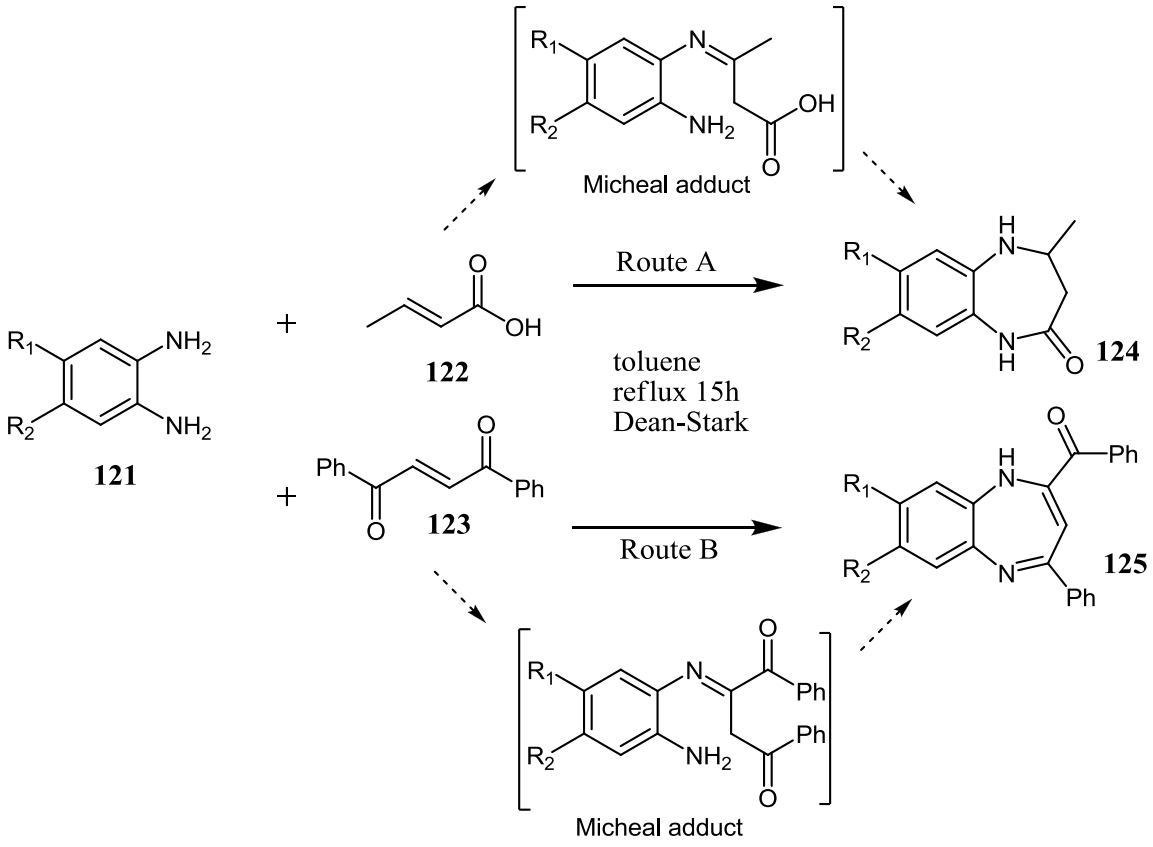

Scheme 31: Generalized methods applied by Loskutov *et al.*,[87] (Route A) and Bindra *et al.*[88] (Route B)

In the above methodologies, variously substituted di-amines **121** were reacted with various unsaturated carbonyls, such as ketones **122** (Route A) or di-ketones **123** (Route B), by refluxing for up to 15 hours in a Dean-Stark apparatus. (**Scheme 31**.) The key intermediates involved are the Michael adducts, which undergo Schiff base formation at either of the two carbonyl functionalities to give the 7-membered rings **124** and **125** (depending on the nature of the carbonyl), after a second condensation. Overall yields for **124** are in the region of 24% and for **125** the overall yields are in the region of 36%

2.3.2.1.2 The one-pot three-component strategy

In this novel one-pot, three-component reaction, benzene-1,2-diamine **126** was condensed with a variety of *β*-keto esters **127**. The reaction proceeded for 4 hours with C_6F_5COOH as acid. This resulted in the formation of an enaminoester intermediate, which then reacted with the aromatic aldehyde **128**. (**Scheme 32**.) The main feature of this reaction is the γ-selective C–C bond formation of β-enaminoesters – probably due to the thermodynamic control derived from intramolecular hydrogen bonding of the enamino esters. Yields for **129** after solvent optimization were in the region of 60%.

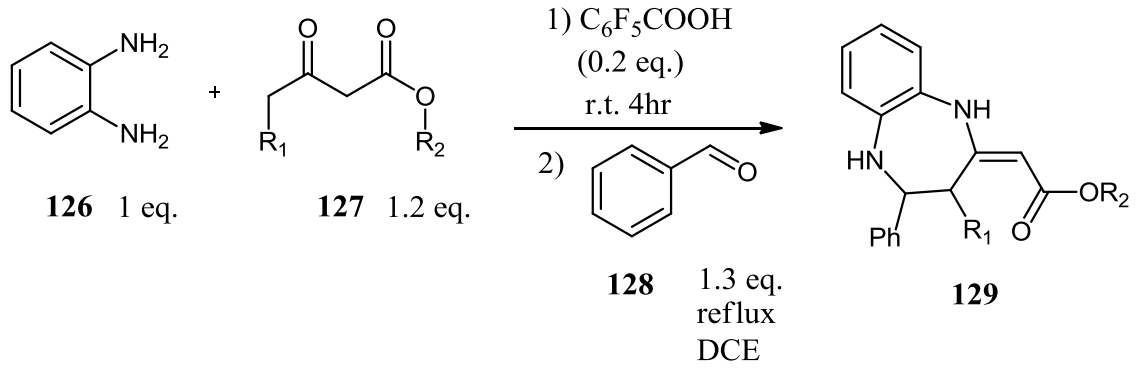

126 1 eq. **127** 1.2 eq. **128** 1.3 eq. reflux DCE **129**

Scheme 32: The *β*-Ketoester methodology of Murai *et al*.[89]

2.3.2.1.3 Synthesis involving the catalytic action of zeolites

The use of synthetic and natural zeolites in the methodology of Tajbakhsh *et al.*[90] represents true heterogeneous catalysis involving heterocyclization. Two equivalents of various ketones **130** were added to 2-aminophenol **126**. The reaction mixture was then refluxed in acetone for 3 to 6 hours, over a variety of zeolites. Types of zeolites used included: heulandite, HY and HZSM-5. Yields obtained for **131** were in the region of 69 – 81%, depending on the ketone and zeolites used. (**Scheme 33**.) Ketones relevant to the generalized reaction scheme below, included: acetone, 3-butanone, 4-methyl-2-pentanone, acetophenone and 6-methyl-5-hepten-2-one.

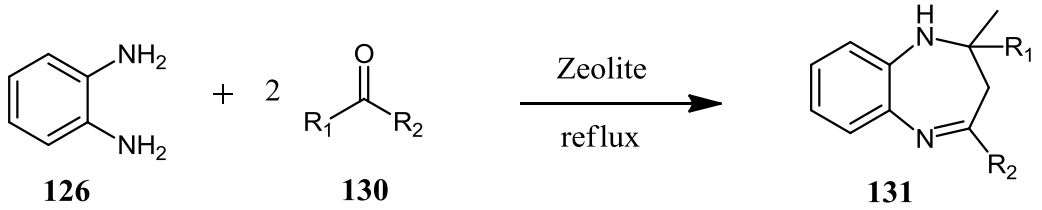

126 **130** **131**

Scheme 33: The highly improved protocol of Tajbakhsh *et al.*[90]

2.3.3 8-Membered *N,N*-benzo-fused heterocycles: the benzodiazocines

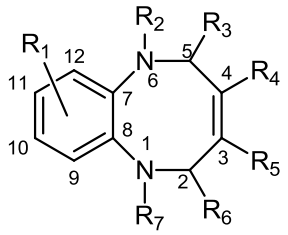

132

Figure 18: The 1,6-benzodiazocine motif

As with its 8-membered 'O,N' counterpart, the 1,6-benzodiazocine motif **132** (**Figure 18**) is rare in naturally occurring compounds with known biological and medicinal effects. These types of bicyclic molecules are, however, potential pharmacological scaffolds with interesting biological activities.[91-92] They have also been used as scaffolds for bridgehead studies[93] and intramolecular flexibility studies.[94] **Figure 19** shows two examples of the 8-membered 1,6-dinitrogen ring system. Compound **133** [95] (KT5720) is a protein kinase A, which regulates multiple signal transduction events *via* protein phoshorylation and is integral to all cellular responses involving the cyclic AMP second messenger system. Compound **134**[96] (K252a) is a potent inhibitor of protein kinase A (as well as kinases C and G) which acts by competing with ATP binding sites that have K_i values in the region of 18-25 nM.

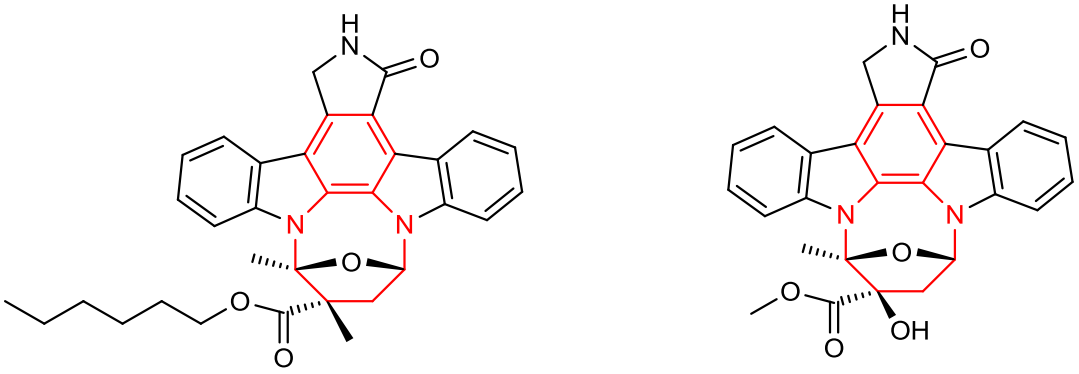

Figure 19: Molecules containing the 1,6-benzodiazacine motif

2.3.3.1 Previous synthetic strategies for the 1,6-benzodiazacines

2.3.3.1.1 Reaction of protected di-amines with *cis*-1,4-dichloro-2-butene

This strategy of Proust *et al.*[93] (**Scheme 34**) involved refluxing the tosylated 1,2-benzodiamine **135** with *cis*-1,4-dichloro-2-butene **136**, in acetonitrile for 24 hours. The reactants were in 1:1 equivalence, with 5 equivalents of K_2CO_3 used as base to initiate the reaction. The yield of **137** was 75%.

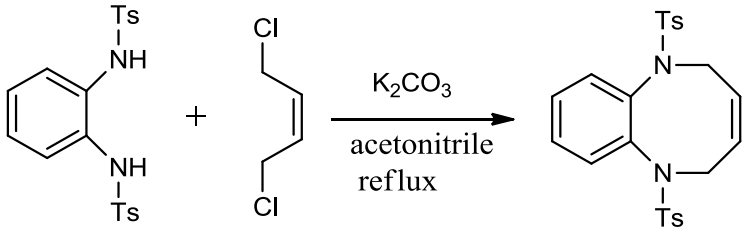

135 **136** **137**

Scheme 34: The synthetic method used by Proust *et al.*[93]

2.3.3.1.2 Methodologies involving RCM of allylated 1,2-benzodiamines

The most common synthetic strategies for 8-membered ring cycles, particularly, those fused to benzene, involve RCM reactions similar to the method used in this project and thus only one example will be given here. References citing other RCM methods include: Mamouni *et al.*,[58] Mori *et al.*[60] and Dragutan *et al.*[97]

The methodology of van Otterlo *et al.*,[59] **(Scheme 35**) utilized a tosylated 1,2-benzodiamine **135** that was subjected to double allylation with allyl bromide and K_2CO_3 (as base). After refluxing in acetone for 20 hours at 60 °C, the double allylated product **138** resulted. **138** was subjected to RCM, using a 5 mol% loading of the GII catalyst **6** in toluene at rt for 5 hours, leading to the formation of the 8-membered ring product **139** with a 94% yield.

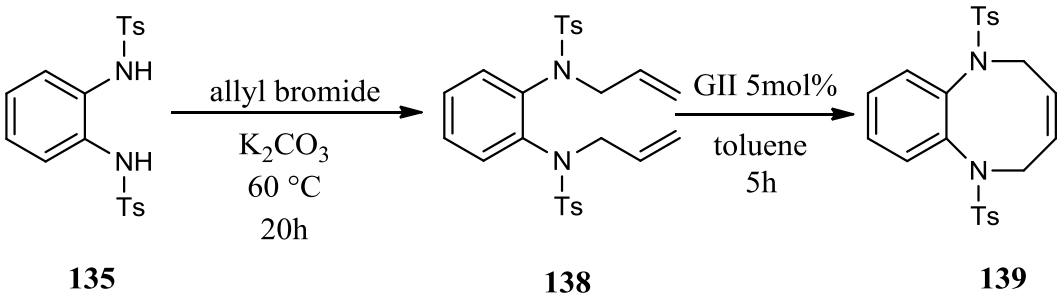

Scheme 35: The synthetic method used by van Otterlo *et al.*[59]

2.4 Conclusion

With the importance of the molecular scaffolds presented, as well as these previous synthetic strategies in mind, attention can now be drawn to the Wits RMI-RCM methodology presented in the next chapter of this dissertation. In doing so, it is hoped that the utility of the methodology can be seen in a more appropriate context.

CHAPTER THREE

DISCUSSION

RESULTS

Chapter 3: Results and discussion

This chapter presents the synthetic work undertaken in this dissertation and will be discussed in some detail. The sections are arranged according to the structural motif produced and will include an in-depth analysis of the synthetic methodology.

3.1 The Wits RMI-RCM approach to benzofurans

The following section will introduce the synthetic methodology undertaken in the production of the benzofuran motif. It begins with the retro-synthetic analysis of the problem at hand and proceeds to the actual methodology implemented towards this aim. The reaction results are then discussed in detail, with note taken of the various yields of the compounds produced, notes of synthetic interest and a discussion of the spectroscopic evidence confirming the identity of the compounds.

3.1.1 Retro-synthetic analysis of the benzofurans

The retro-synthetic methodology towards the Wits RMI-RCM approach to the benzofurans is represented in **Scheme 36**. The required target **A** can be envisaged to form, through RCM, if un-saturated bonds are in the positions shown in synthon **B.** To achieve synthon **B**, it was envisaged that allylic attachments in the required positions shown in synthon **C**, could be subjected to RMI. To achieve these attachments, variously substituted phenols **D** would suffice through dual allylation in the positions shown. Standard allylation reactions would result in attachment of the allyl group to the OH of the phenol. Thus it was envisaged that an allylation reaction followed by a Claisen rearrangement would cause the displacement of the allyl group to the adjacent carbon position. The OH group could then be re-allylated. With this strategy in mind a standardized series of simple reactions was instituted to form the benzofuran motif. This strategy is shown in **Scheme 37**.

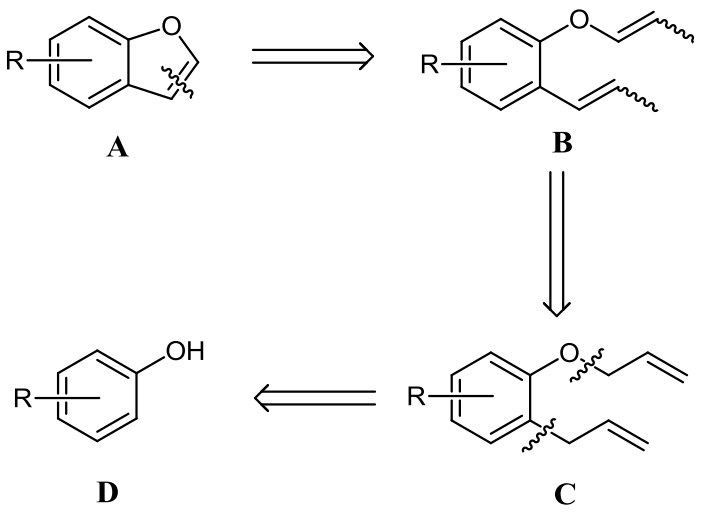

Scheme 36: The disconnection strategy adopted in Wits RMI-RCM methodology towards the synthesis of benzofurans

3.1.2 General methodology implemented towards the benzofurans

Towards the benzofuran synthetic goal – shown in **Scheme 37** – several substituted phenols **140a-e** (with at least one free *ortho* position) were subjected to a simple allylation reaction, utilizing allyl bromide as allylation reagent and potassium carbonate as base, to yield **141a-e**. These compounds were then subjected to a Claisen rearrangement, either *via* conventional heating methods or under microwave radiation, to yield compounds **142a-e.** These compounds were then re-allylated under the same allylation conditions used before, to yield the di-allylated compounds **143a-e**. At this stage the Ru catalysts were introduced. Compounds **143a-e** underwent RMI with catalyst **15,** utilizing an average catalyst loading of 5 mole %, to yield the di-isomerized products **144a-e**. These compounds were then subjected to RCM using the GII catalyst **6**, again with a 5 mole % catalyst loading, resulting in the final benzofuran products **145a-e.**

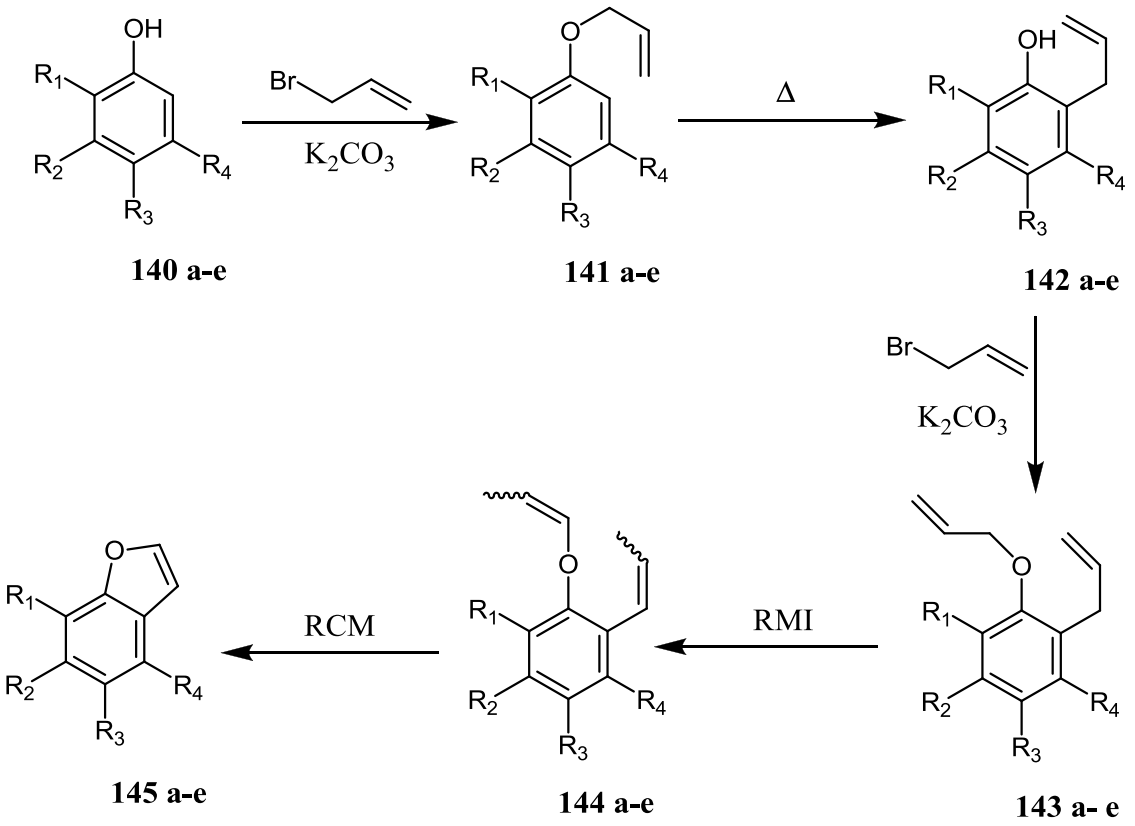

Scheme 37: The Wits RMI-RCM approach to benzofurans

a (R_1 = OMe, R_2 = H , R_3 = H, R_4 =OMe)

b (R_1 = H, R_2 = H, R_3 = Br, R_4 = H)

c (R_1 = H, R_2 = H, R_3 =*t*-butyl, R_4 = H)

d (R_1 = Bz, R_2 = H, R_3 = H, R_4 = H)

e (R_1 , R_2 , R_3 , R_4 = Ar)

(For letter code clarification, please see **Figure 20)**

3.1.3 Substituted phenols and naphthalene-1-ol precursors

A series of commercially available substituted phenols **140a-d** and naphthalene-1-ol **140e** were used as the precursors to the benzofurans (**Figure 20**). The choice of these compounds was based on the type and position of the relevant functionalities attached to the phenol ring – as these functionalities may be used as a means, and position, for the attachment of other structural motifs at a later stage of a complete synthesis of a larger structural complex. None of the compounds required purification prior to use.

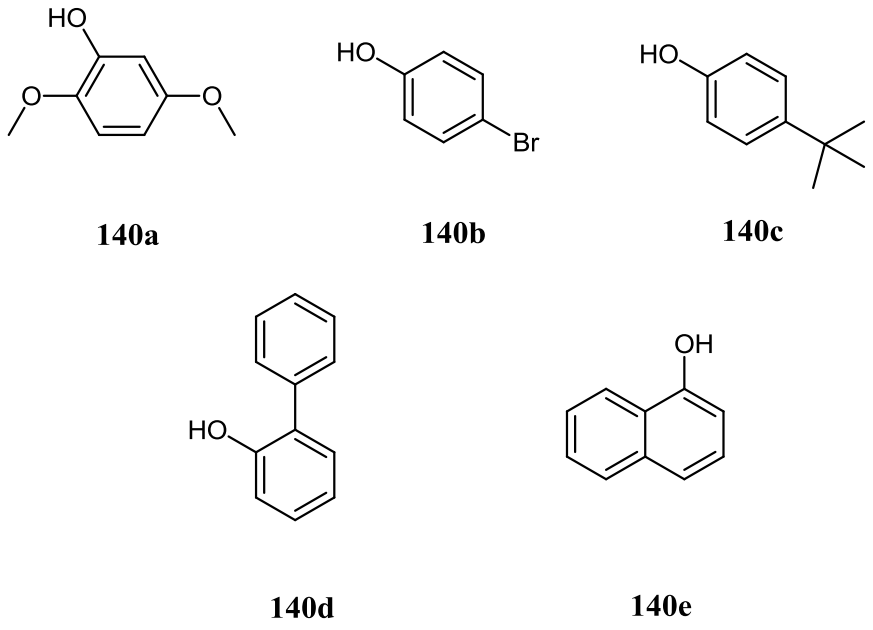

140a **140b** **140c**

140d **140e**

Figure 20: Precursors to the benzofurans

3.1.4 Results and analysis of the individual reaction steps

3.1.4.1 Allylation of the substituted phenols and naphthalene-1-ol

A standardized allylation procedure was adopted as per the generalized mechanistic proposal outlined in **Scheme 38** and proceeded as follows: potassium carbonate (in a molar excess of 2.5 equivalents) was used as a base to deprotonate the hydroxyl group of

the precursors, in the presence of allyl bromide (in a molar excess of 2.5 equivalents) as allylation reagent. All reactions were heated to 60 °C, and left to reflux in acetone for 12 hours under an inert nitrogen atmosphere. The reaction mixtures were then filtered through celite, to remove the base, and the solvent was then removed under reduced pressure. This was followed by purification using silica gel column chromatography with hexane/ethyl acetate mixtures as eluent (optimized according to the retention factor of the individual compounds) to afford the desired compounds.

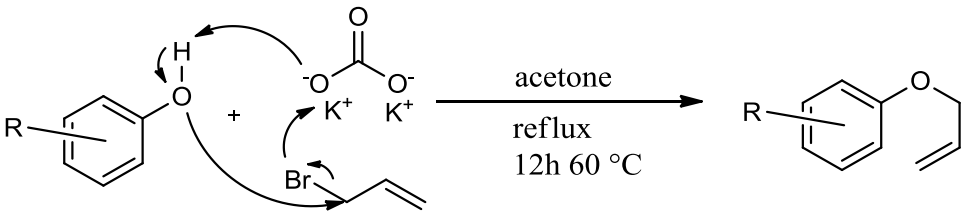

Scheme 38: General mechanistic proposal of the allylation of phenols and naphthalene-1-ol

The following allylated compounds **141a-e** (**Figure 21**) were thus produced.

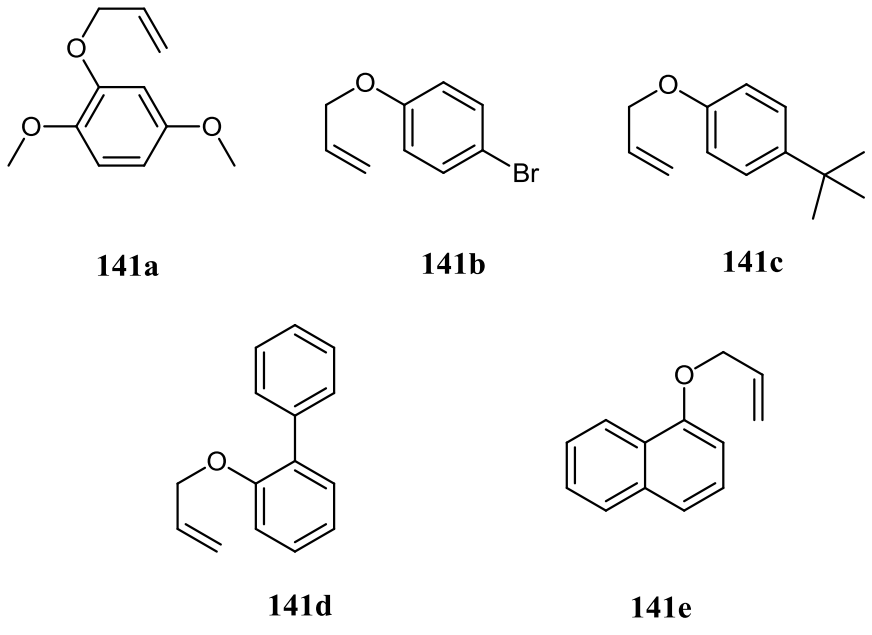

Figure 21: Mono-allylated precursors

3.1.4.1.1 Yield and characterization data regarding the allylation procedures

At this early stage of the synthetic methodology, the identities of the allylated precursors were confirmed primarily *via* HRMS and/or ^{1}H NMR spectroscopy – *only* if they were previously uncharacterized compounds. This was the case with compounds **141a** and **141d**. In the case of compound **141b**, **141c** and **141d**, familiarity with the allylation protocol, along with TLC analysis, indicating that the reaction had run to completion, resulted in these known compounds being submitted directly to the next reaction step without further characterization.

The yield data for the compounds, as well as the *m/z* of the parent ion (unless it was a known compound, in which case the relevant literature reference is given) are presented in **Table 1.**

Table 1: Yields and HRMS data of the allylated compounds

Compound	Yield (%)	HRMS (e/z)	
		Expected	Found
141a	60	194.0943	194.0942
141b	98	211.9837	[98]
141c	99	190.1358	[99]
141d	100	210.1045	210.1045
141e	100	184.0888	[100]

As can be seen from the yields in **Table 1**, only 2,5-dimethoxyphenol (**141a**), did not proceed to completion, due to the possible steric interaction of the adjacent methoxy group. The ^{1}H NMR signals for the allylic substituents on compounds **141a**, **141b** and **141d**, used to confirm that allylation of the OH groups had indeed taken place, are presented in **Table 2.** All signals are in the expected shift ranges.

Table 2: Relevant ^{1}H NMR signals used for identification

Compound	^{1}H NMR			
	Identity	**Shift (ppm)**	**Multiplicity**	**Integration**
141a	$\boldsymbol{H}_2$C=	5.26 – 5.30	m	1
		5.37 – 5.43	m	1
	=C***H***–	6.01 – 6.14	m	1
	–C$\boldsymbol{H}_2$–	4.57 – 4.59	m	2
141b	$\boldsymbol{H}_2$C=	5.27 – 5.44	m	2
	=C***H***–	5.91 – 6.04	m	1
	–C$\boldsymbol{H}_2$–	4.50	d	2
141d	$\boldsymbol{H}_2$C=	5.18	dd	1
		5.31	dd	1
	=C***H***–	5.96	tdd	1
	–C$\boldsymbol{H}_2$–	4.51	td	2

3.1.4.2 Claisen reactions of the allylated precursors

The allylated precursors **141a-e** (**Figure 21**) were then subjected to two separate heating methods to effect the Claisen rearrangement (**Scheme 39**). The first method entailed conventional heating, with the reaction vessel submerged in either an oil bath (for temperatures below 90 °C), or in a Wood's Metal bath (for temperatures above 90 °C). The second method involved subjecting the allylated precursors to focused microwave radiation in a sealed reaction tube. Where conventional heating was used, the reaction progress was checked by TLC every 30 minutes. If no significant conversion had occurred after 1 hour, the reaction temperature was increased by 30 °C and heating continued, until the reaction had either run to completion or decomposition products became evident. When microwave irradiation was used, the reaction progress was monitored *via* TLC every 15 minutes.

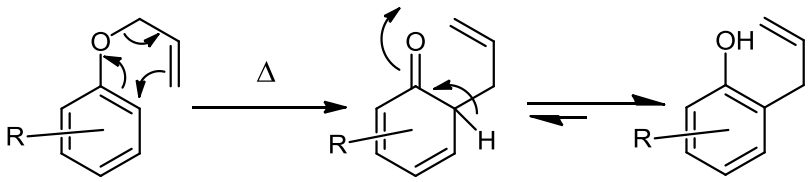

Scheme 39: General mechanistic description for the Claisen rearrangement of the phenols and naphthalene-1-ol

The following compounds **142a-e** (**Figure 22**) were thus produced.

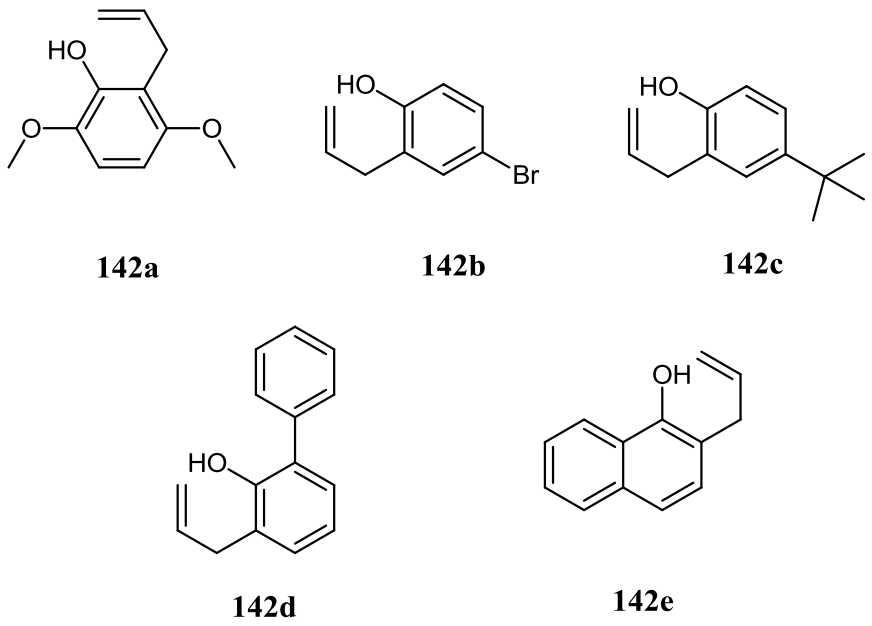

Figure 22: Claisen products

3.1.4.2.1 Yield and characterization data regarding the Claisen procedures

Table 3 shows the comparative yields of the relevant compounds that underwent Claisen rearrangement, as well as heating time, heating temperature and heating method (**M** = microwave radiation, **C** = conventional heating). In the case of microwave radiation the following parameters were used with regards to the CEM Discover microwave device: ramp time = 2 min; pressure = 100 psi; power = 150 W; cooling = on).

Table 3: Yield, reaction time and heating method for the various compounds

Compound	Time (min)	Heating Method	Temp. (°C)	Yield (%)
142a	40	C	230	49
142b	15	M	180	–*
142c	50	M	220	56
142d	90	M	200	60
142e	2	M	180	86

* not isolated, used directly in the next step

Overall, the yields of the Claisen rearrangements were poor to moderate, with an average yield of just 62 %. The heating methodology employed does not, however, represent the optimal heating time or temperature. In each case it was clear that significant decomposition was indeed occurring. Thus a large opportunity is left for yield optimisation, with the potential for the results obtained for **142e** (where the highest yield was 86 %) to be achieved. The molecule most unstable towards heating was **142b**; this was most likely due to the bromine substituent on the ring, which also may have made the precursor compound **141b** unstable and prone to decomposition. This resulted in **142b** being submitted directly to the next reaction step, without purification, as it also appeared to decompose on silica.

On average the microwave method did not represent a significant improvement in reaction times, when compared with conventional heating methods. However, in the case of **142e**, which underwent rearrangement in less than 4 minutes, accompanied by a sudden temperature rise signalling the end of the reaction, a high yield of 86 % was obtained. This may have been due to the increased electronic conjugation in the naphthalene ring, allowing the sigmatrophic shift to proceed more easily. This dramatic temperature rise was not observed in the other compounds undergoing Claisen rearrangement under microwave conditions. In the case of **142a**, the relatively low yield is because the Claisen rearrangement proceeded not only to the required position A, but

also to positions B and C, as per the Claisen mechanism outlined in **Scheme 12** in chapter one.

Table 4 contains spectrographic data used to identify the compounds (with the exception of the bromine containing **142b**). The primary identifying characteristics sought in the ^{1}H NMR spectra were the existence, as well as movement of, the allylic substituent's signals. Where additional confirmation was needed, HRMS was used. All other signals were present in the ^{1}H NMR and ^{13}C NMR spectra which showed all the relevant signals needed to conclusively identify these compounds.

Table 4: HRMS and relevant ^{1}H NMR allylic signals used for identification

Compound	HRMS (e/z)		^{1}H NMR			
	Expected	Found	Identity	Shift (ppm)	Multipl.	Integration
142a	194.0943	194.0943	$\boldsymbol{H_2}C=$	4.92 – 5.07	m	2
			$=C\boldsymbol{H}-$	5.89 – 6.05	m	1
			$-C\boldsymbol{H_2}-$	3.43	br d	2
142c	190.1358	[99]	$\boldsymbol{H_2}C=$	5.14 – 5.20	m	2
			$=C\boldsymbol{H}-$	6.00 – 6.06	m	1
			$-C\boldsymbol{H_2}-$	3.41	br d	2
142d	210.1045	210.1062	$\boldsymbol{H_2}C=$	5.07 – 5.19	m	2
			$=C\boldsymbol{H}-$	6.06	tdd	1
			$-C\boldsymbol{H_2}-$	3.47	br d	2
142e	184.0888	[100]	$\boldsymbol{H_2}C=$	5.23 – 5.32	m	2
			$=C\boldsymbol{H}-$	6.03 – 6.17	m	1
			$-C\boldsymbol{H_2}-$	3.58	d	2

3.1.4.3 Re-allylation of the Claisen products

A standardized allylation procedure was again adopted as per the generalized mechanistic proposal outlined in **Scheme 38** and proceeded as follows: potassium carbonate (in a molar excess of 2.5 equivalents) was used as a base to deprotonate the phenol group of the Claisen precursors **142a-e (Figure 22)**, in the presence of allyl bromide (in a molar excess of 2.5 equivalents) as allylation reagent. All reactions were heated to 60 °C, and left to reflux in acetone for 12 hours under an inert nitrogen atmosphere – with the exception of **142b**, which was only reacted for 2 hours. The reaction mixtures were then filtered through celite and the solvent removed under reduced pressure, followed by purification using silica gel column chromatography with hexane/ethyl acetate mixtures as eluent (optimized according to the retention factor of the individual compounds).

The following re-allylated compounds **143a-e** (**Figure 23**) were thus produced.

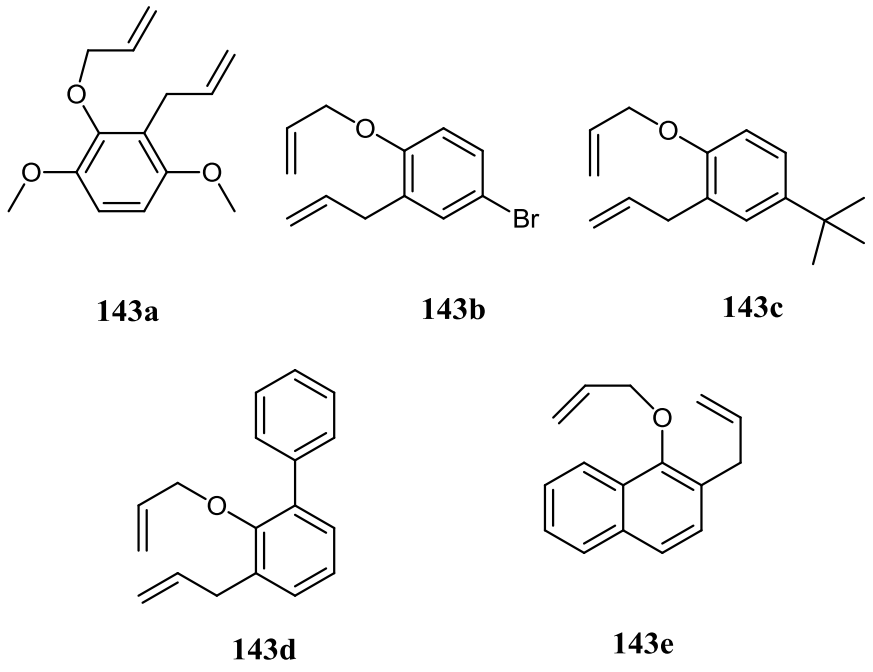

Figure 23: Re-allylated Claisen products

3.1.4.3.1 Yield and characterization data regarding the re-allylation procedures

The yield data for the compounds as well as the m/z of the parent ion, obtained through HRMS, are presented in **Table 5.**

Table 5: Yields and HRMS data of the re-allylated compounds

Compound	Yield (%)	HRMS (e/z)	
		Expected	Found
143a	92	234.1256	234.1258
143b	25	250.1358	250.1360
143c	90	230.1671	230.1648
143d	82	210.1045	210.1045
143e	99	224.1201	224.1204

As can be seen from the yields in **Table 5**, only **143b** gave a poor yield. This was a two-step yield based on **141b**, as its precursor **142b** was used un-purified, due to the silica decomposition problem mentioned earlier. The slightly lower than expect yield for **143d**, is most likely because this reaction was only run for 2 hours and not left overnight, as was done for the others. Nonetheless, the yield for such a short reaction time does indicate the high reactivity between the reagents, which would most likely have resulted in a higher yield, if it was allowed to react for longer, as was evidenced by the presence of a small amount of starting material on the TLC plate.

Table 6 contains ^{1}H NMR spectrographic data also used to identify the compounds. The primary identifying characteristic sought in the ^{1}H NMR spectra, was the existence of two sets of allylic signals – in the regions of those signals found in **Table 2** and **Table 4**. Apart from this, all other signals were present in the ^{1}H NMR spectra. In addition, the ^{13}C NMR spectra showed all the relevant signals needed to conclusively identify these compounds.

Table 6: Relevant ^{1}H NMR spectroscopy signals (* = overlapping signals)

Compound	^{1}H NMR				
	Position	**Identity**	**Shift (ppm)**	**Multiplicity**	**Integration**
143a	O	H_2C=	5.21	dd	2
	O	=CH–	5.32 – 5.43	m	1
	O	–CH_2–	4.48	td	2
	Ar	H_2C=	4.91 – 5.03	m	2
	Ar	=CH–	6.09	tdd	1
	Ar	–CH_2–	3.44	td	2
143b	O	H_2C=	5.27 and 5.40	dd and dd	2
	O	=CH–	5.85 – 6.12*	m	1
	O	–CH_2–	4.51	td	2
	Ar	H_2C=	5.02 – 5.13	m	2
	Ar	=CH–	5.85 – 6.12*	m	1
	Ar	–CH_2–	3.37	br d	2
143c	O	H_2C=	5.23 and 5.41	dd and dd	2
	O	=CH–	6.00 – 6.06*	m	1
	O	–CH_2–	4.52	td	2
	Ar	H_2C=	5.00 – 5.12	m	2
	Ar	=CH–	6.00 – 6.06*	m	1
	Ar	–CH_2–	3.41	br d	2
143d	O	H_2C=	5.03 – 5.15*	m	2
	O	=CH–	5.96 – 6.10	m	1
	O	–CH_2–	3.91	br d	2
	Ar	H_2C=	5.03 – 5.15*	m	2
	Ar	=CH–	5.68 – 5.84	m	1
	Ar	–CH_2–	3.49	d	2
143e	O	H_2C=	5.32	d	2
	O	=CH–	6.16 – 6.28	m	1
	O	–CH_2–	4.51	dd	2
	Ar	H_2C=	5.07 and 5.12	d and dd	2
	Ar	=CH–	5.94 – 6.13	m	1
	Ar	–CH_2–	3.61	dd	2

3.1.4.4 Di-isomerization of the di-allylated compounds

A standardized procedure was adopted in the RMI reactions on the di-allylated products from the previous step. The precursors **143a–e** (**Figure 23**) were placed in a round bottom flask and dissolved in minimal (~2 mL) degassed toluene. The reaction solution was then degassed under reduced pressure and the vessel and then re-gassed with argon. (This was necessary because of the high sensitivity of the catalyst to oxygen.) In each case 5 mole % Ru isomerization catalyst **15** was then added and the vessel, which was again degassed and then re-gassed with argon. All reaction mixtures were then heated to 65 °C and allowed to react for 12 to 14 hours.

The following isomerized compounds **144a-e** (**Figure 24**) were thus produced:

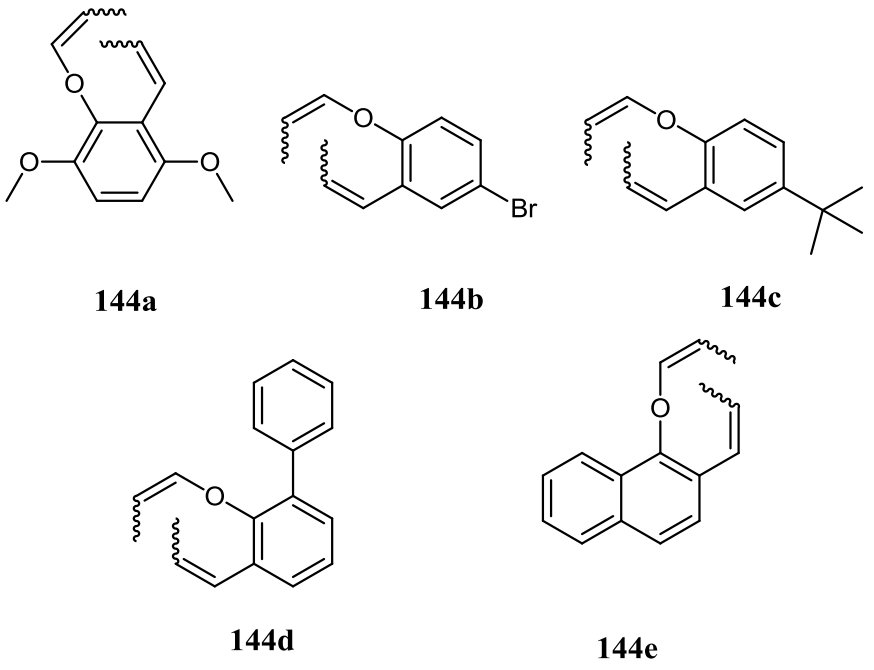

Figure 24: Di-isomerized products

3.1.4.4.1 Yield and characterization data regarding the isomerization procedures

The isomerized compounds were characterized using HRMS and $^{1}H/^{13}C$ NMR spectroscopies. As the molecular weights of the compounds were not expected to change after isomerization, masses of the parent ions, acquired *via* HRMS, were not considered conclusive. All of the masses of the parent ions were, nonetheless, as expected. However, the HRMS fragmentation patterns produced did differ, indicating that some molecular conversion had indeed occurred. The primary means for the identification of the products was left to ^{1}H NMR, with the appearance of 2 methyl group signals, being considered a definitive sign that isomerization had indeed taken place. All other expected signals in both the ^{1}H NMR and ^{13}C NMR spectra were observed.

Table 7 shows the yields found for the di-isomerized compounds **144a–e**, as well as the characteristic methyl group signals that appeared after the compounds were isomerized.

Table 7: Yield and ^{1}H NMR characterization for the isomerized compounds

Compound	Yield (%)	^{1}H NMR			
		Identity	Shift (ppm)	Multipl.	Integration
144a	**98**	O-~-CH_3	1.78	dd	3
		Ar-~-CH_3	1.91	dd	3
144b	**100**	O-~-CH_3	1.86 – 1.92	m	3
		Ar-~-CH_3	1.55 – 1.73	m	3
144c	**86**	O-~-CH_3	1.69	dd	3
		Ar-~-CH_3	1.91	dd	3
144d	**98**	O-~-CH_3	1.85–1.93	m	3
		Ar-~-CH_3	1.57–1.62	m	3
144e	**93**	O-~-CH_3	1.91 – 1.97*	m	3
		Ar-~-CH_3	1.91 – 1.97*	m	3

* = overlapping signals

The isomerization of compound **144d –** which was analyzed only with 200MHz NMR making splitting patterns difficult to discern – had its identity further confirmed *via* the different fragmentation patterns observed in the HRMS spectrum. The fragmentation peaks that differed (as well as those of its precursor) are shown in **Table 8**.

Table 8: HRMS fragmentation patterns used for the characterization of **144d**
(Only non-corresponding peaks are shown; both M^+ = 250)

Precursor (143d)		**Isomerized product (144d)**	
Peak (m/z)	**Intensity (%)**	**Peak (m/z)**	**Intensity (%)**
214	28	236	21
209	28	208	26
181	57	207	37
175	24	191	26
153	16	179	22
139	16		
132	21		
77	17		
41	47		

All of the isomerization reactions proceeded with high yield (with **144c** showing the lowest yield at 86 %). An interesting aspect of these products is that they occur as a mixture of *E*/*Z*-isomers, usually in an approximate ratio of 1:2 (based on the results of those compounds submitted to NMR). The catalyst has shown that it has high versatility, in terms of the substrates it can transform – compound **144b** was unstable towards Claisen reactions and allylation, but underwent isomerization without difficulty. Catalyst removal was also easily effected in this group of compounds. It was sufficient to simply filter the reactant solution though a compacted celite plug and then purify the compounds using silica gel column chromatography.

3.1.4.5 RCM of the di-isomerized compounds

The procedure adopted for the RCM reactions of the di-isomerized compounds **144a-e** proceeded as follows: the di-isomerized precursors were dissolved in ~5 mL distilled degassed toluene and placed in a round bottom flask. The flask was then evacuated under vacuum and flushed with purified nitrogen gas. Grubbs' second generation catalyst **6** was then added at a standard 5 mole % relative to the precursor. The flask was then evacuated again and flushed with additional purified nitrogen. The reaction mixture was then left to stir under nitrogen over a range of times and at an average temperature of 90 °C. Catalyst removal was effected by filtering the reaction solution through a compacted celite plug; after which the solvent was removed under vacuum and the products purified using silica gel column chromatography.

The following benzofuran products **145a-e** (**Figure 25**) were thus obtained:

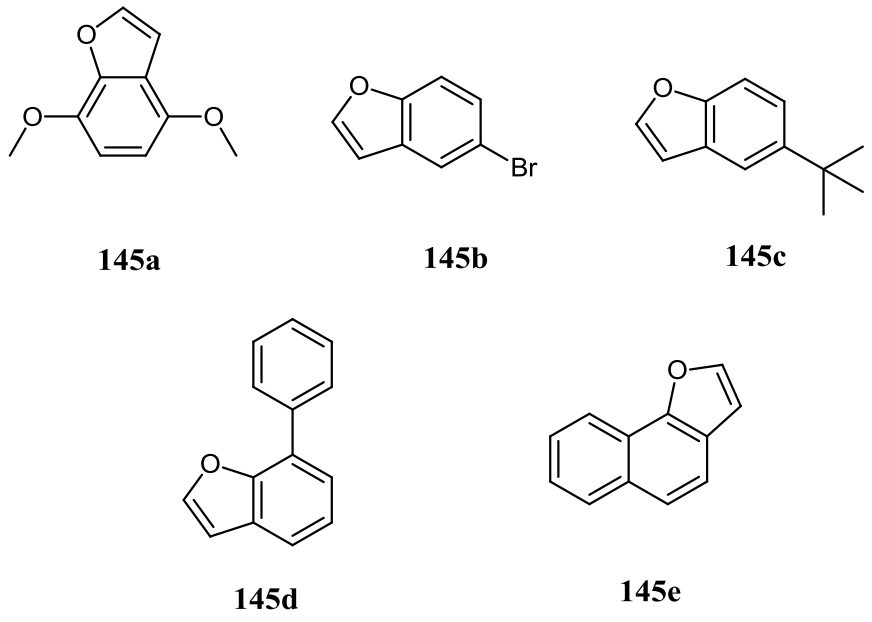

145a **145b** **145c**

145d **145e**

Figure 25: RCM products – the benzofurans

3.1.4.5.1 Yield and characterization data regarding the RCM procedures

The yields, reaction times and temperatures of the RCM reactions are shown in **Table 9**, as well as HRMS data used in the identification of the compounds.

Table 9: Yield, reaction time and temperature for the RCM products and HRMS data

Compound	Time (hr)	Temp. (°C)	Yield (%)	HRMS (e/z)	
				Expected	Found
145a	3	90	100	178.0630	178.0644
145b	14	65	100	195.9524	195.9516
145c	3	90	71	174.1045	174.1029
145d	3	90	63	194.0732	194.0711
145e	12	60	93	168.0575	168.0573

With regard to **Table 9**: compound **145b** was allowed to react at a temperature of 65 °C (instead of the usual temperature of 90 °C used for most RCM reactions in this project) as it was felt that the bromine substituent on the precursor may become unstable at higher temperatures. TLC analysis showed that the compound was slow to convert. However, after a reaction time of 14 hours a 100 % yield was obtained. This prompted a temperature of 60 °C to be used on compound **145e**. This yield was less, despite the reaction time of 12 hours. All other reactions were done at 90 °C, which allowed the reactions to proceed to completion within 3 hours, but resulted in lower yields (with the exception of **145a**) possibly due to decomposition. As can be seen from these results, there appears to be an inverse relationship between reaction temperature and reaction time. There is thus an opportunity to optimize these experimental variables, with regard to the RCM reactions, to maximize the reaction yields.

Table 10 shows selected ^{1}H NMR spectroscopic data used to conclusively identify these products. Only the signals for the 2 carbon substituents on the 5-membered ring are given. All signals shown integrate for 2 hydrogens. All other signals are, nonetheless, accounted for. (See Experimental Section.) ^{13}C NMR spectra also showed that all products contained the relevant number of signals in the required shift ranges.

Table 10: Relevant ^{1}H NMR signals from the 5-membered ring used to identify the benzofuran products

Compound	^{1}H NMR			
	Identity	Shift (ppm)	Multiplicity	Coupling (Hz)
145a	-O-C***H***-CH-	7.55	d	2.1
	-O-CH-C***H***-	6.86	d	2.1
145b	-O-C***H***-CH-	6.72	d	2.2
	-O-CH-C***H***-	7.26	d	2.2
145c	-O-C***H***-CH-	7.43	d	2.9
	-O-CH-C***H***-	6.73	d	2.9
145d	-O-C***H***-CH-	7.67	d	2.2
	-O-CH-C***H***-	6.83	d	2.2
145e	-O-C***H***-CH-	7.75	d	2.1
	-O-CH-C***H***-	6.89	d	2.1

As can be seen from the data in **Table 10**, both saturated carbons on the 5-membered ring show the expected doublet splitting pattern and an expected coupling constant value of around 2.0 Hz. The only exception, in terms of coupling constants, is compound **145c**, which are higher than expected. This anomaly is possibly due to the interaction of the *tert*-butyl group, causing broadening of the observed signals.

3.1.5 Conclusion regarding the benzofuran RMI-RCM methodology

Graph 1 shows the relative yields of all 5 steps of the methodology, although only 3 readings have been given for compound B. As can be seen, there is a downward yield trend at the Claisen step. As discussed earlier, there is an opportunity here to optimise the temperature and reaction times of the Claisen reaction to maximise yields. Both allylation procedures proceeded with high yield (the exception being **141a**, which was not reacted for long enough). The RMI reaction was the most high yielding overall, but could probably be optimised in terms of lowering the amount of catalyst used (i.e. less than 5 mole %) to increase efficiency. The RCM reaction step, also gave generally high yields, but with **145c** and **145d** still leaving room for reaction optimization towards yield improvement. Overall, the synthesis of **145e** was the most efficient; and the synthesis of **145b** the least efficient probably due to the instability of the bromine substituent.

Chart 1: Overall yield trends in the synthesis of the benzofurans

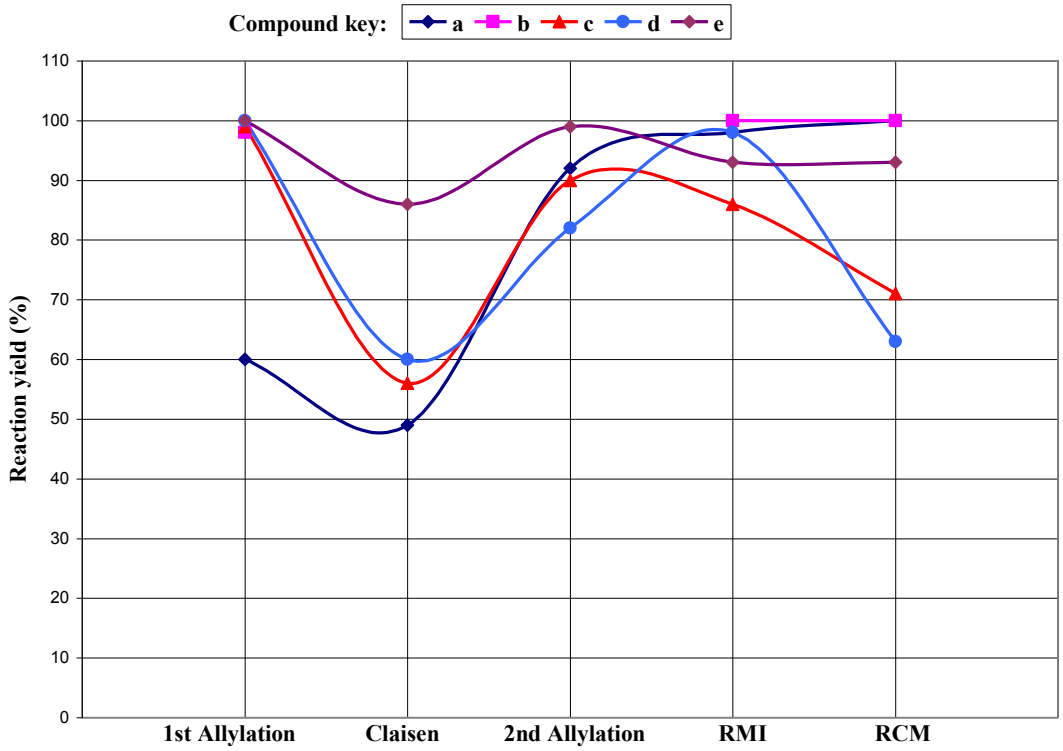

3.2 The Wits RMI-RCM approach to the 6-, 7- and 8-membered *O,N*- and *N,N*-benzo-fused heterocycles

The following section will introduce the synthetic methodology undertaken in the production of the 6-, 7- and 8-membered benzo-fused heterocyclic motif. It begins with the retro-synthetic analysis of the problem at hand and proceeds to the actual methodology implemented towards this aim. Each reaction step of the methodology is then discussed in detail with note taken of: the various yields of the compounds produced, notes of synthetic interest and a discussion of the evidence confirming the identity of the compounds from various spectroscopies.

3.2.1 Retro-synthetic analysis of 6-, 7- and 8-membered benzo-fused heterocycles

The retro-synthetic methodology of the Wits RMI-RCM approach to the 6-, 7- and 8-membered benzo-fused heterocycles is represented in **Scheme 40**. The required targets **A1-3** can be envisaged to form, through RCM, if un-saturated bonds are in the positions shown in synthons **B1-3.** To achieve synthon **B3**, it was envisaged that simple allylic attachments could be subjected to dual RMI. To achieve synthon **B2**, it was envisaged that one of the allylic substituents could be subjected to RMI. To achieve synthon **B1**, it was envisaged that a di-substituted benzene **C** would suffice, through dual allylation. With this strategy in mind, a standardized series of reactions – where the order of the allylation and deployment of the RMI catalyst were key to the methodology – was instituted to form the 6-, 7- and 8-membered benzo-fused heterocycles. Readily available 2-aminophenol **146** was used as starting material for the *O,N*-containing benzo-fused heterocycles (**Scheme 41**); and benzene-1,2-diamine **156** was used as starting material for the *N,N*-containing benzo-fused heterocycles (**Scheme 42**).

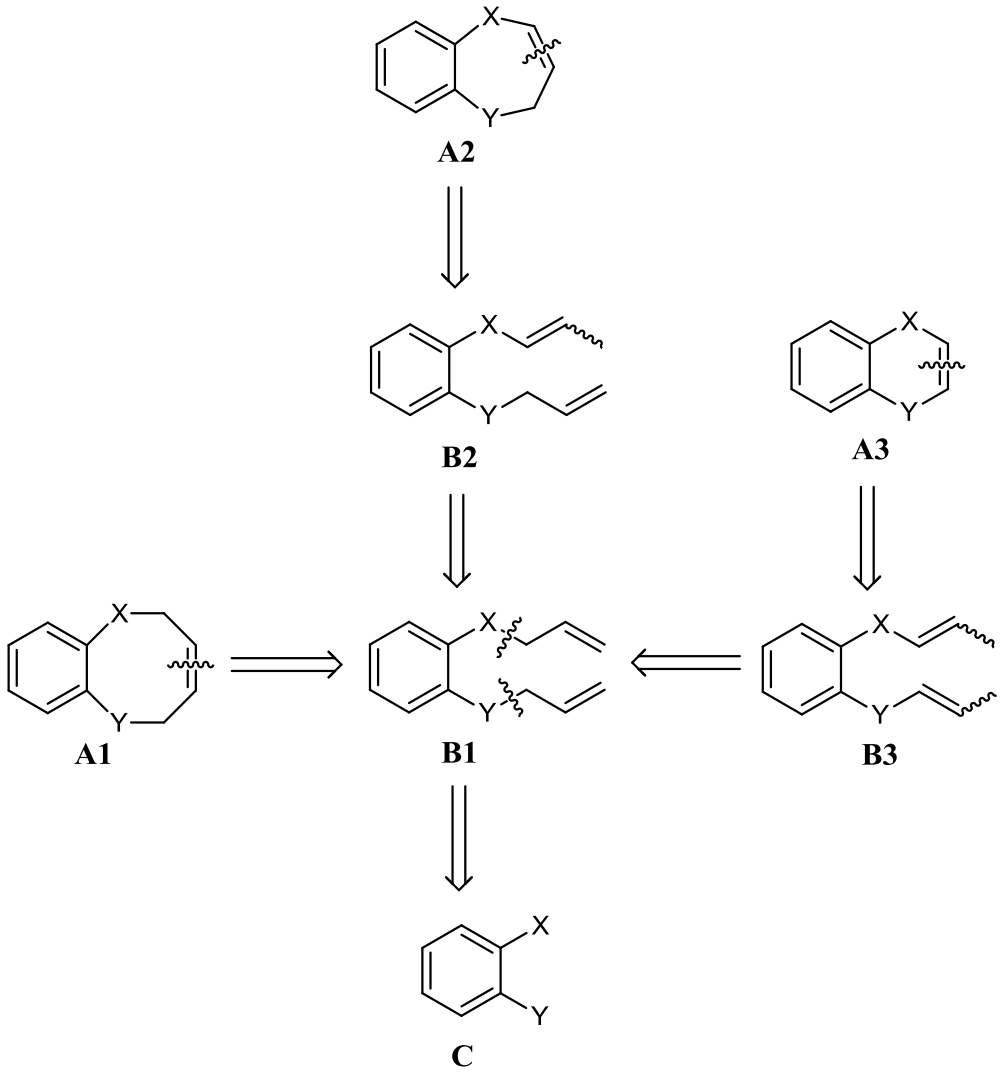

Scheme 40: The disconnection strategy adopted in the Wits RMI-RCM synthesis of the 6-, 7- and 8-membered benzo-fused heterocycles

3.2.2 General methodologies implemented towards the *O,N*- and *N,N*-benzo-fused heterocycles

The next section will give an overview of the synthetic methodology adopted towards the 6-, 7- and 8-membered benzo-fused heterocycles, synthesized in this project. The *O,N*-

benzo-fused heterocycles (**Scheme 41**) are discussed first, followed by the *N,N*-benzofused heterocycles (**Scheme 42**).

3.2.2.1 General methodology towards the *O,N*-benzo-fused heterocycles

2-Aminophenol **146** was subjected to a protection reaction, utilizing benzoyl chloride, to ensure that the amine group would only accept one allyl group in subsequent reaction steps. (**Scheme 41**.)

The next step was to ensure that only allylation at the OH group occurred on the protected product **147**. Potassium carbonate (a base with a suitably weak pK_a) was used to ensure that the protected NH group was not deprotonated. Allyl bromide, in one to one equivalence, was then used as allylation reagent to form the mono-allylated product **148**.

At this stage, the synthesis split into three main reaction paths.

First path:
The mono-allylated product **148** was re-allylated – this time using the stronger base: sodium hydride – followed by the addition of allyl bromide to form the di-allylated product **149**. The di-allylated product was subjected to RCM, using GII **6**, to afford the 8-membered ring product **150**.

Second path:
The di-allylated product **149** was subjected to RMI using catalyst **15**, to afford the di-isomerized product **151**. This in turn was then subjected to RCM, using GII **6**, to afford the 6-membered ring product **152**.

Third path:
The mono-allylated product **148** was subjected to RMI using catalyst **15**, to afford the mono-isomerized product **153**. It was then re-allylated using allyl bromide, with sodium hydride as base, to afford product **154**. This in turn was then subjected to RCM, using GII **6**, to afford the 7-membered ring product **155**.

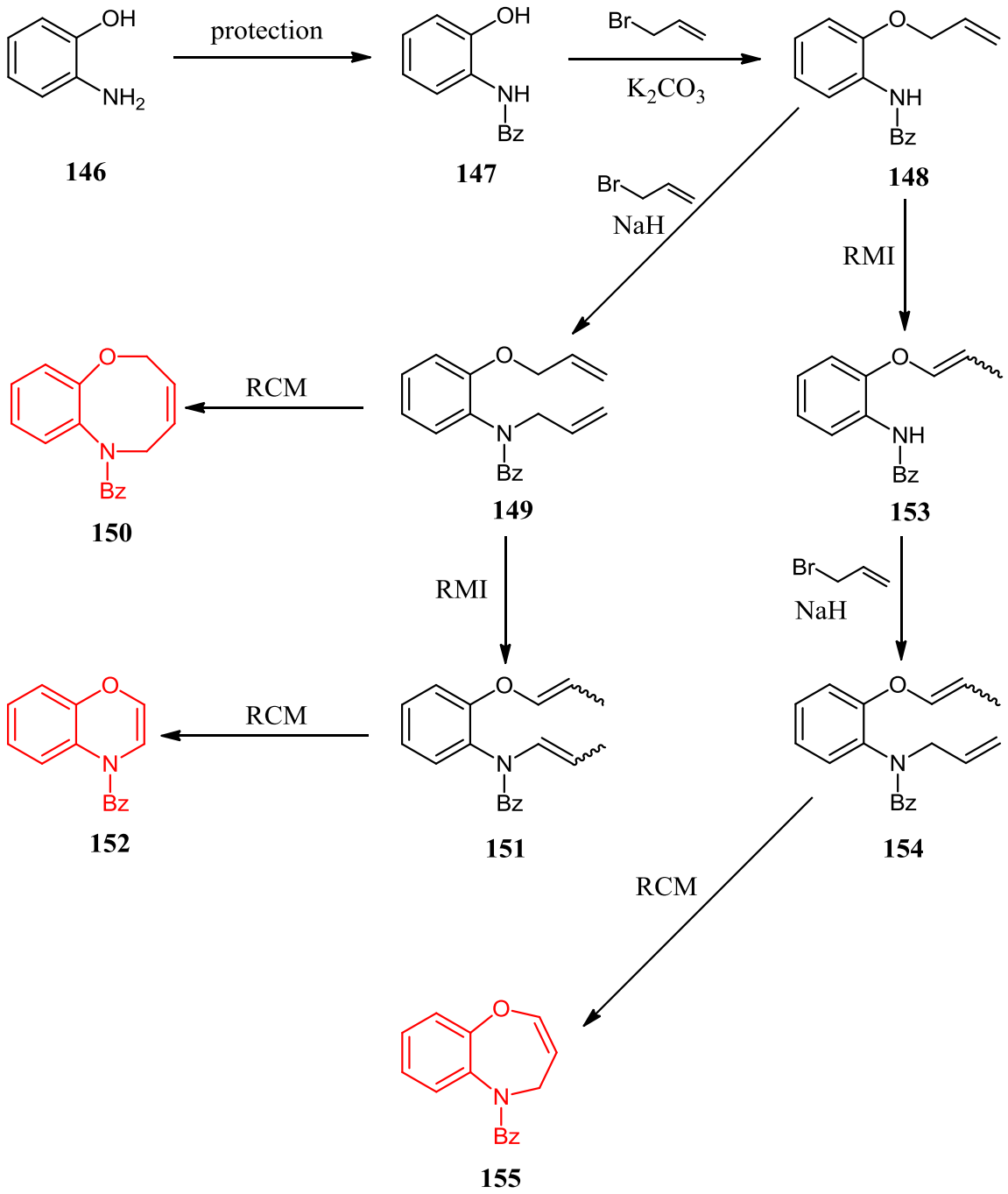

Scheme 41: The Wits RMI-RCM approach to 6-, 7- and 8-membered *O,N*-heterocycles

3.2.2.2 General methodology towards the *N,N*-benzo-fused heterocycles

Benzene-1,2-diamine **156** was subjected to a double protection step, utilizing acetic anhydride, to ensure that the amine groups would only accept one allyl group each, in subsequent reaction steps. (**Scheme 42**.) At this stage, the synthesis split into three main reaction paths.

First path:

To ensure that only one amine group on the protected precursor **157** was deprotonated, a very strict one to one molar ratio of sodium hydride (as base) was used. Allylation using allyl bromide – also in a strict one to one molar ratio – led to the formation of the mono-allylated product **158**. This product was then subjected to RMI using catalyst **15**, to afford the mono-isomerized product **163**. It was then re-allylated using allyl bromide, with sodium hydride as base, to afford product **164**. This in turn was then subjected to RCM, using GII **6**, to afford the 7-membered ring product **165**. (However, after several attempts using different solvents, catalyst loadings, and reactions times and temperatures, results pertaining to the formation of the 7-membered ring were inconclusive – whilst the parent ion was detected using HRMS; ^{1}H and ^{13}C NMR spectra were problematic.)

Second path:

The protected precursor **157** was di-allylated – again using sodium hydride as base, followed by the addition of allyl bromide (2 equivalents) to form the di-allylated product **159**. The di-allylated product was then subjected to RCM, using GII catalyst **6**, to afford the 8-membered ring product **160**.

Third path:

The di-allylated product **149** was then also submitted to RMI using catalyst **15**, to afford the di-isomerized product **161**. This in turn was then subjected to RCM, using GII **6**, in an attempt to afford the 6-membered ring product **162**. (However, after several attempts using different solvents, catalyst loadings, and reactions times and temperatures, formation of the 6-membered ring proved unsuccessful.)

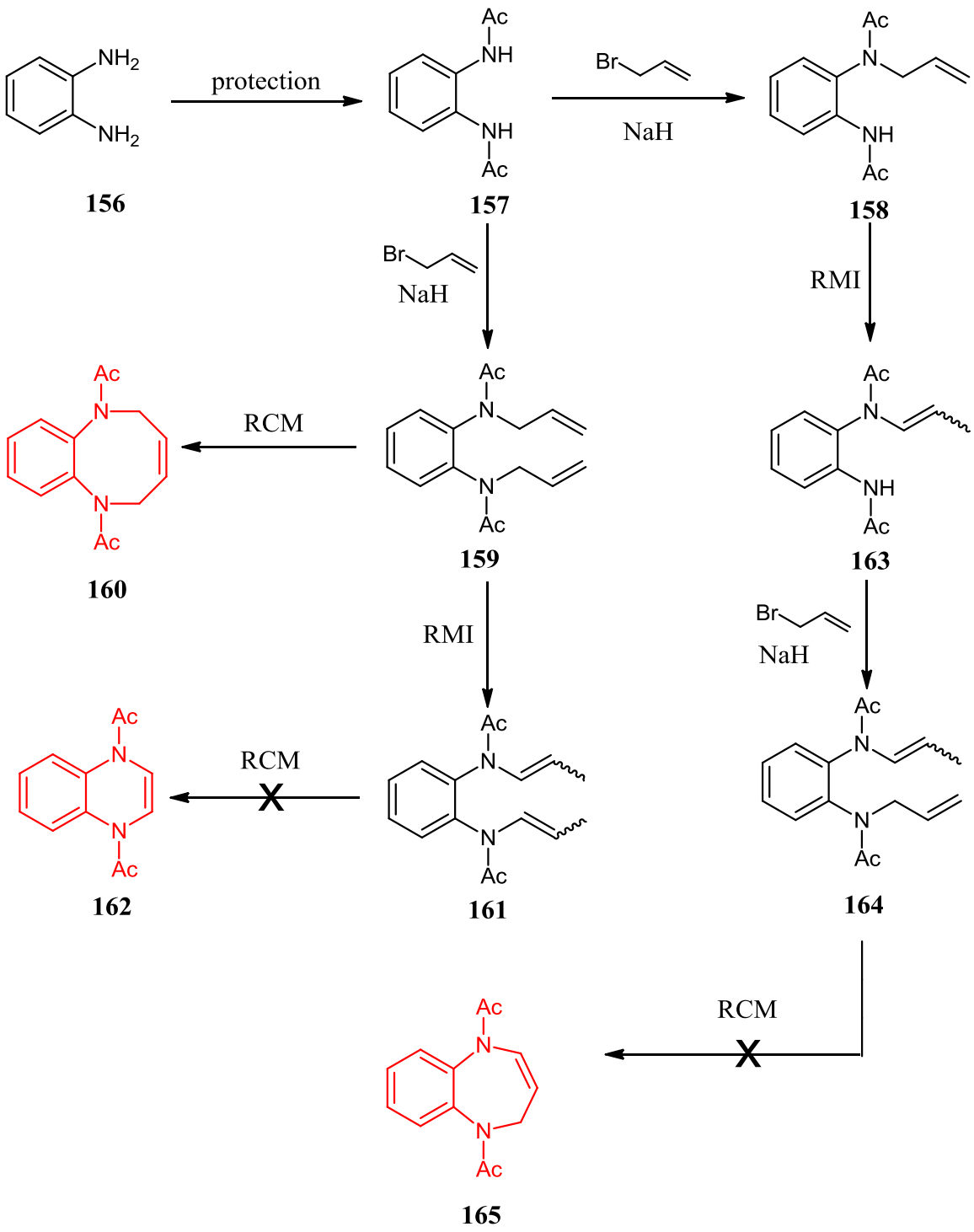

Scheme 42: The Wits RCM approach to 6-, 7- and 8-membered *N,N*-heterocycles

3.3 Results obtained for the individual reaction steps

Each of the individual reaction steps will now be discussed in some detail. Based on the *type* of reaction used, the *N,N*-benzo-fused heterocycles and the *O,N*-benzo-fused heterocycles will be discussed together. Characterization and discussion of the individual compounds will then follow.

3.3.1 Protection of the heterocyclic precursors

Commercially available 2-aminophenol **146** and benzene-1,2-diamine **156** were used as the precursors to the benzo-fused heterocyclic compounds. **156** did require purification prior to use. The purification method used involved refluxing **156** in minimal toluene, in the presence of activated charcoal, for 30 minutes. The charcoal was then removed *via* hot filtration. Upon cooling, pure **156** precipitated out of solution and was removed *via* filtration.

3.3.1.1 Protection of 2-aminophenol with benzoyl chloride

The protection method for 2-aminophenol (**Scheme 42**) involved dissolving precursor **146** in dry dichloromethane, after which the temperature of the reaction mixture was lowered to 0 °C in an ice bath. Pyridine (1 equivalent) was then added, followed by the addition of benzoyl chloride (1 equivalent). The choice of pyridine as base was important, because it was crucial not to deprotonate the hydroxyl group as this would have prevented allylation at a later stage; and pyridine mopped up the hydrogen chloride produced during the reaction. The reaction mixture was stirred under nitrogen at room temperature for 24 hours. It was then quenched with enough saturated solution of sodium hydrogen carbonate to bring the pH to 7. The organic fraction was then dried (using anhydrous magnesium sulphate) and the solvent then removed under reduced pressure. On purification (silica gel column chromatography) the identity of the protected product **147** (100 % yield) was confirmed using ^{1}H NMR spectroscopy (showing additional

signals from new arene ring) and ^{13}C NMR spectroscopy (showing the presence of the carboxyl group).

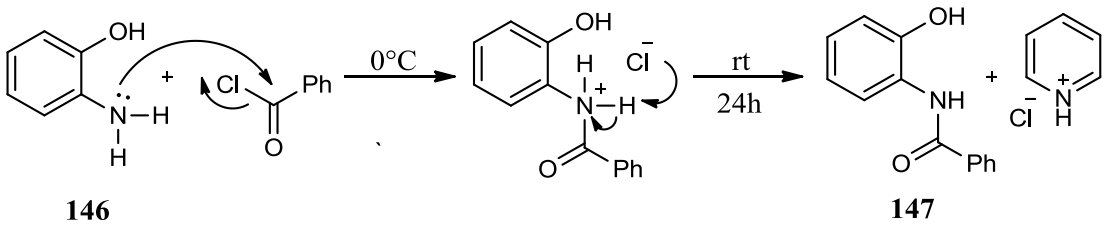

Scheme 42: Protection of 2-aminophenol

3.3.1.2 Protection of benzene-1,2-diamine with acetic anhydride

The protection method for benzene-1,2-diamine (**Scheme 43**) involved dissolving **156** in excess (10 equivalents) of pyridine (used as both base and solvent). The temperature of the mixture was lowered to 0 °C (in an ice bath) followed by the dropwise addition of acetic anhydride (3 equivalents). The reaction mixture was stirred under nitrogen at room temperature for 24 hours. It was then quenched with enough saturated solution of sodium hydrogen carbonate to bring the pH to 7. The organic fraction was dried (using anhydrous magnesium sulphate) and the solvent removed under reduced pressure. On purification (silica gel column chromatography) the identity of the protected product **157** (93 % yield) was confirmed using ^{1}H NMR spectroscopy which showed the presence of the methyl groups.

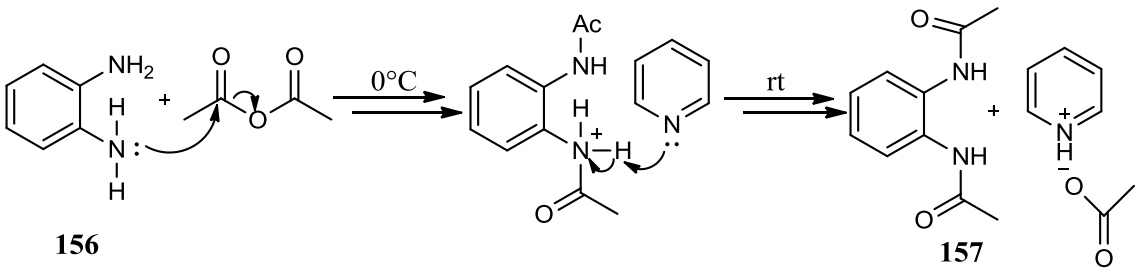

Scheme 43: Protection of Benzene-1.2-diamine

3.3.2 Sequential and dual allylation protocols

The varying pKa values of the functional groups on the protected 2-aminophenol **147**, allowed mono-allylation to be strictly controlled. This was done by varying the type of base used. To deprotonate the phenol group; potassium carbonate (2 equivalents) was used. To deprotonate the protected amine group; sodium hydride (1.2 equivalents) was used. In the protected benezene-1,2-diamine **157**, the precise one to one stochiometric addition of the allyl bromide and sodium hydride was responsible for mono-allylation control; by de-protecting only one of the amine groups on the molecule. For dual allylation the same principles were used, with the hetero-atom on the substrate determining the type of base to be used. The general allylation-reaction mechanistic proposal is outlined in **Scheme 43**, showing a representative synthon undergoing allylation using the two different bases.

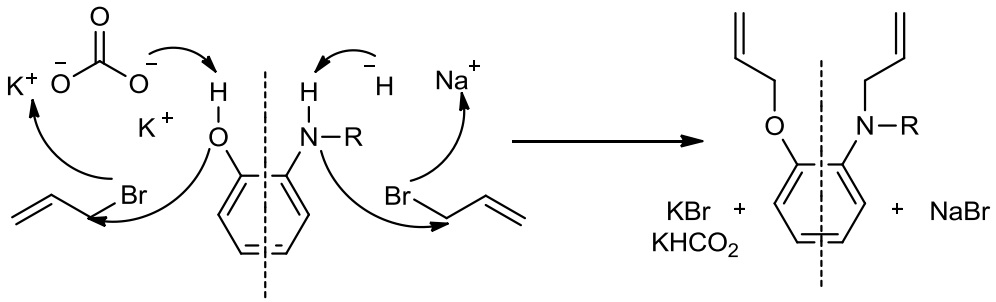

Scheme 43: General allylation protocol

Acetone was the solvent of choice for these reactions, due to its ease of preparation (as it only needed to be distilled prior to use). However, it is known that sodium hydride is sufficiently powerful to deprotonate acetone and thus dimethylformamide (DMF) is recommended as solvent whenever sodium hydride was required.[101] However, it was subsequently found that if strict kinetic control conditions (-14 °C, dropwise reactant addition) were employed, the greater reactivity of the substrates towards sodium hydride, would prevent it from reacting with acetone. Thus acetone was eventually used for all reactions requiring sodium hydride, as long the kinetic reaction conditions were upheld.

The mono-allylated product's (**148** and **158)** and the di-allylated product's (**149** and **159**) spectrographic data (**Table 13**) is presented first, as the NMR signals from these compounds were crucial in assigning the correct signals to the mono-allylated mono-isomerized products **154** and **164** (**Table 15**). This was because the latter compounds existed in two *E,Z*-isomeric forms and as a result, many of their ^{1}H and ^{13}C NMR signals overlapped.

3.3.2.1 Mono- and di-allylations performed on the precursors

Listed below are all the allylation reactions on the precursors, compounds **147** and **157**. The products thus obtained include: the mono-allylated compounds **148** and **158** and the di-allylated compounds **149** and **159**. These products, as well as their precursors are shown in **Scheme 45.** All allylation reactions were left to reflux under a nitrogen atmosphere overnight (~18 hours).

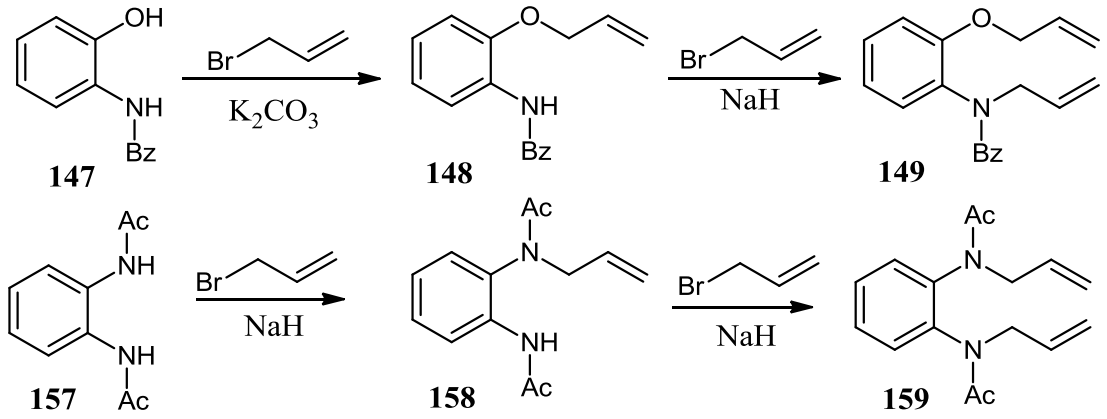

Scheme 45: Allylation reactions performed on precursors

The reaction conditions related to these compounds are listed in **Table 11**. These include: the precursor used; the base used; the stochiometric ratios of the base and allyl bromide to the precursor; the solvent used; the reaction temperature and product yield. With regards to the reaction temperature: if two values are given in the table, it means that the reaction began at the first temperature and was allowed to warm to the second

temperature. This was the case where kinetic conditions were used or where the high reactivity of NaH needed to be curtailed.

Table 11: Yield and reaction conditions employed in the allylation reactions

Pre-cursor	Base used	Stochiometric Ratio		Solvent used	Reaction temp. (°C)	Yield (%)	Product
		Base	Allyl Br				
147	K_2CO_3	2	1.2	acetone	60	80	**148**
148	NaH	1.2	2	DMF	0 to 25	90	**149**
157	NaH	1	1	DMF	0 to 25	94	**158**
157	NaH	1	1	acetone	-14 to 25	95	**158**
157	NaH	2	2.2	acetone	-14 to 25	93	**159**

As can be seen from **Table 11**, all the reactions enjoyed a high yield. The lowest yield found was for compound **148** (80 %). This was most likely due to the incomplete deprotonation of the phenol group on the precursor. Compound **158** was subjected to two synthetic procedures. The first method used DMF as solvent, the second acetone as solvent with full kinetic conditions. Both reactions had almost identical yields (94 %), indicating that NaH can indeed be used with acetone as so long as sufficient care is taken.

3.3.2.1.1 Characterization of the preceding allylation products

The following section will describe the spectrographic data used to confirm reaction outcome, with regards to the allylation reactions performed on the precursors. The characterization of these compounds involved the use of HRMS (**Table 12**); and ^{1}H NMR (**Table 13**) and ^{13}C NMR spectroscopy.

Table 12: HRMS data used to characterize the mono- and di-allylated products

Compound	HRMS (e/z)	
	Expected	Found
148	253.1103	253.1121
149	293.1416	293.1424
158	232.1211	232.1211
159	272.1525	272.1526

As can be seen from **Table 12**, all masses found were as expected.

Table 13: NMR data used to characterize the mono- and di-allylated products' allylic signals

Compound	^{1}H NMR			
	Identity	Shift (ppm)	Multipl.	Integration
148	***H*$_2$**C=	5.33 ; 5.43	dd ; dd	1 ; 1
	=C***H***–	6.08	tdd	1
	–C***H*$_2$**–O	4.64	dt	2
149	***H*$_2$**C=	5.26 ; 5.36	dd ; dd	1 ; 1
	=C***H***–	5.78 – 6.14	m	1
	–C***H*$_2$**–O	4.44 ; 4.64	dd ; dd	1 ; 1
	***H*$_2$**C=	5.08 ; 5.13	dd ; dd	1 ; 1
	=C***H***–	5.78 – 6.14	m	1
	–C***H*$_2$**–N	4.26	dd	2
158	***H*$_2$**C=	5.09 ; 5.15	d ; d	1 ; 1
	=C***H***–	5.90	ddd	1
	–C***H*$_2$**–N	3.93 ; 4.50	dd ; dd	1 ; 1
159	***H*$_2$**C=	5.01 ; 5.10	d ; d	2 ; 2
	=C***H***–	5.75 – 5.91	m	2
	–C***H*$_2$**–N	3.49 ; 4.90	dd ; dd	2 ; 2

As can be seen from **Table 13**, signals for the *O*-allyl substituent on the *O,N*-mono-allylated compound **148**, correspond with the equivalent signals in the di-allylated compound **149**. The same applies to the *N,N*-compounds **158** and **159**. (Keep in mind, of course, that the signals of the symmetrical molecule **159** need to have their integration values doubled.)

3.3.2.2 Allylation reactions performed on the 'isomerized' precursors

Listed below are all the allylation reactions on the 'isomerized' precursors, compounds **153** and **163**. The products thus obtained include: compounds **154** and **164.** (**Scheme 46**.) All allylation reactions were left to reflux under a nitrogen atmosphere overnight (~18 hours).

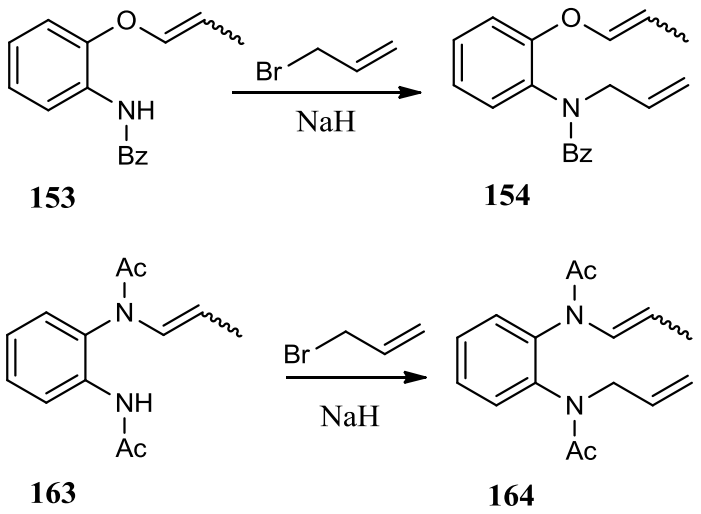

Scheme 46: Allylations performed on the 'isomerized' precursors

The reaction conditions related to these compounds are listed in **Table 14**. (With the same reaction details used in **Table 11**.)

Table 14: Yield and reaction conditions employed in the allylation reactions

Pre-cursor	Base used	Stochiometric Ratio		Solvent used	Reaction temp. (°C)	Yield (%)	Product
		Base	Allyl Br				
153	NaH	1.2	2	DMF	0 to 25	95	**154**
163	NaH	1.2	2.4	acetone	-14 to 25	99	**164**

As can be seen from **Table 14**, all the reactions enjoyed a high yield. Again, the first reaction used DMF as solvent; the second acetone as solvent with full kinetic conditions.

3.3.2.2.1 Characterization of the preceding allylation products

The following section will describe the spectrographic data used to confirm reaction outcome, with regards to the allylation reactions performed on the 'isomerized' precursors. The characterization of these compounds involved the use of HRMS (**Table 15**); and ^{1}H NMR (**Table 16**) and ^{13}C NMR spectroscopy.

Table 15: HRMS data used to characterize 'isomerized' allylated products

Compound	HRMS (e/z)	
	Expected	Found
154	293.1416	293.1424
164	272.1525	272.1529

The HRMS value for **154** is expected to be the same as that of **149**; and the value of **164** is expected to be the same as that of **159**. (See **Table 12**.) It should be noted, however, that the HRMS fragmentation patterns for these molecules were different. (See experimental.)

Table 16: NMR data used to characterize the 'isomerized' allylated products' allylic signals

Compound	^{1}H NMR			
	Identity	**Shift (ppm)**	**Multipl.**	**Integration**
154	***H*$_3$C–**	1.69	dd	3
	–C*H*=	4.84 – 4.94	m	1
	=C*H*–O	5.86 – 6.12	m	1
	***H*$_2$C=**	5.13	dd	2
	=C*H*–	5.86 – 6.12	m	1
	–C*H*$_2$–N	4.37 ; 4.58	dd ; dd	1 ; 1
164	***H*$_3$C–**	1.64	dd	3
	–C*H*=	4.80	dq	1
	=C*H*–N	7.07 – 7.34	m	1
	***H*$_2$C=**	4.93 – 5.29	m	2
	=C*H*–	5.75 – 5.91	m	1
	–C*H*$_2$–N	3.34 – 3.75 4.33 – 4.69	m m	1 1

As can be seen from **Table 16**, the signal shift ranges for the *N*-allylic group of compound **154** corresponds to the *N*-allylic group signal shift ranges of compound **149** (shown in **Table 13**); and the signal shift ranges for the *N*-allylic group of compound **164** corresponds to the *N*-allylic group signal shift ranges of compounds **158** and **159** (shown in **Table 13**).

Furthermore, the signal shift ranges for the isomerized substituent in compound **154** corresponds to the signals shift ranges of its mono-allylated precursor **153**; and the signal shift ranges for the isomerized substituent in compound **164** corresponds to the signals shift ranges of its mono-allylated precursor **163**. The signals assignments for these compounds (**153** and **163**) are shown in **Table 14** in the previous section.

3.3.3 Isomerization (RMI) protocol

The procedure adopted in the RMI reactions on the mono-allylated precursor **158** and di-allylated precursors **149** and **159** proceeded as follows:
The precursors were placed in a round-bottom flask and dissolved in minimal distilled toluene (~ 2 mL). The reaction solution was then degassed under reduced pressure and the vessel and then re-gassed with argon. In each case 5 mole % Ru isomerization catalyst **15** was then added and the vessel was again degassed and then re-gassed with argon. All reaction mixtures were then heated to 65 °C and allowed to reflux under an argon atmosphere for 12 to 14 hours.

In an attempt to demonstrate the utility of the microwave methodology, towards accelerating the isomerization reaction – precursor **148** was placed in a microwave reaction tube and dissolved in minimal (~1 mL) distilled degassed toluene, which was then sealed. 5 Mole % Ru isomerization catalyst **15** was then quickly added to the vessel, followed by irradiation under microwave conditions (power: 150W with cooling, ramp time: 2 °C per min, maximum pressure: 100 psi) in a pressure tube. Under these conditions the isomerization reaction proceeded to completion in just 10 minutes, when an optimised temperature of 90 °C was used.

Catalyst removal was effected by filtering the reaction solutions through a compacted celite plug; after which the solvent was removed under vacuum and the products purified using silica gel column chromatography. Catalyst removal in the di-nitrogen compounds **158** and **159** did, however, prove difficult. These compounds had a very low retention factor in most solvent systems. The most effective removal strategy appeared to be dissolving the crude product in a 2 to 5 % ethyl acetate/hexane mixture and slowly filtering it through a compacted celite plug, up to 4 times, followed by flash silica gel column chromatography using a 100% ethyl acetate.

The following isomerized products (**Figure 26**) were thus obtained:

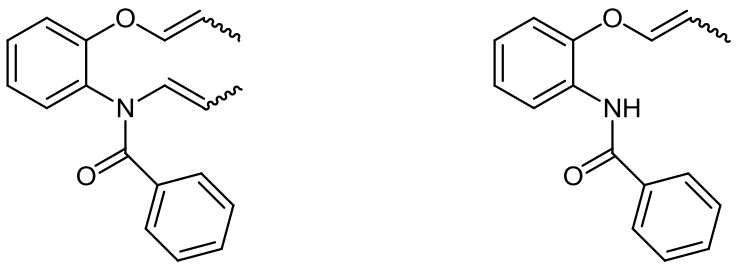

151

153

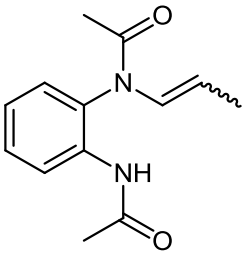

163

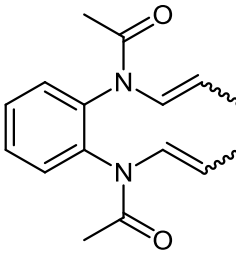

161

Figure 26: Isomerization products

3.3.3.1 Yield and characterization data regarding the RMI procedures

The isomerized compounds were characterized using HRMS and $^{1}H/^{13}C$ NMR spectroscopy. As their molecular weights (acquired through HRMS) were expected to be the same as their non-isomerized counterparts, this data alone was not considered conclusive evidence that isomerization had indeed occurred. The masses of the parent ions acquired were, however, as expected. The HRMS data, as well as the yields for these compounds are given in **Table 17**. It should be noted, however, that the HRMS fragmentation pattern data for the isomerized compounds did differ from their non-isomerized counterparts.

Table 17: Yield and HRMS fragmentation data for the isomerized compounds

Compound	Yield (%)	HRMS (e/z)	
		Expected	Found
151	98	293.1416	293.1416
153	92	253.1103	253.1091
161	93	272.1524	272.1519
163	96	232.1212	232.1214

More important in the characterization of these compounds was the ^{1}H NMR spectroscopy data. **Table 18** presents the methyl signals of the isomerized allylic substituents obtained for these compounds. The existence of one methyl-group signal (for compounds **153** and **163**) in the appropriate region; and two methyl-group signals (for compounds **151** and **162**) in the appropriate region was considered a definitive sign that isomerization had indeed taken place. All other expected signals in both the ^{1}H NMR and ^{13}C NMR spectra were found. It was possible – based on ^{1}H and ^{13}C NMR spectroscopy signal integration ratios – to determine the isomeric *E/Z*-ratios of the compounds produced.

Table 18: Characteristic methyl group signals and isomeric ratio of the isomerized compounds

Compound	^{1}H NMR				
	Identity	Shift (ppm)	Multipl.	Integration	Ratio (*E/Z*)
153	O-~-CH_3	1.68 ; 1.75	dd ; dd	3	1 : 2
151	O-~-CH_3	1.66 ; 1.61	dd ; m	3	1 : 2
	N-~-CH_3	1.66	dd	3	
163	N-~-CH_3	1.64	dd	3	-
161	N-~-CH_3	1.61	br dd	6	~1 : ~1 : ~1

As with the other isomerization reactions in this project, these isomerization reactions proceeded efficiently and with high yield. The mono-isomerized compound **153** occurred as both *E* and *Z* isomers, whereas compound **163** occurred as only one isomer. The di-isomerized *O,N*-compound **151** occurred as two isomers – the signals for which overlapped.

The di-isomerized *N,N*-compound **161** occurred as three isomers: *EE*, *EZ* and *ZZ*. This made the interpretation of its ^{1}H NMR spectrum extremely complex. Therefore all signals are given as multiplets, with compound **163** being used to assign the shift regions correctly. The ^{1}H NMR signals for compounds **163** and **161** are thus given in some detail in **Table 19**. The assignment of the correct identities of compound **161** were also confirmed *via* a ^{13}C-^{1}H correlated spectrum, which is included in Appendix B.

Table 19: Mono-isomerized **163** and di-isomerized **161** ^{1}H NMR signals, showing their congruence

Assignment	Shift (ppm)	
	163	**161**
NCHCH-C***H*₃**	1.64	1.54 – 1.65
C-(=O)-C***H*₃**	1.82	1.74 – 1.88
C-(=O)-C***H*₃**	2.18	2.12 – 2.25
NCH=C***H***-CH_3	4.40 – 4.58	4.39 – 4.93
N-C***H***=$CHCH_3$	7.11	7.02 – 7.29
ArC***H***'s	7.21	7.31 – 7.60
ArC***H***'s	7.38 – 7.52	

From **Table 19** it can be seen that the regions in the complex ^{1}H NMR spectrum of compound **161**, match up with the known regions in the much simpler spectrum of compound **163**, thereby confirming that the correct shift assignment have been made.

3.3.4 RCM protocol

The procedure adopted in the RCM reactions on the *O,N*-precursors **149**, **151** and **154**; and the *N,N*-precursors **159** and **161** was as follows: The precursors were placed in a round bottom flask and dissolved in minimal distilled toluene (~ 5 mL). The reaction solution was then degassed under reduced pressure and the vessel and then re-gassed with argon. The GII RCM catalyst **6** was then added to the vessel, which was again degassed and then re-gassed with argon. All reaction mixtures were then heated to between 80 and 90 °C and allowed to reflux under an argon atmosphere for 8 to 18 hours – with reaction progress checked *via* TLC every 4 hours. All reactions proceeded to completion, except for compound **161** (which failed to ring close, despite several attempts at various catalyst loadings, temperatures and reaction times) and compound **164**, which resulted in only trace amounts of the expected product **165.**

The microwave methodology was again investigated towards accelerating the RCM reaction, using precursors **161** and **164**. Each precursor was placed in a microwave reaction tube and dissolved in minimal (~1 mL) distilled degassed toluene, which was then kept sealed. 5 Mole % RCM catalyst **6** was then added to the vessel, followed by irradiation under microwave conditions (power: 150W with cooling, ramp time: 2 °C per min, maximum pressure: 100 psi) in a pressure tube. Under these conditions the RCM reaction for **164** appeared to proceed to completion in just 20 minutes, when an optimised temperature of 90 °C was used. Compound **161**, however, failed to ring-close.

Catalyst removal was effected by filtering the reaction solution through a compacted celite plug. After which the solvent was removed under vacuum and the products purified using silica gel column chromatography.

The relevant precursors and their **RCM** products and their precursors are shown in **Scheme 47**:

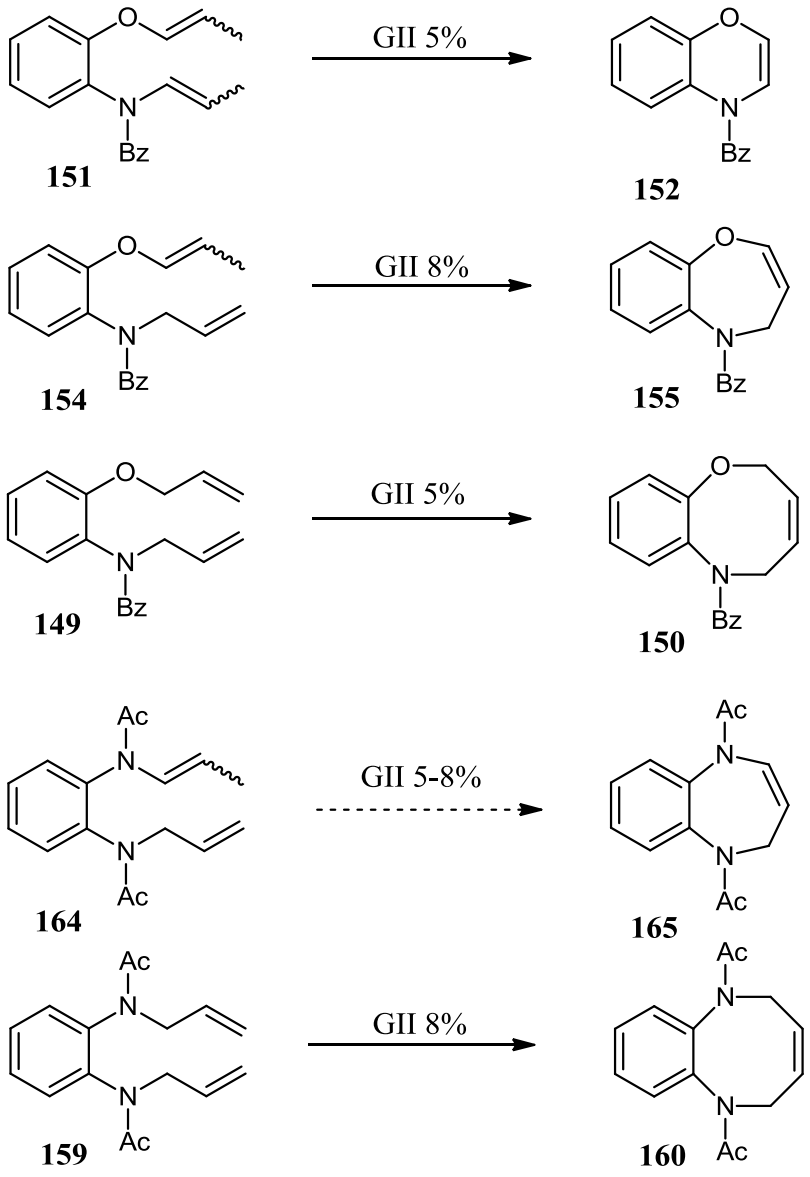

Scheme 47: RCM products obtained

3.3.4.1 Yield and characterization data regarding the successful RCM products

The yields, optimized reaction conditions and HRMS data for the successful RCM reactions are shown in **Table 20**. All the expected HRMS masses for these compounds were found.

Table 20: Yield, HRMS, optimized reaction times and temperature for the RCM products

Com-pound	% GII loading	Time (hr)	Temp. (°C)	Yield (%)	HRMS (e/z)	
					Expected	Found
152	8	8	90	96	237.0790	237.0789
155	5	8	80	100	251.0946	251.0946
150	5	18	90	88	265.1103	265.1118
160	8	18	90	90	244.1212	244.1212
165	5	20 min *	90	trace**	230.1055	230.1056
165	8	18	90	trace**		

* = microwave reaction time

** = largest product not the required 7-membered benzo-fused ring

Regarding the data for compound **165** – when the reaction was performed under conventional heating conditions, the parent ion for the expected product **165** was not obtained and the ^{1}H and ^{13}C NMR spectra showed that significant amounts of starting material **164** were still present, and the product obtained was clearly a decomposition product. When the reaction was performed under microwave conditions, the expected parent ion of **165** *was* detected, but the primary product could not be conclusively identified using ^{1}H and ^{13}C NMR. (Spectra shown in Appendix A).

Table 21 shows selected ^{1}H NMR spectroscopic data used to conclusively identify the *O,N*-ring-closed products **152**, **155** and **150**. Only the hydrogen signals from the bridge carbons along the ring are presented. All other signals are, nonetheless, accounted for.

(See Experimental Section.) ^{13}C NMR spectra also showed that all products contained the relevant number of signals in the required shift ranges.

Table 21: NMR data used to characterize the *O,N*-RCM Products

Compound	^{1}H NMR				
	Identity	**Shift (ppm)**	**Multipl.**	**Integration**	**Coupling (Hz)**
152	–O–C***H***=	6.05	d	1	4.5
	=C***H***–N–	6.27	br d	1	2.5
155	–O–C***H***=	6.51 – 6.58	m	1	-
	–CH=C***H***–	4.94	d	1	3.1
	–C***H*$_2$**–N–	3.37 ; 5.36	br s ; br s	2	-
150	–O–C***H*$_2$**–	3.95 – 5.48*	m	2	-
	O–CH$_2$–C***H***=	5.80	dt	1	10.4 and 8.3
	=C***H***–CH$_2$–N	5.95	dt	1	10.4 and 4.0
	–C***H*$_2$**–N–	3.95 – 5.48*	m	2	-

* = overlapping signals

Where coupling values could be obtained in compound **152**, the apparent difference in the values obtained for the saturated carbons in the heterocyclic ring (which should be the same) is most likely due to the close proximity of the highly electronegative nitrogen atom's lone-pair interacting with the hydrogen on the carbon adjacent to the nitrogen, which led to significant broadening of the signal. The value given for this hydrogen is thus only approximate. A similar effect is also noted in compound **150**, where significant ring movement is expected, and the second coupling constant is around half the value of its counterpart.

Table 22 shows selected ^{1}H NMR spectroscopic data used to conclusively identify the *N,N*-ring-closed product **160**. Only the hydrogen signals from the bridge carbons along the 6-membered ring are presented. All other signals are, nonetheless, accounted for. (See Experimental Section.) ^{13}C NMR spectra also showed that the product contained the relevant number of signals in the required shift ranges.

Table 22: NMR data used to characterize the *N,N*-RCM Product

Compound	^{1}H NMR				
	Identity	**Shift (ppm)**	**Multipl.**	**Integration**	**Coupling (Hz)**
160	–N–C***H*$_2$**–	3.47–5.19	m	4	-
	–CH$_2$–C***H*=**	5.82–6.11	m	2	-

It was very difficult to purify compound **160** completely, as its high polarity and apparent tendency to adhere to silica required the use of a highly polar solvent system. The use of pure ethyl acetate was found to be the most effective eluent which gave a retention factor of 0.28 to the compound in the column. The catalyst was less polar than **160** and was substantially removed *via* gradient elution utilizing a 10% ethyl acetate/hexane mixture, which left the compound unmoved on the column. Re-crystallization was attempted, as a means of purification, but was unsuccessful.

3.3.4.2 Data regarding the unsuccessful RCM products

Despite several efforts, compound **161** failed to ring-close. All the reaction conditions employed towards the attempted ring closure of compound **161** are presented in **Table 23.** The failure of di-nitrogen containing compounds, of this type, to ring-close is not, however, unprecedented and will be discussed in some detail in **Chapter 4**.

Table 23: Reaction conditions employed towards the attempted RCM of **161**

% GII loading	Heating method	Time	Temp. (°C)
5	C	8 hr	90
5	M	40 min	90
8	C	12 hr	80

8	M	50 min	90
12	C	24 hr	95

Most disappointing, were the results regarding the attempted synthesis of compound **165**. As stated earlier, HRMS did find the expected parent-ion and the subsequent mass fragmentation pattern was obtained, but this product most likely formed only in trace amounts. Subsequent ^{1}H and ^{13}C NMR analysis indicated that the major products isolated were not the expected 7-membered benzo-fused ring, but most likely resulted from single or dual de-allylation of the precursor. This result will be discussed in detail in **Chapter 4**.

3.4 Conclusion regarding the *O,N*- and *N,N*-benzofused heterocycles

The yields of all the individual reaction steps leading up the final RCM step of the methodology were very high, and proceeded without much difficulty. These yields were all in the region of 90–100%. Where ring-closure could be affected, the yields were similarly high in the region of 88–100%. There did not appear to be any correlation between the size and the ring produced and the yield obtained.

Numerous attempts at RCM to form the 6-membered di-nitrogen product **162**, all met with failure. Previous attempts in these laboratories in similar di-nitrogen compounds, albeit with different protecting groups, have also met with failure.[59] The attempted synthesis of the 7-membered di-nitrogen product **165** was met with some success, but overall it cannot be conclusively stated that the methodology was successful.

CHAPTER FOUR

4.1 Conclusions and future work regarding the benzofurans

The most successful part of this project involved the formation of the benzofurans, utilizing the Wits RMI-RCM methodology – a simple, versatile method for the synthesis of substituted benzofurans involving the novel use of RMI on *C*- and *O*-allyl functional groups, followed by RCM. A large range of arene-ring substituents has been demonstrated to be tolerated by the methodology.

The Wits RMI-RCM methodology proved to be most efficient for compounds containing electron rich substituents on the arene ring, such as **145a** (dimethoxy) and **145b** (bromo), as well as the naphtho-compound **145e.** While the yields were lower, bulky groups *para* or *ortho* to the phenol group, such as **145c** (tert-butyl) and **145d** (benzo) did not prevent RCM from occurring. The high level of tolerance to all these arene substituents, in terms of both their identity and position is useful, as they may be converted to other functional groups as part of a later complete synthesis, requiring the attachment of a benzofuran motif.

The Claisen reactions performed in this project showed the lowest yields overall, with the di-allylated 4-bromophenol **143b** showing extensive decomposition during the reaction. There is thus scope left to optimise this reaction, with the hope of finding an ideal reaction time and temperature, to increase the overall efficiency of the methodology.

The most efficient part of the methodology involved RMI, with the Ru-catalyst **15** proving itself to be most versatile (being reacted both with and without solvent) and with a seemingly universal tolerance to its substrate.

The utilization of microwave radiation, not only as a method of affecting the Claisen rearrangement, but also for RMI and RCM reactions, has shown to improve the efficiency of the methodology in terms of both time and energy.

4.2 Conclusions and future work regarding the *O,N*-benzo-fused heterocycles

The deployment of RMI to mono- and di-allylated *O,N*-precursors, was successful. The methodology showed high tolerance to both the *N*- and *O*-allyl functional groups, with very high yields obtained. The RCM reactions occurred readily and with high yield on both the *O,N*-di-allylated; *O,N*-di-isomerised; and *O*-mono-allylated-isomerized and *N*-allylated functionalities – leading to the formation of the required 8-, 6- and 7-membered ring-closed products.

The reaction most notable is the formation of the 6-membered ring product **152**, in which the precursor **151** had an allylic amine group (shown in red) but nonetheless underwent RCM with a high yield. (**Scheme 48.**) This is of interest, as the *N,N*-precursors **161** and **164** with this same allylic amine configuration did not undergo ring-closure, but instead underwent allylic cleavage, followed by possible secondary metathesis reactions.

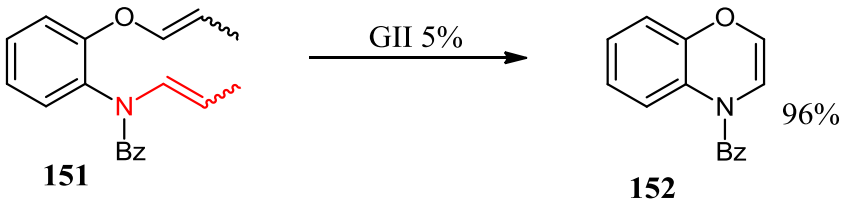

151 **152**

Scheme 48: Formation of the 6-membered *O,N*-product

Future work regarding the formation of 6-, 7 and 8-membered benzo-fused heterocycles may include the use of *O,N*-precursors with a wide variety of substituents on the arene-ring, to determine if the Wits RMI-RCM methodology is still applicable to such systems.

This is of interest because such systems would allow for the formation of more complicated motifs, with such functionalities acting as useful attachment points of the heterocyclic motif to other molecules, or they may be converted to other functional groups as part of a later complete synthesis, potentially towards medicinally useful molecules such as those discussed in **Chapter 2**.

4.3 Conclusions and future work regarding the *N,N*-benzo-fused heterocycles

The Wits RMI-RCM methodology met with failure, with regards to the formation of 6- and 7-membered di-nitrogen benzo-fused heterocycles, but was successful in the formation of the 8-membered di-nitrogen heterocycle. One possible explanation for this failure involves the allylic amine system (shown in red in **Scheme 49**). The presence of two of these systems in similar molecules (but with different protecting groups) has resulted in other failures to ring close.[59]

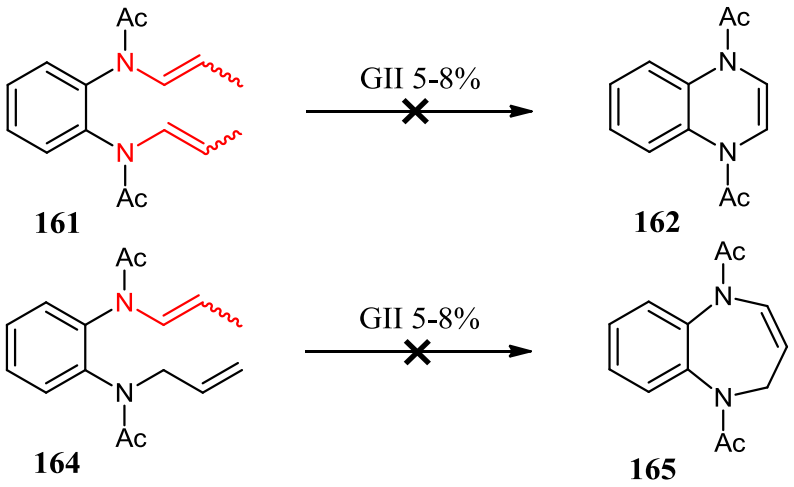

Scheme 49: Non-formation of the 6- and 7-membered *N,N*-products

As mentioned in the previous section, however, this system is present in the *O,N*-precursor **151**, but did not affect the reaction outcome. This result, and the presence of trace amounts of the 7-membered product **165**, but none of the 6-membered product **162**,

may indicate that the GII catalyst **6** is tolerant to only one such system in a molecule. It also leaves open the possibility that the formation of the 7-membered product is indeed possible, with further study involving catalyst loading, reaction time, reaction temperature, and solvent system needed. The ^{1}H and ^{13}C NMR spectra obtained for the expected **165**, formed using the microwave reaction methodology but not the conventional heating methodology, reiterates the possibility that reaction conditions affect outcome. Several papers[102-105] have discussed the Ru-initiated de-allylation of such allylic amine systems, and the tolerance of certain substrates (such as **151**) to this phenomenon and not others (such as **161** and **164**) warrants further investigation.

Finally, a steric argument for the failure of these precursors to ring-close may be proposed, in that the positions of the allylic and isomerized-allylic substituents on the precursor are beyond the bite-angle of the catalyst. A method of investigating this would involve a molecular modeling study. In such a study, a crystal structure of the relevant precursor is obtained and submitted to a force field methodology (e.g. MM+). The following steps for such a methodology are envisaged (**Chart 1**):

Step 1: The Single-point energy optimized model of the molecule, has its isomerized-allylic substituent's atoms restrained by an external torsional force. (A common procedure in the HyperChem software suite.)

Step 2: The molecule is then submitted to a Geometry Optimization method such as Newton Raphson and/or Polak Ribiere, followed by the new determination of its Single-point energy.

Step 3: The angle of the restrained isomerized-allylic substituent is then altered by a small amount, and Step 2 is then repeated.

Steps 2 and 3 are then repeated until the isomerized-allylic substituent has been rotated through 360°. At each step, the Single-point energy, along with the associated

conformation of the molecule, is stored. The procedure can be repeated on the other isomerized-allylic substituent.

From the resulting data, a plot of the Single-point energy of the molecule versus torsional angle can be produced. The conformation of the computationally determined molecule with the lowest energy is expected to be the most likely conformation of the molecule in reality. If the isomerized-allylic substituents on this molecule are in positions that make them unlikely to come within the bite-angle of the GII catalyst **6,** then this may be a reason for the failure to ring-close.

Precursors with different protecting groups (such as benzoyl, tosyl, etc.) can also be subjected to this computational methodology, to determine if a suitable protecting group exists that may bring the isomerized-allylic substituents on the molecule into more favourable positions, with regards to the bite-angle of the catalyst.

Chart 1: Program methodology envisaged for determining the most stable conformation of a precursor

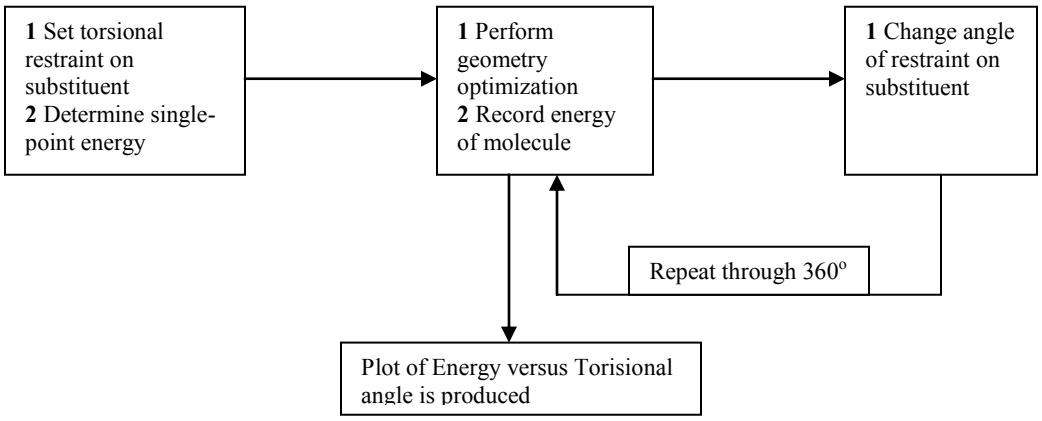

CHAPTER 5

EXPERIMENTAL SECTION

5.0 General experimental procedures

Spectroscopy

^{1}H spectra were recorded either on a Bruker AC-200 or a Bruker 300 spectrometer at the frequency indicated. Chemical shifts (δ) are reported in parts per million (ppm) relative to tetramethylsilane as the internal standard. Abbreviations used: s = singlet, d = doublet, dd = double doublet, t = triplet, dt = double triplet, ddt = double double triplet, q = quartet, m = multiplet and b = broad.
^{13}C spectra were recorded on a Bruker 300 spectrometer at 75 MHz. Chemical shifts (δ) are reported relative to the central signal of deuterated chloroform taken as 77.00 ppm.
The probe temperature for all experiments was 300 K ±1 K. All spectra were recorded in deuterated chloroform in 5 mm NMR tubes. All spectra were subjected to Fourier transform using the Mestrec Nova software package for interpretation.

Infrared spectra were recorded on either a Bruker IFS 25 Fourier transform spectrometer using KBr plates or on a Bruker Vector 22 Fourier Transform spectrometer on a diamond cell platform. The absorptions are reported on the wave number (cm^{-1}) scale in the 600–3500 cm^{-1} range.

Mass spectra were recorded on a Kratos MS 9/50, VG 70E MS or a VG 70 SEQ mass spectrometer. The polarity was positive, ionization employed was EI, with a resolution of 3000, a mass range of 3000 amu (8 kV) and a scan rate of 5 secs/decade. Data are quoted in relative abundance (*m/z*).

Solvents and separations

Macherey–Nagel kieselgel 60 (particle size 0.063 – 0.200 mm) was used for conventional silica gel chromatography. Flash Silica was used where indicated. The R_f values quoted are those obtained from thin layer chromatography on aluminium backed Macherey-Nagel ALUGRAM Sil G/UV254 plates, pre-coated with 0.25mm silica gel.

All solvents used for reactions and chromatography were distilled and purified *via* standard laboratory methods prior to use. Tetrahydrofuran and diethyl ether were distilled from sodium metal wire and benzophenone. Benzene and toluene were distilled from sodium metal lumps. Dichloromethane and DMF were stored over 4Å molecular sieves after low pressure distillation. Acetic anhydride was distilled from 4Å molecular sieves. Pyridine was distilled from potassium hydroxide. Hexane and ethyl acetate were distilled at atmospheric pressure.

Miscellaneous

All melting points were obtained on a Reichert hot-stage microscope and are uncorrected.

Grubbs' II catalyst **6** and the Ru-isomerization catalyst **15** were stored in Schlenk tubes under argon and protected from light.

Celite® was used as filtration medium in a Hirsh apparatus for all filtrations performed.

All microwave reactions were performed in a CEM Corporation Discover Focused Microwave Synthesis system, with the following parameters: Ramp time = 2 min; Pressure = 100 psi; Power = 150 W (unless otherwise indicated); and Cooling = On.

All reactions were performed under an inert Nitrogen or Argon atmosphere as indicated.

Solvent evaporations were performed first on a rotary evaporator (± 20 mmHg, 40–50 °C) followed by final drying under high vacuum conditions utilizing an oil pump manifold (± 1–2 mmHg) at room temperature.

5.1 The benzofurans

5.1.1 Mono-allylation of the precursors

5.1.1.1 1,4-Dimethoxy-2-(prop-2-en-1-yloxy)benzene 141a

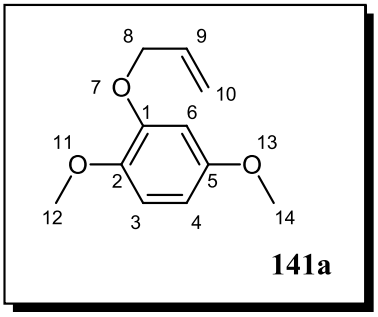

141a

Allyl bromide (5.5 g, 45 mmol, 3.9 mL) and K_2CO_3 (9.5 g, 69 mmol) were added to 2,5-dimethoxyphenol **140a** (5.0 g, 32 mmol) dissolved in dry acetone (500 mL). The reaction mixture was then heated at reflux (60 °C) under N_2 overnight. The resulting crude residue was then passed through a silica gel column (10% EtOAc/hexane) to afford 1,4-dimethoxy-2-(prop-2-en-1-yloxy)benzene **141a** as a light yellow oil (3.7 g, 60%). *m/z* (EI): 195 (M^+ +1, 55%), 194 (M^+, 90), 153 (100), 125 (90), 110 (30), 79 (35), 69 (40), 52 (40), 41 (53); HRMS: calcd for $C_{11}H_{14}O_3$ 194.0943, found: 194.0942; ν_{max} ($CHCl_3$)/cm^{-1}: 1610, 1602, 1510; ^1H NMR (300 MHz, $CDCl_3$): δ(ppm) = 3.75 (3H, s, $ArOC^{14}H_3$), 3.82 (3H, s, $ArOC^{12}H_3$), 4.57–4.59 (2H, m, $OC^8H_2CHCH_3$), 5.26–5.30 (1H, m, $OCH_2CHC^{10}H_AH_B$), 5.37–5.43 (1H, m $OCH_2CHC^{10}H_AH_B$), 6.01–6.14 (1H, m, $OCH_2C^9HCH_2$), 6.40 (1H, dd, *J* = 8.7 Hz and 2.8 Hz, ArC^4H), 6.52 (1H, d, *J* = 2.8 Hz, ArC^6H), 6.79 (1H, d, *J* = 8.8 Hz, ArC^3H); ^{13}C NMR (75 MHz, $CDCl_3$); δ(ppm) = 55.5 ($OC^{14}H_3$), 56.6 ($OC^{12}H_3$), 69.8 ($OC^8H_2CHCH_3$), 102.2 (ArC^6H), 103.6 (ArC^4H), 112.6 (ArC^3H), 117.8 ($OCH_2CHC^{10}H_2$), 133.3 ($OCH_2C^9HCH_2$), 143.9 (ArC^2), 148.9 (ArC^{10}), 154.2 (ArC^5).

5.1.1.2 1-Bromo-4-(prop-2-en-1-yloxy)benzene 141b

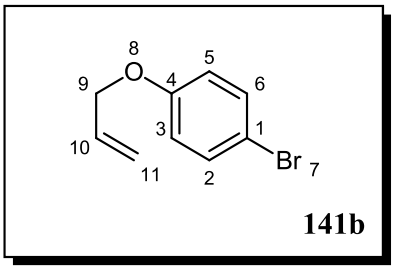

141b

Allyl bromide (8.741 g, 72.25 mmol, 6.25 mL, 2.5 equiv.) and K_2CO_3 (9.986 g, 72.25 mmol, 2.5 equiv.) were added to 4-bromophenol **140b** (5.002 g, 28.91 mmol, 1.eqiv.) dissolved in dry acetone (100 mL). The reaction mixture was then stirred at 60 °C under N_2 overnight. After cooling the reaction slurry was passed through a Celite plug to remove the base and the resulting crude residue was then passed through a silica gel column (10% EtOAc/hexane) to afford 1-bromo-4-(prop-2-en-1-yloxy)benzene **141b** as a yellow oil (6.026 g, 98%). R_f = 0.66 (10% EtOAc/hexane); ^{1}H NMR (200 MHz, $CDCl_3$):δ(ppm) = 4.50 (2H, d, *J* = 5.2 Hz, OC^9*H*$_2$CHCH$_2$), 5.27 – 5.44 (2H, m, OCH$_2$CHC^{11}*H*$_2$), 5.91–6.04 (1H, m, OCH$_2$C^{10}*H*CH$_2$), 6.70 (2H, dd, *J* = 10.0 Hz and 8.8 Hz, ArC^{3}H and ArC^{5}H), 7.19–7.38 (2H, m, ArC^{2}H and ArC^{6}H);. {The ^{1}H NMR spectrum confirmed that allylation had taken place and this known compound[98] was used without further characterisation.}

5.1.1.3 1-*tert*-Butyl-4-(prop-2-en-1-yloxy)benzene 141c

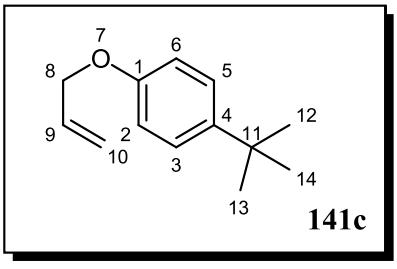

141c

Allyl bromide (10.07 g, 83.21 mmol, 7.20 mL, 2.5 equiv.) and K_2CO_3 (11.50 g, 83.21 mmol, 2.5 equiv.) were added to 4-*tert*-butylphenol **140c** (5.000 g, 33.28 mmol, 1.equiv.) dissolved in dry acetone (100 mL). The reaction mixture was then stirred at 60 °C under N_2

overnight. After cooling the reaction slurry was passed through a Celite plug to remove the base and the solvent removed under reduced pressure. The resulting crude residue was then subjected to silica gel column chromatography (10% EtOAc/hexane) to afford 1-*tert*-butyl-4-(prop-2-en-1-yloxy)benzene **141c** as a yellow oil (6.284 g, 99%). R_f = 0.84 (10% EtOAc/hexane). {This known compound[99] was submitted directly to the next reaction step.}

5.1.1.4 2-(Prop-2-en-1-yloxy)biphenyl 141d

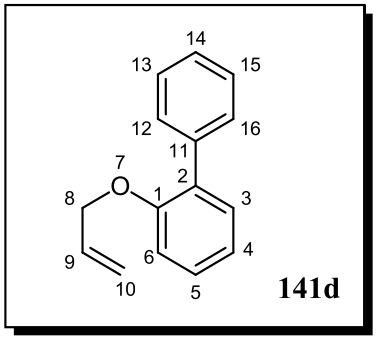

141d

Allyl bromide (9.11 g, 75.3 mmol, 6.37 mL) and K_2CO_3 (10.2 g, 73.8 mmol) were added to biphenyl-2-ol **140d** (5.00 g, 29.4 mmol) dissolved in dry acetone (100 mL). The reaction mixture was then stirred at 60 °C under N_2 overnight. After cooling the reaction slurry was passed through a Celite plug to remove the base and the resulting crude residue was then passed through a silica gel column (10% EtOAc/hexane) to afford 2-(prop-2-en-1-yloxy)biphenyl **141d** as a yellow oil (6.18 g, 100%). *m/z* (EI): 211 (M^+ +1, 17%), 210 (M^+, 100), 195 (12), 191 (11), 181 (18), 168 (14), 167 (20), 165 (29), 153 (13), 152 (21), 139 (10), 115 (21), 77 (13); HRMS: calcd for $C_{15}H_{14}O$ 210.1045, found: 210.1045; ν_{max} ($CHCl_3$)/cm^{-1}: 1638, 1590, 1497, 1458, 1433; ^{1}H NMR (300 MHz, $CDCl_3$): δ(ppm) = 4.51 (2H, td, J = 4.7 Hz, 1.6 Hz and 1.6 Hz, $OC^8H_2CHCH_2$), 5.18 (1H, dd, *J* = 10.6 Hz and 1.5 Hz, $OCH_2CHC^{10}H_AH_B$), 5.31 (1H, dd, *J* = 17.3 Hz and 1.7 Hz $OCH_2CHC^{10}H_AH_B$), 5.96 (1H, tdd, *J* = 17.2 Hz, 10.4 Hz, 4.8 Hz and 4.8 Hz, $ArOCH_2C^9HCH_2$), 6.95 (1H, d, *J* = 8.2 Hz, ArC^6H), 7.02 (1H, dt, *J* = 7.5 Hz, 7.5 Hz and 0.9 Hz, ArC^4H), 7.26 (1H, dd, *J* = 8.0 Hz and 1.5 Hz, ArC^5H), 7.28–7.35 (2H, m, ArC^3H and $ArC^{14}H$), 7.35–7.42 (2H, m, $ArC^{13}H$ and $ArC^{15}H$), 7.52–7.58 (2H, m, $ArC^{12}H$ and $ArC^{16}H$); ^{13}C NMR (75 MHz, $CDCl_3$): δ(ppm) = 69.1 ($OC^8H_2CHCH_2$), 113.0 (ArC^6H), 116.8 ($OCH_2CHC^{10}H_2$), 121.1 (ArC^4H), 126.8 (ArC^5H), 127.9 ($ArC^{12}H$ and $ArC^{16}H$), 128.5 ($ArC^{14}H$), 129.6 ($ArC^{13}H$ and $ArC^{15}H$), 130.9 (ArC^3H), 131.1 (ArC^2), 133.3 ($OCH_2C^9HCH_2$), 138.5 (ArC^{11}), 155.4 (ArC^1).

5.1.1.5 1-(Prop-2-en-1-yloxy)naphthalene 141e

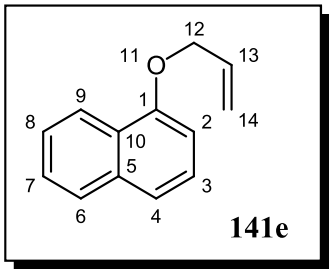

141e

Allyl bromide (10.71 g, 88.54 mmol, 7.662 mL, 2.5 equiv.) and K_2CO_3 (12.24 g, 88.54 mmol, 2.5 equiv.) were added to naphthalen-1-ol **140e** (5.106 g, 35.42 mmol, 1 equiv.) dissolved in dry acetone (100 mL). The reaction mixture was then stirred at 60 °C under N_2 overnight. After cooling the reaction slurry was passed through a Celite plug to remove the base and the resulting crude residue was then passed through a silica gel column (10% EtOAc/hexane) to afford 1-(prop-2-en-1-yloxy)naphthalene **141e** as a yellow oil (6.525 g, 100%). R_f = 0.66 (10% EtOAc/hexane). {This known compound[100] was submitted directly to the next reaction step.}

5.1.2 Claisen reactions on the mono-allylated precursors

5.1.2.1 3,6-Dimethoxy-2-(prop-2-en-1-yl)phenol 142a

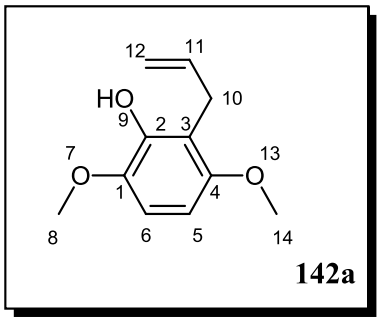

142a

1,4-Dimethoxy-2-(prop-2-en-1-yloxy)benzene **141a** (1.0 g, 5.2 mmol) was heated without solvent, under N_2, at 220–240 °C for 40 min. The dark brown residue was then subjected to purification by silica gel chromatography (20% EtOAc/hexane) to afford 3,6-dimethoxy-2-(prop-2-en-1-yl)phenol **142a** as a light oily semi-solid (0.49g, 49%). *m/z* (EI): 195 (M^+ +1, 45%), 194 (M^+, 91), 179 (100), 151 (84), 147 (50), 136 (35), 123 (24), 119 (26), 91 (46), 79 (22), 77 (26), 65 (20), 53 (30), 39 (20); HRMS: calcd for $C_{11}H_{14}O_3$ 194.0943, found: 194.0943; ν_{max} ($CHCl_3$)/cm^{-1}: 3506 br, 1639, 1601, 1493, 1464, 1440; ^{1}H NMR (300 MHz, $CDCl_3$): δ(ppm) = 3.43 (2H, br d, *J* = 5.6 Hz, $ArC^{10}\mathit{H_2}CHCH_2$), 3.76 (3H, s, $OC^{14}\mathit{H_3}$), 3.82 (3H, s, $OC^{8}\mathit{H_3}$), 4.92–5.07 (2H, m, $ArCH_2CHC^{12}\mathit{H_2}$), 5.76 (1H, s, OH), 5.89–6.05 (1H, m, $ArCH_2C^{11}\mathit{H}CH_2$), 6.33 (1H, d, *J* = 8.8 Hz, ArC^5H), 6.65 (1H, d, *J* = 8.8 Hz, ArC^6H); ^{13}C NMR (75 MHz, $CDCl_3$): δ(ppm) = 27.4 ($ArC^{10}H_2CHCH_2$), 55.8 ($OC^{14}H_3$), 56.1 (OC^8H_3), 100.9 (ArC^5H), 108.1 (ArC^6H), 114.1 (ArC^3), 114.9 ($ArCH_2CHC^{12}H_2$), 136.3 ($ArCH_2C^{11}HCH_2$), 141.0 (ArC^1), 144.2 (ArC^2OH), 152.4 (ArC^4).

5.1.2.2 4-Bromo-2-(prop-2-en-1-yl)phenol 142b

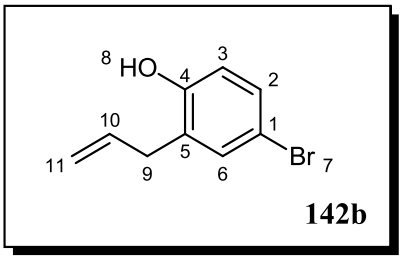

142b

1-Bromo-4-(prop-2-en-1-yloxy)benzene **141b** (1.399 g, 6.566 mmol) was irradiated in 3 mL Dichloromethane, under microwave conditions (power: 150W, ramp time: 2 °C per min, temperature: 180 °C, maximum pressure 100 psi) in a pressure tube. The irradiation was continued for 15 min. The resulting crude residue was then submitted directly to the next reaction step, after TLC revealed that significant decomposition was occurring on the silica as well as with heating times greater than 15 min. R_f = 0.30 (10% EtOAc/hexane). {A ^{1}H NMR showed that a mixture product as well as decomposition products were evident, thus the compound was used without further characterisation.}

5.1.2.3 4-*tert*-Butyl-2-(prop-2-en-1-yl)phenol 142c

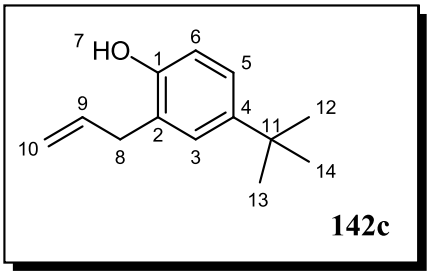

142c

1-*tert*-Butyl-4-(prop-2-en-1-yloxy)benzene **141c** (2.011 g, 10.57 mmol) was irradiated without solvent, under microwave conditions (power: 100W, ramp time: 2 °C per min, temperature: 220 °C, maximum pressure 100 psi) in a pressure tube. The irradiation was continued at 15 min intervals, at which time the reaction progress checked *via* TLC. After a total irradiation time of 50 min the dark brown residue was subjected to purification by silica gel chromatography (10% EtOAc/hexane) to afford 4-*tert*-butyl-2-

(prop-2-en-1-yl)phenol **142c** as a clear yellow oil (1.131 g, 56%). R_f = 0.26 (10% EtOAc/hexane); ^{1}H NMR (300 MHz, $CDCl_3$): δ(ppm) = 1.29 (9H, s, $C^{11}(CH_3)_3$), 3.41 (2H, br d, *J* = 6.0 Hz, $C^8H_2CHCH_2$), 4.85 (1H, br d, *J* = 16.4 Hz, OH),), 5.14–5.20 (2H, m, $CH_2CHC^{10}H_2$), 6.00–6.06 (1H, m, $CH_2C^9HCH_2$), 6.75 (1H, d, *J* = 8.2 Hz, ArC^3H), 7.11–7.16 (2H, m, ArC^5H and ArC^6H). {The identity of this known compound[99] was confirmed with ^{1}H NMR and submitted directly to the next reaction step.}

5.1.2.4 3-(Prop-2-en-1-yl)biphenyl-2-ol 142d

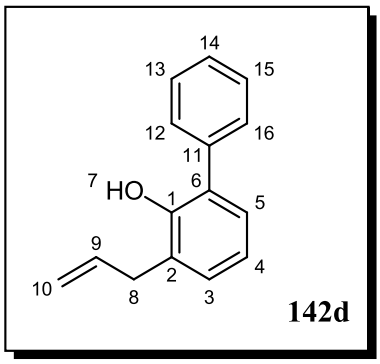

142d

2-(Prop-2-en-1-yloxy)biphenyl **141d** (2.0 g, 9.5 mmol) was irradiated without solvent, under microwave conditions (power: 100W, ramp time: 2 °C per min, temperature: 200 °C, maximum pressure 100 psi) in a pressure tube. The irradiation was continued at 15 min intervals, at which time the reaction progress checked *via* TLC. After a total irradiation time of 90 min the dark brown residue was subjected to purification by silica gel chromatography (10% EtOAc/hexane) to afford 3-(prop-2-en-1-yl)biphenyl-2-ol **142d** as a clear yellow oil (1.2 g, 60%). *m/z* (EI): 211 (M^+ +1, 12%), 210 (M^+, 63), 195 (13), 178 (12), 176 (35), 169 (100), 168 (23), 163 (18), 141 (38), 139 (21), 115 (37), 41 (10); HRMS: calcd for $C_{15}H_{14}O$ 210.1045, found: 210.1062; ν_{max} ($CHCl_3$)/cm^{-1}: 3062, 3025, 1649, 1597, 1584, 1504, 1481, 1455, 1434; ^{1}H NMR (300 MHz, $CDCl_3$): δ(ppm) = 3.47 (2H, br d, *J* = 6.5 Hz, $ArC^8H_2CHCH_2$), 5.07–5.19 (2H, m, $ArCH_2CHC^{10}H_2$), 5.31 (1H, s, ArOH), 6.06 (1H, tdd, *J* = 16.7 Hz, 10.0 Hz and 6.6 Hz, $ArCH_2C^9HCH_2$), 6.93 (1H, t, *J* = 7.5 Hz, ArC^4H), 7.13 (2H, ddd, *J* = 7.3 Hz, 5.9 Hz and 1.3 Hz, ArC^3H and ArC^5H), 7.34–7.42 (1H, m, $ArC^{14}H$), 7.43–7.51 (4H, m, $ArC^{12}H$, $ArC^{13}H$, $ArC^{15}H$ and $ArC^{16}H$); ^{13}C NMR (75 MHz, $CDCl_3$): δ(ppm) = 34.8 ($ArC^8H_2CHCH_2$), 115.9 ($ArCH_2CHC^{10}H_2$), 120.5 (ArC^4H), 127.8 (ArC^5H), 127.9 (ArC^6), 128.4 ($ArC^{12}H$), 128.5 ($ArC^{16}H$), 129.2 ($ArC^{13}H$ and $ArC^{15}H$), 129.3 ($ArC^{14}H$), 129.7 (ArC^3H), 129.8 (ArC^2), 136.6 ($ArCH_2C^9HCH_2$), 137.3 (ArC^{11}), 150.4 (ArC^1).

5.1.2.5 2-(Prop-2-en-1-yl)naphthalen-1-ol 142e

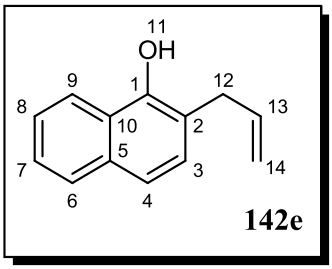

142e

1-(Prop-2-en-1-yloxy)naphthalene **141e** (2.022 g, 10.97 mmol) was irradiated without solvent under microwave conditions (power: 100W, ramp time: 2 °C per min, temperature: 180 °C, maximum pressure 100 psi) in a pressure tube. The irradiation was continued for just 2 min, after a sudden temperature and pressure increase was noted. TLC showed that the reaction had run to completion. The resulting crude residue was then was then passed through a silica gel column (10% EtOAc/hexane) to afford 2-(prop-2-en-1-yl)naphthalen-1-ol **142e** as a yellow oil (1.735 g, 86%). R_f = 0.47 (10% EtOAc/hexane); ^{1}H NMR (200 MHz, $CDCl_3$): δ(ppm) = 3.58 (2H, d, *J* = 6.1 Hz, $ArC^{12}\mathit{H}_2CHCH_2$), 5.23–5.32 (2H, m, $ArCH_2CHC^{14}\mathit{H}_2$), 5.71 (1H, s, OH), 6.03–6.17 (1H, m, $ArCH_2C^{13}\mathit{H}CH_2$), 7.25 (1H, d, *J* = 8.3 Hz, ArC^3H), 7.44–7.55 (3H, m, ArC^4H, ArC^7H and ArC^8H), 7.81–7.85 (1H, m, ArC^6H) and 8.22–8.27 (1H, m, ArC^9H). {The identity of the known compound[100] was confirmed by ^{1}H NMR and submitted directly to the next reaction step.}

5.1.3 Re-allylation of the Claisen precursors

5.1.3.1 1,4-Dimethoxy-2-(prop-2-en-1-yl)-3-(prop-2-en-1-yloxy)benzene 143a

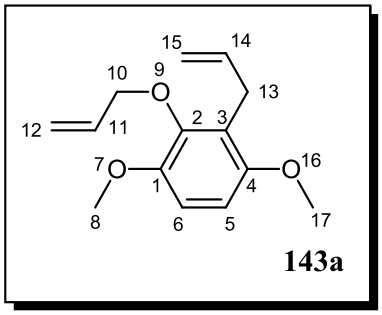

143a

Allyl bromide (0.599 g, 4.95 mmol, 0.42 mL) and K_2CO_3 (0.685 g, 4.95 mmol) were added to 1,4-dimethoxy-2-(prop-2-en-1-yloxy)benzene **142a** (0.481 g, 2.48 mmol) dissolved in acetone (50 mL) and the reaction slurry was then stirred at 60 °C for 2 h. After cooling, the base was removed by filtration through a Celite plug and the solvent was removed under reduced pressure. The brown residue was then purified using silica gel column chromatography (10% EtOAc/hexane) to afford 1,4-dimethoxy-2-(prop-2-en-1-yl)-3-(prop-2-en-1-yloxy)benzene **143a** as a clear oil (0.532 g, 92%). *m/z* (EI): 234 (M^+, 100%), 220 (21), 219 (39), 193 (94), 165 (44), 163 (33), 150 (26), 135 (23), 133 (26), 130 (62), 118 (18), 100 (18), 91 (28), 79 (22), 77 (27), 69 (97), 41 (31); HRMS: calcd for $C_{14}H_{18}O$ 234.1256, found: 234.1258; ν_{max} ($CHCl_3$)/cm^{-1}: 1638, 1593, 1487, 1465, 1439; ^{1}H NMR (300 MHz, $CDCl_3$): δ(ppm) = 3.44 (2H, td, *J* = 6.1 Hz and 1.4 Hz, ArC^{13}*H*$_2$CHCH$_2$), 3.77 (3H, s, OC^8*H*$_3$), 3.80 (3H, s, OC^{17}*H*$_3$), 4.48 (2H, td, *J* = 5.7 Hz and 1.3 Hz, Ar*C*^{10}H$_2$CHCH$_2$), 4.91–5.03 (2H, m, ArCH$_2$CHC^{15}*H*$_2$), 5.21 (1H, dd, *J* = 10.4 Hz and 1.6 Hz, OCH$_2$CHC^{12}*H*$_A$H$_B$), 5.20 (1H, dd, *J* = 17.2 Hz and 1.6 Hz, OCH$_2$CHC^{12}H$_A$*H*$_B$), 5.32–5.43 (1H, m, OCH$_2$C^{11}*H*CH$_2$), 6.09 (1H, tdd, *J* = 14.7 Hz, 9.1 Hz and, 5.0 Hz, ArCH$_2$C^{14}*H*CH$_2$), 6.56 (1H, d, *J* = 8.9 Hz, ArC^{5}H), 6.73 (1H, d, *J* = 8.9 Hz. ArC^{6}H); ^{13}C NMR (75 MHz, $CDCl_3$); δ(ppm) = 28.3 (Ar*C*^{13}H$_2$CHCH$_2$), 56.0 (OC^{17}H$_3$), 56.2 (OC^{8}H$_3$), 73.8 (O*C*^{10}H$_2$CHCH$_2$), 105.6 (ArC^{5}H), 110.2 (ArC^{6}H), 114.3

($ArCH_2CHC^{15}H_2$), 116.9 ($OCH_2CHC^{12}H_2$), 123.2 (ArC^3), 134.4 ($OCH_2C^{11}HCH_2$), 137.0 ($ArCH_2C^{14}HCH_2$), 146.9 (ArC^2O), 147.2 (ArC^1), 152.2 (ArC^4).

5.1.3.2 4-Bromo-2-(prop-2-en-1-yl)-1-(prop-2-en-1-yloxy)benzene 143b

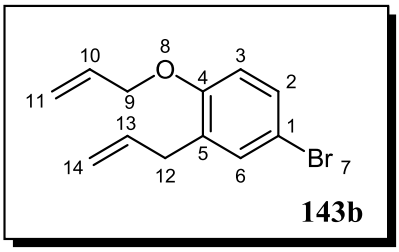

143b

Allyl bromide (1.60 g, 13.2 mmol, 1.12 mL) and K_2CO_3 (1.83 g, 13.2 mmol) were added to 4-bromo-2-(prop-2-en-1-yl)phenol **142b** (1.41 g, 6.62 mmol) dissolved in acetone (50 mL) and the reaction slurry was then stirred at 60 °C for 2 h. After cooling, the base was removed by filtration through a Celite plug and the solvent was removed under reduced pressure. The brown residue was then purified using silica gel column chromatography (10% EtOAc/hexane) to afford 4-bromo-2-(prop-2-en-1-yl)-1-(prop-2-en-1-yloxy)benzene **143b** as a yellow oil (1.40 g, 25% quantitative). R_f = 0.66 (5% EtOAc/hexane); *m/z* (EI): 254, (M^+ +2, 56%), 252 (M^+, 56), 220 (31), 210 (37), 209 (20), 185 (18), 132 (100), 118 (19), 104 (33), 103 (17), 55 (14); HRMS: calcd for $C_{12}H_{13}BrO$ 252.0150, found: 252.0133; ν_{max} ($CHCl_3$)/cm^{-1}: 1638, 1591, 1487, 1455, 1424, 1410; ^1H NMR (300 MHz, $CDCl_3$): δ(ppm) = 3.37 (2H, br d, *J* = 6.7 Hz, $ArC^{12}H_2CHCH_2$), 4.51 (2H, td, *J* = 4.9 Hz, 1.4 Hz and 1.4 Hz, $OC^9H_2CHCH_2$), 5.02–5.13 (2H, m, $ArCH_2CHC^{14}H_2$), 5.27 (1H, dd, *J* = 10.6 Hz and 1.5 Hz, $OCH_2CHC^{11}H_AH_B$), 5.40 (1H, dd, *J* = 17.3 Hz and 1.6 Hz, $OCH_2CHC^{11}H_AH_B$), 5.85–6.12 (2H, m, $OCH_2C^{10}HCH_2$ and $ArCH_2C^{13}HCH_2$), 6.70 (1H, d, *J* = 9.3 Hz, ArC^3H), 7.23–7.28 (2H, m, ArC^2H and ArC^6H); ^{13}C NMR (75 MHz, $CDCl_3$): δ(ppm) = 34.0 ($ArC^{12}H_2CHCH_2$), 68.9 ($OC^9H_2CHCH_2$), 112.9 (ArC^1), 113.2 (ArC^3H), 116.1 ($OCH_2CHC^{11}H_2$), 117.2 ($ArCH_2CHC^{14}H_2$), 129.7 (ArC^6H), 131.3 (ArC^5), 132.4 (ArC^2H), 133.0 ($OCH_2C^{10}HCH_2$), 135.9 ($ArCH_2C^{13}HCH_2$), 155.3 (ArC^4).

5.1.3.3 4-*tert*-Butyl-2-(prop-2-en-1-yl)-1-(prop-2-en-1-yloxy)benzene 143c

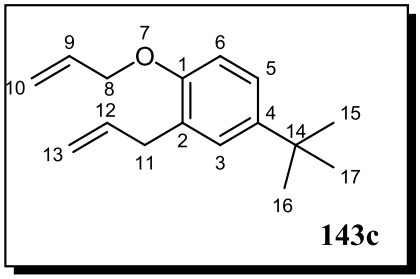

143c

Allyl bromide (0.66 g, 5.5 mmol, 0.46 mL) and K_2CO_3 (0.76 g, 5.5 mmol) were added 4-*tert*-butyl-2-(prop-2-en-1-yl)phenol **142c** (0.52 g, 2.7 mmol) dissolved in acetone (25 mL) and the reaction slurry was then stirred at 60 °C for 3 h. After cooling, the base was removed by filtration through a Celite plug and the solvent was removed under reduced pressure. The brown residue was then purified using silica gel column chromatography (10% EtOAc/hexane) to afford 4-*tert*-butyl-2-(prop-2-en-1-yl)-1-(prop-2-en-1-yloxy) benzene **143c** as a yellow oil (0.57 g, 90%). R_f = 0.66 (5% EtOAc/hexane); *m/z* (EI): 230 (M^+, 24%), 216 (17), 215 (100), 173 (7), 159 (13), 128 (8), 115 (11), 91 (9), 41 (13); HRMS: calcd for $C_{16}H_{22}O$ 230.1671, found: 230.1648; ^{1}H NMR (300 MHz, $CDCl_3$): δ(ppm) = 1.29 (9H, s, $C^{14}(CH_3)_3$), 3.41 (2H, br d, *J* = 6.6 Hz, $ArC^{11}H_2CHCH_2$), 4.52 (2H, td, *J* = 4.9 Hz, 1.5 Hz and 1.5 Hz, $OC^8H_2CHCH_2$), 5.00–5.12 (2H, m, $ArCH_2CHC^{13}H_2$), 5.23 (1H, dd, *J* = 10.6Hz and 1.6 Hz, $OCH_2CHC^{10}H_AH_B$), 5.41 (1H, dd, *J* = 17.3 Hz and 1.6 Hz, $OCH_2CHC^{10}H_AH_B$), 6.00–6.06 (2H, m, $OCH_2C^9HCH_2$ and $ArCH_2C^{12}HCH_2$), 6.76 (1H, d, *J* = 9.2 Hz, ArC^3H), 7.15–7.17 (2H, m, ArC^5H and ArC^6H);

5.1.3.4 3-(Prop-2-en-1-yl)-2-(prop-2-en-1-yloxy)biphenyl 143d

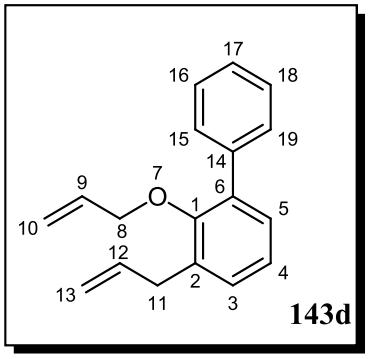

143d

Allyl bromide (0.794 g, 6.56 mmol, 0.555 mL) and K_2CO_3 (0.907 g, 6.56 mmol) were added to 2-(prop-2-en-1-yloxy)biphenyl **142d** (0.690 g, 3.28 mmol) dissolved in acetone (50 mL) and the reaction slurry was then stirred at 60 °C for 2 h. After cooling, the base was removed by filtration through a Celite plug and the solvent was removed under reduced pressure. The brown residue was then purified using silica gel column chromatography (10% EtOAc/hexane) to afford 3-(prop-2-en-1-yl)-2-(prop-2-en-1-yloxy)biphenyl **143d** as a light yellow oil (0.670 g, 82%). *m/z* (EI): 250 (M^+, 55%), 235 (15), 221 (16), 214 (28), 209 (28), 194 (42), 181 (57), 178 (25), 175 (24), 168 (100), 166 (20), 165 (65), 153 (16), 152 (26), 139 (16), 132 (21), 115 (29), 77 (17), 41 (47); HRMS: calcd for $C_{18}H_{18}O$ 250.1358, found: 250.1360; ν_{max} ($CHCl_3$)/cm^{-1}: 1638, 1600, 1498, 1459, 1431; ^1H NMR (300 MHz, $CDCl_3$): δ(ppm) = 3.49 (2H, br d, *J* = 6.6 Hz, $ArC^{11}\mathit{H}_2CHCH_2$), 3.91 (2H, br d, *J* = 5.7 Hz, $OC^{8}\mathit{H}_2CHCH_2$), 5.03–5.15 (4H, m, $ArCH_2CHC^{13}\mathit{H}_2$ and $OCH_2CHC^{10}\mathit{H}_2$), 5.68–5.84 (1H, m, $ArCH_2C^{12}\mathit{H}CH_2$), 5.96–6.10 (1H, m, $OCH_2C^{9}\mathit{H}CH_2$), 7.09–7.15 (1H, m, ArC^4H), 7.15–7.23 (2H, m, ArC^5H and ArC^3H), 7.27–7.36 (1H, m, $ArC^{17}H$), 7.36–7.43 (2H, m, $ArC^{16}H$ and $ArC^{18}H$), 7.54–7.61 (2H, m, $ArC^{15}H$ and $ArC^{19}H$); ^{13}C NMR (75 MHz, $CDCl_3$, one quaternary carbon not observable): δ(ppm) = 34.4 ($ArC^{11}H_2CHCH_2$), 73.7 ($OC^{8}H_2CHCH_2$), 115.8 ($OCH_2CHC^{10}H_2$), 117.2 ($ArCH_2CHC^{13}H_2$), 124.1 (ArC^4H), 127.1 (ArC^5H), 128.2 ($ArC^{15}H$ and $ArC^{19}H$), 129.1 ($ArC^{16}H$ and $ArC^{18}H$), 129.2 ($ArC^{17}H$),

129.4 (ArC^{3}H), 133.8 (OCH$_2$*C*^{8}HCH$_2$), 135.1 (ArC$^{6/2}$), 137.4 (ArCH$_2$*C*^{12}HCH$_2$), 138.9 (ArC^{14}), 154.3 (ArC^{1}).

5.1.3.5 2-(Prop-2-en-1-yl)-1-(prop-2-en-1-yloxy)naphthalene 143e

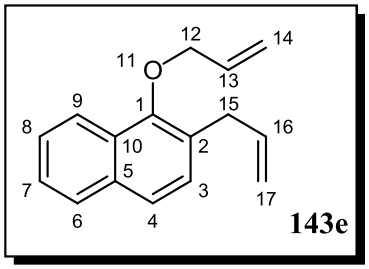

143e

Allyl bromide (1.168 g, 9.651 mmol, 0.835 mL, 2.5 equiv.) and K_2CO_3 (1.334 g, 9.651 mmol, 2.5 equiv.) were added to 2-(prop-2-en-1-yl)naphthalen-1-ol **142e** (0.7112 g, 3.860 mmol, 1 equiv.) dissolved in dry acetone (50 mL) and the reaction slurry was then stirred at 60 °C for 12 h. After cooling, the base was removed by filtration through a Celite plug and the solvent was removed under reduced pressure. The brown residue was then purified using silica gel column chromatography (5% EtOAc/hexane) to afford 2-(prop-2-en-1-yl)-1-(prop-2-en-1-yloxy)naphthalene **143e** as a yellow oil (0.8564 g, 99%). R_f = 0.81 (10% EtOAc/hexane); *m/z* (EI): 224, (M^+, 63%), 183 (100), 165 (58), 155 (70), 139 (12), 128 (26), 102 (6), 77 (10), 41 (10); HRMS: calcd for $C_{16}H_{16}O$ 224.12012, found: 224.12044; ν_{max} ($CHCl_3$)/cm^{-1}: 3076, 3009, 2978, 2911, 2863, 1638, 1572, 1386, 1360, 1343, 1260, 1246, 1181, 1078, 992, 918, 814, 757; ^{1}H NMR (300 MHz, $CDCl_3$) δ ppm = 3.61 (2H, dd, *J* = 6.4 Hz and 0.8 Hz, ArCH$_2$C^{15}*H*CH$_2$), 4.51 (2H, dd, *J* = 5.5 Hz and 1.0 Hz, OCH$_2$C^{12}*H*CH$_2$), 5.07 (1H, d, *J* = 1.4 Hz, ArCH$_2$CHC^{17}*H$_A$*H$_B$), 5.12 (1H, dd, *J* = 4.5 Hz and 1.4 Hz, ArCH$_2$CHC^{17}H$_A$*H$_B$*), 5.32 (1H, d, *J* = 10.4 Hz, OCH$_2$CHC^{14}*H$_A$*H$_B$), 5.51 (1H, d, *J* = 17.2 Hz, OCH$_2$CHC^{14}H$_A$*H$_B$*), 5.94–6.13 (1H, m, ArCH$_2$C^{16}*H*CH$_2$), 6.13–6.28 (1H, m, OCH$_2$C^{13}*H*CH$_2$), 7.32 (1H, d, *J* = 8.4 Hz, ArC^{6}H), 7.52–7.39 (2H, m, ArC^{7}H and ArC^{8}H), 7.58 (1H, d, *J* = 8.5 Hz, ArC^{4}H), 7.81 (1H, d, *J* = 7.9 Hz, ArC^{3}H), 8.09 (1H, d, *J* = 8.1 Hz, ArC^{9}H); ^{13}C NMR (75 MHz, $CDCl_3$): δ(ppm) = 34.0 (Ar*C*^{15}H$_2$CHCH$_2$), 75.2 (O*C*^{12}H$_2$CHCH$_2$), 115.8 (OCH$_2$CH*C*^{14}H$_2$), 117.3 (ArCH$_2$CH*C*^{17}H$_2$), 118.1 (ArC^{2}), 122.1

(ArC^4H), 124.0 (ArC^3H), 125.4 (ArC^{10}), 125.5 (ArC^9H), 125.8 (ArC^8H), 127.8 (ArC^7H), 128.2 (ArC^6H), 128.6 (ArC^5), 133.9 ($OCH_2C^{13}HCH_2$), 137.2 ($ArCH_2C^{15}HCH_2$), 152.2 (ArC^1O).

5.1.4 Di-isomerization of the di-allylated precursors

5.1.4.1 1,4-Dimethoxy-2-(prop-1-en-1-yl)-3-(prop-1-en-1-yloxy)benzene 144a

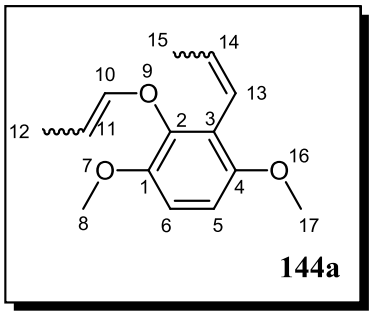

144a

1,4-Dimethoxy-2-(prop-2-en-1-yl)-3-(prop-2-en-1-yloxy) benzene **143a** (0.31g, 1.3mmol) and $[RuClH(CO)(PPh_3)_3]$ **15** (0.063g, 0.066mmol, 5 mol%) were dissolved in distilled, degassed toluene (5 mL). The reaction was heated at 65 °C for 14 h with the completion of the reaction confirmed by NMR spectroscopy of a crude sample. The reaction solution was then purified by filtration through a short silica gel pad (5% EtOAc/hexane) to remove the catalyst and evaporated under reduced pressure to 1,4-dimethoxy-2-(prop-1-en-1-yl)-3-(prop-1-en-1-yloxy)benzene **144a** (a mixture of E,Z isomers) as a dark oil (0.30g, 98%). ^1H NMR (200 MHz, $CDCl_3$): δ(ppm) = 1.78 (3H, dd, J = 7.1 Hz and 1.3 Hz, $ArCHCHC^{15}H_3$), 1.91 (3H, d, J = 5.1 Hz, $OCHCHC^{12}H_3$), 3.80 (6H, br d, J = 1.0 Hz, OC^8H_3 and $OC^{17}H_3$), 4.53–4.62 (1H, m, $OCHC^{11}HCH_3$), 6.05–6.08 (1H, m, $ArCHCHC^{14}H_3$), 6.44–6.85 (4H, m, $OC^{10}HCHCH_3$, $ArC^{13}HCHCH_3$, ArC^5H and ArC^6H). {The ^1H NMR spectrum confirmed that dual isomerization had taken place and the compound was used without further characterisation.}

5.1.4.2 4-Bromo-2-(prop-1-en-1-yl)-1-(prop-1-en-1-yloxy)benzene 144b

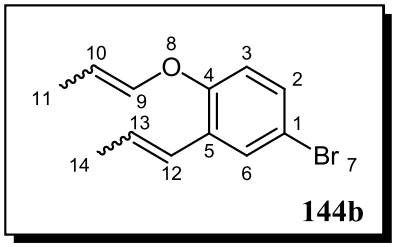

144b

4-Bromo-2-(prop-2-en-1-yl)-1-(prop-2-en-1-yloxy) benzene **143b** (0.23 g, 0.91 mmol) and [RuClH(CO)(PPh_3)$_3$] **15** (0.043 g, 0.047 mmol, 5 mol%) were dissolved in distilled, degassed toluene (5 mL). The reaction was heated at 65 °C for 14 h with the completion of the reaction confirmed by NMR spectroscopy of a crude sample. The reaction solution was then purified by filtration through a short silica gel pad (5% EtOAc/hexane) to remove the catalyst and evaporated under reduced pressure to produce 4-bromo-2-(prop-1-en-1-yl)-1-(prop-1-en-1-yloxy)benzene **144b** (a mixture of E,Z isomers in a ratio of 1:2) as a dark oil (0.23 g, 100%). R_f = 0.78 (5% EtOAc/hexane); *m/z* (EI): 254 (M^+ +2, 52%), 252 (M^+, 54), 239 (33), 237 (35), 225 (59), 223 (60), 218 (26), 210 (23), 198 (28), 196 (27), 173 (40), 158 (100), 145 (21), 144 (22), 132 (55), 130 (32), 116 (21), 115 (87), 103 (30), 89 (26), 69 (20), 63 (23), 41 (20); HRMS: calcd for $C_{12}H_{13}BrO$ 252.0150, found: 252.0150; ^{1}H NMR (200 MHz, $CDCl_3$): δ(ppm) = 1.55–1.73 (3H, m, ArCHCHC$^{14}H_3$), 1.86–1.92 (3H, m, OCHCHC$^{11}H_3$), 4.88 (dt, *J* = 6.2 Hz and 0.6 Hz) and 5.32 (dt, *J* = 6.9 Hz and 5.1 Hz) [1H, OCHC^{10}HCH$_3$], 6.08–6.31 (2H, m, ArCHC^{13}HCH$_3$ and OC^9HCHCH$_3$), 6.54–6.68 (1H, m, ArC^{12}HCHCH$_3$), 6.77 (1H, dd, *J* = 5.7 Hz and 2.9 Hz, ArC^{3}H), 7.22 (1H, dd, *J* = 6.3 Hz and 2.2 Hz, ArC^{2}H), 7.52 (1H, d, *J* = 2.2 Hz, ArC^{6}H).

5.1.4.3 4-*tert*-butyl-2-(prop-1-en-1-yl)-1-(prop-1-en-1-yloxy)benzene 144c

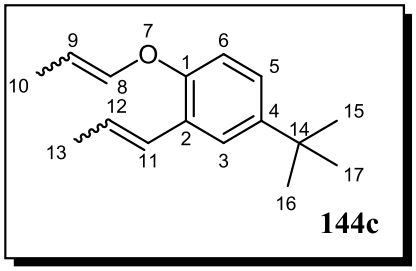

144c

4-*tert*-butyl-2-(prop-2-en-1-yl)-1-(prop-2-en-1-yloxy) benzene **143c** (0.22 g, 0.96 mmol) and [RuClH(CO)(PPh_3)$_3$] **15** (0.046 g, 0.048 mmol, 5 mol%) were dissolved in distilled, degassed toluene (5 mL). The reaction was heated at 65 °C for 14 h with the completion of the reaction confirmed by NMR spectroscopy of a crude sample. The reaction solution was then purified by filtration through a short silica gel pad (5% EtOAc/hexane) to remove the catalyst and evaporated under reduced pressure to afford 4-tert-butyl-2-(prop-1-en-1-yl)-1-(prop-1-en-1-yloxy)benzene **144c** (a mixture of E,Z isomers) as a light oil (0.19 g, 86%). R_f = 0.78 (5% EtOAc/hexane); *m/z* (EI): 230 (M^+, 24%), 216 (17), 215 (100), 173 (7), 159 (13), 128 (8), 115 (11), 91 (9), 41 (13); HRMS: calcd for $C_{16}H_{22}O$ 230.1671, found: 230.1648; ^{1}H NMR (200 MHz, $CDCl_3$): δ(ppm) = 1.31 (9H, s, $C^{14}(CH_3)_3$), 1.69 (3H, ddd, *J* = 9.8 Hz, 5.3 Hz and 1.6 Hz, $OCHCHC^{10}H_3$), 1.91 (3H, dd, *J* = 2.6 Hz and 1.6 Hz, $ArCHCHC^{13}H_3$), 5.05 (1H, m, $OCHC^9HCH_3$), 6.23–6.34 (2H, m, $ArCHC^{12}HCH_3$ and OC^8HCHCH_3), 6.76 (1H, td, *J* = 12.1 Hz and 1.7 Hz, $ArC^{11}HCHCH_3$), 6.86 (1H, d, *J* = 2.0 Hz, ArC^6H), 7.17 (1H, d, *J* = 8.5 Hz, ArC^5H), 7.44 (1H, s, ArC^3H). {The HRMS and ^{1}H NMR results confirmed that isomerization had taken place, and the compound was used without further characterization.}

5.1.4.4 3-(Prop-1-en-1-yl)-2-(prop-1-en-1-yloxy)biphenyl 144d

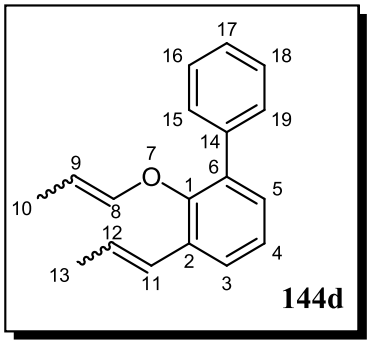

144d

3-(Prop-2-en-1-yl)-2-(prop-2-en-1-yloxy)biphenyl **143d** (0.24 g, 0.96 mmol) and [RuClH(CO)(PPh_3)$_3$] **15** (0.046 g, 0.048 mmol, 5 mol%) were dissolved in distilled, degassed toluene (5 mL). The reaction was heated at 65 °C for 14 h with the completion of the reaction confirmed by NMR spectroscopy of a crude sample. The reaction solution was then purified by filtration through a short silica gel pad (5% EtOAc/hexane) to remove the catalyst and evaporated under reduced pressure to afford 3-(prop-1-en-1-yl)-2-(prop-1-en-1-yloxy)biphenyl **144d** (a mixture of *E,Z* isomers) as a dark oil (0.23 g, 98%). *m/z* (EI): 250 (M^+, 100%), 236 (21), 235 (98), 221 (64), 208 (26), 207 (37), 194 (80), 191 (26), 179 (22), 178 (50), 168 (21), 166 (28), 165 (89), 152 (46), 115 (41); HRMS: calcd for $C_{18}H_{18}O$ 250.1358, found: 250.1333; ^{1}H NMR (200 MHz, $CDCl_3$): δ(ppm) = 1.57–1.62 (3H, m, ArCHCHC$^{13}H_3$), 1.85–1.93 (3H. m, OCHCHC$^{10}H_3$), 4.27–4.66 (1H, m, OCHC^9HCH$_3$), 5.76–5.81 (1H, m, ArCHC^{12}HCH$_3$), 6.25–6.29 (1H, m, OC^8HCHCH$_3$), 6.63–6.73 (1H, m, ArC^{11}HCHCH$_3$), 7.14–7.48 (8H, m, 8 × ArC*H*). {The HRMS and ^{1}H NMR results confirmed that isomerization had taken place, and the compound was used without further characterization.}

5.1.4.5 2-(Prop-1-en-1-yl)-1-(prop-1-en-1-yloxy)naphthalene 144e

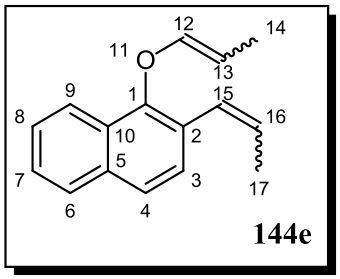

144e

2-(Prop-2-en-1-yl)-1-(prop-2-en-1-yloxy)naphthalene **143e** (0.2919 g, 1.301 mmol) and [RuClH(CO)(PPh_3)$_3$] **15** (61.97 mg, 0.06507 mmol, 5 mol%) were dissolved in distilled, degassed toluene (5 mL). The reaction was heated at 60 °C for 12 h under a N_2 atmosphere. The reaction mixture was then filtered through a compacted Celite plug (3 ×) to remove the catalyst and the solvent was then removed under reduced pressure. The resulting crude residue was passed through a silica gel column (5% EtOAc/hexane) to afford 2-(prop-1-en-1-yl)-1-(prop-1-en-1-yloxy)naphthalene **144e** (a mixture of *E,Z*-isomers) as a yellow oil (0.2713 g, 93%). R_f = 0.78 (5% EtOAc/hexane); *m/z* (EI): 224 ($M^{+\cdot}$ 65%), 209 (95), 195 (100), 181 (40), 165 (68), 139 (21), 115 (31), 101 (6), 77 (7), 63 (4), 39 (12); HRMS: calcd for $C_{16}H_{16}O$ 224.1201, found: 224.1205; ^{1}H NMR (200 MHz, $CDCl_3$): δ(ppm) = 1.91–1.97 (6H, m, OCHCHC$^{14}H_3$ and ArCHCHC$^{17}H_3$), 4.60–4.86 (1H, m, OCHC^{13}HCH$_3$), 6.11–6.14 (1H, m, ArCHC^{16}HCH$_3$), 6.33–6.41 (1H, m, OC^{12}HCHCH$_3$), 6.77–6.88 (1H, m, ArC^{15}HCHCH$_3$), 7.39–7.52 (2H, m, ArC^{3}H and ArC^{4}H), 7.54–7.61 (2H, m, ArC^{7}H and ArC^{8}H), 7.77 (1H, dd, *J* = 4.1 Hz and 2.1 Hz, ArC^{6}H), 8.04 (1H, d, *J* = 7.4 Hz, ArC^{9}H).

5.1.5 RCM of the di-isomerized precursors

5.1.5.1 4,7-Dimethoxybenzofuran 145a

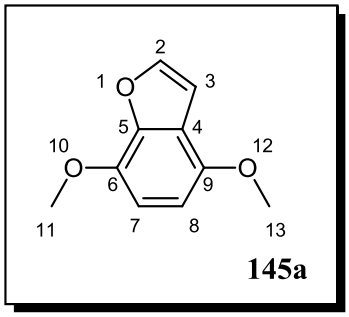

145a

1,4-Dimethoxy-2-(prop-1-en-1-yl)-3-(prop-1-en-1-yloxy) benzene **144a** (0.17 g, 0.74 mmol) and Grubbs' II catalyst **6** (0.031 g, 0.037 mmol, 5 mol%) were dissolved in distilled, degassed toluene (5 mL). The reaction mixture was then stirred at 90 °C for 3 h under a N_2 atmosphere. After cooling, the reaction mixture was filtered through a Celite plug to remove the catalyst and the solvent was removed under vacuum. The dark oil was purified by column chromatography (10% EtOAc/hexane) to afford 4,7-dimethoxybenzofuran **145a** as a low melting point solid (0.13 g, 100%). *m/z* (EI): 178 (M^+, 65%), 163 (100), 135 (8), 120 (8), 92 (6), 76 (5), 63 (6); HRMS: calcd for $C_{10}H_{10}O_3$ 178.0630, found: 178.0644; ν_{max} ($CHCl_3$)/cm^{-1}: 1607, 1590, 1540, 1504, 1461; ^{1}H NMR (300 MHz, $CDCl_3$): δ(ppm) = 3.89 (3H, s, $OC^{11}H_3$), 3.96 (3H, s, $OC^{13}H_3$), 6.53 (1H, d, *J* = 8.5 Hz, ArC^8H), 6.70 (1H, d, *J* = 8.5 Hz, ArC^7H), 6.86 (1H, d, *J* = 2.1 Hz, CC^3HCHOC), 7.55 (1H, d, *J* = 2.1 Hz, $CCHC^2HOC$); ^{13}C NMR (75 MHz, $CDCl_3$): δ(ppm) = 55.8 ($OC^{11}H_3$), 56.5 ($OC^{13}H_3$), 102.7 (CC^3HCHO), 104.4 (ArC^8H), 106.8 (ArC^7H), 119.5 (ArC^4), 132.0 (ArC^6), 140.4 (ArC^9), 143.9 (OC^2HCHC), 147.6 (ArC^5).

5.1.5.2 5-Bromobenzofuran 145b

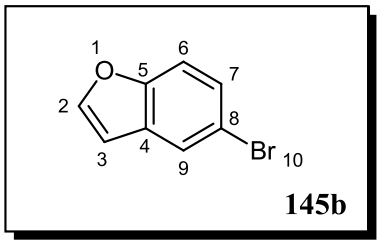

145b

4-Bromo-2-(prop-1-en-1-yl)-1-(prop-1-en-1-yloxy) benzene **144b** (0.15 g, 0.59 mmol) and Grubbs' II catalyst **6** (0.025 g, 0.030 mmol, 5 mol%) were dissolved in distilled, degassed toluene (5 mL). The reaction mixture was then stirred at 90 °C for 3 h under a N_2 atmosphere. After cooling, the reaction mixture was filtered through a Celite plug to remove the catalyst and the solvent was removed under vacuum. The dark oil was purified by column chromatography (10% EtOAc/hexane) to afford 5-bromobenzofuran **145b** as yellow oil (0.026 g, 22%). *m/z* (EI): 198 (M^+ +2, 72%), 196 (M^+, 43), 194 (30), 180 (23), 165 (19), 149 (22), 132 (46), 115 (24), 111 (30), 109 (22), 97 (43), 89 (38), 85 (50), 83 (57), 82 (20), 81 (35), 72 (35), 71 (60), 70 (25), 69 (62), 67 (24), 63 (33), 57 (100), 55 (81), 43 (92), 41 (64); HRMS: calcd for C_8H_5BrO 195.9524, found: 195.9516; ^{1}H NMR (300 MHz, $CDCl_3$): δ(ppm) = 6.72 (1H, d, *J* = 2.1 Hz, CC^3*H*CHOC), 7.38 (2H, br d, *J* = 0.9 Hz, ArC^{6}H and ArC^{7}H), 7.62 (1H, d, *J* = 2.2 Hz, CCHC^2*H*OC), 7.73 (1H, br s, ArC^{9}H); ^{13}C NMR (75 MHz, $CDCl_3$): δ(ppm) = 106.0 (C*C*^{3}HCHOC), 112.8 (ArC^{6}H), 115.7 (ArC^{8}Br), 123.8 (ArC^{9}H), 127.1 (ArC^{7}H), 129.4 (ArC^4), 146.1 (CCH*C*^{2}HOC), 153.7 (ArC^5).

5.1.5.3 5-*tert*-Butyl-benzofuran 145c

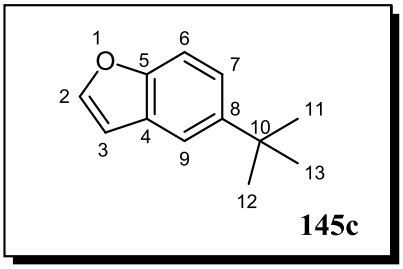

145c

4-*tert*-Butyl-2-(prop-1-en-1-yl)-1-(prop-1-en-1-yloxy) benzene **144c** (0.10 g, 0.44 mmol) and Grubbs' II catalyst **6** (0.020 g, 0.022 mmol, 5 mol%) were dissolved in distilled, degassed toluene (5 mL). The reaction mixture was then stirred at 90 °C for 3 h under a N_2 atmosphere. After cooling, the reaction mixture was filtered through a Celite plug to remove the catalyst and the solvent was removed under vacuum. The dark oil was purified by column chromatography (10% EtOAc/hexane) to afford 5-*tert*-butyl-benzofuran **145c** as a clear oil (0.055 g, 71%). *m/z* (EI): 174 (M^+, 23%), 160 (12), 159 (100), 115 (16), 91 (14), 89 (7), 77 (6), 63 (6), 63 (7), 40 (9); HRMS: calcd for $C_{12}H_{14}O$ 174.1045, found: 174.1029; ν_{max} ($CHCl_3$)/cm^{-1}: 1699, 1607, 1541; ^1H NMR (300 MHz, $CDCl_3$): δ(ppm) = 1.38 (9H, s, $C(CH_3)_3$), 6.73 (1H, d, J = 2.9 Hz, CC^3HCHOC), 7.36 (1H, dd, J = 8.7 Hz and 1.9 Hz, ArC^7H), 7.42 (1H, d, J = 8.7 Hz, $CCHC^2HOC$), 7.58–7.60 (2H, m, ArC^6H and ArC^9H); ^{13}C NMR (75 MHz, $CDCl_3$): δ(ppm) = 31.5 ($C^{10}(CH_3)_3$), 31.9 ($C^{11}H_3$, $C^{12}H_3$, $C^{13}H_3$), 106.7 (CC^3HCHOC), 110.6 (ArC^6H), 116.2 (ArC^4), 117.3 (ArC^9H), 122.2 (ArC^7H), 127.1 (ArC^8), 145.0 ($CCHC^2HOC$), 145.8 (ArC^5).

5.1.5.4 7-Phenyl-1-benzofuran 145d

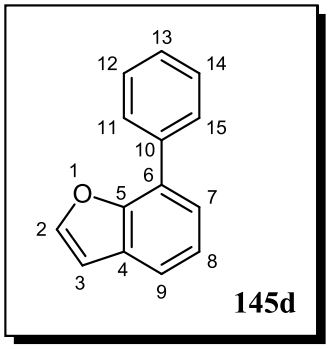

145d

3-(Prop-1-en-1-yl)-2-(prop-1-en-1-yloxy)biphenyl **144d** (0.10 g, 0.42 mmol) and Grubbs' II catalyst **6** (0.018 g, 0.021 mmol, 5 mol%) were dissolved in distilled, degassed toluene (5 mL). The reaction mixture was then stirred at 90 °C for 3 h under a N_2 atmosphere. After cooling, the reaction mixture was filtered through a Celite plug to remove the catalyst and the solvent was removed under vacuum. The dark oil was purified by column chromatography (10% EtOAc/hexane) to afford 7-phenylbenzofuran **145d** as yellow oil (0.051 g, 63%). *m/z* (EI): 195 (M^+ +1, 17%), 194 (M^+, 100), 165 (53), 163 (10), 139 (12), 115 (9), 63 (7); HRMS: calcd for $C_{14}H_{10}O$ 194.0732, found: 194.0711; ν_{max} ($CHCl_3$)/cm^{-1}: 1668, 1596, 1542, 1499, 1474, 1451, 1412; ^1H NMR (300 MHz, $CDCl_3$): δ(ppm) = 6.83 (1H, d, *J* = 2.2 Hz, CHC^3*H*CHOC), 7.33 (1H, d, *J* = 7.6 Hz, ArC^{8}H), 7.40 (1H, d, *J* = 4.3 Hz, ArC^{7}H), 7.48 (3H, ddd, *J* = 9.7 Hz, 8.3 Hz and 0.9 Hz, ArC^{12}H, ArC^{13}H and ArC^{14}H), 7.58 (1H, dd, *J* = 7.7 Hz and 1.1 Hz, ArC^{9}H), 7.67 (1H, d, J = 2.2 Hz, CCHC^2*H*OC), 7.83–7.88 (2H, m, ArC^{11}H and ArC^{15}H); ^{13}C NMR (75 MHz, $CDCl_3$): δ(ppm) = 106.7 (CC^3*H*CHOC), 120.3 (ArC^{9}H), 123.2 (ArC^{7}H), 123.8 (ArC^{8}H), 127.6 (ArC^{13}H), 127.9 (ArC^4), 128.5 (ArC^{11}H and ArC^{15}H), 128.6 (ArC^{14}H and ArC^{14}H), 129.2 (ArC^6), 136.5 (ArC^{10}), 144.9 (CCHC^2*H*OC), 152.2 (ArC^5).

5.1.5.5 Naphtho[1,2-*b*]furan 145e

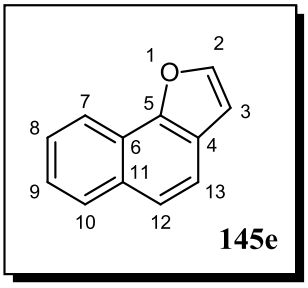

145e

2-(prop-1-en-1-yl)-1-(prop-1-en-1-yloxy)naphthalene **144e** (0.1202 g, 0.5359 mmol) and Grubbs' II catalyst **6** (22.75 mg, 0.02679 mmol, 5 mol%) were dissolved in distilled, degassed toluene (5 mL). The reaction mixture was then stirred at 60 °C for 12 h under a N_2 atmosphere. After cooling, the reaction mixture was filtered through a Celite plug to remove the catalyst and the solvent was removed under vacuum. The dark oil was purified by column chromatography (10% EtOAc/hexane) to afford Naphtho[1,2-*b*]furan **145e** as yellow oil (83.31 mg, 93%). *m/z* (EI): 168 (M^+, 62%), 139 (38), 131 (47), 119 (10), 100 (12), 69 (76); HRMS: calcd for $C_{12}H_8O$ 168.0575, found: 168.0573; ν_{max} ($CHCl_3$)/cm^{-1}: 3057, 2926, 1511, 1392, 1322, 1269, 1170, 1128, 1069, 1022, 882, 809, 739, 686, 598, 561; ^{1}H NMR (300 MHz, $CDCl_3$): δ(ppm) = 6.89 (1H, d, *J* = 2.1 Hz, OCHC^3*H*), 7.48 (1H, ddd, *J* = 8.1 Hz, 7.0 Hz and 1.2 Hz, ArC^{8}H), 7.58 (1H, ddd, *J* = 8.2 Hz, 7.1 Hz and 1.2 Hz, ArC^{9}H), 7.65 (2H, br s, ArC^{7}H and ArC^{8}H), 7.75 (1H, d, *J* = 2.1 Hz, OC^2*H*CH), 7.92 (1H, d, *J* = 8.2Hz, ArC^{12}H), 8.31 (1H, d, *J* = 8.2 Hz, ArC^{13}H); ^{13}C NMR (75 MHz, $CDCl_3$): δ(ppm) = 107.6 (C*C*^{3}HCHO), 119.7 (ArC^{13}H), 120.0 (ArC^{12}H), 122.9 (ArC^6), 123.4 (ArC^{8}H), 125.1 (ArC^{9}H), 126.1 (ArC^4), 126.3 (ArC^{7}H), 128.3 (ArC^{10}H), 131.4 (ArC^{11}), 144.1 (CCH*C*^{2}HO), 150.6 (ArC^5).

5.2 The *O,N*-benzo-fused heterocycles

5.2.1 Protection of the precursor

5.2.1.1 *N*-(2-Hydroxyphenyl)benzamide 147

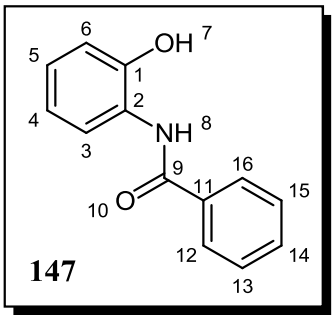

147

2-Aminophenol **146** (5.89 g, 53.9 mmol, 1 equiv.) was dissolved in dry CH_2Cl_2 (100 mL) and the temperature of the mixture lowered to 0 °C, followed by the sequential addition of pyridine (4.4 mL, 54 mmol, 1 equiv.) and benzoyl chloride (6.3 mL, 54 mmol, 1 equiv.). The reaction mixture was stirred at r. t. for 24 h under a N_2 atmosphere. The reaction mixture was then quenched with saturated $NaHCO_3$ solution to bring the pH to 7. The mixture was separated and the organic fraction dried ($MgSO_4$) and the solvent removed under reduced pressure to afford *N*-(2-hydroxyphenyl)benzamide **147** as a white crystalline powder (11.5 g, 100%). R_f = 0.10 (20% EtOAc/hexane); ^{1}H NMR (300 MHz, $CDCl_3$): δ(ppm) = 1.70 (1H, s, OH), 4.81 (1H, s, NH), 6.85–7.20 (1H, m, ArC^{6}H), 7.20–7.45 (2H, m, ArC^{5}H and ArC^{4}H), 7.46–7.65 (2H, m, ArC^{13}H and ArC^{15}H), 7.65–7.82 (1H, m, ArC^{12}H), 7.84–7.99 (1H, m, ArC^{14}H), 8.20–8.37 (1H, m, ArC^{16}H), 8.10 (0.3H, s) and 8.69 (0.7H, s) [ArC^{3}H]; ^{13}C NMR (75 MHz, $CDCl_3$): δ(ppm) = 119.4 (ArC^{6}H), 120.6 (ArC^{4}H), 122.2 (ArC^{5}H), 123.4 (ArC^{3}H), 126.9 (ArC^{12}H), 127.3 (ArC^{16}H), 128.8 (ArC^{13}H), 128.8 (ArC^{15}H), 130.2 (ArC^{14}H), 132.4 (ArC^2), 134.3 (ArC^{11}), 148.5 (ArC^1), 167.0 (C=O). {The identity of this compound was confirmed with ^{1}H and ^{13}C NMR and submitted directly to the next reaction step.}

5.2.2 Allylation reactions

5.2.2.1 *N*-(2-(Prop-2-en-1-yloxy)phenyl)benzamide 148

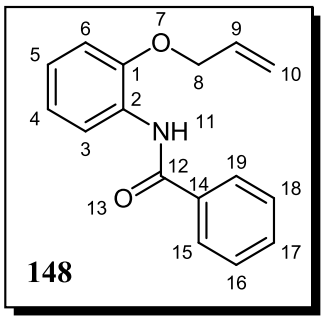

148

Allyl bromide (3.00 g, 24.8 mmol, 2.1 mL, 1.2 equiv.) and K_2CO_3 (5.71 g, 41.3 mmol, 2 equiv.) were added to *N*-(2-hydroxyphenyl)benzamide **147** (4.40 g, 20.7 mmol, 1 equiv.) dissolved in dry acetone (100 mL). The reaction mixture was then stirred at reflux (60 °C) for 24 h under a N_2 atmosphere. After cooling, the reaction slurry was passed through a celite plug to remove the base and the resulting crude residue was then passed through a silica gel column (20% EtOAc/hexane) to afford *N*-(2-(prop-2-en-1-yloxy)phenyl)benzamide **148** as a pale yellow solid (4.188 g, 80%). R_f = 0.48 (20% EtOAc/hexane), mp = 50–51 °C; *m/z* (EI): 253 (M^+ , 30%), 212 (15), 105 (100), 77 (36), 51 (8) ,41 (5); HRMS: calcd for $C_{16}H_{15}NO_2$ 253.1103, found: 253.1121; ν_{max} (ATR)/cm^{-1}: 3317, 1738, 1648, 1601, 1518, 1482, 1452, 1375, 1324, 1294; ^{1}H NMR (300 MHz, $CDCl_3$): δ(ppm) = 4.64 (2H, dt, *J* = 5.2 Hz and 1.3 Hz, $OC^8H_2CHCH_2$), 5.33 (1H, dd, *J* = 10.5 Hz and 1.3 Hz, $OCH_2CHC^{10}H_AH_B$), 5.43 (1H, dd, *J* = 17.3 Hz and 1.4 Hz, $CH_2CHC^{10}H_AH_B$), 6.08 (1H, tdd, *J* = 17.1 Hz, 10.6 Hz and 5.3 Hz, $OCH_2C^9HCH_2$), 6.88–6.97 (1H, m, ArC^6H), 6.97–7.10 (2H, m, ArC^5H and ArC^4H), 7.45–7.58 (3H, m, $ArC^{16}H$, $ArC^{17}H$ and $ArC^{18}H$), 7.89 (2H, dd, *J* = 8.0 Hz and 1.5 Hz, $ArC^{15}H$ and $ArC^{19}H$), 8.52–8.59 (1H, m, ArC^3H), 8.63 (1H, br s, NH); ^{13}C NMR (75 MHz, $CDCl_3$): δ(ppm) = 69.5 ($OC^8H_2CHCH_2$), 111.4 ($OCH_2CHC^{10}H_2$), 118.1 (ArC^6H), 119.9 (ArC^4H), 121.4 (ArC^3H), 123.7 (ArC^5H), 126.9

(ArC^{15}H and ArC^{19}H), 128.1 (ArC^{2}), 128.7 (ArC^{16}H and ArC^{18}H), 131.7 (ArC^{17}H), 132.7 (OCH$_2$*C*^{9}HCH$_2$), 135.3 (ArC^{14}), 147.1 (ArC^{1}), 165.1 (C=O).

5.2.2.2 *N*-(Prop-2-en-1-yl)-*N*-[2-(prop-2-en-1-yloxy)phenyl]benzamide 149

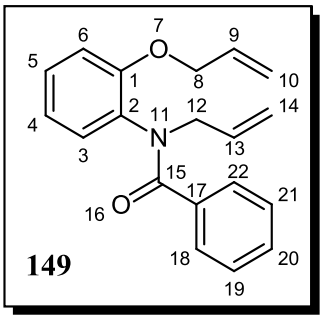

149

N-(2-(Prop-2-en-1-yloxy)phenyl)benzamide **148** (1.05 g, 4.13 mmol, 1 equiv.) was dissolved in dry DMF (30 mL) and the temperature of the mixture lowered to 0 °C, followed by the sequential addition of NaH (60% in oil, 0.190 g, 4.96 mmol, 1.2 equiv.) and allyl bromide (1.0 g, 8.3 mmol, 0.72 mL, 2 equiv.). The reaction mixture was then stirred at r.t. for 24 h under a N_2 atmosphere. Water (80 mL) was added to quench the reaction mixture, after which it was extracted with EtOAc (3 × 50 mL) and the combined fractions dried ($MgSO_4$). The solvent was then removed under reduced pressure and the resulting crude residue passed through a silica gel column (20% EtOAc/hexane) to afford *N*-(prop-2-en-1-yl)-*N*-[2-(prop-2-en-1-yloxy)phenyl]benzamide **149** as a pale yellow oil (1.10 g, 90%). R_f = 0.30 (20% EtOAc/hexane); *m/z* (EI): 293 (M^+, 28%), 236 (11), 188 (10), 120 (5), 105 (100), 77 (33) and 41 (7); HRMS: calcd for $C_{19}H_{19}NO_2$ 293.1416, found: 293.1424; ν_{max} (ATR)/cm^{-1}: 1647, 1601, 1518, 1496, 1481, 1452, 1324, 1294, 1265, 1246, 1208, 1125; ^{1}H NMR (300MHz; $CDCl_3$) δ (ppm) = 4.26 (2H, dd, *J* = 14.4 Hz and 7.2 Hz, NC^{12}*H*$_2$CHCH$_2$), 4.44 (1H, dd, *J* = 12.3 Hz and 3.4 Hz, OC^{8}*H*$_A$H$_B$CHCH$_2$), 4.64 (1H, dd, *J* = 14.5 Hz and 5.2 Hz, OC^{8}H$_A$*H*$_B$CHCH$_2$), 5.08 (1H, dd, *J* = 9.8 Hz and 1.0 Hz, NCH$_2$CHC^{14}*H*$_A$H$_B$), 5.13 (1H, dd, *J* = 15.0 Hz and 1.1 Hz, NCH$_2$CHC^{14}H$_A$*H*$_B$), 5.26 (1H, dd, *J* = 10.6 Hz and 1.4 Hz, OCH$_2$CHC^{10}*H*$_A$H$_B$), 5.36 (1H, dd, *J* = 17.3 Hz and 1.4 Hz, OCH$_2$CHC^{10}H$_A$*H*$_B$), 5.78–6.14 (2H, m, OCH$_2$C^{9}*H*CH$_2$ and NCH$_2$C^{13}*H*CH$_2$), 6.71 (1H, d, *J* = 8.1 Hz, ArC^{6}H), 6.80 (1H, t, *J* = 7.5 Hz and 7.5 Hz, ArC^{5}H), 6.99–7.23 (5H, m,

ArC^{4}H, ArC^{19}H, ArC^{21}H, ArC^{3}H and ArC^{20}H), 7.32 (2H, d, *J* = 7.2 Hz, ArC^{18}H and ArC^{22}H); ^{13}C NMR (75MHz; $CDCl_3$) δ (ppm) = 52.0 (NC^{12}H$_2$CHCH$_2$), 68.5 (OC^{8}H$_2$CHCH$_2$), 112.5 (NCH$_2$CHCH$_2$), 117.2 (OCH$_2$CHCH$_2$), 117.5 (ArC^{6}H), 120.6 (ArC^{4}H), 127.1 (ArC^{3}H), 128.0 (ArC^{5}H), 128.4 (ArC^{18}H and ArC^{22}H), 129.2 (ArC^{19}H and ArC^{21}H), 129.9 (ArC^{20}H), 132.0 (ArC^{2}), 132.5 (OCH$_2$C^{9}HCH$_2$), 133.4 (NCH$_2$C^{13}HCH$_2$), 136.3 (ArC^{17}), 153.5 (ArC^{1}), 171.1 (C=O).

5.2.2.3 *N*-(Prop-2-en-1-yl)-*N*-(2-(prop-1-en-1-yloxy)phenyl)benzamide 154

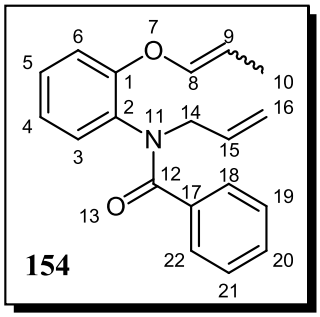

154

N-(2-(Prop-1-en-1-yloxy)phenyl)benzamide **153** (0.297 g, 1.17 mmol, 1 equiv.) was dissolved in dry DMF (30 mL) and the temperature of the mixture lowered to 0 °C, followed by the sequential addition of NaH (60% in oil, 54.0 mg, 1.41 mmol, 1.2 equiv.) and allyl bromide (0.28 g, 2.35 mmol, 0.20 mL, 2 equiv.). The reaction mixture was then stirred at r.t. for 24 h under a N_2 atmosphere. Water (80 mL) was added to quench the reaction mixture, which was then extracted with EtOAc (3 × 50 mL) and the combined fractions dried ($MgSO_4$). The solvent was then removed under reduced pressure and the resulting crude residue passed through a silica gel column (20% EtOAc/hexane) to afford *N*-(prop-2-en-1-yl)-*N*-(2-(prop-1-en-1-yloxy)phenyl)benzamide **154** as a pale yellow oil (0.327 g, 95%) as a mixture of *E/Z* isomers (ratio 65:35). R_f = 0.17 (10% EtOAc/hexane); *m/z* (EI): 293 (M^+, 28%), 236 (38), 188 (5), 160 (28), 105 (75), 77 (44), 51 (6); HRMS: calcd for $C_{19}H_{19}NO_2$ 293.1416 found: 293.1424; ν_{max} (ATR)/cm^{-1}: 1639, 1496, 1384, 1255, 1213, 1124, 1018, 907, 791, 725, 646; ^{1}H NMR (300MHz; $CDCl_3$, ***cis*[1]** and ***trans*[2]** isomers) δ (ppm) = 1.63[2] and 1.69[1] (3H, dd and dd, *J* = 6.9 Hz and 1.5 Hz, and *J* = 6.9 Hz and 1.6 Hz, OCHCHC^{10}*H$_3$*), 4.20–4.60 (2H, br m, NC^{12}*H$_2$*CHCH$_2$), 4.84–4.94[1] and 5.29–5.41[2] (1H, 2 × m, OCHC^{9}*H*CH$_3$), 5.09–5.15 (2H, m, NCH$_2$CHC^{14}*H$_2$*), 5.86–6.12 (2H, m, OC^{8}*H*CHCH$_3$ and NCH$_2$C^{13}*H*CH$_2$), 6.80–6.92 (2H, m, 2 × ArH), 7.03–7.23 (5H, m, 5 × ArH), 7.32–7.36 (2H, m, 2 × ArH); ^{13}C NMR (75MHz; $CDCl_3$, *cis*{*trans*}) δ (ppm) = 9.4 and 12.1 (OCHCH*C*^{10}H$_3$), 52.3 and 52.2 (NC^{12}H$_2$CHCH$_2$), 108.6 and 109.8

(OCH*C*^{9}HCH$_3$), 115.5 and 115.6 (ArC^{6}H), 117.7 and 117.6 (NCH$_2$CH*C*^{14}H$_2$), 122.4 and 122.3 (ArC^{4}H), 127.3 and 127.3 (ArC^{3}H), 128.1 (ArC^{5}H), 128.6 and 128.5 (ArC^{18}H), 128.6 and 128.5 (ArC^{22}H), 129.4 (ArC^{2}), 130.0 and 129.9 (ArC^{19}H), 130.0 and 129.9 (ArC^{21}H), 132.4 and 132.3 (ArC^{20}H), 133.2 and 133.3 (NCH$_2$*C*^{13}HCH$_2$), 136.1 (ArC^{17}), 140.0 and 140.9 (OCH*C*^{8}HCH$_3$), 152.6 (ArC^{1}), 171.0 (C=O).

5.2.3 Isomerization reactions

5.2.3.1 *N*-[2-(Prop-1-en-1-yloxy)phenyl]benzamide 153

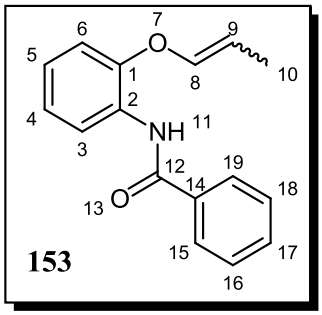

153

N-[2-(Prop-2-en-1-yloxy)phenyl]benzamide **148** (0.401 g, 1.58 mmol) and [RuClH(CO)(PPh$_3$)$_3$] **15** (60.3 mg, 0.0633 mmol, 4 mol%) were reacted under solventless conditions. The reaction mixture was heated at 65 °C for 24 h under an Ar atmosphere. The reaction solution was then diluted with a 5% EtOAc/hexane mixture (150 mL) and filtered through a compacted celite plug to remove the catalyst; the solvent was then removed under reduced pressure and the resulting crude residue passed through a silica gel column (10% EtOAc/hexane) to afford *N*-[2-(prop-1-en-1-yloxy)phenyl]benzamide **153** as a yellow oil (0.368 g, 92%) as a mixture of *E/Z* isomers (ratio 1:2). R_f = 0.57 (20% EtOAc/hexane); *m/z* (EI): 253 (M^+, 34%), 196 (35), 105 (100), 77 (23), 51 (8); HRMS: calcd for $C_{16}H_{15}NO_2$ 253.1103, found: 253.1091; ν_{max} (ATR)/cm^{-1}: 3433, 3019, 2401, 1672, 1604, 1525, 1477, 1453, 1332, 1256, 1205, 1128, 1017, 928, 709, 667; ^{1}H NMR (300MHz; $CDCl_3$, *cis*^{1} and *trans*^{2} and isomers) δ (ppm) = 1.68^{2} and 1.75^{1} (3H, dd and dd, *J* = 6.9 Hz and 1.4 Hz and *J* = 6.9 Hz and 1.6 Hz, OCHCHC^{10}*H*$_3$), 4.92–5.10^{1} and 6.33–6.43^{2} (1H, 2 × m, OCHC^{9}*H*CH$_3$), 6.34–6.40 (1H, m, OC^{8}*H*CHCH$_3$), 6.98–7.10 (3H, m, 3 × ArH), 7.43–7.58 (3H, m, 3 × ArH), 7.89 (2H, dd, *J* = 6.5 Hz and 1.6 Hz, 2 × ArH), 8.46–8.59 (2H, m, ArH and NH); ^{13}C NMR (75MHz; $CDCl_3$, δ (ppm) = 9.3 and 12.6 (OCHCH*C*^{10}H$_3$), 108.7 and 109.6 (OCH*C*^{9}HCH$_3$), 114.0 and 114.6 (ArC^{6}H), 120.3

(ArC^4H), 122.9 and 123.0 (ArC^3H), 123.8 (ArC^5H), 126.8 and 126.9 ($ArC^{15}H$ and $ArC^{19}H$), 128.3 (ArC^2), 128.7 and 128.6 ($ArC^{16}H$ and $ArC^{18}H$), 131.7 ($ArC^{17}H$), 135.0 (ArC^{14}), 140.4 and 141.5 (OC^8HCHCH_3), 146.1 and 146.0 (ArC^1), 165.0 and 165.1 (C=O).

5.2.3.2 *N*-(Prop-1-en-1-yl)-*N*-(2-(prop-1-en-1-yloxy)phenyl)benzamide 151

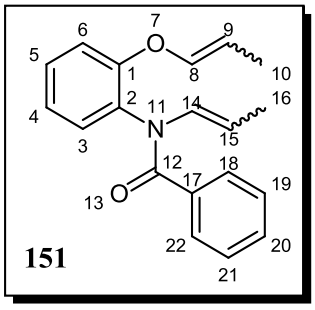

N-(Prop-2-en-1-yl)-*N*- [2-(prop-2-en-1-yloxy) phenyl] benzamide **149** (0.329 g, 1.12 mmol) and $[RuClH(CO)(PPh_3)_3]$ **15** (53.4 mg, 0.0561 mmol, 5 mol%) were reacted without solvent. The reaction mixture was heated at 65 °C for 24 h under an Ar atmosphere. The reaction solution was then diluted with a 5% EtOAc/hexane mixture (150 mL) and filtered through a compacted celite plug to remove the catalyst. The solvent was then removed under reduced pressure and the resulting crude residue passed through a silica gel column (10% EtOAc/hexane) to afford *N*-(prop-1-en-1-yl)-*N*-(2-(prop-1-en-1-yloxy)phenyl)benzamide **151** as a yellow oil (0.321 g, 98%) as a mixture of *E/Z* isomers (ratio 1:2). R_f = 0.47 (20% EtOAc/hexane); *m/z* (EI): 293 (M^+, 34%), 264 (68), 253 (4), 236 (100), 220 (15), 188 (10), 176 (4), 161 (4); HRMS: calcd for $C_{19}H_{19}NO_2$ 293.1416, found: 293.1416; ν_{max} (ATR)/cm^{-1}: 2920, 1650, 1588, 1495, 1447, 1386, 1355, 1319, 1272, 1247, 1159, 1117, 1017, 944, 877; ^1H NMR (300MHz; $CDCl_3$) δ (ppm) = 1.45–1.87 (6H, m, $OCHCHC^{10}H_3$ and $NCHCHC^{16}H_3$), 4.55–4.76 (1H, m, $NCHC^{15}HCH_3$), 4.79–4.99 and 5.22–5.46 (1H, 2 × m, $OCHC^9HCH_3$), 5.88–6.26 (1H, m, OC^8HCHCH_3), 6.80–6.91 (1H, m, ArC^6H), 6.92–7.02 (1H, m, $NC^{14}HCHCH_3$), 7.11–7.54 (8H, m, ArC^{3-5} and $ArC^{18-22}H$); ^{13}C NMR (75MHz; $CDCl_3$) δ (ppm) = 9.4 and 12.1 ($OCHCHC^{10}H_3$), 15.0 and 15.1 ($NCHCHC^{16}H_3$), 108.8 and 109.9 ($OCHC^9HCH_3$), 109.3 ($NCHC^{15}HCH_3$), 115.8 and 116.2 (ArC^6H), 122.6 (ArC^4H), 127.5 (ArC^3H and ArC^5H), 128.0 ($ArC^{18}H$ and

ArC^{22}H), 129.3 (ArC^{2}), 129.4 (ArC^{19}H and ArC^{21}H), 129.7 (N*C*^{14}HCHCH$_3$), 130.9 (ArC^{20}H), 135.9 (ArC^{17}), 140.0 and 140.1 (O*C*^{8}HCHCH$_3$), 152.9 (ArC^{1}), 169.1 (C=O).

5.2.4 RCM reactions

5.2.4.1 4*H*-1,4-Benzoxazin-4-yl(phenyl)methanone 152

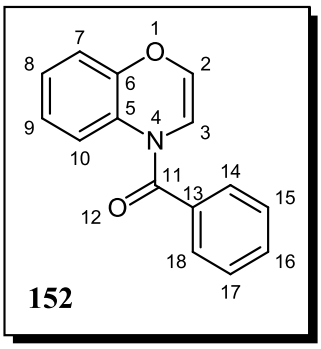

152

N-(Prop-1-en-1-yl)-*N*-(2-(prop-1-en-1-yloxy)phenyl) benzamide **151** (0.362 g, 1.24 mmol) and Grubbs' II catalyst **6** (83.9 mg, 0.0988 mmol, 8 mol%) were dissolved in distilled, degassed toluene (15 mL). The reaction mixture was then stirred at 90 °C for 8 h under an Ar atmosphere. After cooling, the reaction mixture was diluted with a 10% EtOAc/hexane mixture (100 mL) and filtered through a compacted celite plug to remove the catalyst. The solvent was then removed under reduced pressure and the resulting crude residue passed through a silica gel column (10% EtOAc/hexane) to afford 4*H*-1,4-benzoxazin-4-yl(phenyl)methanone **152** as a yellow oil (0.281 g, 96%). R_f = 0.30 (10% EtOAc/hexane); *m/z* (EI): 237 (M^+, 33%), 238 (6), 219 (23), 132 (18), 105 (100), 77 (62), 51 (16); HRMS: calcd for $C_{15}H_{11}NO_2$ 237.0790, found: 237.0789; ν_{max} (ATR)/cm^{-1}: 1640, 1585, 1492, 1462, 1444, 1352, 1304, 1276, 1205, 1169, 1127, 1081, 1050, 1018, 936, 906, 856, 813; ^{1}H NMR (300MHz; $CDCl_3$) δ (ppm) = 6.05 (1H, d, *J* = 4.5 Hz, OC^{2}*H*CHN), 6.27 (1H, br d, *J* = 2.5 Hz, NC^{3}*H*CHO), 6.84 (1H, dd, *J* = 8.0 Hz and 1.1 Hz, ArC^{7}H), 6.90 (1H, dt, *J* = 8.1 Hz, 8.0 Hz and 1.0 Hz, ArC^{9}H), 7.04 (1H, dt, *J* = 7.8 Hz, 7.8 Hz and 1.2 Hz, ArC^{8}H), 7.37–7.50 (3H, m, ArC^{15}H, ArC^{16}H and ArC^{17}H), 7.56 (2H, dd, *J* = 7.7 Hz and 1.4 Hz, ArC^{14}H and ArC^{18}H), 7.65 (1H, br d, *J* = 1.14 Hz,

ArC^{10}H); ^{13}C NMR (75MHz; $CDCl_3$) δ (ppm) = 111.6 (N*C*^{3}HCHO), 116.6 (O*C*^{2}HCHN), 116.6 (ArC^{7}H), 122.4 (ArC^{10}H), 123.5 (ArC^{9}H), 126.5 (ArC^{8}H), 127.9 (ArC^{14}H and ArC^{18}H), 128.5 (ArC^{15}H and ArC^{17}H), 130.7 ArC^{16}H), 131.7 (ArC^{5}), 134.9 (ArC^{13}), 147.4 (ArC^{6}), 166.7 (C=O).

5.2.4.2 1,5-Benzoxazepin-5(4*H*)-yl(phenyl)methanone 155

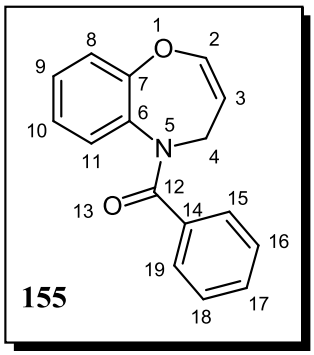

155

N-(Prop-2-en-1-yl)-*N*-(2-(prop-1-en-1-yloxy) phenyl) benzamide **154** (0.301 g, 1.10 mmol) and Grubbs' II catalyst **6** (43.6 mg, 0.0513 mmol, 5 mol%) were dissolved in distilled, degassed toluene (15 mL). The reaction mixture was then stirred at 80 °C for 8h under an Ar atmosphere. After cooling, the reaction mixture was diluted with a 10% EtOAc/hexane mixture (100 mL) and filtered through a compacted celite plug to remove the catalyst. The solvent was then removed under reduced pressure and the resulting crude residue passed through a silica gel column (10% EtOAc/hexane) to afford 1,5-benzoxazepin-5(4*H*)-yl(phenyl)methanone **155** as a low melting point solid (0.13 g, 100%). R_f = 0.14 (10% EtOAc/hexane), mp = 27–28 °C; *m/z* (EI): 252 (M^+ +1, 94%), 251 (M^+ , 30%), 196 (8), 154 (40), 136 (38), 131 (15), 120 (9); HRMS: calcd for $C_{16}H_{13}NO_2$ 251.0946, found: 251.0946; ν_{max} (ATR)/cm^{-1}: 1657, 1593, 1537, 1469, 1414, 1364, 1325, 1287, 1264, 1202, 1168, 1123, 1093, 1040, 1007, 940, 887, 865, 813, 785, 724, 700, 658, 629; ^{1}H NMR (300 MHz, $CDCl_3$, one proton for NCH_2 not observed* in spectrum due to very broad peaks caused by amide rotamers): δ (ppm) = 3.76 and 5.36 (1H*, 2 × br s, N*C*^{4}*H*$_2$CHCHO), 4.94 (1H, d, *J* = 3.1 Hz, NCH_2C^{3}*H*CHO), 6.51–6.58 (1H, m, NCH_2CHCH^{2}O), 6.70 (1H, br s, ArC^{8}H), 6.80 (1H, br s, ArC^{9}H), 7.10–7.31 (7H, m, 7 × ArCH); ^{13}C NMR (75 MHz, $CDCl_3$): δ(ppm) = 44.5 (N*C*^{4}H$_2$CHCHO), 105.0 (NCH_2*C*^{3}HCHO), 121.1 (ArC^{8}H), 124.5 (ArC^{11}H), 127.8 (ArC^{10}H), 128.0 (ArC^{9}H),

128.4 (ArC^{15}H and ArC^{19}H), 129.5 (ArC^{16}H and ArC^{18}H), 129.9 (ArC^{17}H), 134.8 (ArC^{6}), 135.4 (ArC^{14}), 142.9 (O*C*^{2}HCHCH$_2$O), 153.2 (ArC^{7}), 169.8 (C=O).

5.2.4.3 2,5-Dihydro-6*H*-1,6-benzoxazocin-6-yl(phenyl)methanone 150

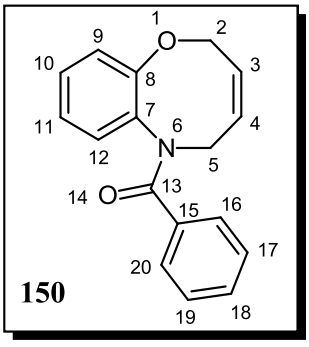

150

N-(Prop-2-en-1-yl)-*N*-[2-(prop-2-en-1-yloxy)phenyl] benzamide **149** (0.201 g, 0.682 mmol, 1 equiv.) and Grubbs' II catalyst **6** (29.0 mg, 0.0341 mmol, 5 mol%) were dissolved in distilled, degassed toluene (15 mL). The reaction mixture was then stirred at 90 °C for 18 h under an Ar atmosphere. After cooling, the reaction mixture was diluted with a 10% EtOAc/hexane mixture and filtered through a compacted celite plug (3 ×) to remove the catalyst. The solvent was then removed under reduced pressure and the resulting crude residue passed through a silica gel column (15% EtOAc/hexane) to afford 2,5-dihydro-6*H*-1,6-benzoxazocin-6-yl(phenyl)methanone **150** as a low melting point solid (0.142 g, 88%). R_f = 0.13 (20% EtOAc/hexane), mp = 29–30 °C; *m/z* (EI): 265 (M^+, 4%), 251 (30), 234 (5), 146 (6), 131 (24), 105 (100), 77 (42), 51 (9); HRMS: calcd for $C_{17}H_{15}NO_2$ 265.1103, found: 265.1118; ν_{max} (ATR)/cm^{-1}: 1645, 1497, 1360, 1325, 1274, 1249, 1134, 1018, 906, 725, 647; ^{1}H NMR (300 MHz, $CDCl_3$): δ(ppm) = 3.95–5.48 (4H, m, NC^{5}*H*$_2$ and OC^{2}*H*$_2$), 5.8 (1H, dt, *J* = 10.4 Hz and 8.3 Hz, OCH$_2$C^{3}*H*), 5.95 (1H, dt, *J* = 10.3 Hz and 4.0 Hz, NCH$_2$C^{4}*H*), 6.79 (2H, dq, *J* = 8.0 Hz, 7.9 Hz and 1.0 Hz, ArC^{10}H and ArC^{11}H), 6.89 (1H, br dd, *J* = 8.2 Hz and 0.6 Hz, ArC^{9}H), 7.06–7.14 (1H, m, ArC^{12}H), 7.14–7.27 (3H, m, ArC^{17}H, ArC^{19}H and ArC^{18}H), 7.38 (2H, d, *J* = 7.6 Hz and 1.0 Hz, ArC^{16}H and ArC^{20}H); ^{13}C NMR (75 MHz, $CDCl_3$): δ(ppm) = 49.1 (NC^{5}H$_2$), 65.2 (OC^{2}H$_2$), 121.3 (Ar*C*^{9}H), 122.3 (Ar*C*^{12}H), 124.7 (ArC^{11}H), 27.4 (ArC^{10}H),

127.6 (OCH_2C^3H), 128.1 ($ArC^{16}H$ and $ArC^{20}H$), 129.4 ($ArC^{17}H$ and $ArC^{19}H$), 130.1 (NCH_2C^4H), 131.4 ($ArC^{18}H$), 132.8 (ArC^7), 135.6 (ArC^{15}), 153.1 (ArC^8), 171.2 (C=O).

5.3 The *N,N*-benzo-fused heterocycles

5.3.1 Protection of the precursor

5.3.1.1 *N,N'*-Benzene-1,2-diyldiacetamide 157

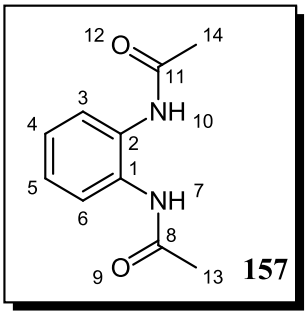

157

Benzene-1,2-diamine **156** (2.29 g, 21.2 mmol, 1 equiv.) was dissolved in pyridine (6.49 g, 63.6 mmol, 10.0 mL, 10.7 equiv.) and the temperature of the mixture lowered to 0 °C in an ice bath. Acetic anhydride (3.53 g, 34.5 mmol, 3.26 mL, 3 equiv.) was then added drop wise over 5 minutes. The reaction mixture was then stirred at r.t. for 24 h under a N_2 atmosphere. The reaction mixture was then quenched with enough $NaHCO_3$ to bring the pH to ~8. The reaction mixture was then extracted with ethyl acetate (3 × 50 mL) and dried ($MgSO_4$), after which the solvent was removed under reduced pressure to afford *N,N'*-benzene-1,2-diyldiacetamide **157** as a white crystalline powder (3.78 g, 93%). ^{1}H NMR (300 MHz, $CDCl_3$): δ(ppm) = 2.09 (6H, s, $OC^{13}H_3$ and $OC^{14}H_3$), 7.17 (2H, dd, J = 5.7 Hz and 3.7 Hz, ArC^4H and ArC^5H), 7.29 (2H, dd, J = 5.6 Hz and 3.7 Hz, ArC^3H and ArC^6H), 8.44 (2H, s, N^7H and $N^{10}H$); ^{13}C NMR (75 MHz, $CDCl_3$): δ(ppm) = 23.8 ($OC^{13}H_3$ and $OC^{14}H_3$), 125.5 (ArC^4H and ArC^5H), 126.1 (ArC^3H and ArC^6H), 130.5 (ArC^1 and ArC^2), 169.9 (C^8=O and C^{11}=O). {The identity of this compound was confirmed with ^{1}H and ^{13}C NMR and submitted directly to the next step.}

5.3.2 Allylation reactions

5.3.2.1 *N*-[2-(Acetylamino)phenyl]-*N*-(prop-2-en-1-yl)acetamide 158

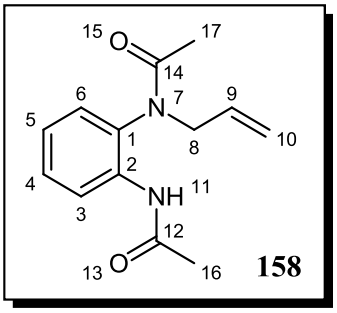

158

[Method 1] *N*,*N*'-Benzene-1,2-diyldiacetamide **157** (0.200 g, 1.04 mmol, 1 equiv.) was dissolved in dry acetone (30 mL) and the temperature of the solution lowered to –14 °C (using an ice and salt slurry), followed by the sequential addition of NaH (60% in oil, 40.0 mg, 1.04 mmol, 1 equiv.) and allyl bromide (0.138 g, 1.15 mmol, 0.10 mL, 1.1 equiv.). The reaction mixture was then stirred at r.t. for 12 h under a N_2 atmosphere. The reaction mixture was then quenched with water (100 mL) and extracted with EtOAc (3 × 50 mL) and the combined fractions dried ($MgSO_4$). The solvent was then removed under reduced pressure and the resulting crude residue passed through a silica gel column (100% EtOAc) to afford *N*-[2-(acetylamino)phenyl]-*N*-(prop-2-en-1-yl)acetamide **158** as a pale yellow oil (0.229 g, 95%).

[Method 2] *N*,*N*'-Benzene-1,2-diyldiacetamide **157** (0.274 g, 1.43 mmol, 1 equiv.) was dissolved in dry DMF (30 mL) and the temperature of the solution lowered to 0 °C, followed by the sequential addition of NaH (60% in oil, 54.7 mg, 1.43 mmol, 1 equiv.) and allyl bromide (0.172 g, 1.43 mmol, 0.12 mL, 1 equiv.). The reaction mixture was then stirred at r.t. for 12 h under a N_2 atmosphere. The reaction mixture was then

quenched with water (100 mL) and extracted with EtOAc (3 × 50 mL), the combined fractions were then dried ($MgSO_4$). The solvent was then removed under reduced pressure and the resulting crude residue passed through a silica gel column (100% EtOAc) to afford *N*-[2-(acetylamino)phenyl]-*N*-(prop-2-en-1-yl)acetamide **158** as a pale yellow oil (0.312 g, 94%).

R_f = 0.40 (100% EtOAc); *m/z* (EI): 232 (M^+, 20%), 213 (30), 189 (90), 172 (100), 147 (75), 130 (68), 119 (100), 107 (32), 77 (15); HRMS: calcd for $C_{13}H_{16}N_2O_2$ 232.12118, found: 232.12117; ν_{max} (ATR)/cm^{-1}: 3278, 1696, 1641, 1592, 1525, 1452, 1395, 1289, 1231, 1112, 1080, 1038, 980, 929, 875, 759, 678; ^{1}H NMR (300 MHz, $CDCl_3$): δ(ppm) = 1.83 (3H, m, $OC^{16}H_3$), 2.25 (3H, m, $OC^{17}H_3$), 3.93 (1H, dd, *J* = 14.2 Hz and 7.2 Hz, $NCH_2CHCH_AH_B$), 4.50 (1H, dd, *J* = 14.2 Hz and 5.9 Hz, $NCH_2CHCH_AH_B$), 5.12 (2H, dd, *J* = 17.6 Hz and 14.0 Hz, $NC^8H_2CHCH_2$), 5.75–6.02 (1H, m, $NCH_2C^9HCH_2$), 7.04–7.20 (2H, m, ArC^3H and $N^{11}H$), 7.32–7.43 (1H, m, ArC^4H), 8.38 (1H, br d, *J* = 8.0 Hz ArC^5H), 8.57 (1H, br s, ArC^6H); ^{13}C NMR (75 MHz, $CDCl_3$): δ(ppm) = 22.6 ($OC^{17}H_3$), 24.4 ($OC^{16}H_3$), 50.8 ($NC^8H_2CHCH_2$), 119.3 ($NCH_2CHC^{10}H_2$), 122.6 (ArC^3H), 124.2 (ArC^6H), 129.1 (ArC^4H), 129.1 (ArC^5H), 131.1 ($NCH_2C^9HCH_2$), 132.1 (ArC^1), 135.2 (ArC^2), 169.3 (C^{14}=O), 171.0 (C^{12}=O).

5.3.2.2 *N*,*N*'-Benzene-1,2-diyl*bis*[*N*-(prop-2-en-1-yl)acetamide] 159

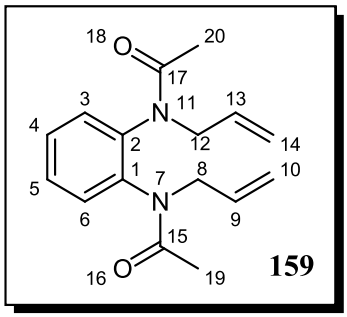

159

N,*N*'-Benzene-1,2-diyldiacetamide **157** (0.478 g, 2.49 mmol, 1 equiv.) was dissolved in dry acetone (15 mL) and the temperature of the mixture lowered to –14 °C (using an ice and salt slurry), followed by the sequential addition of NaH (60% in oil, 0.191 g, 4.97 mmol, 2 equiv.) and Allyl bromide (0.662 g, 5.47 mmol, 0.47 mL, 2.2 equiv.). The reaction mixture was then stirred at r.t. for 24 h under a N_2 atmosphere. The reaction mixture was then quenched with water (100 mL) and extracted with EtOAc (3 × 50 mL) and the combined fractions dried ($MgSO_4$). The solvent was then removed under reduced pressure and the resulting crude residue passed through a silica gel column (100% EtOAc) to afford *N*,*N*'-benzene-1,2-diyl*bis*[*N*-(prop-2-en-1-yl)acetamide] **159** as a white solid (0.626 g, 93%). mp 25–26 °C; R_f = 0.27 (100% EtOAc); *m/z* (EI): 272 (M^+, 2%), 230 (22), 213 (100), 187 (46), 172 (20), 159 (48), 145 (32), 119 (34), 92 (8), 77 (9); HRMS: calcd for $C_{16}H_{20}N_2O_2$ 272.1525, found: 272.1526; ν_{max} (ATR)/cm^{-1}: 2916, 1645, 1594, 1499, 1441, 1378, 1333, 1298, 1281, 1250, 1228, 1205, 1114, 1081, 1018, 982, 939; ^{1}H NMR (300 MHz, $CDCl_3$): δ(ppm) = 2.04 (6H, s, $OC^{19}H_3$ and $OC^{20}H_3$), 3.78 (1H, dd, *J* = 15.0 Hz and 7.6 Hz, $NCH_2CHC^{10/14}H_AH_B$), 5.20 (1H, dd, *J* = 15.0 Hz and 5.1 Hz, $NCH_2CHC^{10/14}H_2$), 5.26–5.44 (2H, m, $NC^{8/12}H_2CHCH_2$), 6.02–6.23 (m, 1H, $NCH_2C^{9/13}HCH_2$), 7.47 (2H, dd, *J* = 5.8 Hz and 3.6 Hz, ArC^3H and ArC^6H), 7.71 (2H, dd, *J* = 5.8 Hz and 3.6 Hz, ArC^5H and ArC^4H); ^{13}C NMR (75 MHz, $CDCl_3$): δ(ppm) =

22.7 ($OC^{19}H_3$ and $OC^{20}H_3$), 49.9 ($NC^8H_2CHCH_2$ and $NC^{12}H_2CHCH_2$), 118.1 ($NCH_2CHC^{10}H_2$ and $NCH_2CHC^{14}H_2$), 129.0 (ArC^3H and ArC^6H), 131.9 (ArC^4H and ArC^5H), 132.5 ($NCH_2C^9HCH_2$ and $NCH_2C^{13}HCH_2$), 138.7 (ArC^1 and ArC^2), 169.8 (C^{19}=O and C^{20}=O).

5.3.2.3 *N*-{2-[Acetyl(prop-1-en-1-yl)amino]phenyl}-*N*-(prop-2-en-1-yl)acetamide 164

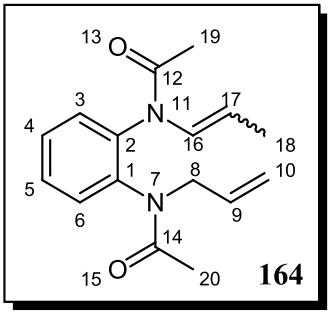

164

N-[2-(Acetylamino)phenyl]-*N*-(prop-2-en-1-yl)acetamide **163** (0.100 g, 0.431 mmol, 1 equiv.) was dissolved in dry acetone (10 mL) and the temperature of the mixture lowered to –14 °C (using an ice and salt slurry), followed by the sequential addition of NaH (60% in oil, 19.8 mg, 0.517 mmol, 1.2 equiv.) and allyl bromide (0.125 g, 1.03 mmol, 0.10 mL, 2.4 equiv.). The reaction mixture was then stirred at r.t. for 24 h under a N_2 atmosphere. The reaction mixture was then quenched with water (100 mL) and extracted with EtOAc (3 × 50 mL) and the combined fractions dried ($MgSO_4$). The solvent was then removed under reduced pressure and the resulting residue passed through a silica gel column (100% EtOAc) to afford *N*-{2-[acetyl(prop-1-en-1-yl)amino]phenyl}-*N*-(prop-2-en-1-yl) acetamide **161** as a pale yellow oil (0.116 g, 99%). R_f = 0.57 (100% EtOAc); *m/z* (EI): 272 (M^+, 4%), 257 (2), 229 (56), 213 (100), 187 (52), 159 (35), 146 (42), 130 (25), 119 (54), 92 (9), 77 (5); HRMS: calcd for $C_{16}H_{20}N_2O_2$ 272.1525, found: 272.1529; ν_{max} (ATR)/cm^{-1}: 2924, 1644, 1596, 1496, 1447, 1382, 1304, 1257, 1214, 1160, 1124, 1086, 1018, 925, 792, 734, 698, 640; ^{1}H NMR (300 MHz, $CDCl_3$): δ(ppm) = 1.54–1.70 (3H, m, $NCHCHC^{18}H_3$), 1.75–2.33 (6H, m, $OC^{19/20}H_3$), 3.36–4.30 (1H, m, $NCH_2CHCH_AH_B$), 4.31–4.70 (1H, m, $NCH_2CHCH_AH_B$), 4.70–4.94 (1H, m, $NCHC^{17}HCH_3$), 4.93–5.29 (2H, m, $NC^8H_2CHCH_2$), 5.63–6.03 (1H, m, $NCH_2C^9HCH_2$), 7.09–7.34 (2H, m, $NC^{16}HCHCH_3$ and ArC^5H), 7.34–7.58 (3H, m, 3 × ArCH); ^{13}C NMR (75 MHz, $CDCl_3$):

δ(ppm) = 14.8 (NCHCH*C*^{18}H$_3$), 22.2 (O*C*^{19}H$_3$), 22.3 (O*C*^{20}H$_3$), 50.3 (N*C*^{8}H$_2$CHCH$_2$), 112.7 (NCH*C*^{17}HCH$_3$), 117.4 (NCH$_2$CH*C*^{10}H$_2$), 128.2 (Ar*C*^{3}H), 128.6 (Ar*C*^{6}H), 128.9 (Ar*C*^{4}H), 129.2 (Ar*C*^{5}H), 131.1 (Ar*C*^{1}), 131.8 (Ar*C*^{2}), 132.6 (N*C*^{16}HCHCH$_3$), 136.8 (NCH$_2$*C*^{9}HCH$_2$), 169.0 (*C*^{12}=O), 169.8 (*C*^{14}=O).

5.3.3 Isomerization reactions

5.3.3.1 *N,N′*-Benzene-1,2-diyl*bis*[*N*-(prop-1-en-1-yl)acetamide] 161

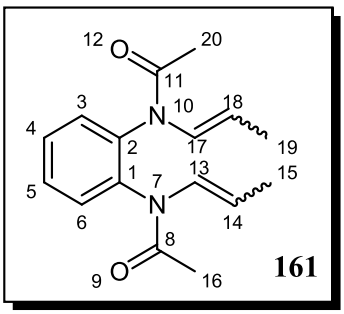

161

[Method 1] *N,N*′-Benzene-1,2-diyl*bis*[N-(prop-2-en-1-yl) acetamide] **159** (0.351 g, 1.29 mmol, 1 equiv.) and [RuClH(CO)(PPh$_3$)$_3$] **15** (61.4 mg, 0.0664 mmol, 5 mol%) were reacted directly. The reaction mixture was stirred at 80 °C for 20 h under an Ar atmosphere. The reaction solution was then diluted with 10% EtOAc/hexane mixture (50 mL) and passed through a compacted Celite plug (4 ×) to remove the catalyst and the solvent then removed under reduced pressure. The resulting crude residue was passed through a silica gel column (100% EtOAc) to afford *N,N*′-benzene-1,2-diyl*bis*[*N*-(prop-1-en-1-yl)acetamide] **161** (a complex mixture of 3 isomers) as a pale yellow oil (0.325 g, 93%).

[Method 2] *N,N*′-Benzene-1,2-diyl*bis*[*N*-(prop-2-en-1-yl)acetamide] **159** (0.101 g, 0.371 mmol, 1 equiv.) and [RuClH(CO)(PPh$_3$)$_3$] **15** (17.7 mg, 0.0184 mmol, 5 mol%) were dissolved in degassed toluene (1 mL) and irradiated under microwave conditions (power: 200W with cooling, ramp time: 2 °C per min, temperature: 80 °C, maximum pressure 100 psi) in a pressure tube for 22 min. The reaction solution was then diluted with EtOAc (50 mL) and passed through a compacted Celite plug (4 ×) to remove the catalyst. The solvent then removed under reduced pressure and the resulting crude residue passed through a Flash silica gel column (15% EtOAc/hexane) to afford *N,N*′-benzene-1,2-

diyl*bis*[*N*-(prop-1-en-1-yl)acetamide] **161** (a complex mixture of 3 isomers) as a pale yellow oil (96.5 mg, 96%).

R_f = 0.67 (10% EtOAc/Hexane); *m/z* (EI): 274 (M^+ +2, 4%), 273 (M^+ +1, 18%), 272 (M^+, 100%), 271 (6), 270 (1), 268 (1); HRMS: calcd for $C_{16}H_{20}N_2O_2$ 272.1524, found: 272.1519; ν_{max} (ATR)/cm^{-1}: 2921, 1656, 1597, 1495, 1453, 1369, 1347, 1314, 1294, 1273, 1133, 1095, 1036, 948, 919, 729, 646; ^{1}H NMR (300 MHz, $CDCl_3$,) δ (ppm) = 1.54–1.65 (6H, m, NCHCHC$^{15/19}H_3$), 1.74–1.88 (3H, m, OC$^{16}H_3$), 2.12–2.25 (3H, m, OC$^{20}H_3$), 4.39–4.93 (2H, m, NCHC$^{14/18}H$CH$_3$), 7.02–7.29 (2H, m, NCHC$^{14/18}H$CH$_3$), 7.31–7.60 (4H, m, 4 × ArCH); ^{13}C NMR (75 MHz, $CDCl_3$, *major*{*minor*}): δ(ppm) = 14.7 {14.8, 14.9} (NCHCHC$^{15/19}H_3$), 22.5 {22.7, 22.8} (OC$^{16/20}H_3$), 111.0 {113.3, 115.9} (NCHC$^{14/18}$HCH$_3$), 126.8 {128.4, 128.5} (ArC$^{3/6}$H), 128.8 {129.1, 129.5} {(ArC$^{4/5}$H), 131.0 {131.8, 131.9} (NC$^{13/17}$HCHCH$_3$), 136.9 {137.5, 137.7} (ArC$^{1/2}$), 168.5 {169.1, 169.2} (C$^{8/11}$=O).

5.3.3.2 *N*-[2-(Acetylamino)phenyl]-*N*-(prop-1-en-1-yl)acetamide 163

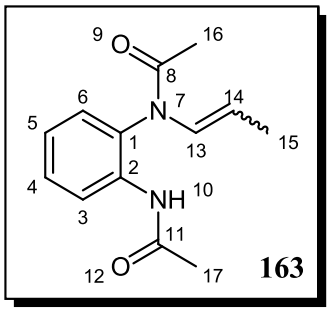

163

N-[2-(Acetylamino)phenyl]-*N*-(prop-2-en-1-yl)acetamide **158** (0.150 g, 0.646 mmol, 1 equiv.) and [RuClH(CO)(PPh_3)$_3$] **15** (30.8 mg, 0.0323 mmol, 5 mol%) were dissolved in degassed toluene (1 mL) and irradiated under microwave conditions (power: 150W with cooling, ramp time: 2 °C per min, temperature: 90 °C, maximum pressure: 100 psi) in a pressure tube for 10 min. The reaction solution was then diluted with a 5% EtOAc/hexane mixture (30 mL) and filtered through a compacted Celite plug (4 × 50 mL) to remove the catalyst. The solvent was then removed under reduced pressure and the resulting crude residue passed through a silica gel column (100% EtOAc) to afford *N*-[2-(acetylamino) phenyl]-*N*-(prop-1-en-1-yl)acetamide **163** (a single isomer) as a pale yellow oil (0.144 g, 96%). R_f = 0.60 (100% EtOAc); *m/z* (EI): 232 (M^+, 5%), 213 (4), 190 (18), 172 (100), 147 (24), 132 (28), 119 (74), 77 (5), 65 (8); HRMS: calcd for $C_{13}H_{16}N_2O_2$ 232.1212, found: 232.1214; ν_{max} (ATR)/cm^{-1}: 3428 (br), 2925, 1701, 1658, 1528, 1450, 1367, 1297, 1229,

1095, 723; ^{1}H NMR (300 MHz, $CDCl_3$): δ(ppm) = 1.64 (3H, dd, *J* = 6.7 Hz and 1.5 Hz, NCHCHC$^{15}H_3$), 1.82 (3H, s, OC$^{17}H_3$), 2.18 (3H, s, OC$^{16}H_3$), 4.49 (1H, qd, *J* = 13.6 Hz, 6.6 Hz, 6.6 Hz, and 6.6 Hz, NCHC^{14}HCH$_3$), 7.11 (br d, 1H, *J* = 7.8 Hz, NC^{13}HCHCH$_3$), 7.21 (dt, 1H, *J* = 7.6 Hz, 7.5 Hz and 1.2 Hz, ArC^{4}H), 7. 38–7.52 (3H, m, ArC^{5}H, ArC^{6}H and N^{10}H), 8.42 (1H, br d, *J* = 7.8 Hz, ArC^{3}H); ^{13}C NMR (75 MHz, $CDCl_3$): δ(ppm) = 15.0 (NCHCH*C*^{15}H$_3$), 22.9 (OC^{16}H$_3$), 24.8 (OC^{17}H$_3$), 109.2 (NCH*C*^{14}HCH$_3$), 122.5 (ArC^{6}H), 125.1 (ArC^{5}H), 126.4 (ArC^{4}H), 128.4 (ArC^{3}H), 129.9 (N*C*^{13}HCHCH$_3$), 132.0 (ArC^{2}), 135.1 (ArC^{1}), 168.7 (C^{8}=O), 169.0 (C^{11}=O).

5.3.4 RCM Reactions

5.3.4.1 Attempted synthesis of 1,1'-(1*H*-1,5-Benzodiazepine-1,5(2*H*)-diyl)diethanone 165

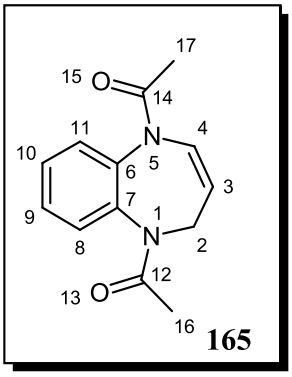

165

[Method 1] *N*-{2-[Acetyl(prop-1-en-1-yl)amino]phenyl}-*N*-(prop-2-en-1-yl) acetamide **164** (50.0 mg, 0.140 mmol. 1 equiv.) and Grubbs' II catalyst **6** (7.8 mg, 0.0092 mmol, 5 mol%) were dissolved in distilled, degassed toluene (1 mL) and irradiated under microwave conditions (power: 150W with cooling, ramp time: 2 °C per min, temperature: 90 °C, maximum pressure 100 psi) in a pressure tube for 20 min. After cooling, the reaction solution was then diluted with a 10% EtOAc/hexane mixture and filtered through a compacted Celite plug (4 ×) to remove the catalyst. The solvent was then removed under reduced pressure and the resulting crude residue passed through a silica gel column (100% EtOAc) to afford an unknown product as a dark oil (33.0 mg, 78%) and trace amounts of 1,1'-(1*H*-1,5-Benzodiazepine-1,5(2*H*)-diyl)diethanone **165** detected using HRMS. *m/z* (EI): 230 (M^{+}, 55%), 213 (4), 188 (65), 161 (12), 145 (100), 130 (32), 119 (74), 92 (8), 65 (8); HRMS: calcd for $C_{13}H_{14}N_2O_2$ 230.10553, found: 230.10563.

[Method 2] *N*-{2-[Acetyl(prop-1-en-1-yl)amino]phenyl}-*N*-(prop-2-en-1-yl) acetamide **164** (0.166 g, 0.610 mmol) and Grubbs' II catalyst **6** (41.4 mg, 0.0488 mmol, 8 mol%)

were dissolved in distilled, degassed toluene (10 mL). The reaction mixture was then stirred at 90 °C for 18 h under an Ar atmosphere. The reaction mixture was then evaporated under reduced pressure and the resultant crude product was purified by silica gel column chromatography utilizing gradient elution: 10% EtOAc/hexane mixture, to remove the catalyst, followed by 100% EtOAc to afford to afford an unknown product as a dark oil (20 mg, 15%).

5.3.4.1 1,1'-[(3*Z*)-2,5-Dihydro-1,6-benzodiazocine-1,6-diyl]diethanone 160

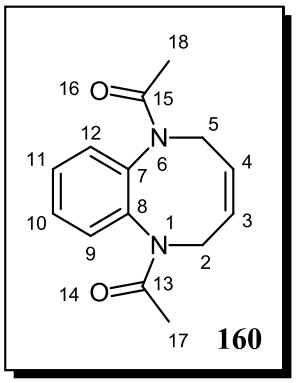

160

N,*N*'-benzene-1,2-diyl*bis*[*N*-(prop-2-en-1-yl)acetamide] **159** (0.141 g, 0.518 mmol) and Grubbs' II catalyst **6** (35.2 mg, 0.0414 mmol, 8 mol%) were dissolved in distilled, degassed toluene (15 mL). The reaction mixture was then stirred at 90 °C for 18 h under an Ar atmosphere. The reaction mixture was then evaporated under reduced pressure and the resultant crude product was purified by silica gel column chromatography utilizing gradient elution: 10% EtOAc/hexane mixture, to remove the catalyst, followed by 100% EtOAc to afford 1,1'-[(3*Z*)-2,5-dihydro-1,6-benzodiazocine-1,6-diyl]diethanone **160** as a dark oil (0.101 g, 80%). R_f = 0.28 (100% EtOAc); *m/z* (EI): 244 (M+, 34%), 230 (8), 202 (100), 184 (82), 159 (93), 143 (64), 119 (84), 93 (6), 92 (16), 77 (18), 65 (9); HRMS: calcd for $C_{14}H_{16}N_2O_2$ 244.1212, found: 244.1212; ν_{max} (ATR)/cm^{-1}: 2931, 1712, 1662, 1599, 1500, 1362, 1304, 1283, 1223, 1094, 1039, 905, 848, 772, 737, 707; ^{1}H NMR (300 MHz, $CDCl_3$): δ(ppm) = 1.82–2.00 (6H, m $OC^{17/18}H_3$), 3.47–5.19 (4H, m, $NC^2H_2CHCHC^5H_2N$), 5.82–6.11 (2H, m, $NCH_2C^3HC^4HCH_2N$), 7.25 (2H, br d, *J* = 2.7 Hz, $ArC^{10/11}H$), 7.40 (2H, br d, *J* = 3.3 Hz, $ArC^{9/12}H$); ^{13}C NMR (75 MHz, $CDCl_3$): δ(ppm) = 22.4 ($OC^{17/18}H_3$), 45.2 ($NC^2H_2CHCHC^5H_2N$), 128.7 ($ArC^{10/11}H$), 129.1 ($ArC^{9/12}H$), 130.1 ($NC^2H_2CHCHC^5H_2N$), 139.1 ($C^{7/8}$), 169.2 ($C^{13/15}$=O).

CHAPTER SIX

REFERENCES

1) Fecik, R. A.; Frank, K. E.; Gentry, E. J.; Mitscher, L. A.; and Shibata, M.; *Pure Appl. Chem.*, **1999**, 71, p. 559

2) Thayer, A. M.; *Chem. Eng. News*, **2007**, 85, p. 37

3) van Otterlo, W. A. L.; Ngidi, E. L.; de Koning, C. B.; and Fernandes, M. A.; *Tetrahedron Lett.*, **2004**, 45, p. 659

4) Schrock, R. R.; *J. Chem. Soc., Dalton Trans.*, **2001**, p. 2541

5) Nguyen, S. T.; Johnson, L. K.; Grubbs, R. H.; and Ziller, J. W.; *J. Am. Chem. Soc.*, **1992**, 114, 10, p. 3974

6) Schwab, P.; France, M. B.; Ziller, J. W.; and Grubbs, R. H.; *Angew. Chem.*, **1995**, 107, 18, p. 2179

7) Herisson, J. L.; and Chauvin, Y.; *Makromol. Chem.*, **1971**, 141, p. 161

8) Dias, E.L.; Nguyen, S.T.; and Grubbs, R.H.; *J. Am. Chem. Soc.*, **1997**, 119, p. 3887

9) Sanford, M. S.; Love, J.A.; and Grubbs, R.H.; *J. Am. Chem. Soc.*, **2001**, 123, p. 6543

10) Scholl, M.; Trnka, T.M.; Morgan, J.P.; and Grubbs, R.H.; *Tetrahedron Lett.*, **1999**, 40, p. 2247

11) Scholl, M.; Ding, S.; Lee, C.W.; and Grubbs, R.H.; *Org. Lett.*, **1999**, 1, p. 953

12) Sanford, M. S.; Love, J. A.; and Grubbs, R. H.; *J. Am. Chem. Soc.*, **2003**, 115, 27, p. 1010

13) Maynard, H. D., and Grubbs, R. H., *Tetrahedron Let*, **1999**, 40, p. 4137

14) Bourgeois , D.; Pancrazi, A.; Ricard, L.; and Prunet, J.; *Angew. Chem. Int. Ed*, **2000**, 112, p. 742

15) Bourgeois, D.; Pancrazi, A.; Nolan, S. P.; and Prunet, J.; *J. Organomet. Chem.*, **2002**, 643, p. 247

16) Krompiec, S.; Pigulla, M.; Krompiec, M.; Baj, S.; Mrowiec-Bialoń, J.; Kasperczyk, J.; Kubicki, M.; and Borowiak, T.; *Tetrahedron Lett.*, **2001**, 42, p. 7095

17) Krompiec, S.; Pigulla, M.; Krompiec, M.; Baj, S.; Mrowiec-Bialoń, J.; and Kasperczyk, J.; *Tetrahedron Lett.*, **2004**, 45, p. 5257

18) Mundy, B. P., Ellerd, M. G., Favaloro, F. G., *Name Reactions and Reagents in Organic Synthesis*, **2005,** 2nd Ed, John Wiley & Sons, New Jersey, p. 150

18a) Talams, F.X.; Smith, D.B.; Cervantes, A.; Franco, F.; Cutler, S.T.; Loughhead, D.G.; Morgans, D.J.; and Weikert, R.J.; *Tetrahedron Lett.*, **1997**, 38 , p. 4125

18b) Smith, D.B.; Elworthy, T. R.; Morgans, D.J.; Lenson, J.T.; Patterson, J.W.; Vasquez, A.; and Waltos, A.M.; *Tetrahedron Lett.*, **1996**, 37, p. 21

19) Horton, D. A.; Bourne, G. T.; and Smythe, M. L.; *Chem. Rev.*, **2003**, 103, p. 893

20) van Wijngaarden, I.; Kruse, C. G.; Van der Heyden, J. A. M.; and Tulp. M. T. M.; *J. Med. Chem.*, **1988**, 31, 10, p. 1934

21) Halfpenny, P.R.; Horwell, D.C.; Hughes, J.; Hunter, J.C.; and Rees, D. C.; *J. Med. Chem.*, **1990**, 33, 1, p. 286

22) Morris, J.; Wishka, D. G.; Humphrey, W. R.; Lin, A. H.; Wiltse, A. L.; Benjamin, C. W.; Gorman, R. R.; and Shebuski, R. J.; *Bioorg. Med. Chem. Lett.*, **1994**, 4, 21, p. 2621

23) Gammill, R. B.; and Hyde, B. R.; *J. Org. Chem.*, **1983**, 48, p. 3863

24) Stermitz, F. R.; Thomas, R. D.; and Coburn Williams, M.; *Phytochemistry*, **1975**, 14, p. 1681

25) Hu, Y., and Yang, Z., *Org. Lett.*, **2001**, 3, p. 1387

26) Katritzky, A. R., Rees, C. W., Scriven, E. F. V., Eds.; *Comprehensive Heterocyclic Chemistry II*; Pergamon Oxford, **1996**; Vol. 2, pp 368–377

27) Stephans, R.D.; and Castro, C. E.; *J. Org. Chem.*, **1963**, 28, p. 3313

28) Capozzi, G.; and Modena, G.; *J.Chem. Soc., Perkin Trans. 1*, **1972**, p. 216

29) Schroeder, D. C.; Corcoran, P. O.; Holden, C. A.; and Mulligan, M.C.; *J. Org. Chem.*, **1962**, 27, p. 586

30) Pandey, G.; Krishna, A.; and Bhalerao, U. T.; *Tetrahedron. Lett.*, **1989**, 30, 14, p. 1867

31) Liebeskind, L. S.; and Wang, J.; *J. Org. Chem.*, **1993**, 58, p. 3550

32) Mundy, B. P., Ellerd, M. G., Favaloro, F. G., *Name Reactions and Reagents in Organic Synthesis*, **2005,** 2nd Ed, John Wiley & Sons, New Jersey, p. 317

33) Bowden, K.; and Battah, S.; *J. Chem. Soc. Perkin Tran. 2*, **1998**, p. 1603

34) Habermann, J.; Ley, S. V.; and Smits, R. J.; *J. Chem. Soc., Perkin Trans.,* 1, **1999**, p. 2421

35) Wang, Y.; and Huang, T. N.; *Tetrahedron Lett.,* **1998**, 39, 52, p. 9605

36) Nicolaou, K. C.; Snyder, S. A.; Bigot, A.; and Pfefferkorn, J. A.; *Ange. Chem. Int. Ed*., **2000**, 39, p. 1093

37) Wu, J. H.; Chang, F. R.; Hayashi, K.; Shiraki, H.; Liaw, C. C.; Nakanishi, Y.; Bastow, K. F.; Yu, D.; Chen, I. S.; and Lee K. H.; *Bioorg. Med. Chem. Lett.*, **2003**, 13, 13, p. 2223

38) Rybczynski, P. J.; Zeck, R. E.; Combs, D. W.; Turchi, I; Burris, T. P.; Xu, J. Z.; Yang, M.; and Demares, K. T.; *Bioorg. Med. Chem. Lett.*, **2003**, 13, p. 2359

39) Bergman, J., Rosenzweig-Lipson, S., and Spealman, R. D., *J. Pharmacol. Exp. Ther.*, **1995**, 273, p. 40

40) Madhavan, G. R.; Iqbal, J.; Bhuniya, D.; Chakrabarti, R.; and Das, S. K.; WO Patent Appl. 03033481, **2003**.

41) Lestage, P.; Lockhart, B.; Fleury, M. B.; and Largeron, M.; WO Patent Appl. 9962889, **1999**.

42) Buon, C.; Chacun-Lefevre, L.; Rabot, R.; Bouyssou, P.; and Coudert, G.; *Tetrahedron*, **2000**, 56, p. 605

43) Chacun-Lefevre, L.; Buon, C.; Bouyssou, P.; and Coudert. G.; *Tetrahedron Lett.*, **1998,** 39, p. 5763

44) Bartsch, H; Kropp, W.; and Pailer, M.; *Monatsh. Chem.*, **1979**, 110, p. 267

45) McKillop, A.; and Sayer, T. S. B.; *J. Org. Chem.,* **1976**, 41, p. 1079

46) Willand, N.; Beghyn, T.; Nowogrocki, G.; Gesquierea, J. C.; and Depreza, B.; *Tetrahedron Lett.*, **2004**, 45, p. 1051

47) Matsumoto, Y.; Tsuzuki, R.; Matsuhisa, A.; Yoden, T.; Yamagiwa, Y.; Yanagisawa, I.; Shibanuma, T.; and Nohira, H.; *Bioorg. Med. Chem.*, **2000**, 8, 2, p. 393

48) Dudykina, N. V.; and Zagorevskii, V. A.; *Khimiya Geterotsiklicheskikh Soedinenii*, **1967**, 3, p. 250

49) Bonsignore, L.; De Logu, A.; Loy, G.; Lavagna, S. M.; and Secci, D.; *Eur. J. Med. Chem.*, **1994**, 29, p. 479

50) Bright, S. A.; Greene, L. M.; Greene, T. F.; Campiani, G.; Butini, S.; Brindisi, M.; Lawler, M. Meegan, M. J.; Williams, D. C.; and Zisterer, D. M.; *Biochemical Pharmacology*, **2009**, 77, p. 310

51) Bennasar, M. L.; Roca, T.; Monerris, M.; - , D.; *J. Org. Chem.*, **2006**, 71, p. 7028

52) Mizuno, K.; Sawa, M.; Harada, H.; Taoka, I.; Yamashita, H.; Oue, M.; Tsujiuchi, H.; Arai, Y.; Suzuki, S.; Furutani, Y.; and Kato, S.; *Bioorg. Med. Chem.*, **2005**, 13, p. 855

53) Lakshmi, Ch. S.; Rehaman, H.; and Bhaskar Rao, A.; *Monatsh. Chem.*, **2009**, 140, p. 611

54) Novelli, A. -Trelles, R.; Groppetti, A.; -Sanchez, M. T.; *Amino Acids*, **2005**, 28, p. 183

55) Suemitsu, R.; Ohnishi, K.; Horiuchi, M.; Kitaguchi, A.; and Odamura, K.; *Phytochemistry,* **1992**, 31, p. 2325

56) Shinkevich, E. Yu.; Novikov, M. S.; Khlebnikov, A. F.; Kostikov, R. R.; Kopf, J.; and Magullc, J.; *Russ. J. Org. Chem.*, **2007**, 43, p. 1065

57) Ibrahim, Y. A.; Behbehani, H.; and Ibrahim, M. R.; *Tetrahedron Lett.*, **2002**, 43, p. 4207

58) Mamouni, R.; Soukri, M.; Lazar, S.; Akssira, M.; and Guillaumet, G.; *Tetrahedron Lett.*, **2004**, 45, p. 2631

59) van Otterlo, W. A. L.; Morgans, G. L.; Khanye, S. D.; Aderibigbe, B. A. A.; Michael, J. P. and Billing, D. G.; *Tetrahedron Lett.*, **2004**, 45, p. 9171

60) Mori, M.; Kitamura, T.; Sakakibara, N.; and Sato, Y.; *Org. Lett.,* **2000**, 2, p. 543

61) De Clercq, E., *Antiviral Res.*, **1998**, 38, p. 153

62) Vierfond, J. M.; Legendre, L.; Martin, C.; Rinjard, P.; and Miocque, M.; *Eur. J. Med. Chem.*, **1990**, 25, p. 251

63) Dalgaard, L.; Hjortkjaer, R.; Regnier, B.; and Nordholm, L.; *Drug. Metab. Dispos.*, **1994**, 22, p. 289

64) Kaim, W.; *J. Am. Chem. Soc*., **1983**, 105, p. 707

65) Anantha Lakshmi, P.V.; Saritha Reddy, P.; and Jayatyaga Raju, V.; *Spectrochimica Acta Part A*, **2009**, 74, p. 52

66) Jaso, A.; Zarranz, B.; and Aldana, I.; *Eur. J. Med. Chem.*, **2003**, 38, p. 791

67) Nunoshiba, T.; and Nishioka, H.; *Mutation Res.*, **1989**, 217, p. 203

68) Amin, K. M.; Ismail, M. M. F.; Noaman, E.; Soliman, D. H.; and Ammar, Y. A.; *Bioorg. Med. Chem.*, **2006**, 14, 20, p. 6917

69) Lopatinskaya, K.; Sheinkman, A. K.; and Terent'ev, B. P.; *Khimiya Geterotslklicheskikh Soedinenii*, **1984**, 2, p. 1573

70) Hamer, J.; and Holliday, J. A.; *J. Org. Chem.*, **1963**, 28, p. 2488

71) Gomtsyan, A.; Bayburt, E. K.; Schmidt, R. G.; Guo Zheng, Z.; Perner, R. J.; Didomenico, S.; Koenig, R. J.; Turner, S.; Jinkerson, T.; Drizin, I.; Hannick, S. M.; Macri, B. S.; McDonald, H. A.; Honore, P.; Wismer, C. T.; Marsh, K. C.; Wetter, J.; Stewart, K. D.; Oie, T.; Jarvis, M. F.; Surowy, C. S.; Faltynek,C. R.; and Lee, Ch-L.; *J. Med. Chem.,* **2005**, 48, p. 744

72) Tene Ghomsi, N.; Hammou Ahabchane, N-.E.; Es-Safi, N. E.; Garrigues, B.; and Essassi, El. M.; *Spectros. Lett.*, **2007**, 40, p. 741

73) Hazarika, H.; Gogoi, P.; and Konwar, D.; *Synth. Commun.*, **2007**, 37, p. 3447

74) Jaso, A.; Zarranz, B.; and Aldana, I.; *J. Med. Chem.*, **2005,** 48, p. 2019

75) Carta, A.; Paglietti, G.; Rahbar Nikookar, M. E.; Sanna. P.; Sechi, L.; and Zanetti, S.; *Eur. J. Med. Chem.*, **2002**, 37, p. 355

76) Marin, A.; Lima, L. M.; Solano, B.; Vicente, E.; Perez Silanes, S.; Maurel, S.; Sauvain, M.; Aldana, I.; Monge, A.; and Deharo, E.; *Experimental Parasitology*, **2008**, 118, p. 25

77) Mundy, B. P., Ellerd, M. G., Favaloro, F. G., *Name Reactions and Reagents in Organic Synthesis*, **2005,** 2nd Ed, John Wiley & Sons, New Jersey, p. 82

78) Grineva, N. A.; and Safonova, T. S.; *Khimiko-Farmatsevticheskii Zhurnal*, **1977**, 2, p. 28

79) Di Braccio, M.; and Grossi, G.; *Eur. J. Med. Chem.*, **2001**, 36, p. 935

80) Pozarentzi, M.; Stephanidou-Stephanatou, J.; Tsoleridis, C. A.; Zika, C.; and Demopoulos, V.; *Tetrahedron*, **2009**, 65, p. 7741

81) Natsu, N.; and Haruna, H.; *Carbohydrate Res.*, **2000**, 329, p. 681

82) Failli, A. A.; Shumsky, J. S.; Steffan, R. J.; Caggiano, T. J.; Williams, D. K.; Trybulski, E. J.; Ning, X.; Lock, Y.; Tanikella, T.; Hartmann, D.; Chan, P. S.; and Park, C. H.; *Bioorg. Med. Chem. Lett.*, **2006**, 16, 4, p. 954

83) McGowan, D.; Nyanguile, O.; Cummings, M. D.; Vendeville, S.; Vandyck, k.; van den Broeck, W.; Boutton, C. W.; de Bondt, H.; Quirynen, L.; Amssoms, K.; Bonfanti, J. F.; Last, S.; Rombauts, K.; Tahri, A.; Hu, L.; Delouvroy, F.; Vermeiren, K.; Vandercruyssen, G.; van der Helm, L.; and Cleiren, E.; *Bioorg. Med. Chem. Lett.*, **2009**, 19, p. 2492

84) Kakyanam, N.; and Manyunatha, S.G.; *Heterocycles*, **1991**, 32, p. 1131

85) Ried, W.; and Torinus, E.; *Chem. Ber.* **1957**, 90, p. 815

86) Herbert, J. A.; and Suschitzky, H.; *J. Chem. Soc. Perkin I*, **1974**, p. 2657

87) Loskutov, V. A.; Konstantinova, A. V.; and Fokin, E. P.; *Khimiya Geterotsiklicheskikh Soedinenii*, **1979**, 1, p.121.

88) Bindra, A. P.; and LeGoff, E.; *Tetrahedron Lett.*, **1974**, 16, p. 1523

89) Murai, K.; Nakatani, R.; Kita, Y.; and Fujioka, H.; *Tetrahedron*, **2008**, 64, p. 11034

90) Tajbakhsh, M.; Heravi, M. M.; Mohajerani, B.; and Ahmadi, A. N.; *J. Mol. Cat. A: Chemical*, **2006**, 247, p. 213

91) Souers, A. J.; and Ellman, J. A.; *Tetrahedron*, **2001**, 57, p. 7431

92) Thompson, L. A.; and Ellman, J. A.; *Chem. Rev.*, **1996**, 96, p. 555

93) Proust, N.; Gallucci, J. C.; and Paquette, L. A.; *J. Org. Chem.* **2008**, *73*, p. 6279

94) Kleinpeter, E.; Gabler, M.; and Schroth. W.; *Monatsh. Chem.*, **1998**, 119, p. 233

95) Knusel, B; and Hefi, F.; *J. Neurochem.*, **1992**, 59, p. 1987

96) Kase, H.; Iwahashi, K.; Nakanishi, S.; Matsuda, Y.; Yamada, k.; Takahashi, M.; Murakata, C.; Sata, A.; and Kaneko, M.; *Biochem. Biophys. Res. Commun.*, **1987**, 142, 2, p.436

97) Dragutan, V.; Dragutan, I.; *J. Organomet. Chem.*, **2006**, 691, p. 5129

98) Kurasawa, W.; Kan, T.; and Fukuyma, T.; *J. Am. Chem. Soc.*, **2003**, 125, p. 8112

99) Staubli, B.; Fretz, H.; Piantini, U.; and Woggen, W.D.; *Helv. Chim. Acta*, **1987**, 70, p. 1173

100) kiyama, R.; and Kobayashi, S.; *J. Am. Chem. Soc.*, **2003**, 125, p. 3412

101) Dias, M.; Gibson, M.; Grimshaw, J.; Hill, I.; Troch-Grimshaw, J.; and Hammerich, O.; *Acta Chem*. *Scand*., **1998**, 52, p. 549.

102) Alcaide, B.; Almendros, P.; and Alonso, J.M.; *Chem. Eur. J.*, **2003**, 9, p. 5793

103) Alcaide, B.; Almendros, P.; and Alonso, J.M.; *Tetrahedron Lett.*, **2003**, 44, p. 8693

104) Cadot, C.; Dalko, P.I.; and Cossy, J.; *Tetrahedron Lett.*, **2002**, 43, p. 1839

105) Alcaide, B.; Almendros, P.; Alonso, J.M.; and Moustafa, F.A.; *Org. Lett.*, **2001**, 3, 23, p. 3781

APPENDIX A

SELECTED NMR SPECTRA

^{1}H and ^{13}C NMR spectra for the benzofurans and selected precursors

4,7-Dimethoxybenzofuran **154a**

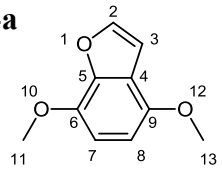

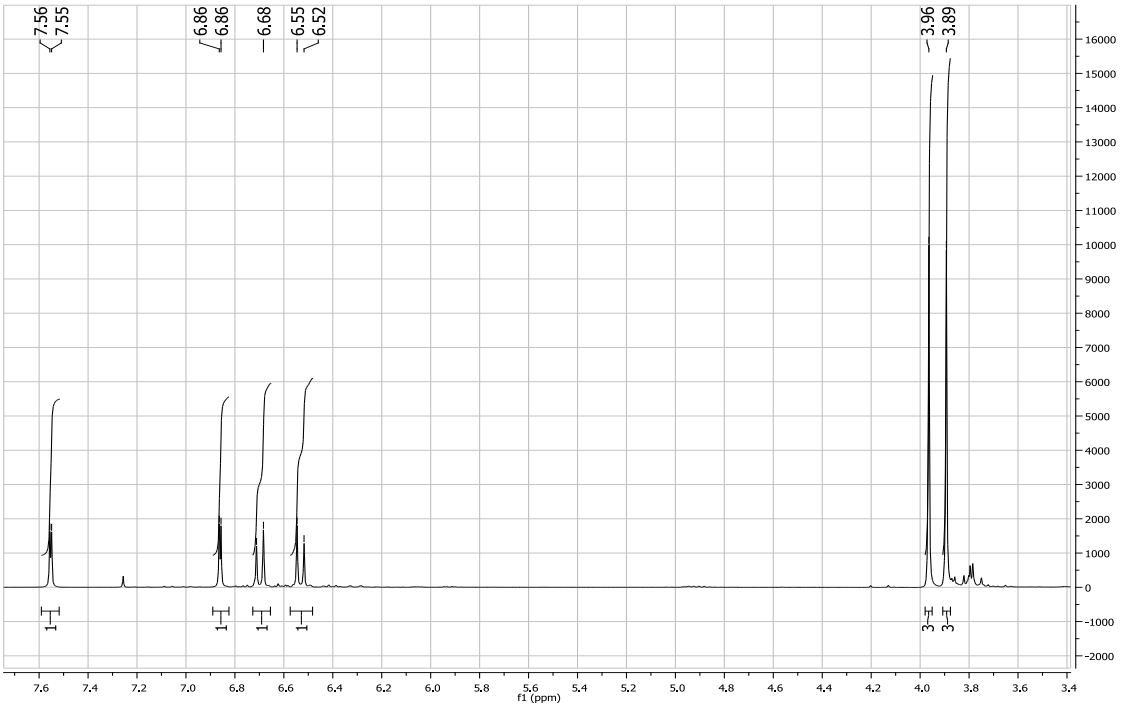

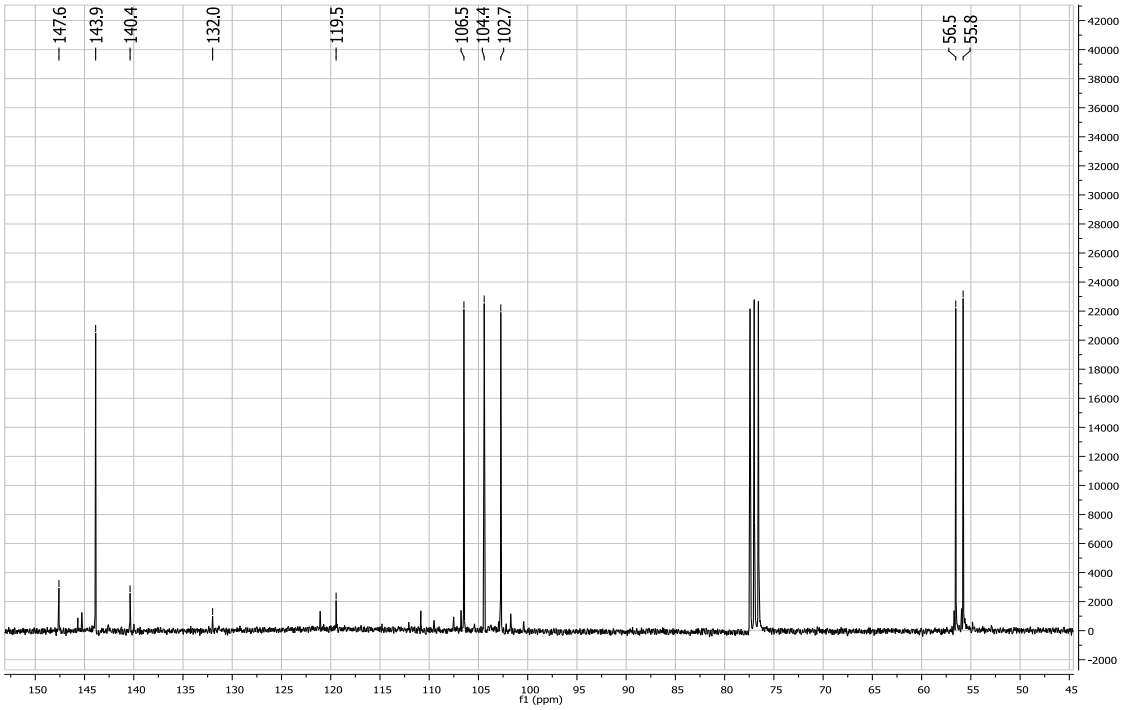

1,4-Dimethoxy-2-(prop-2-en-1-yl)-3-(prop-2-en-1-yloxy)benzene 143a

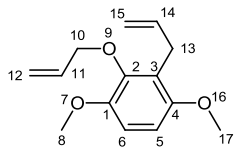

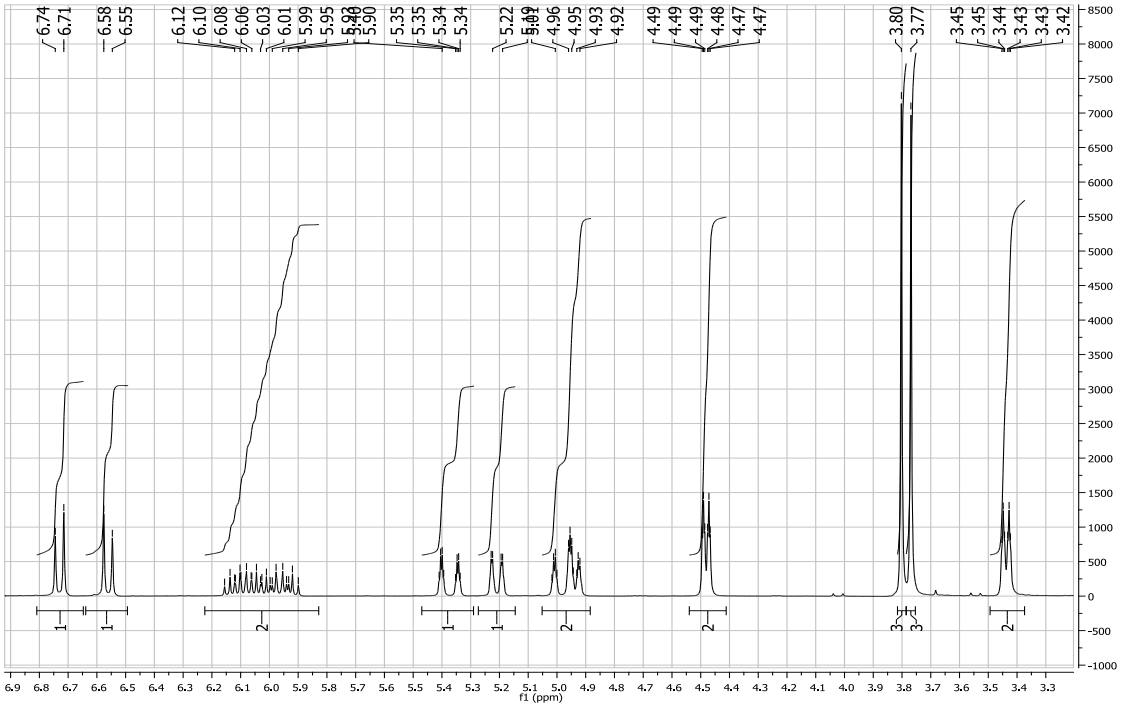

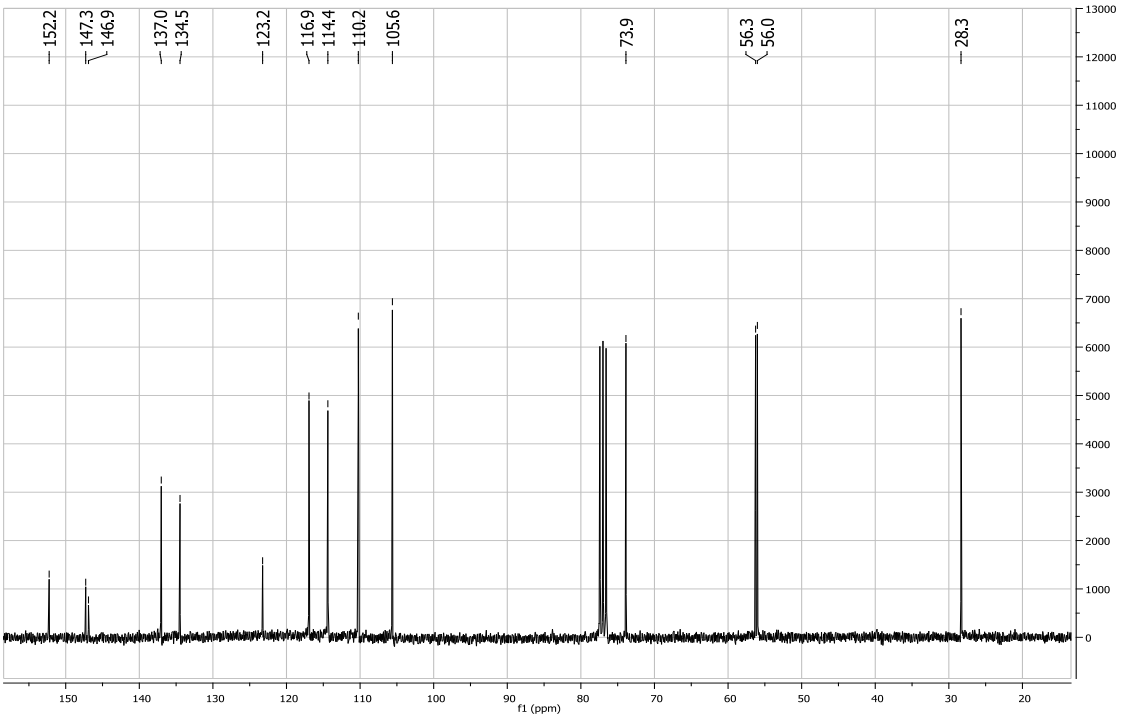

5-Bromobenzofuran

145b

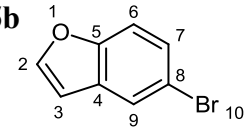

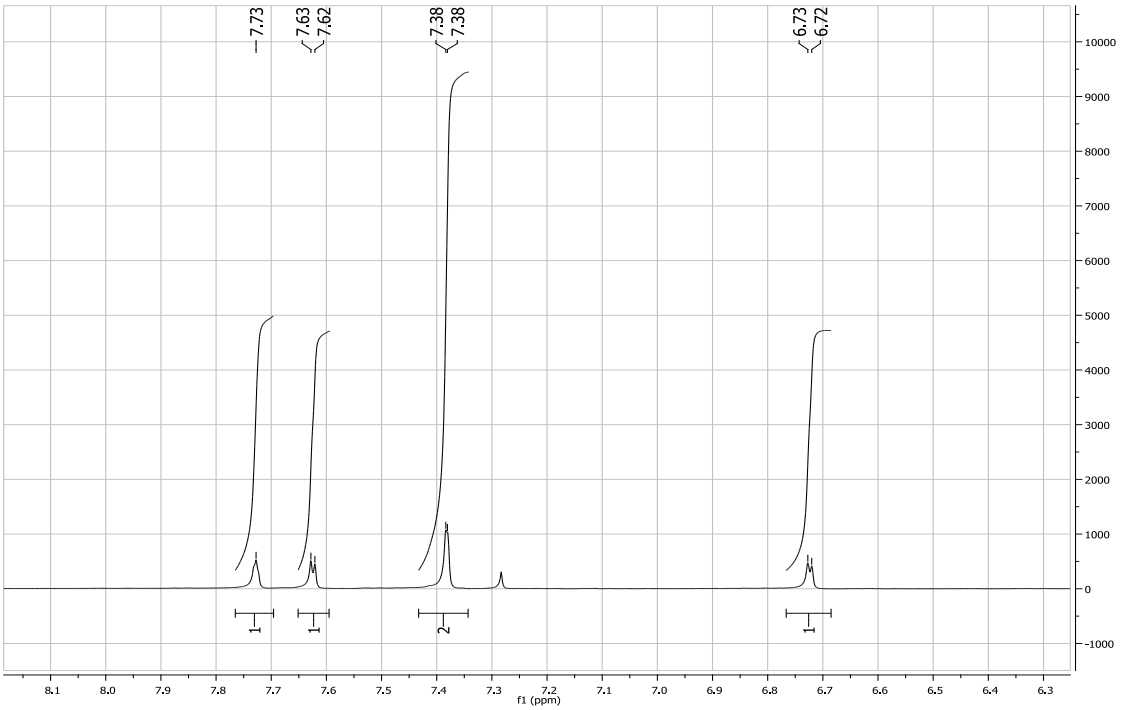

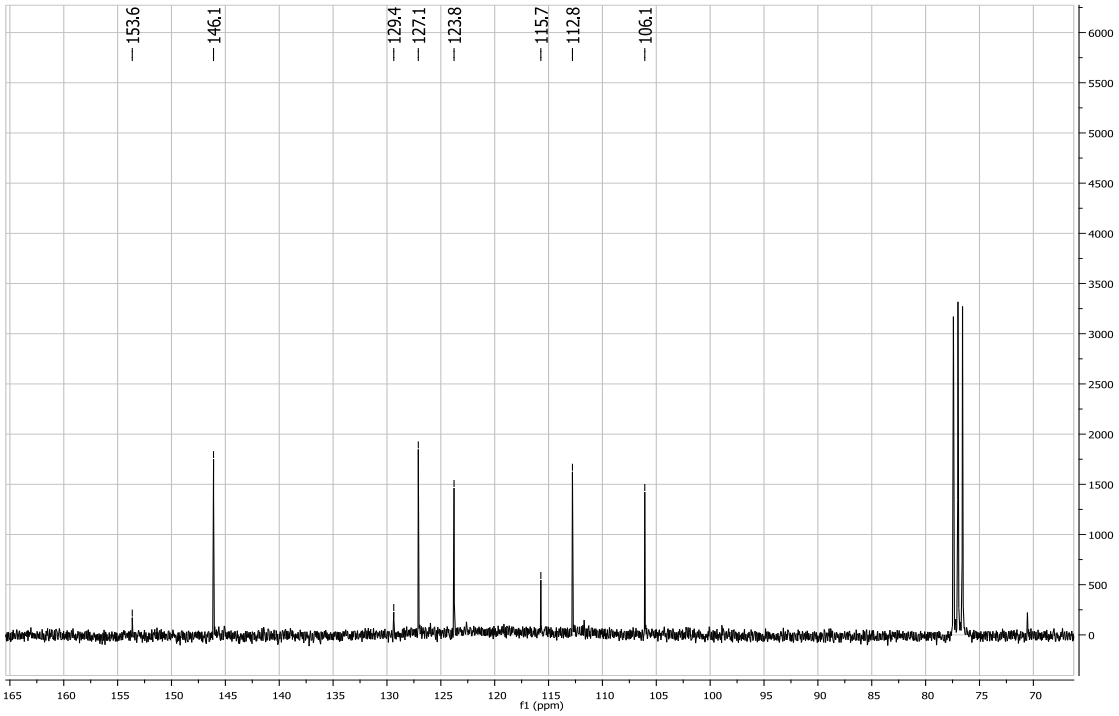

4-Bromo-2-(prop-2-en-1-yl)-1-(prop-2-en-1-yloxy)benzene **143b**

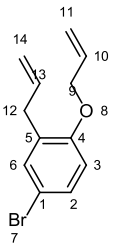

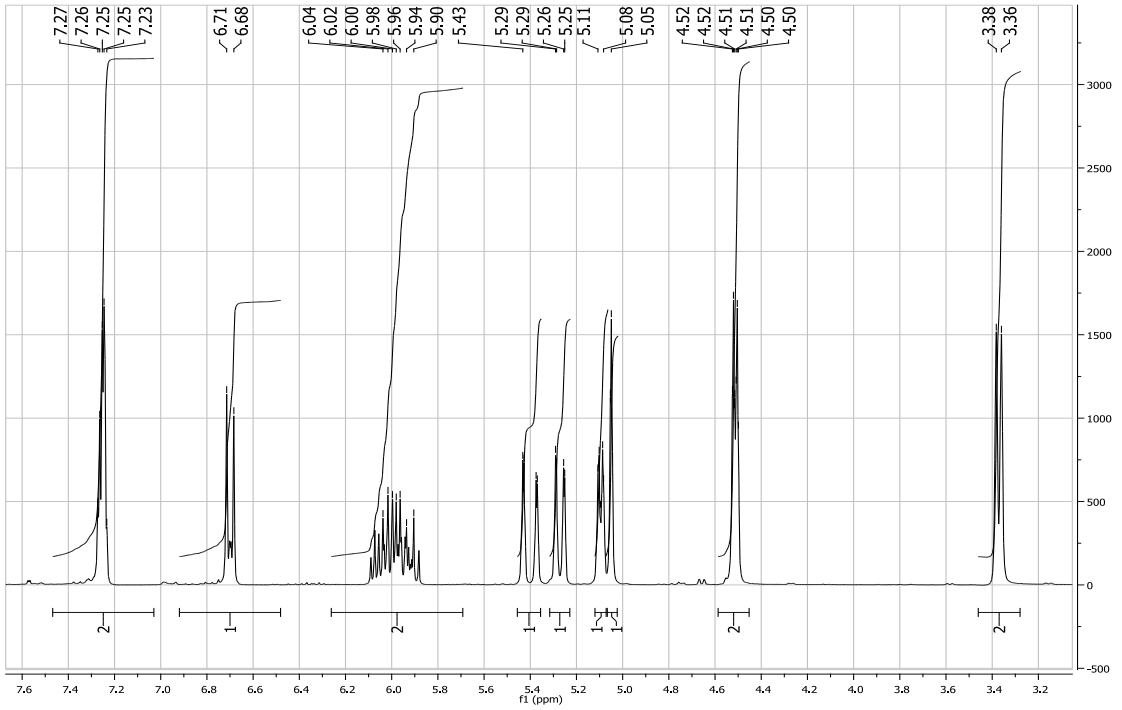

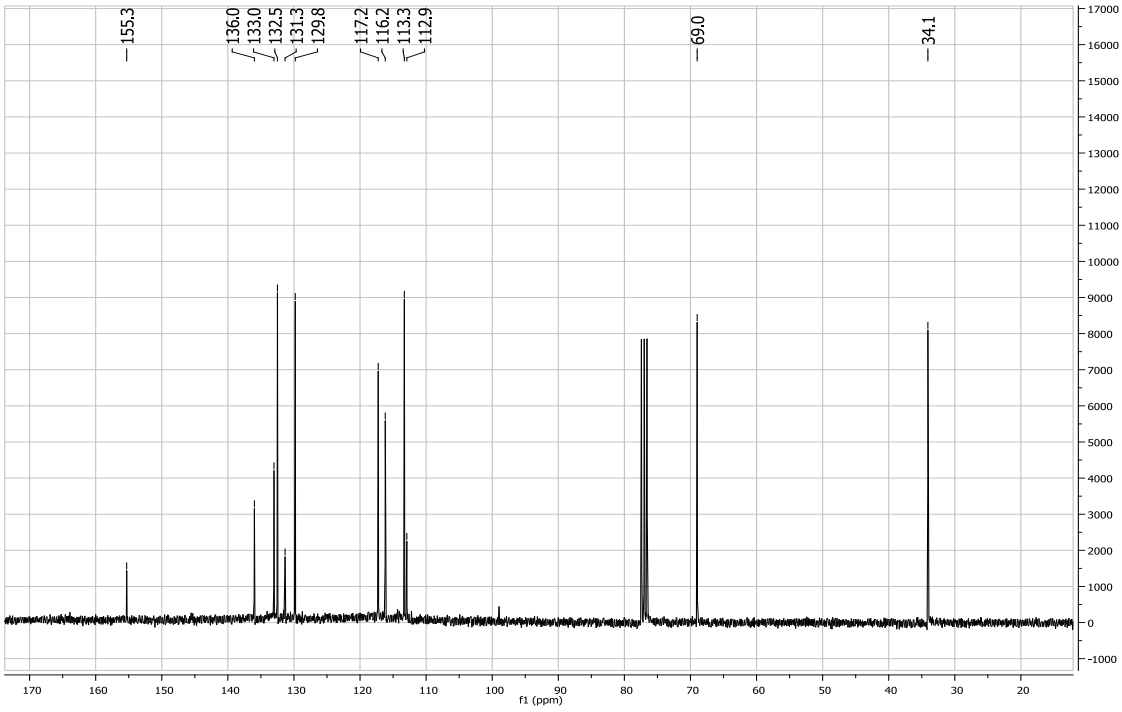

5-*tert*-Butyl-benzofuran **145c**

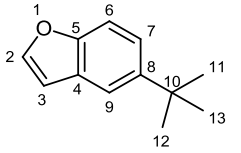

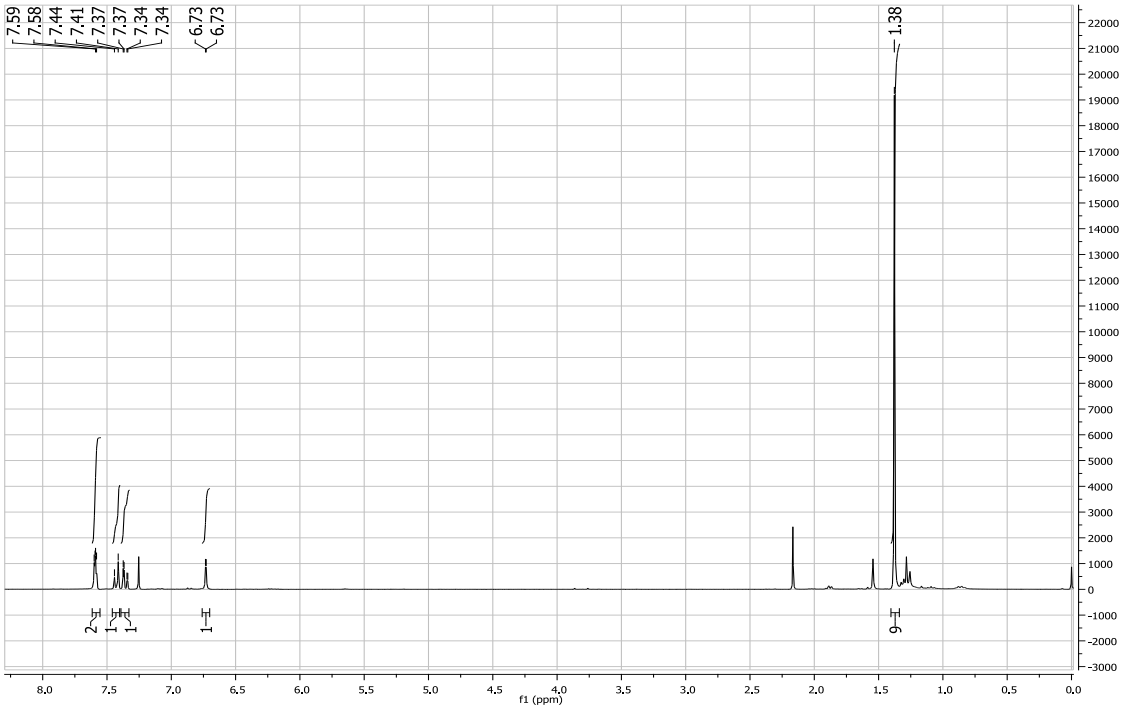

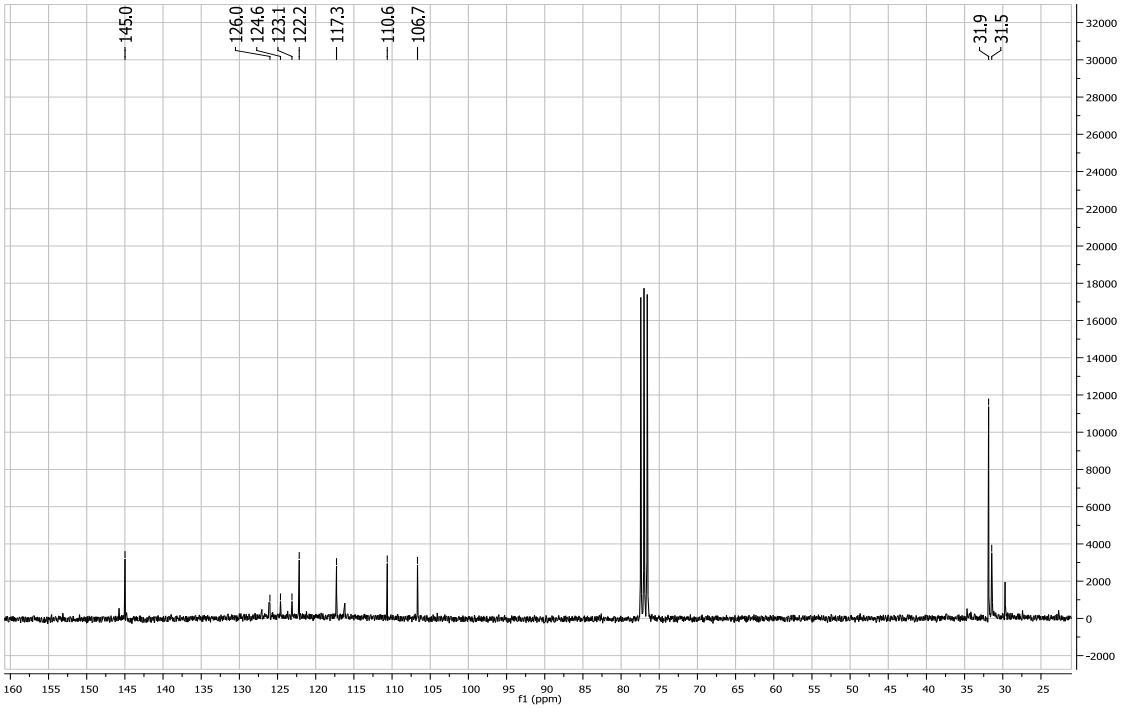

4-*tert*-Butyl-2-(prop-2-en-1-yl)-1-(prop-2-en-1-yloxy)benzene 143c

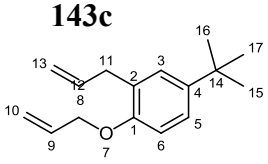

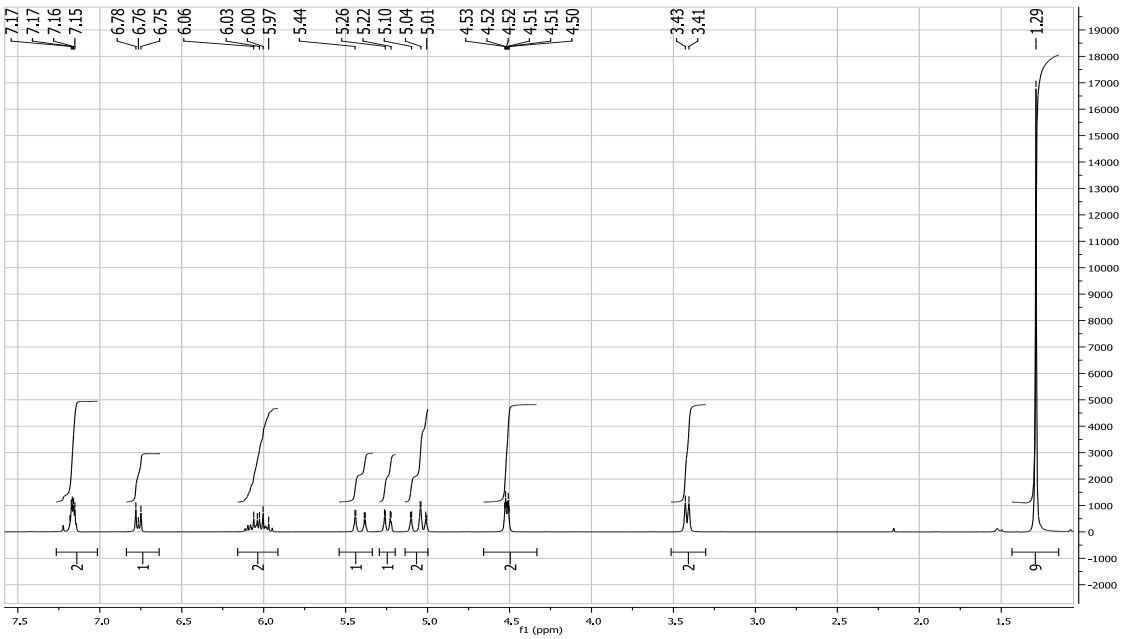

4-*tert*-butyl-2-(prop-1-en-1-yl)-1-(prop-1-en-1-yloxy)benzene **144c**

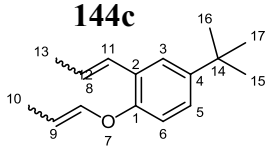

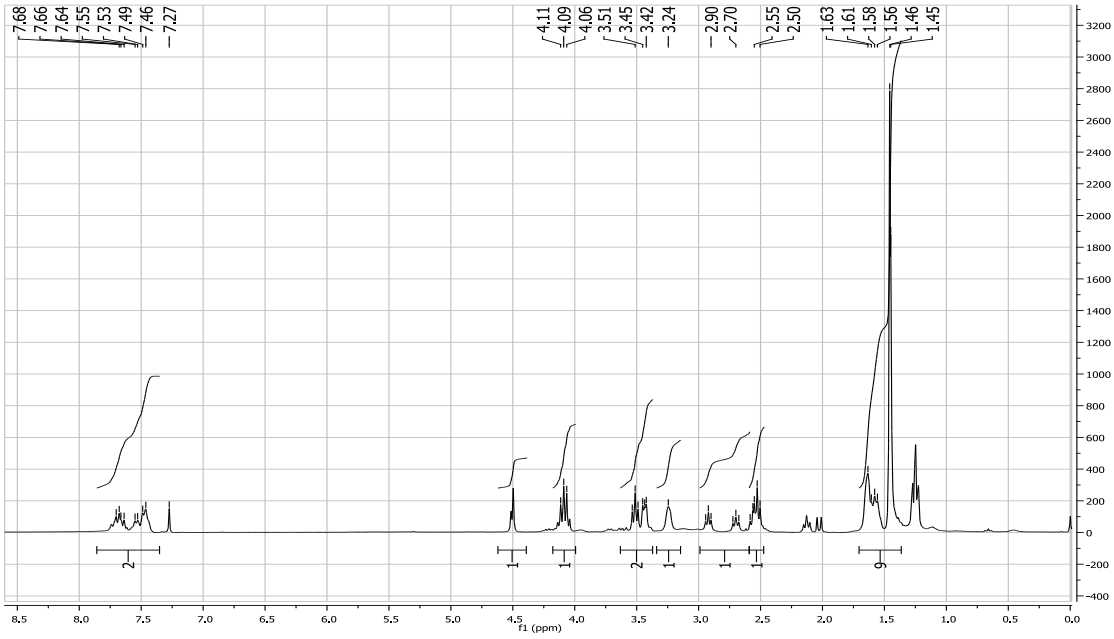

7-Phenyl-1-benzofuran **145d**

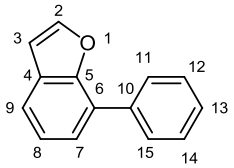

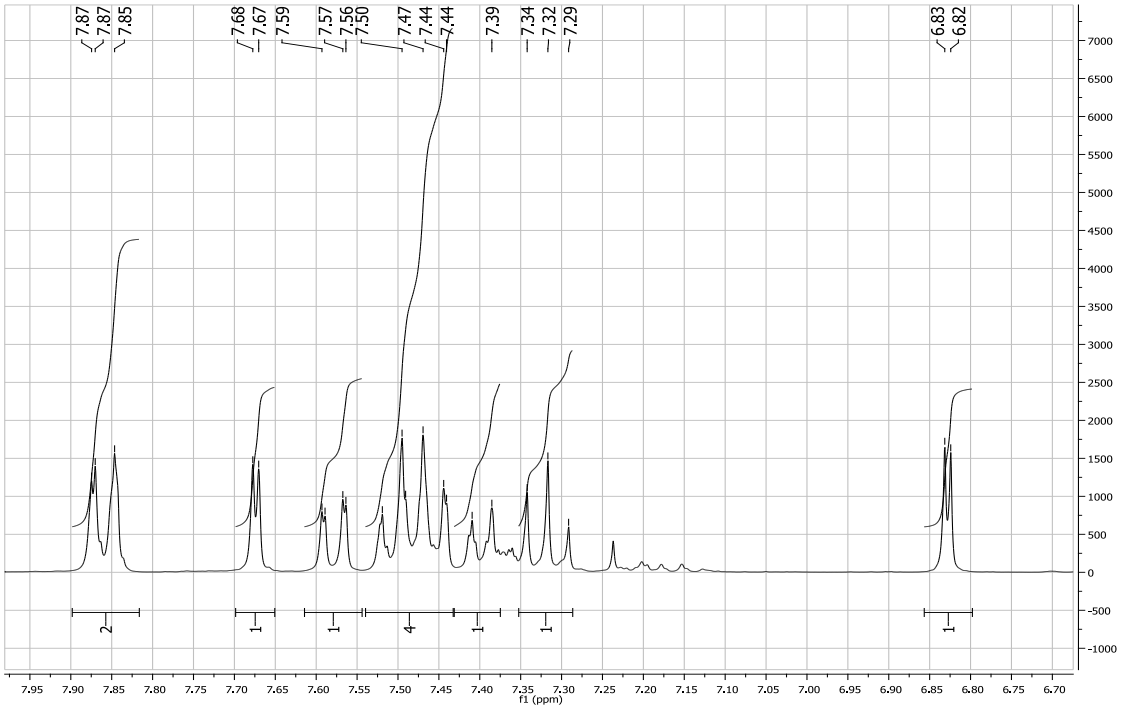

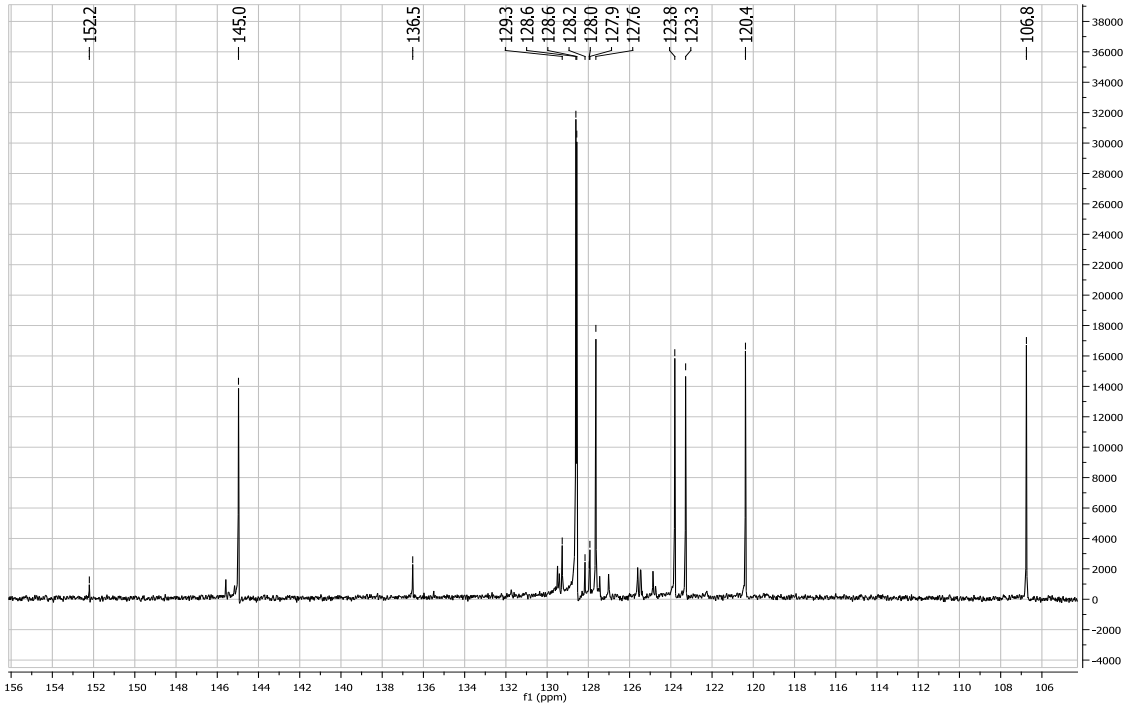

5.1.3.4 3-(Prop-2-en-1-yl)-2-(prop-2-en-1-yloxy)biphenyl 143d

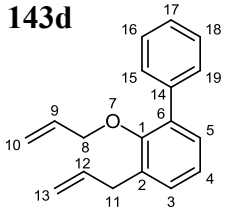

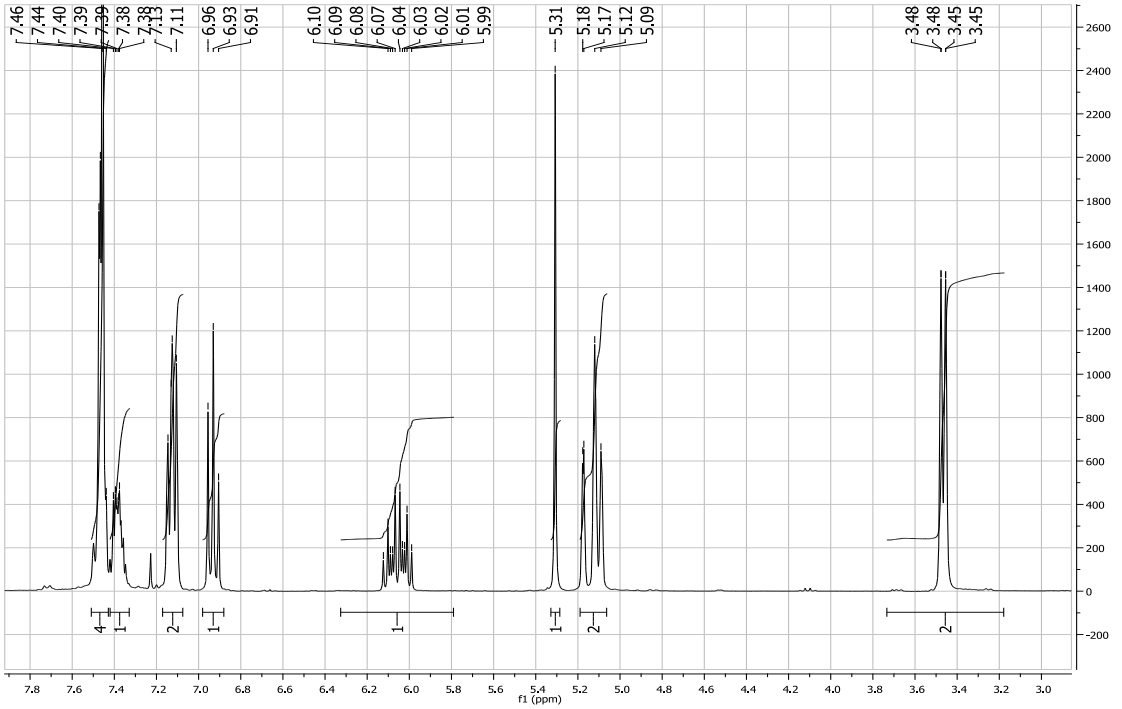

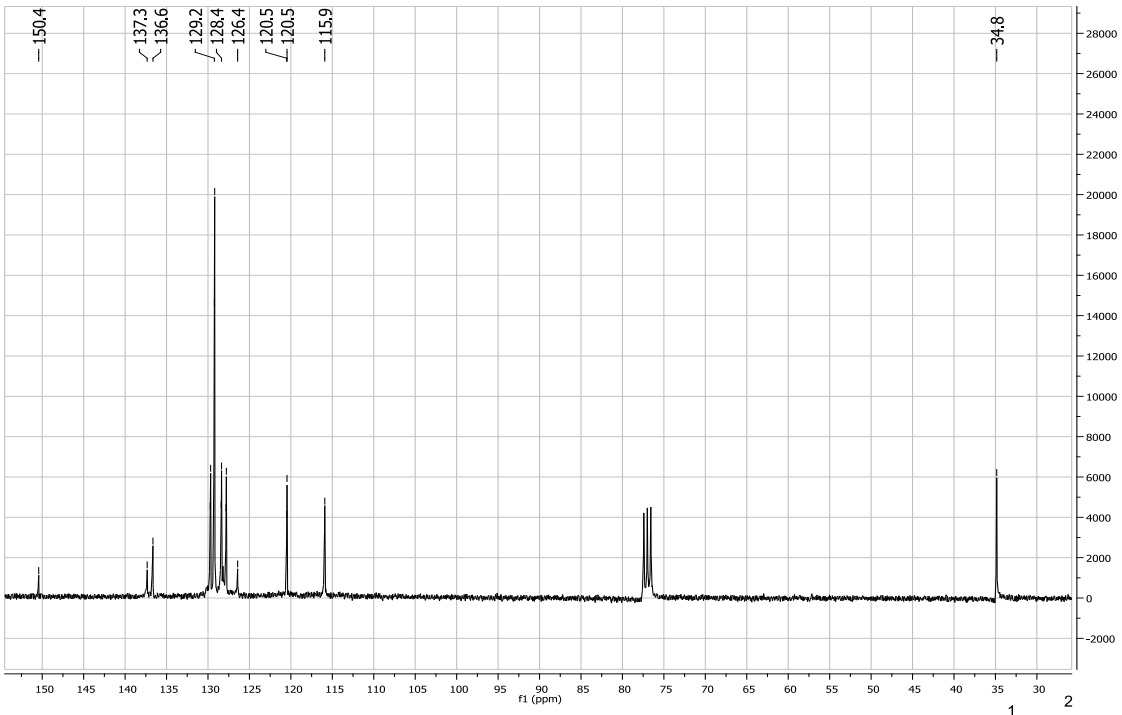

Naphtho[1,2-*b*]furan **145e**

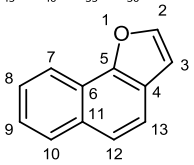

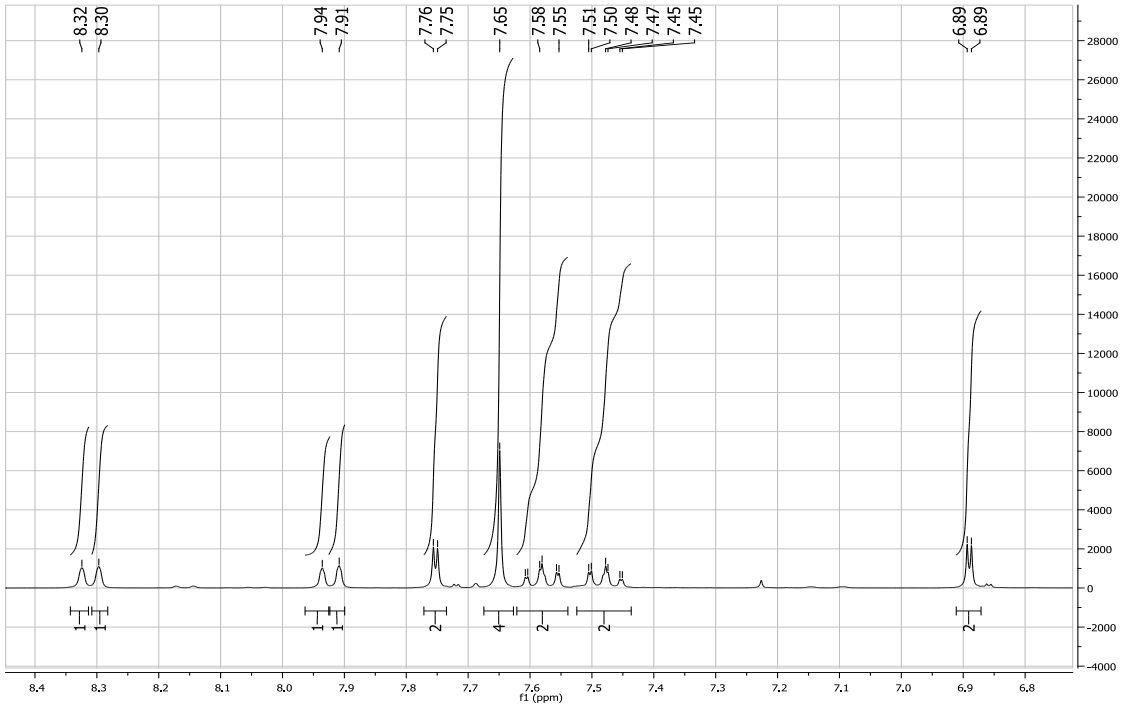

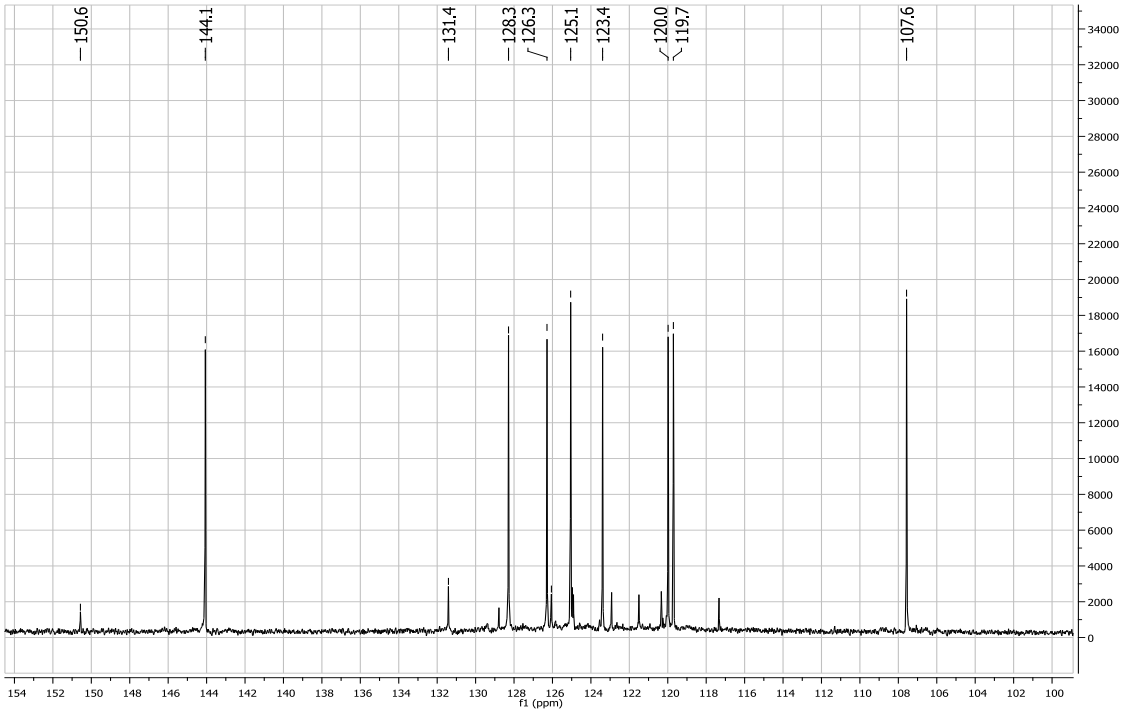

2-(prop-2-en-1-yl)-1-(prop-2-en-1-yloxy)naphthalene **143e**

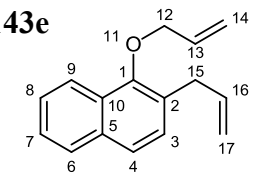

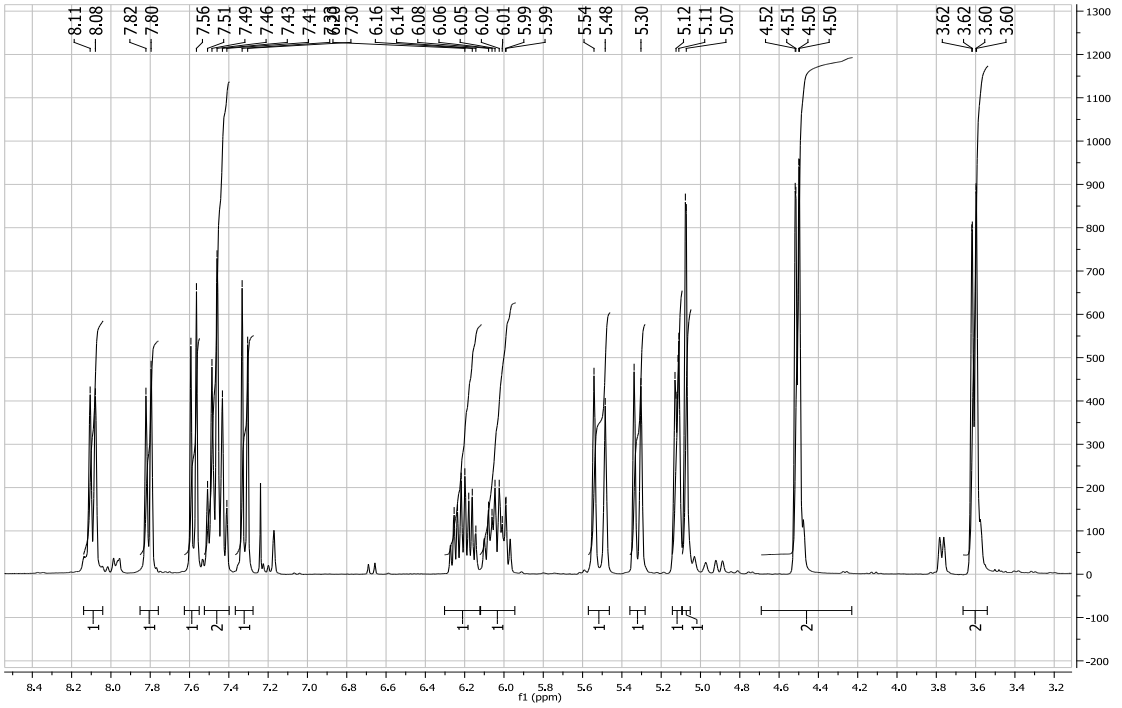
8.11
8.08
7.82
7.80
7.56
7.51
7.49
7.46
7.43
7.41
7.30
6.16
6.14
6.08
6.06
6.05
6.02
6.01
5.99
5.99
5.54
5.48
5.30
5.12
5.11
5.07
4.52
4.51
4.50
4.50
3.62
3.62
3.60
3.60
f1 (ppm)

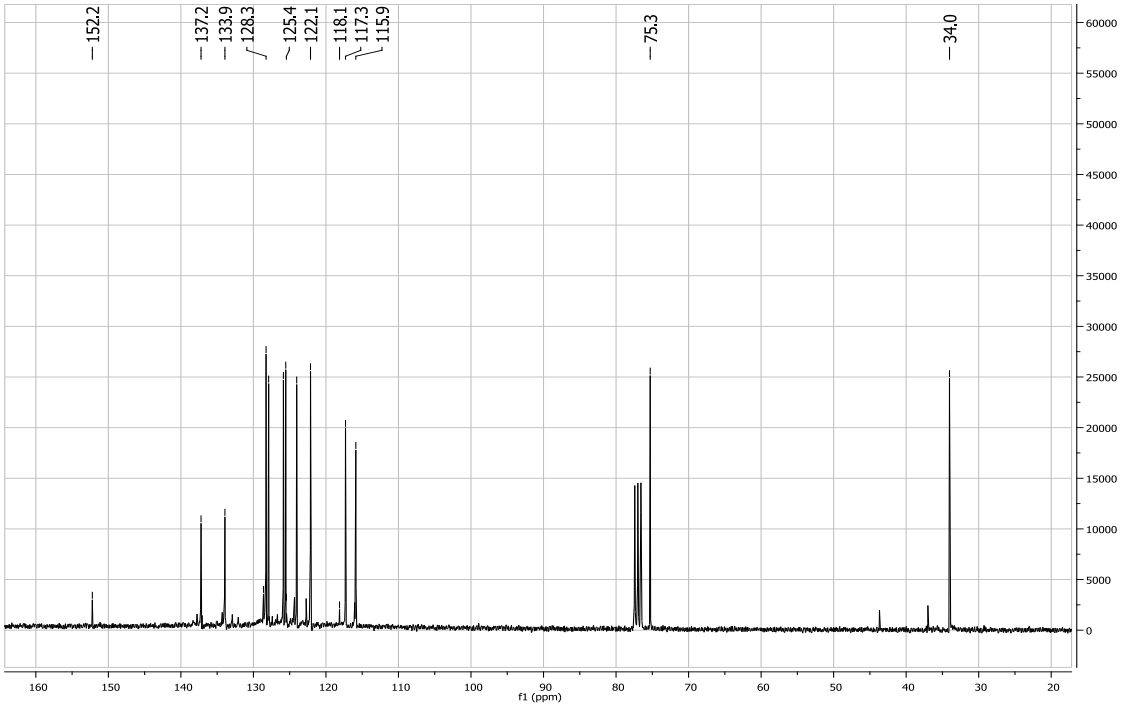
152.2
137.2
133.9
128.3
125.4
122.1
118.1
117.3
115.9
75.3
34.0
f1 (ppm)

^{1}H and ^{13}C NMR spectra for the 6-, 7- and 8-membered *O,N*-benzo-fused heterocycles and precursors

4*H*-1,4-benzoxazin-4-yl(phenyl)methanone **152**

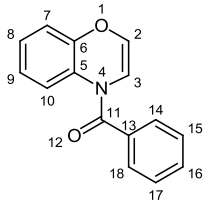

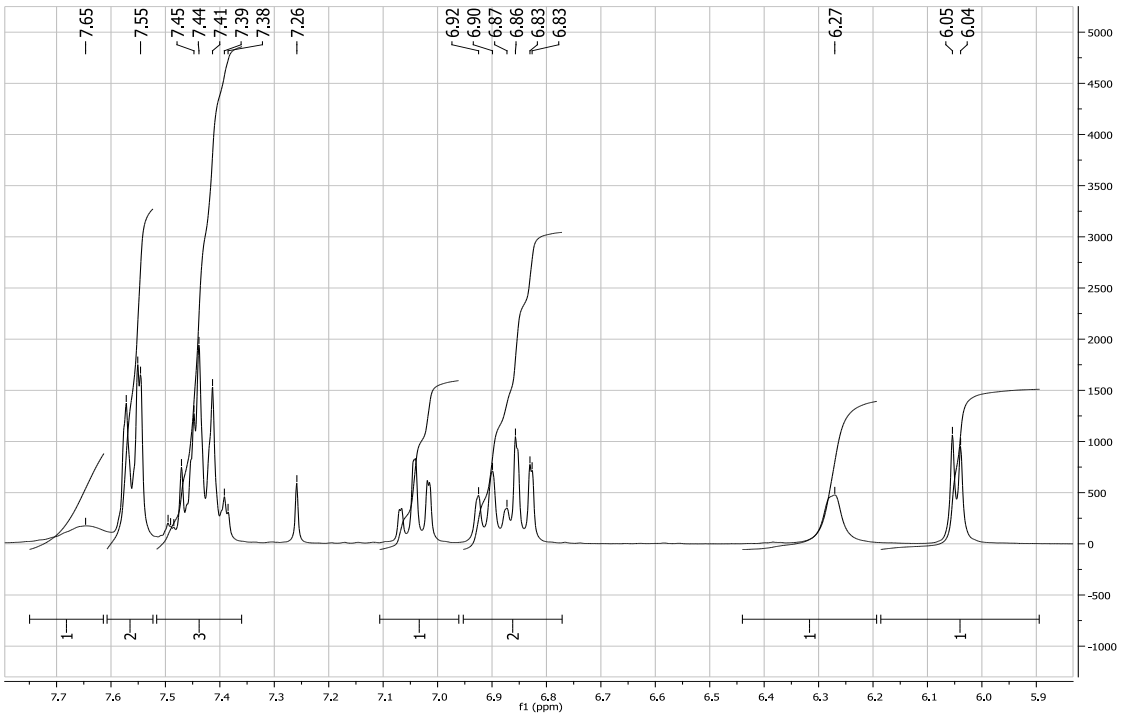

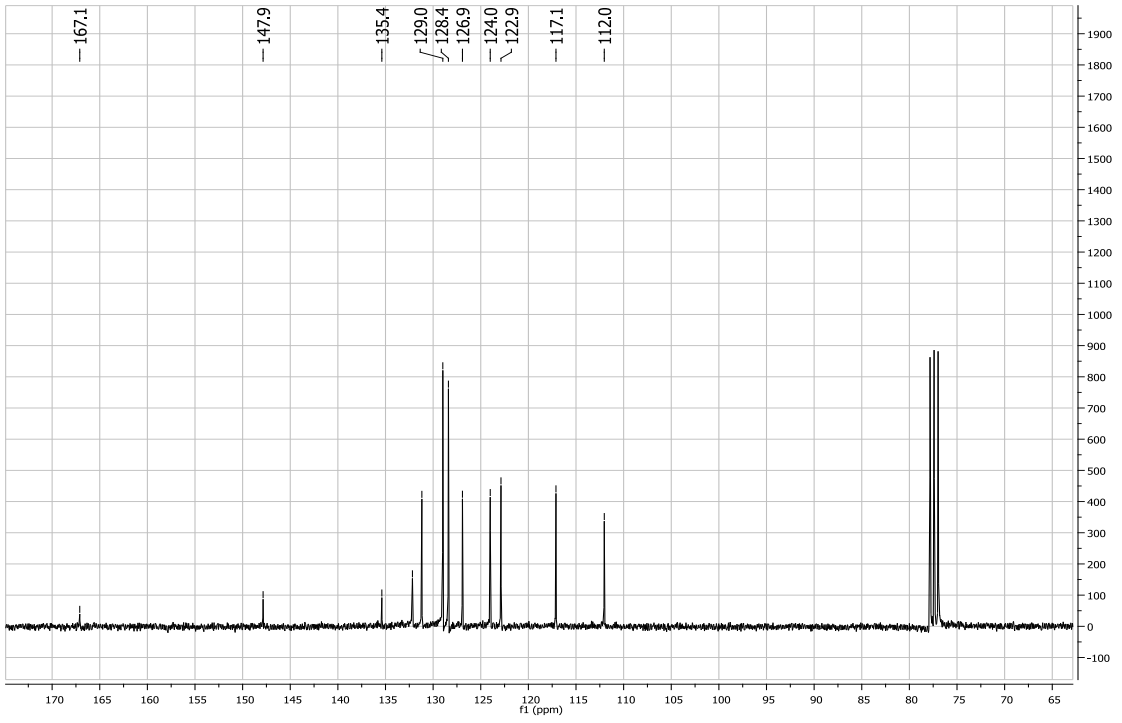

1,5-benzoxazepin-5(4*H*)-yl(phenyl)methanone **155**

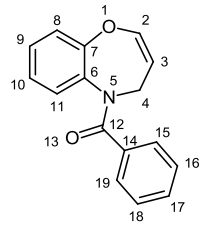

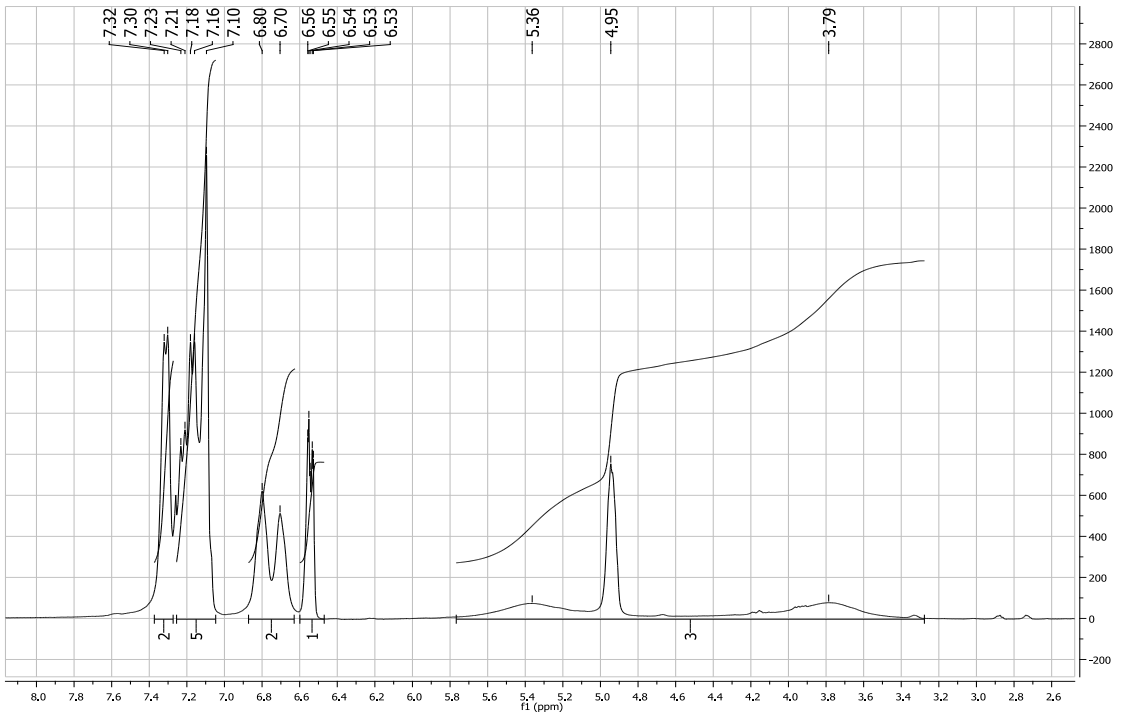

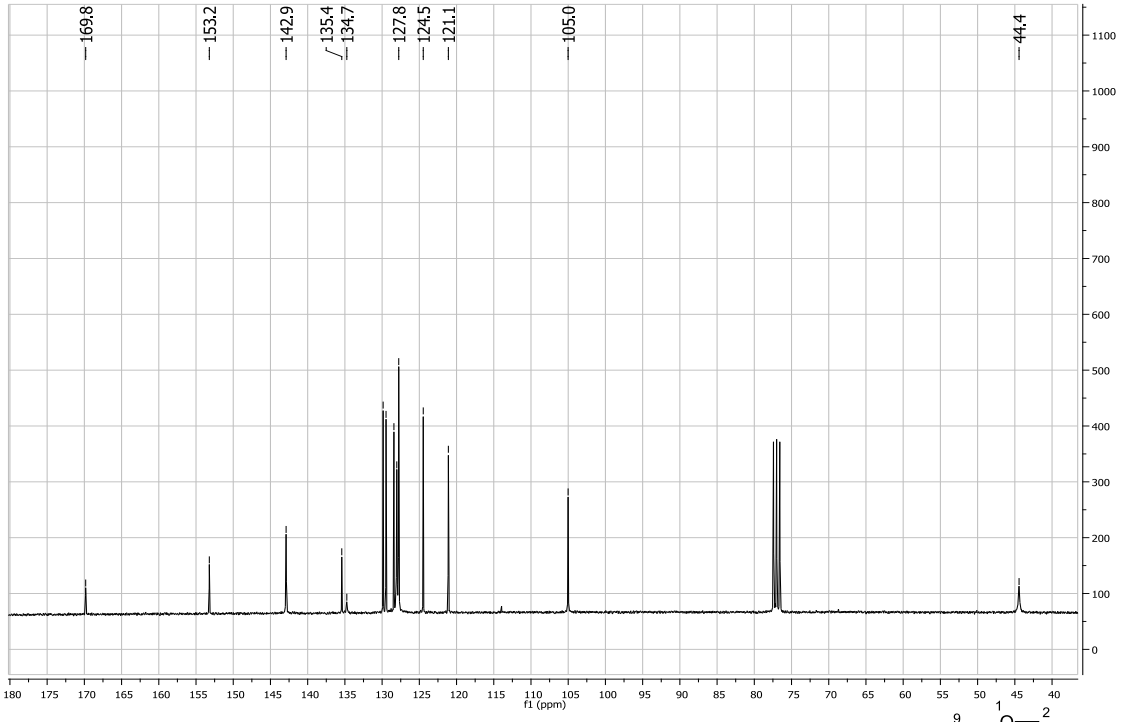

2,5-dihydro-6*H*-1,6-benzoxazocin-6-yl(phenyl)methanone **150**

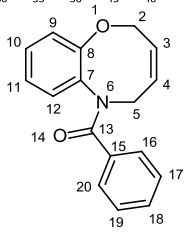

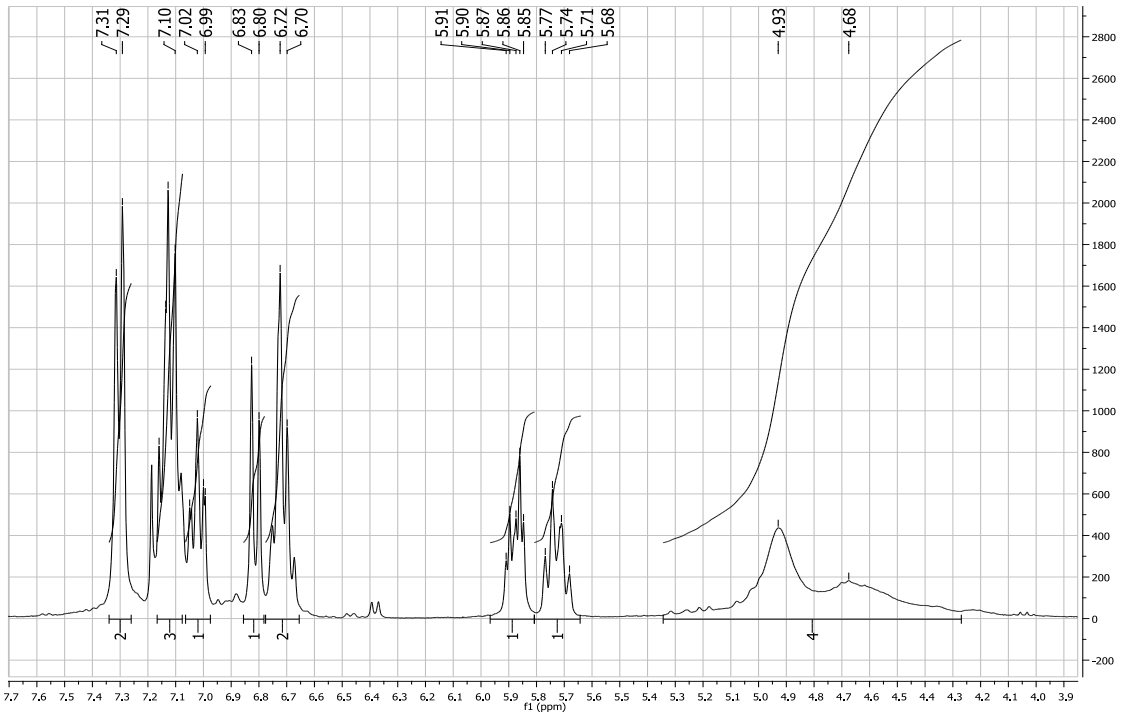

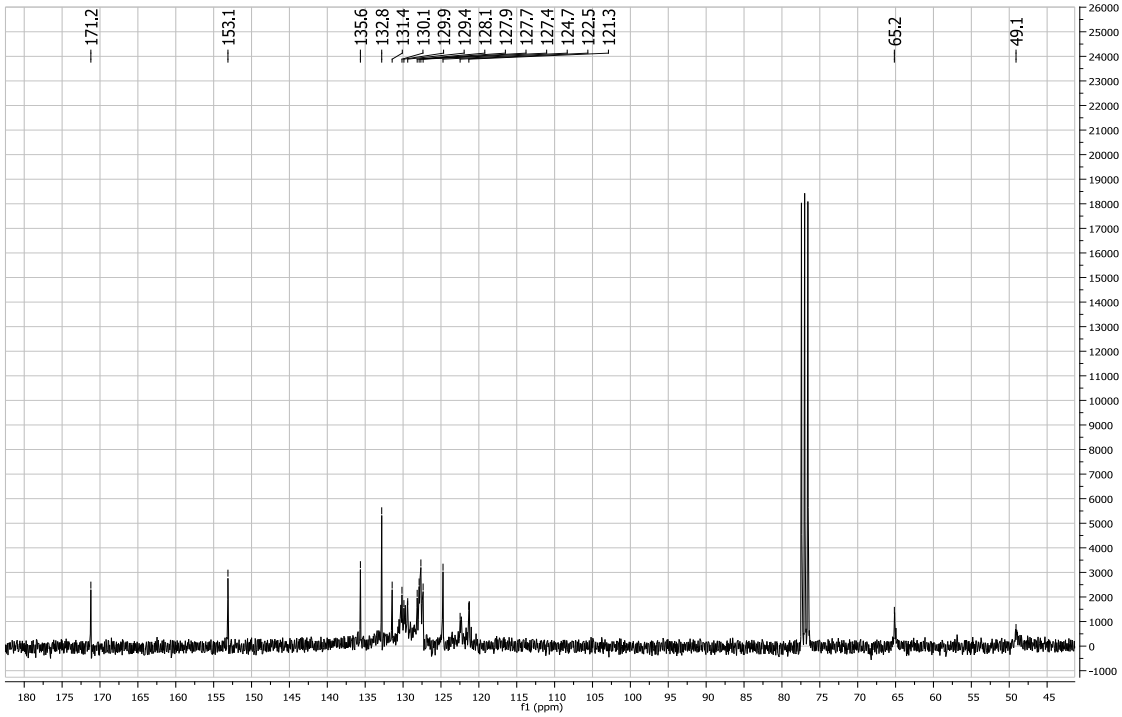

_N_-(prop-1-en-1-yl)-_N_-(2-(prop-1-en-1-yloxy)phenyl)benzamide 151

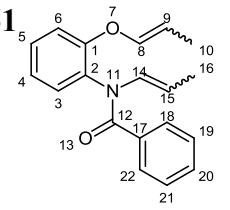

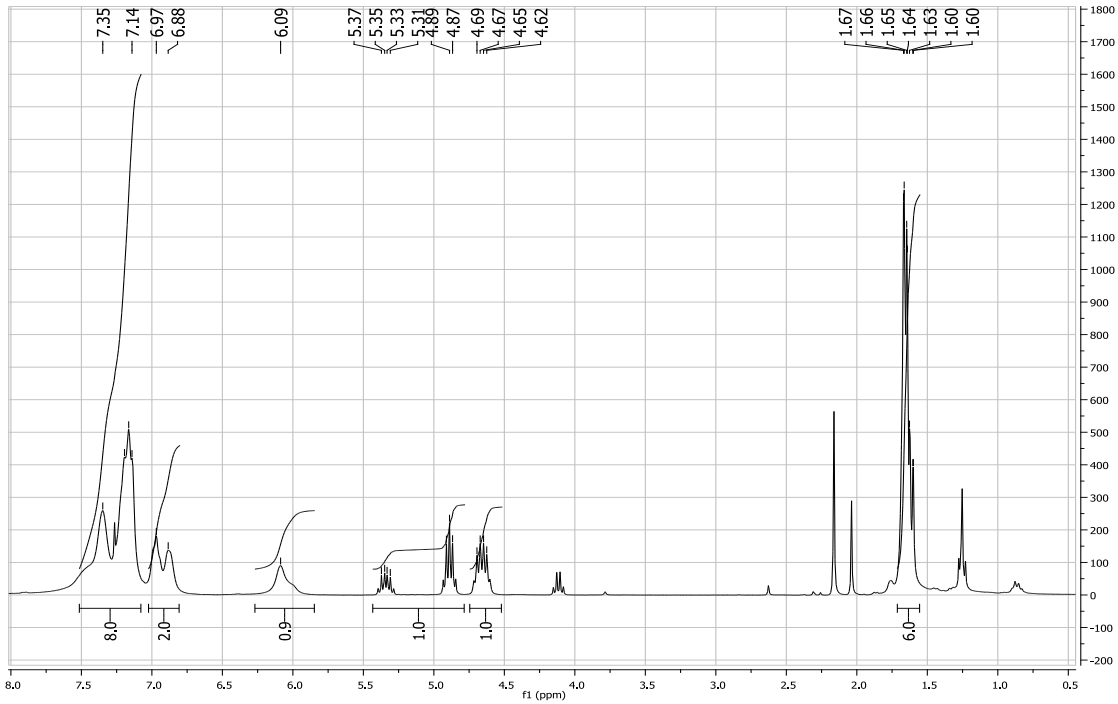

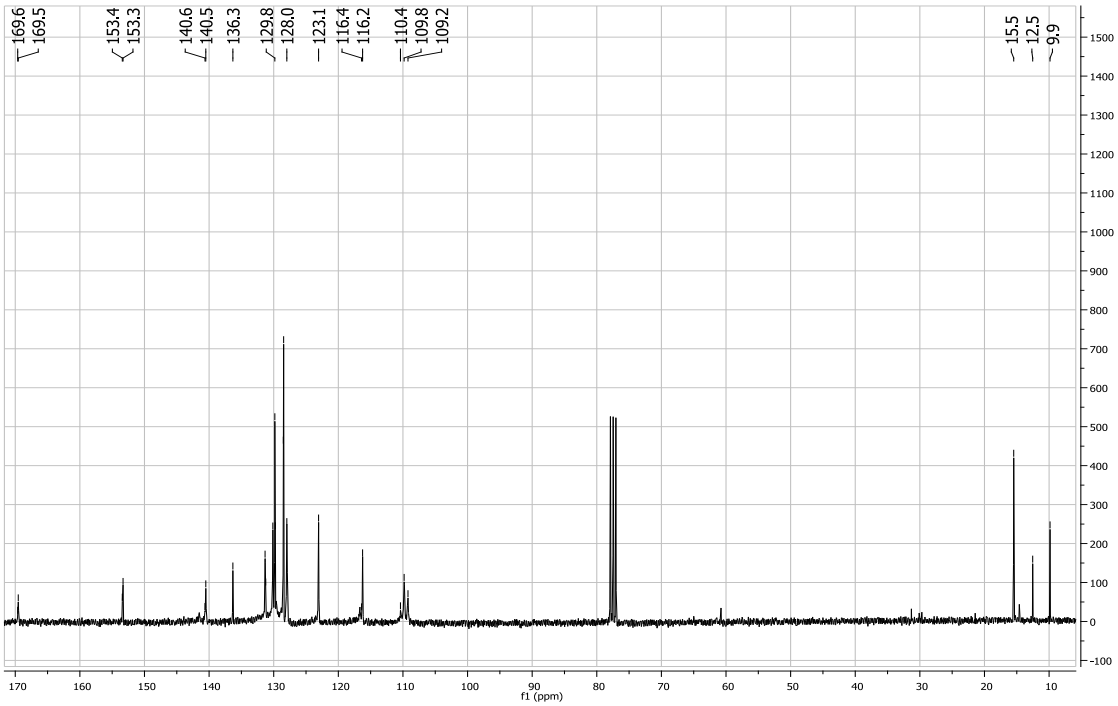

_N_-(2-(prop-1-en-1-yloxy)phenyl)benzamide **153**

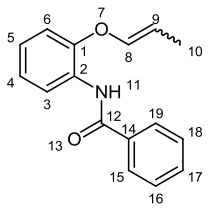

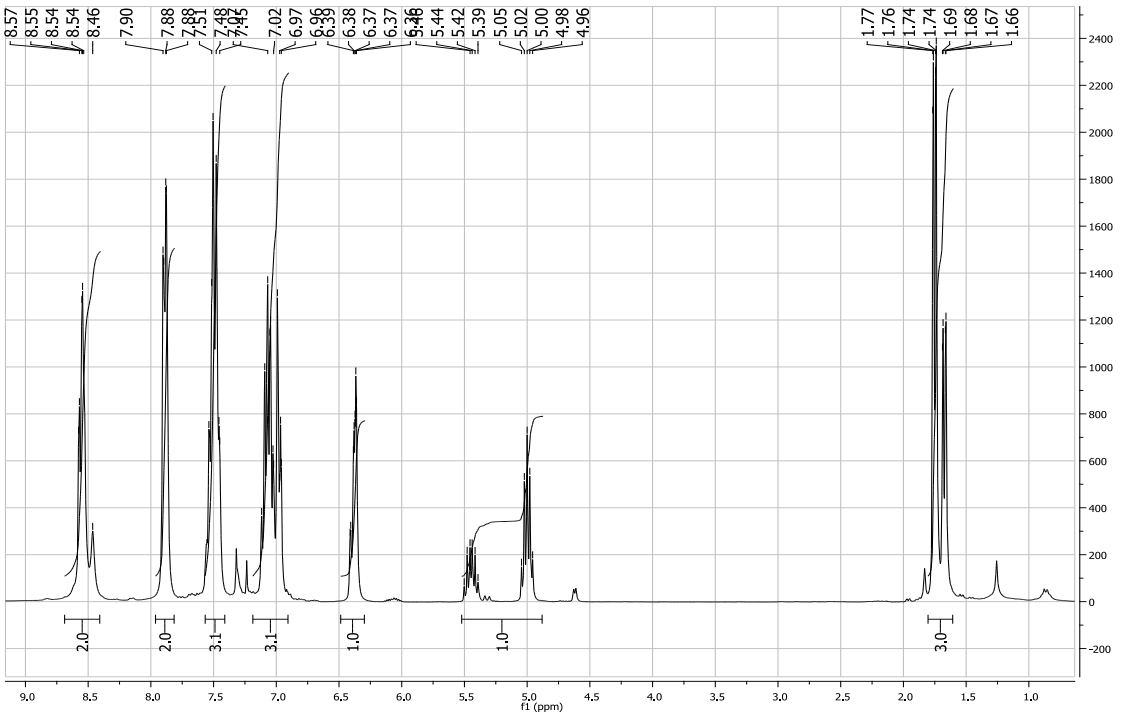

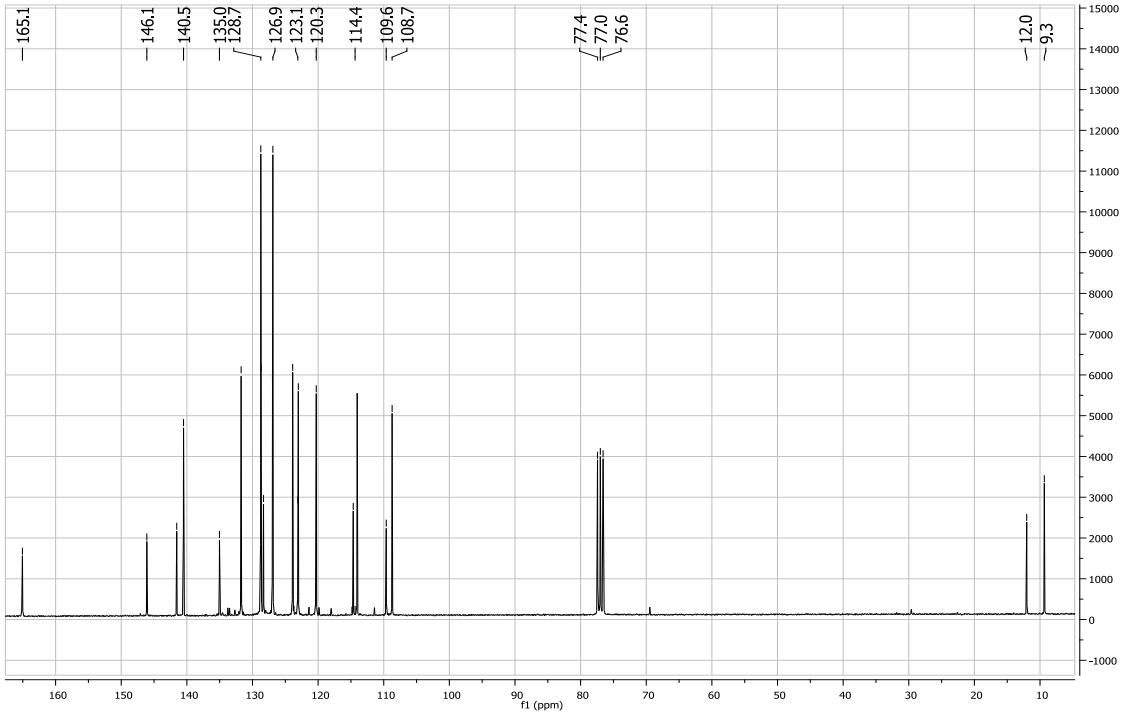

_N_-(prop-2-en-1-yl)-_N_-(2-(prop-1-en-1-yloxy)phenyl)benzamide 154

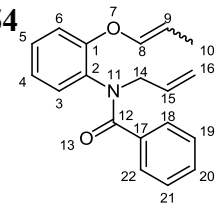

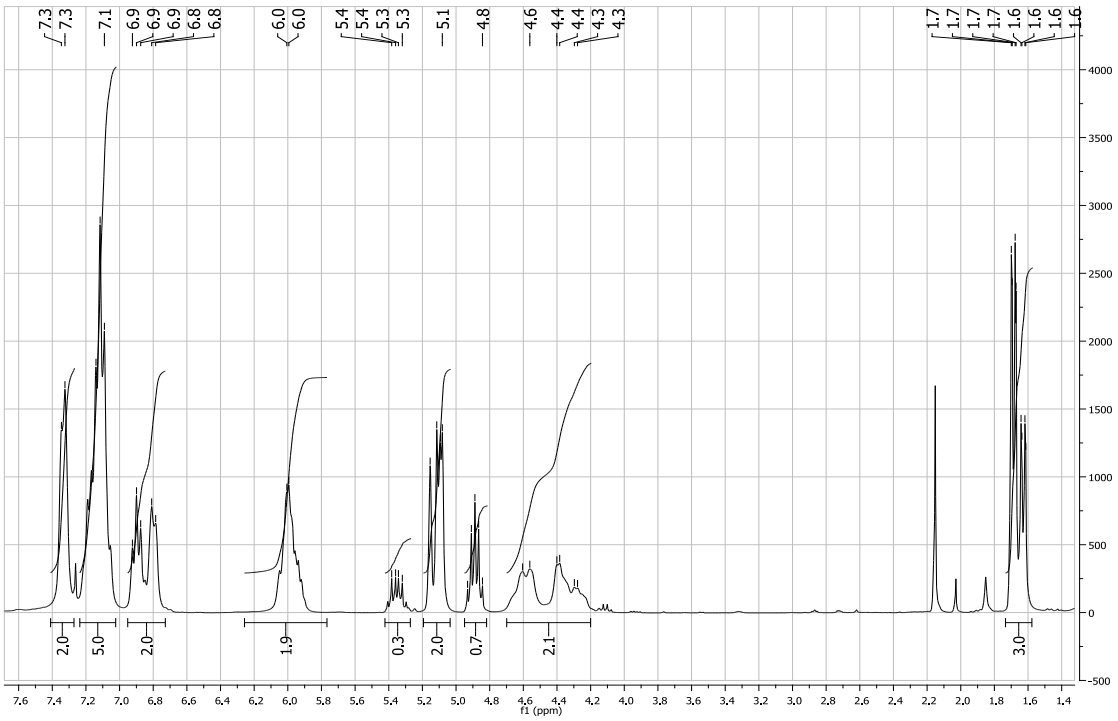

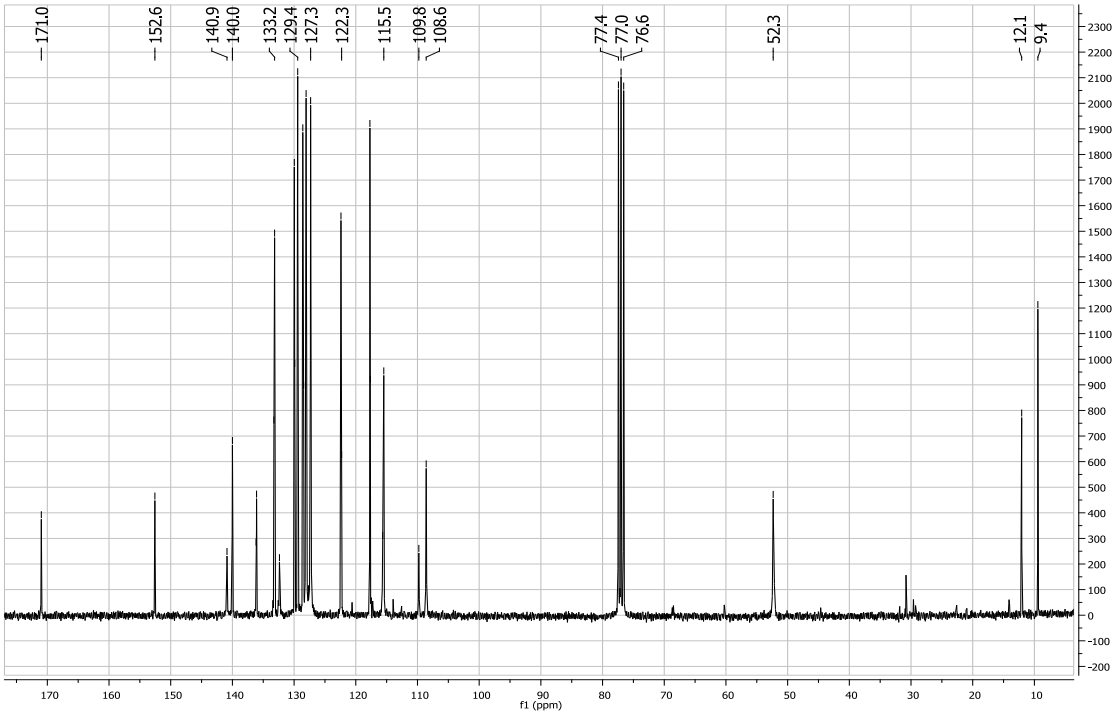

_N_-(prop-2-en-1-yl)-_N_-[2-(prop-2-en-1-yloxy)phenyl]benzamide 149

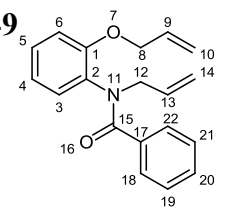

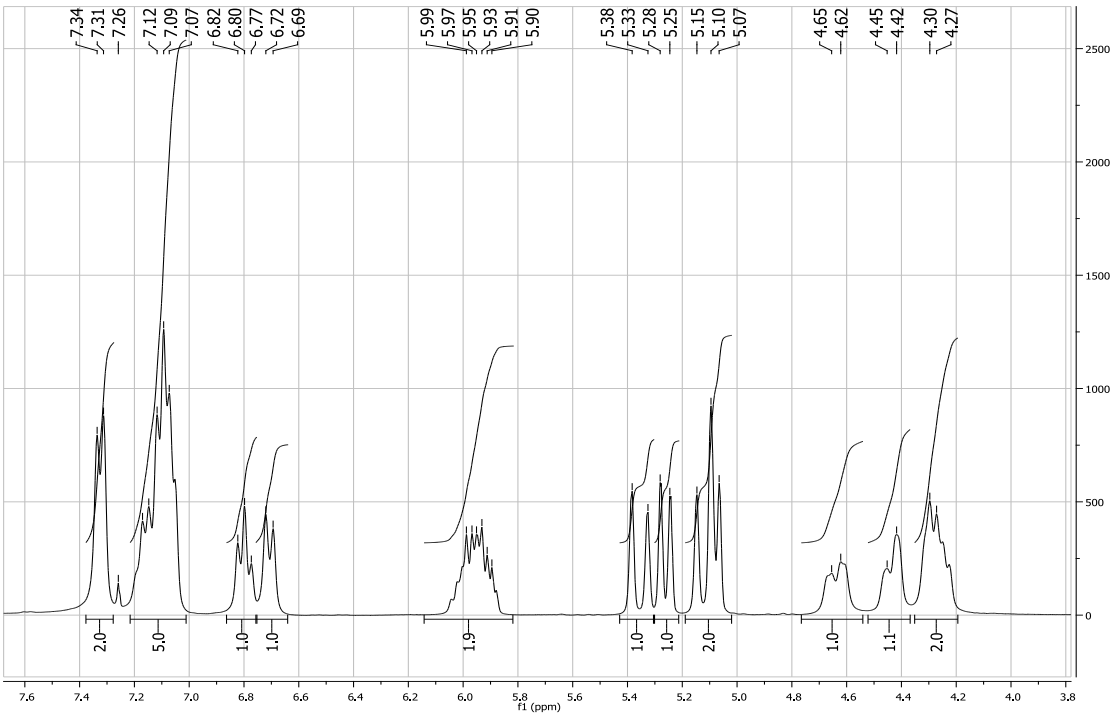

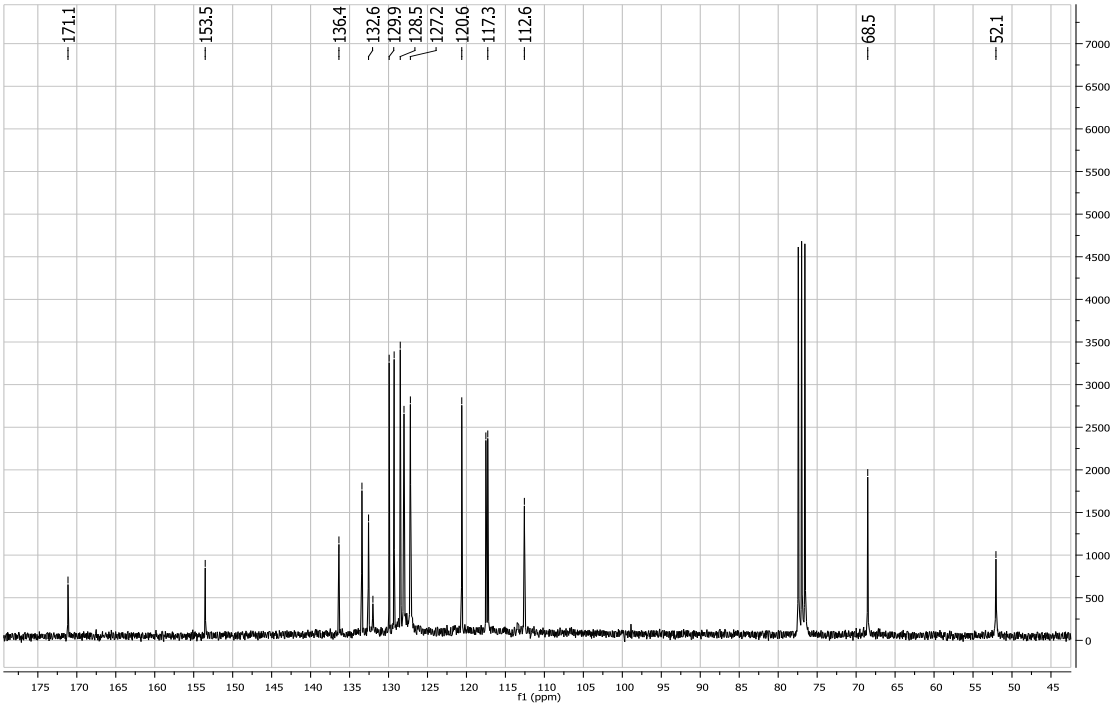

***N*-(2-(prop-2-en-1-yloxy)phenyl)benzamide** **148**

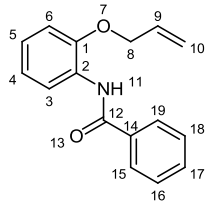

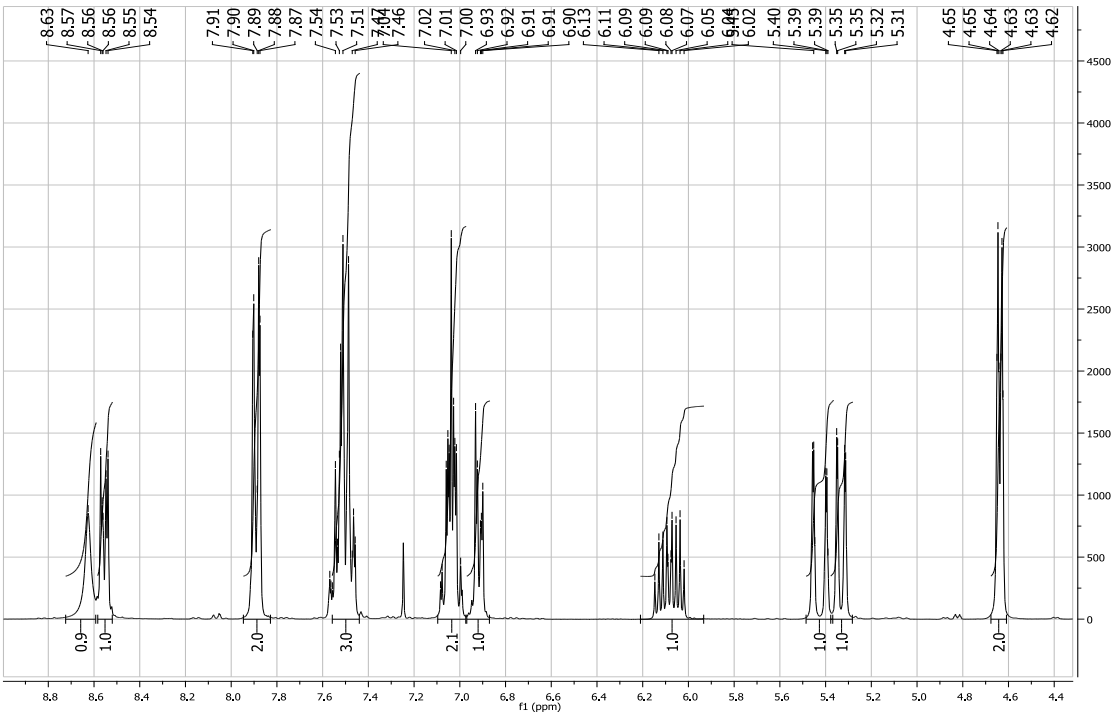
8.63
8.57
8.56
8.56
8.55
8.54
7.91
7.90
7.89
7.88
7.87
7.54
7.53
7.51
7.47
7.46
7.02
7.01
7.00
6.93
6.92
6.91
6.91
6.90
6.13
6.11
6.09
6.09
6.08
6.07
6.05
6.02
5.40
5.39
5.39
5.35
5.35
5.32
5.31
4.65
4.65
4.64
4.63
4.63
4.62
0.9
1.0
2.0
3.0
2.1
1.0
1.0
1.0
1.0
2.0
f1 (ppm)

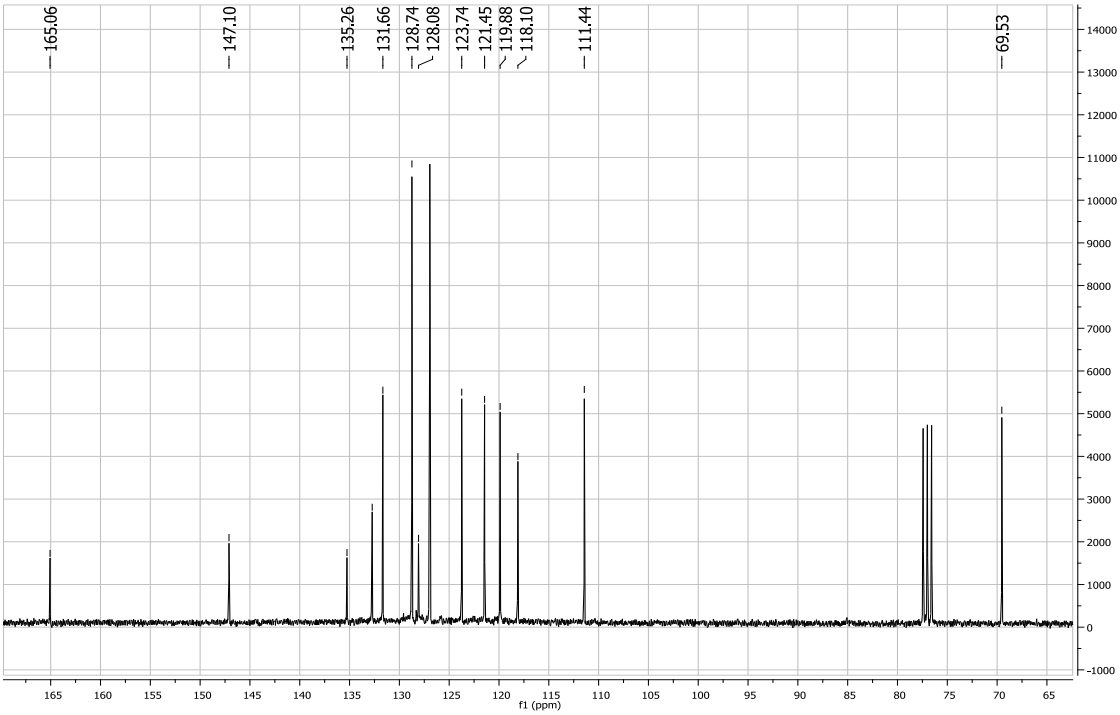
165.06
147.10
135.26
131.66
128.74
128.08
123.74
121.45
119.88
118.10
111.44
69.53
f1 (ppm)

^{1}H and ^{13}C NMR spectra for the 6-, 7- and 8-membered *N,N*-benzo-fused heterocycles and precursors

_N_-[2-(acetylamino)phenyl]-_N_-(prop-2-en-1-yl)acetamide **160**

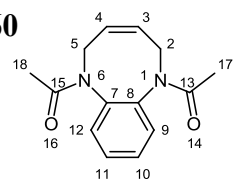

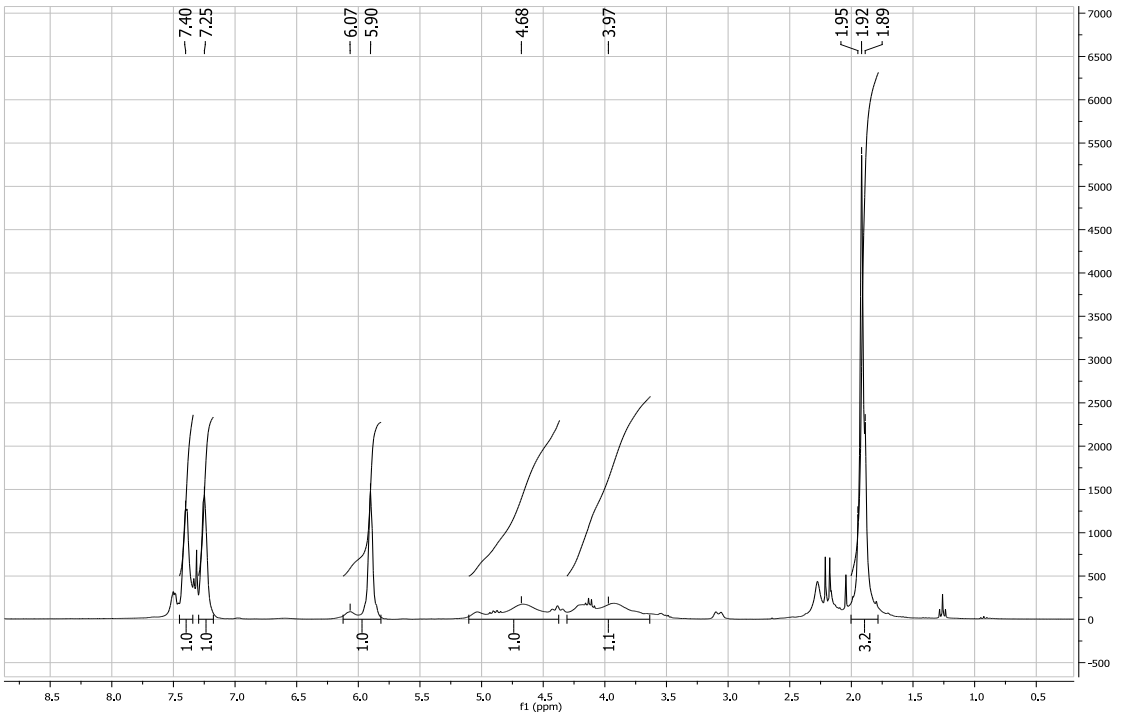

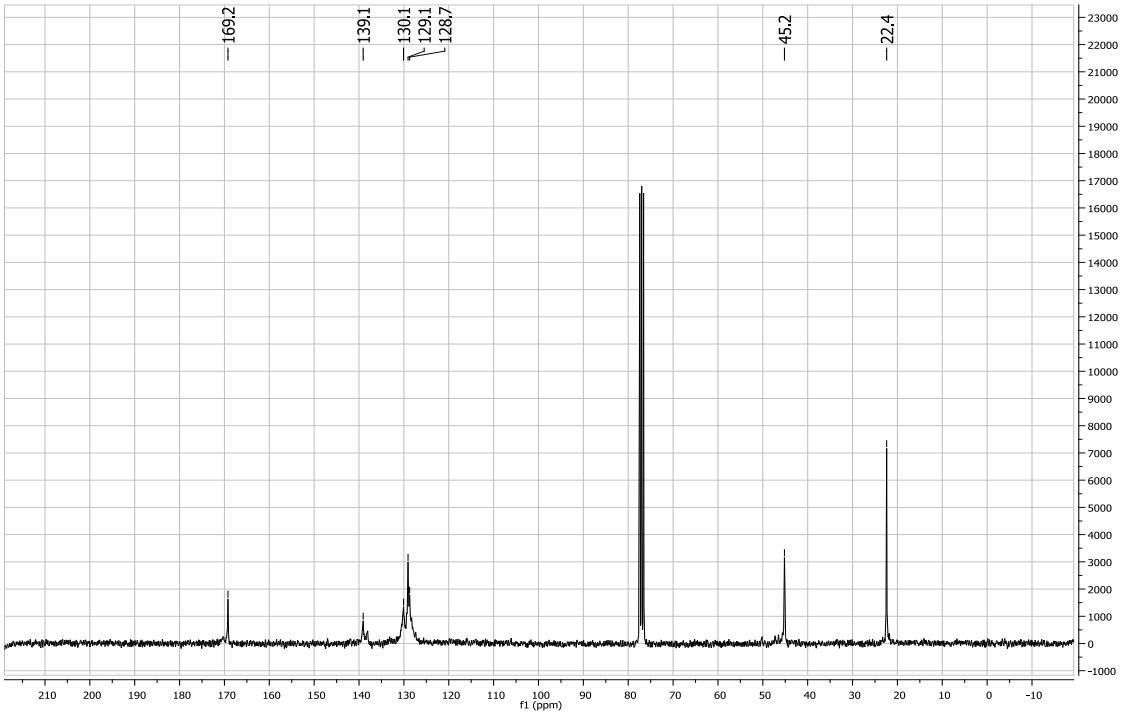

Unknown product spectra for the attempted formation of 1,1'-(1*H*-1,5-benzodiazepine-1,5-(2*H*)-diyl)diethanone 165

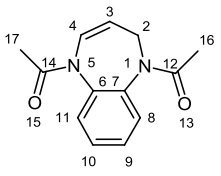

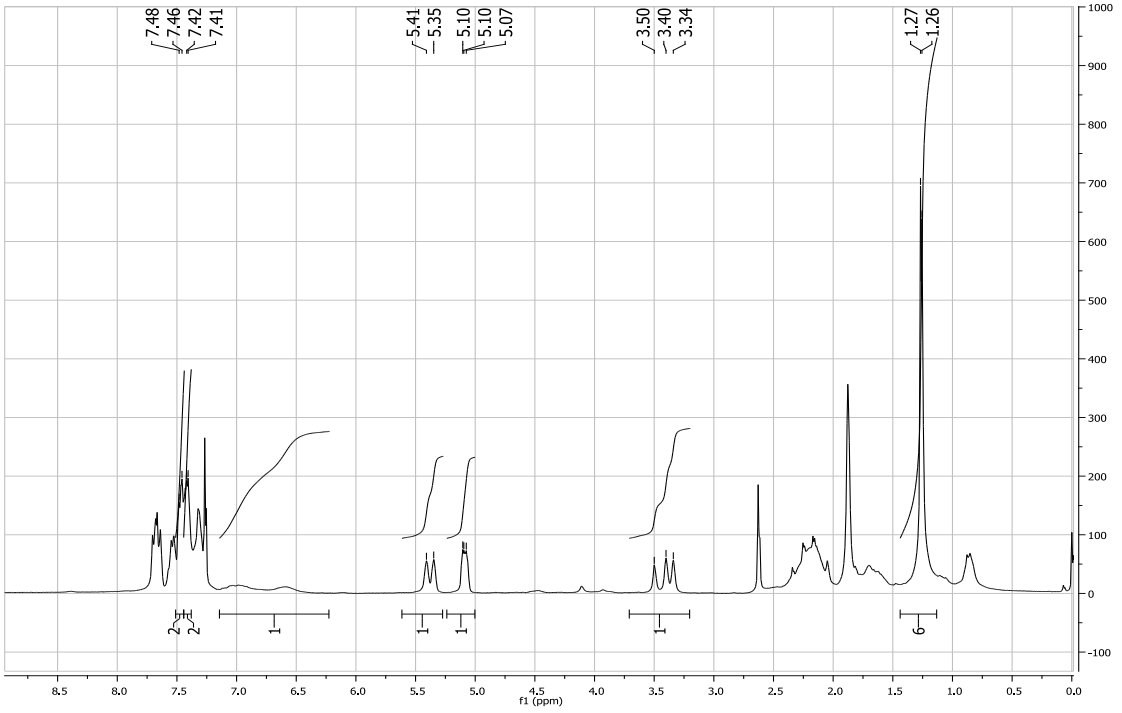

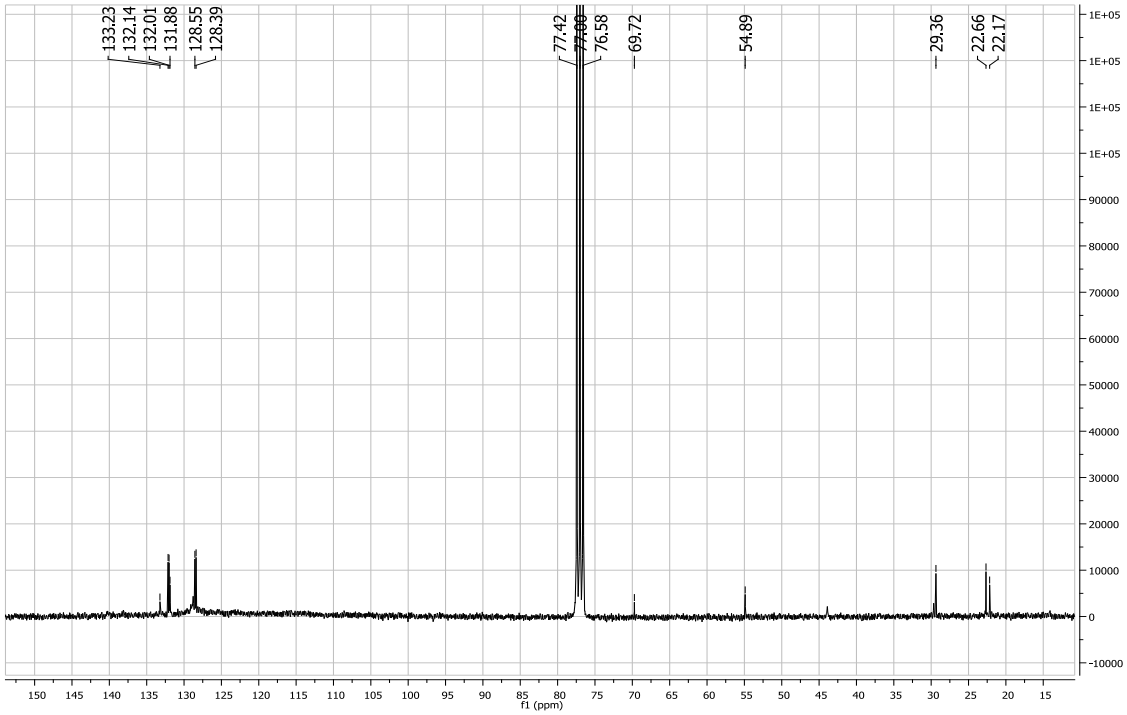

***N*-[2-(acetylamino)phenyl]-*N*-(prop-1-en-1-yl)acetamide** **163**

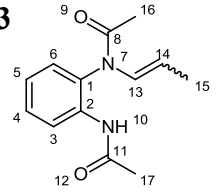

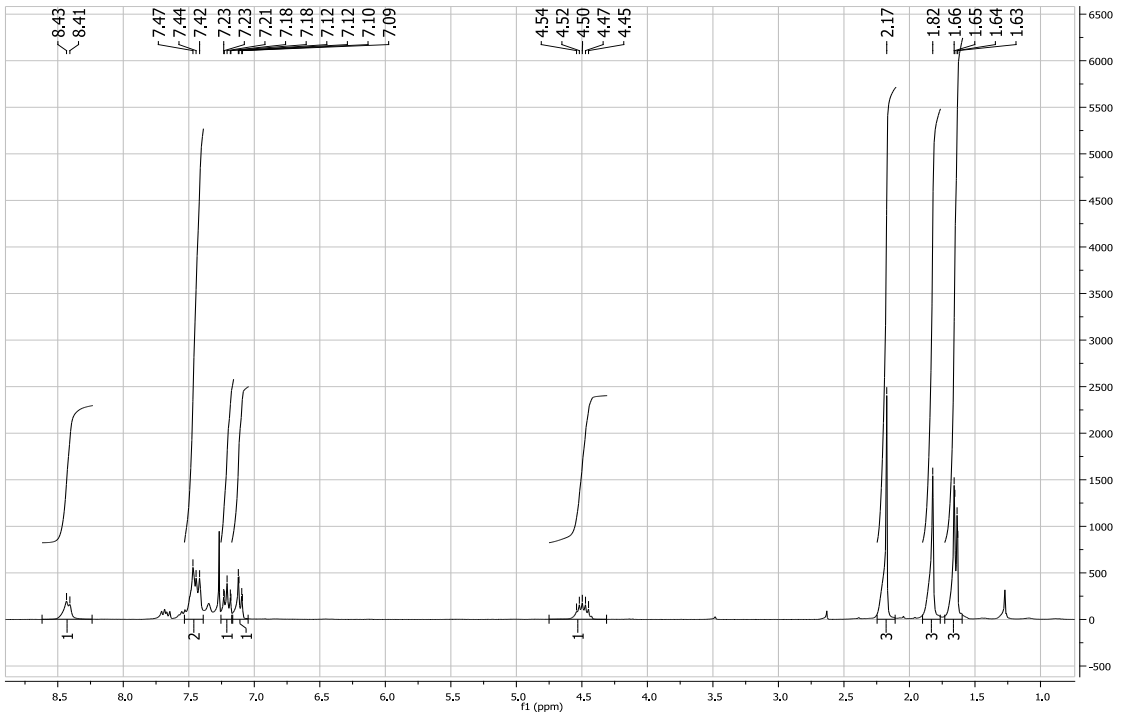

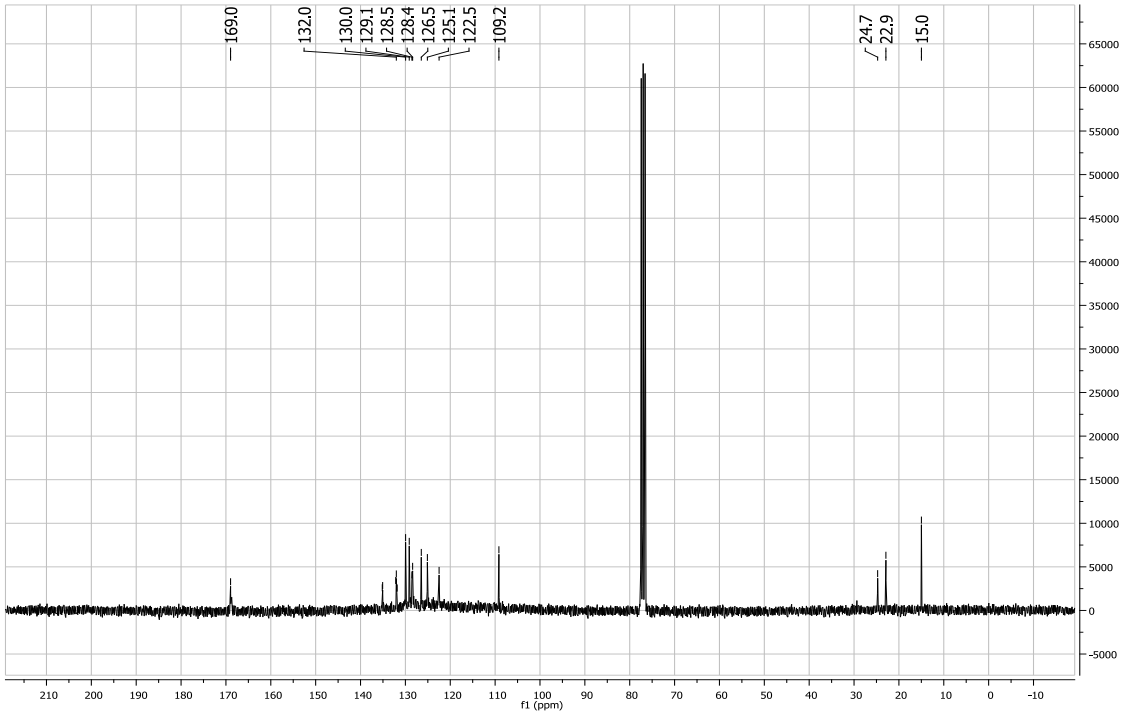

_N,N′_-benzene-1,2-diylbis[_N_-(prop-1-en-1-yl)acetamide] **161**

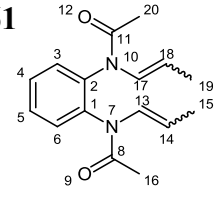

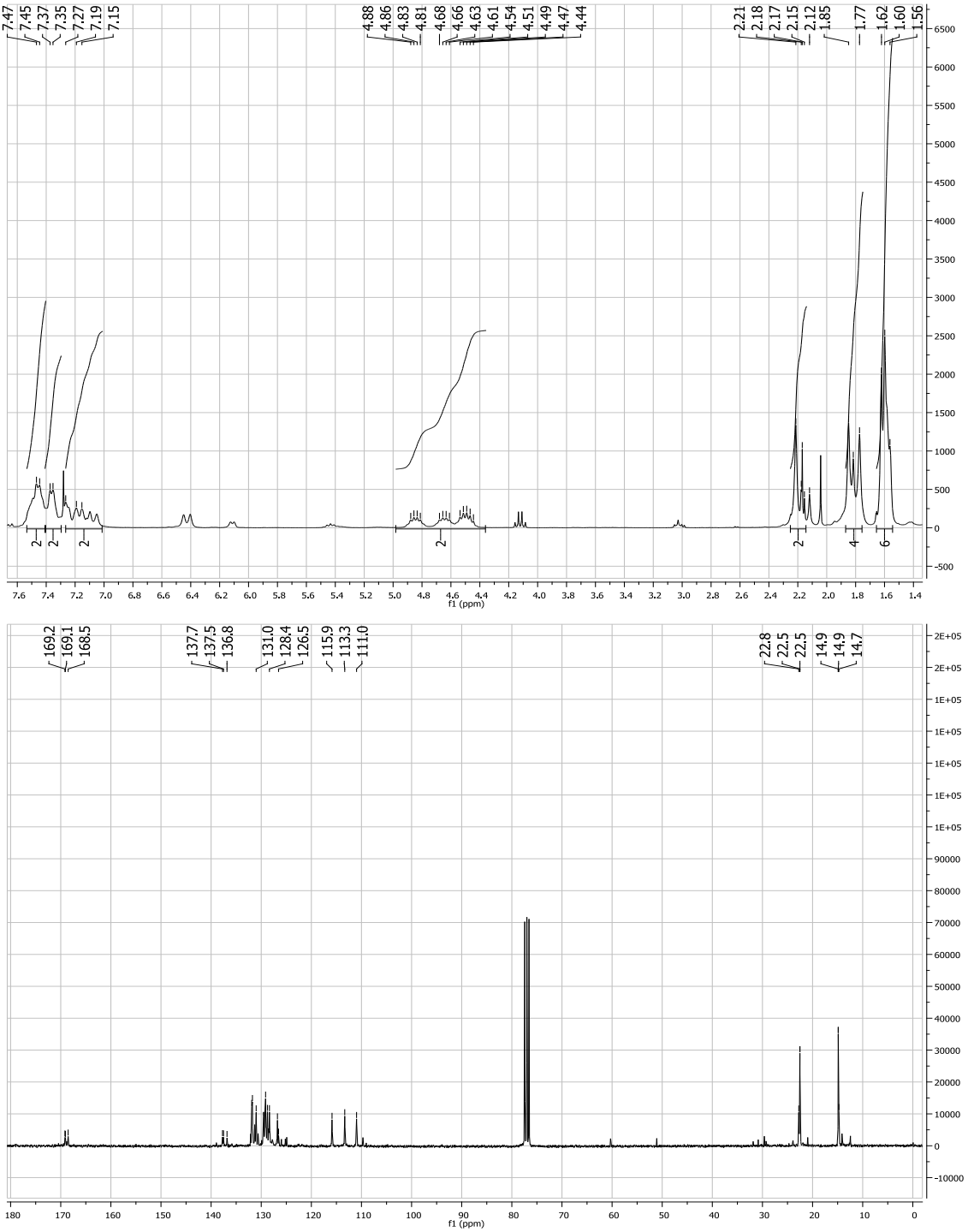

_N_-{2-[acetyl(prop-1-en-1-yl)amino]phenyl}-_N_-(prop-2-en-1-yl)acetamide 161

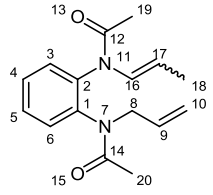

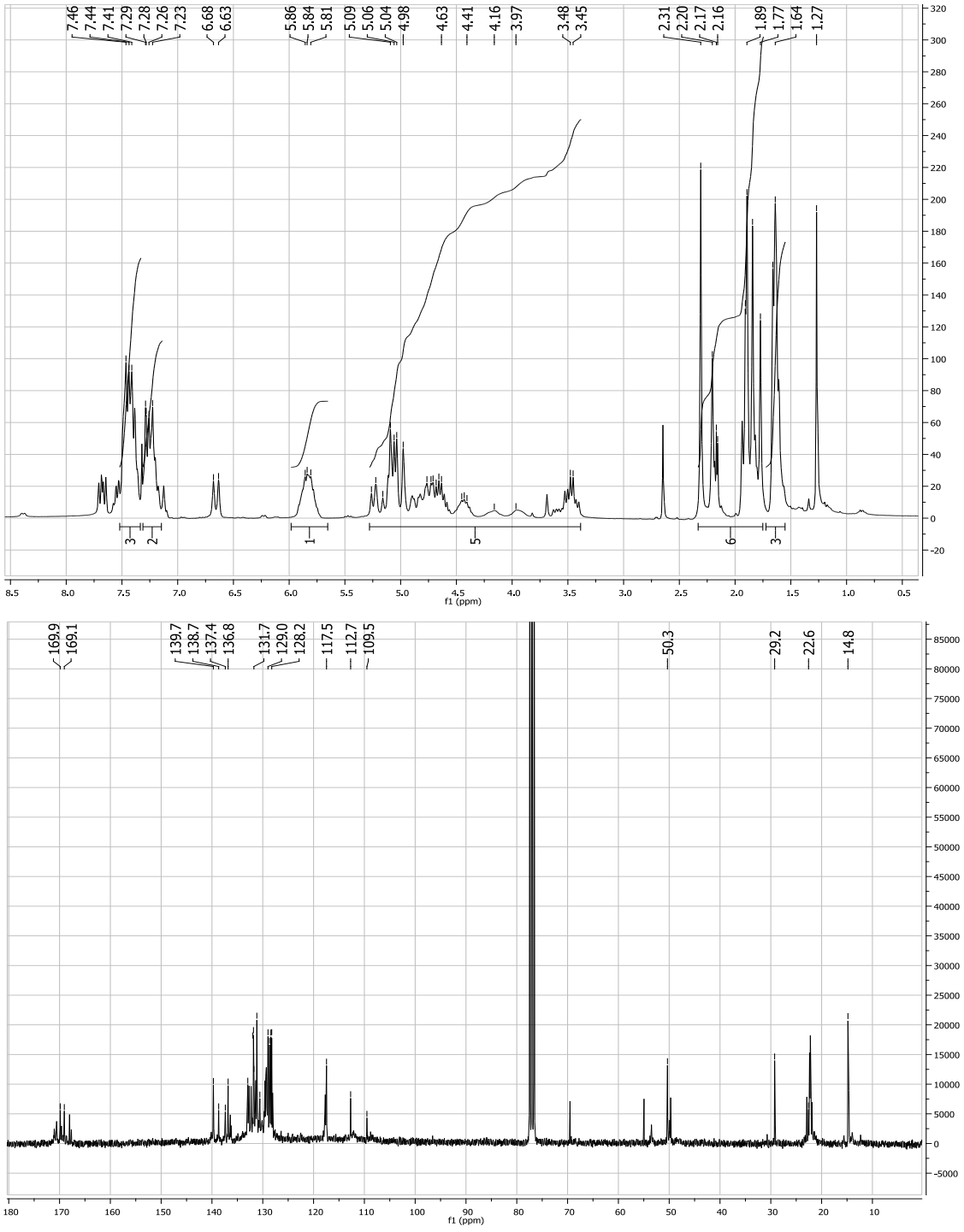

C-H correlated spectrum of 161

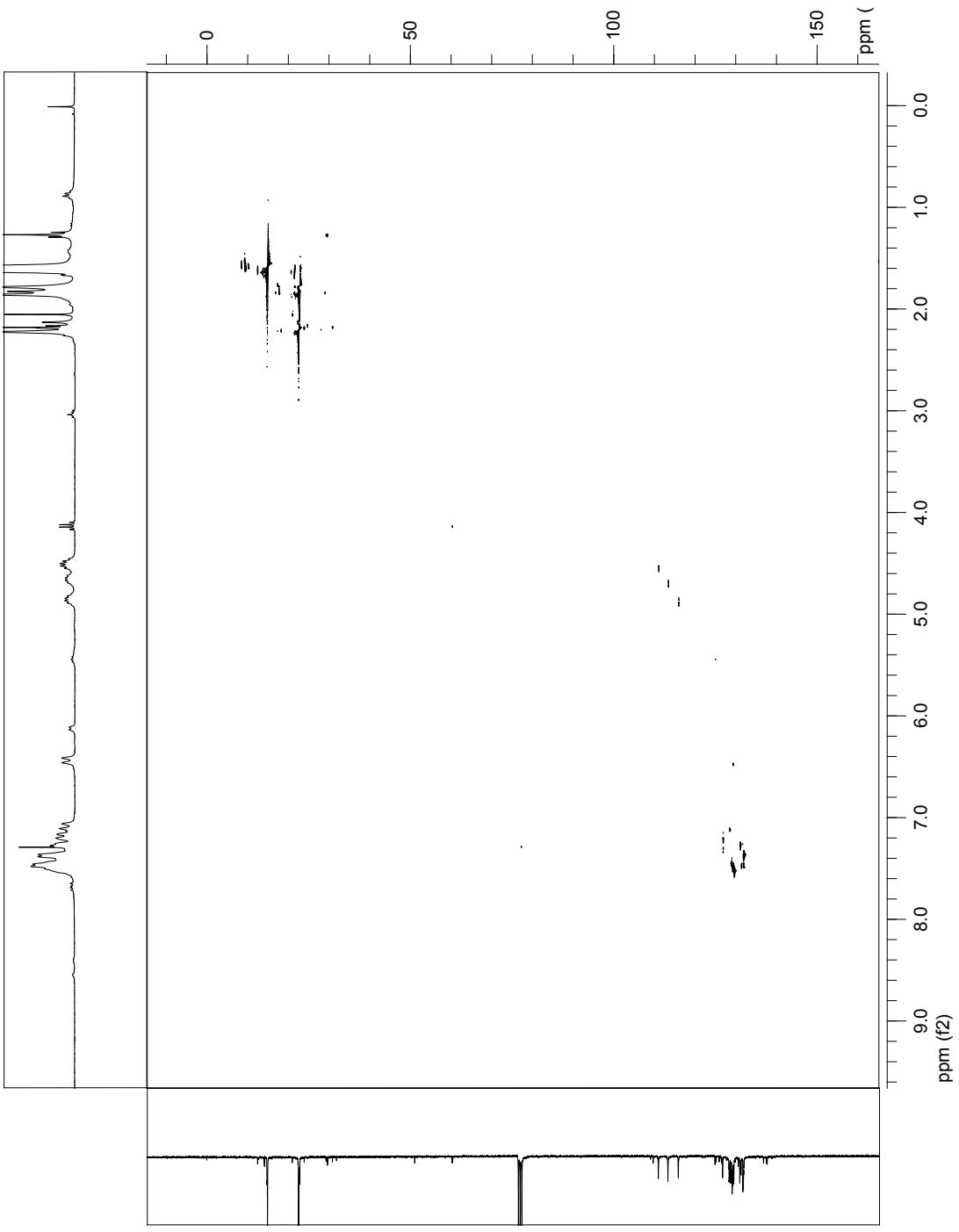

***N*,*N*'-benzene-1,2-diylbis[*N*-(prop-2-en-1-yl)acetamide]** **159**

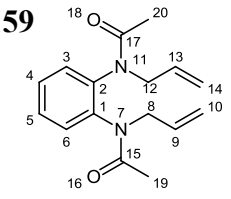

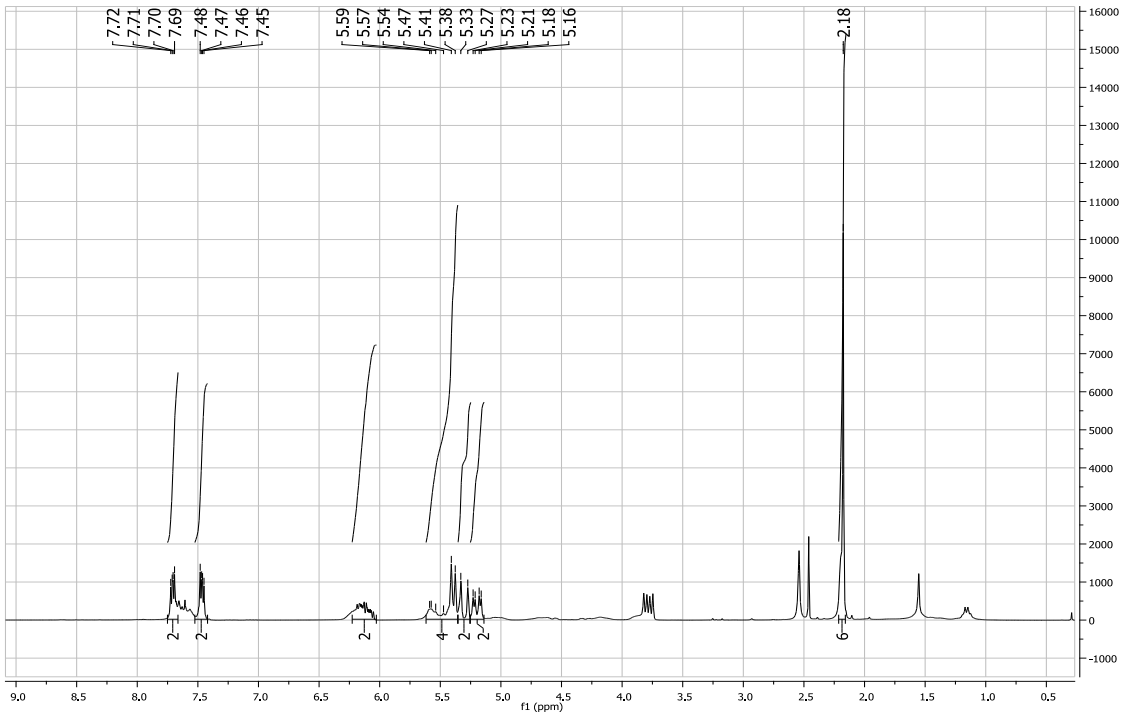

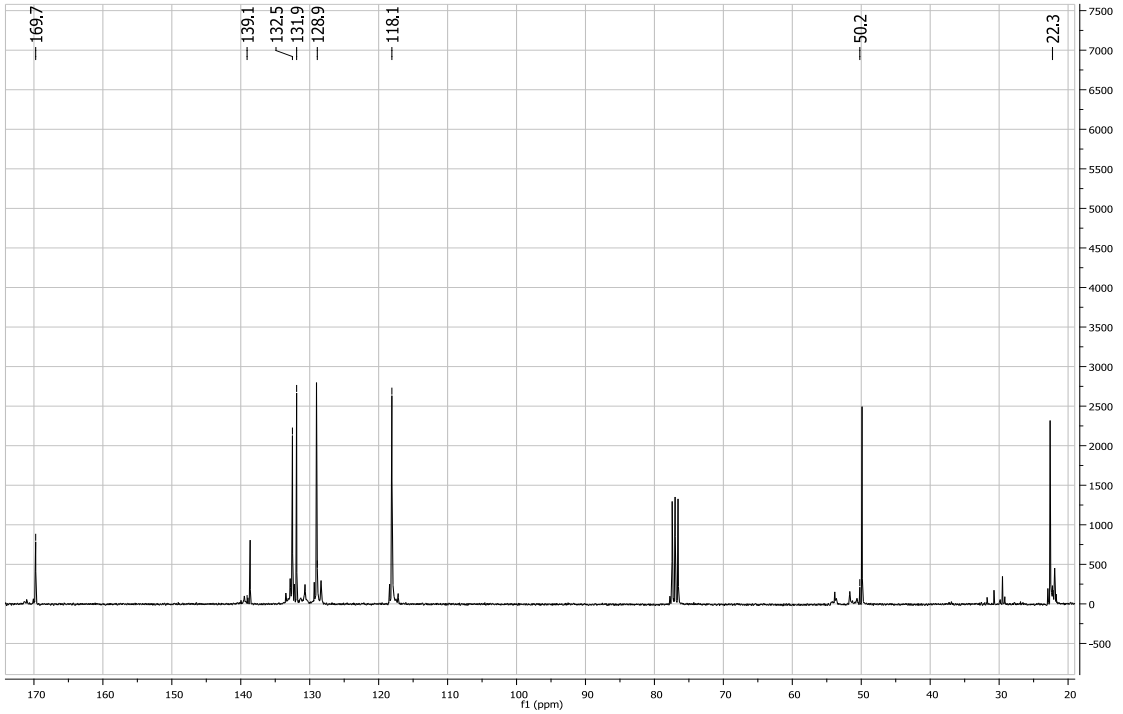

_N_-[2-(acetylamino)phenyl]-_N_-(prop-2-en-1-yl)acetamide **158**

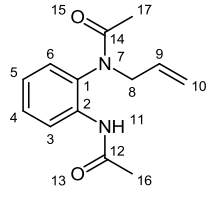

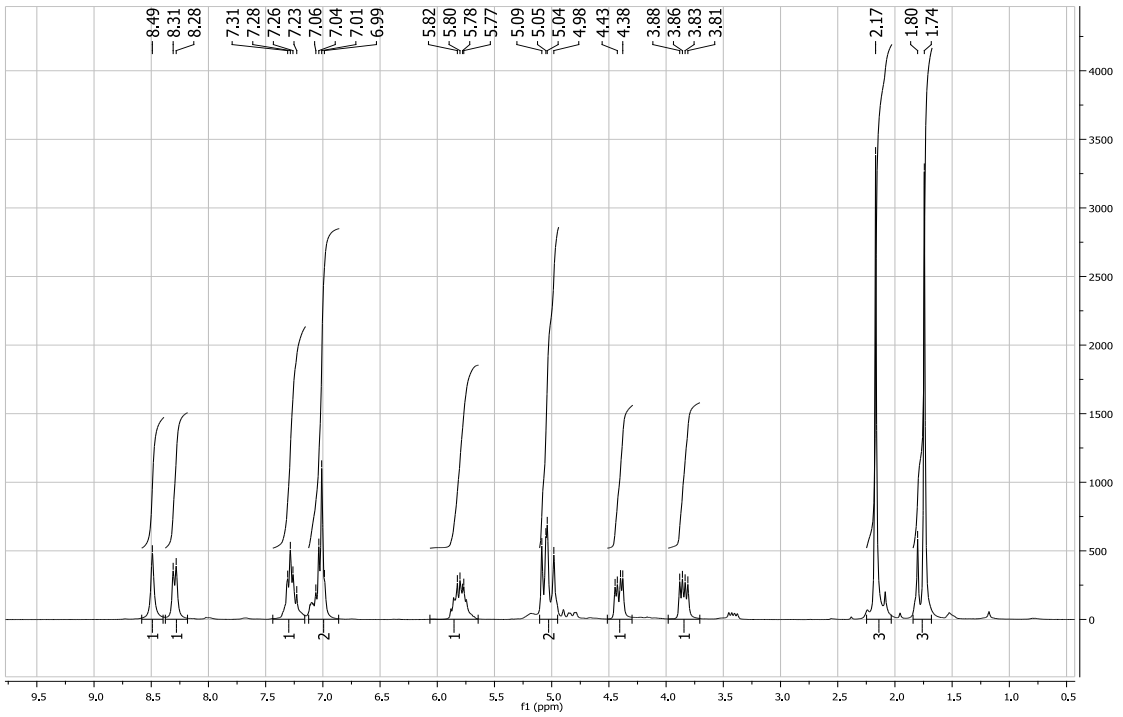
8.49
8.31
8.28
7.31
7.28
7.26
7.23
7.06
7.04
7.01
6.99
5.82
5.80
5.78
5.77
5.09
5.05
5.04
4.98
4.43
4.38
3.88
3.86
3.83
3.81
2.17
1.80
1.74
f1 (ppm)

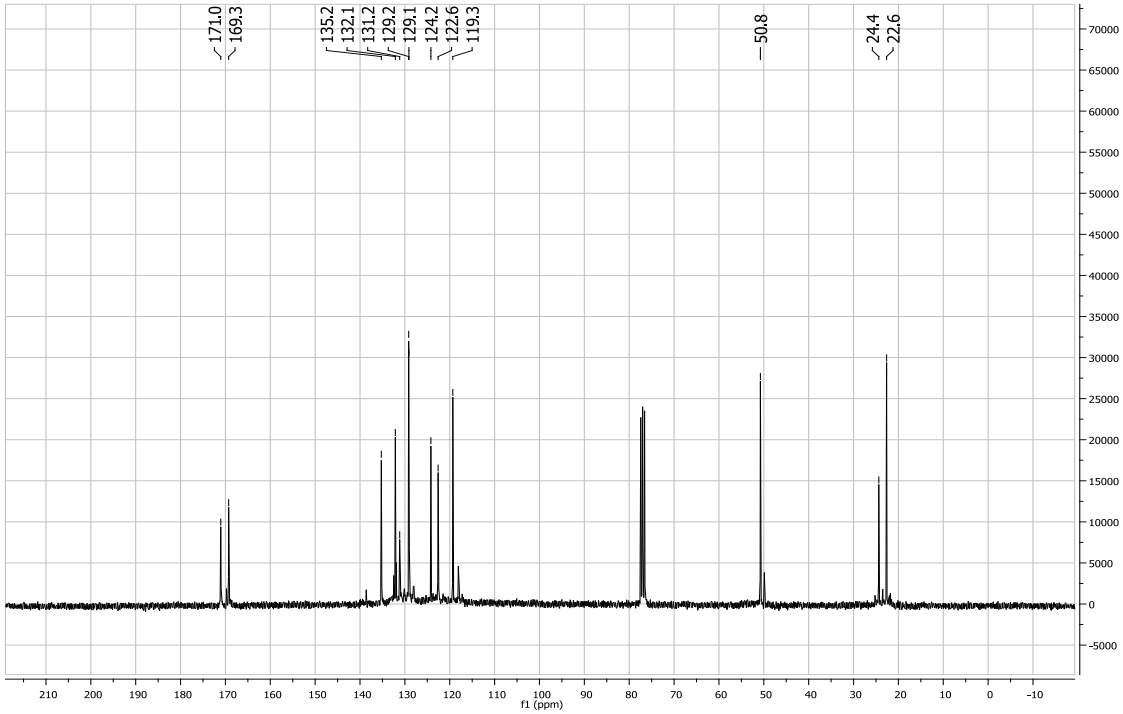
171.0
169.3
135.2
132.1
131.2
129.2
129.1
124.2
122.6
119.3
50.8
24.4
22.6
f1 (ppm)

APPENDIX B

SELECTED MS SPECTRA

5.1.5.1 4,7-Dimethoxybenzofuran 145a

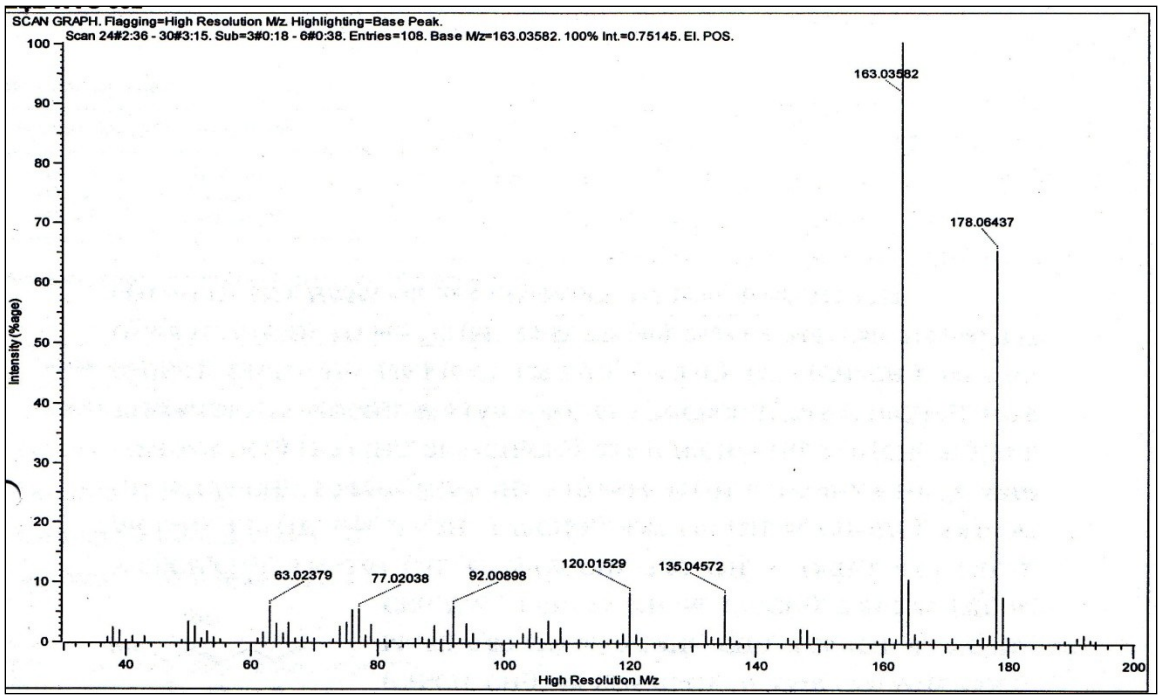

5.1.3.1 1,4-Dimethoxy-2-(prop-2-en-1-yl)-3-(prop-2-en-1-yloxy)benzene 143a

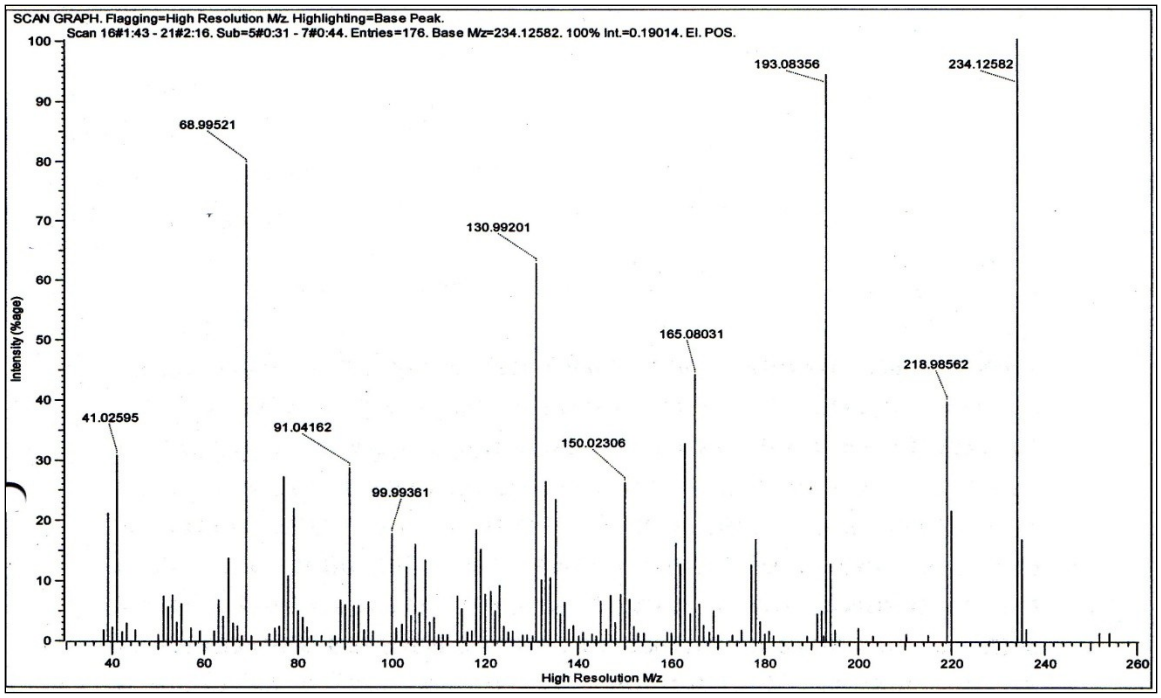

5.1.5.2 5-Bromobenzofuran 145b

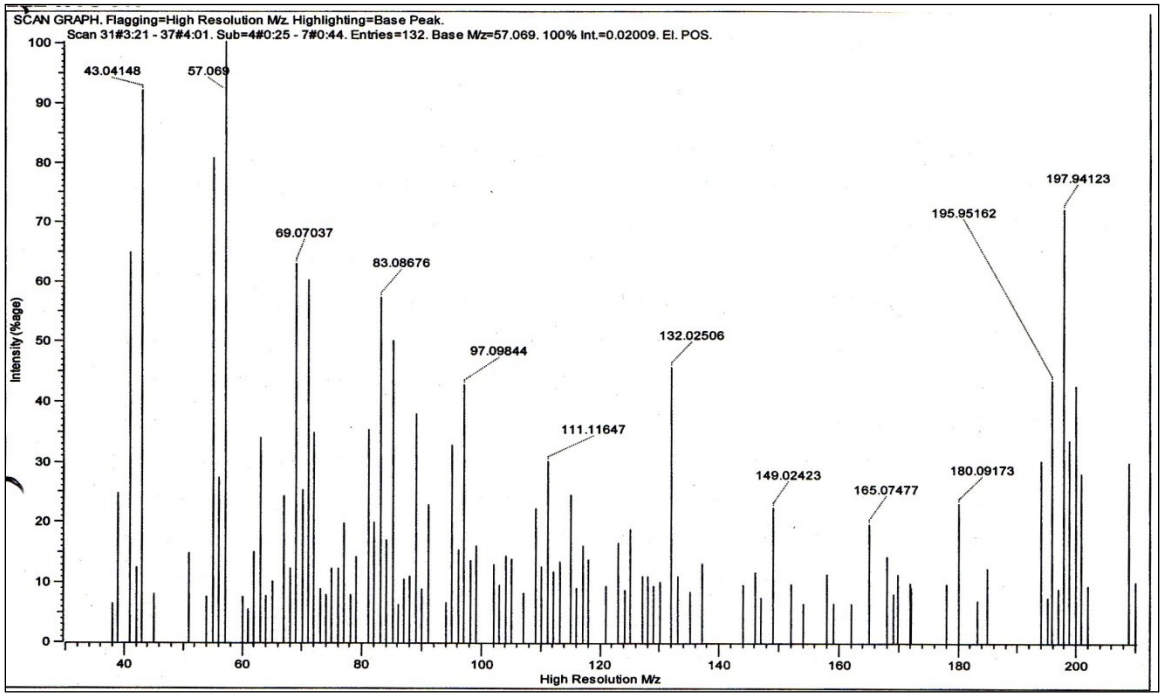

5.1.4.2 4-Bromo-2-(prop-1-en-1-yl)-1-(prop-1-en-1-yloxy)benzene 144b

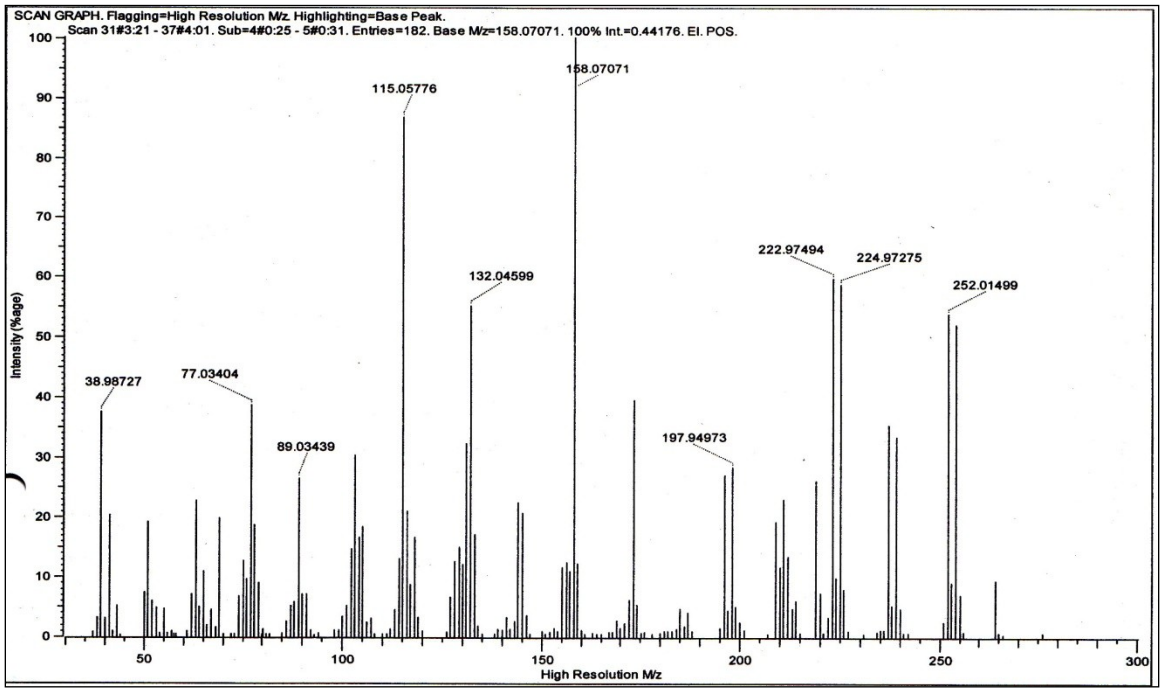

5.1.3.2 4-Bromo-2-(prop-2-en-1-yl)-1-(prop-2-en-1-yloxy)benzene 143b

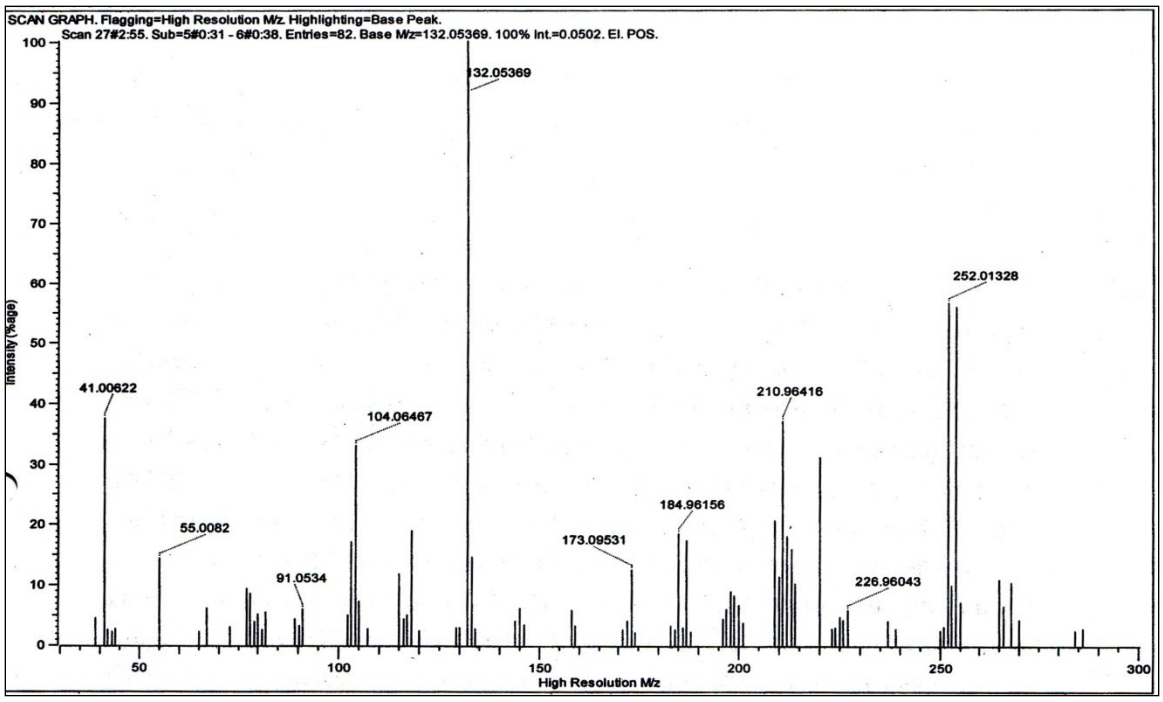

5.1.5.3 5-*tert*-Butyl-benzofuran 145c

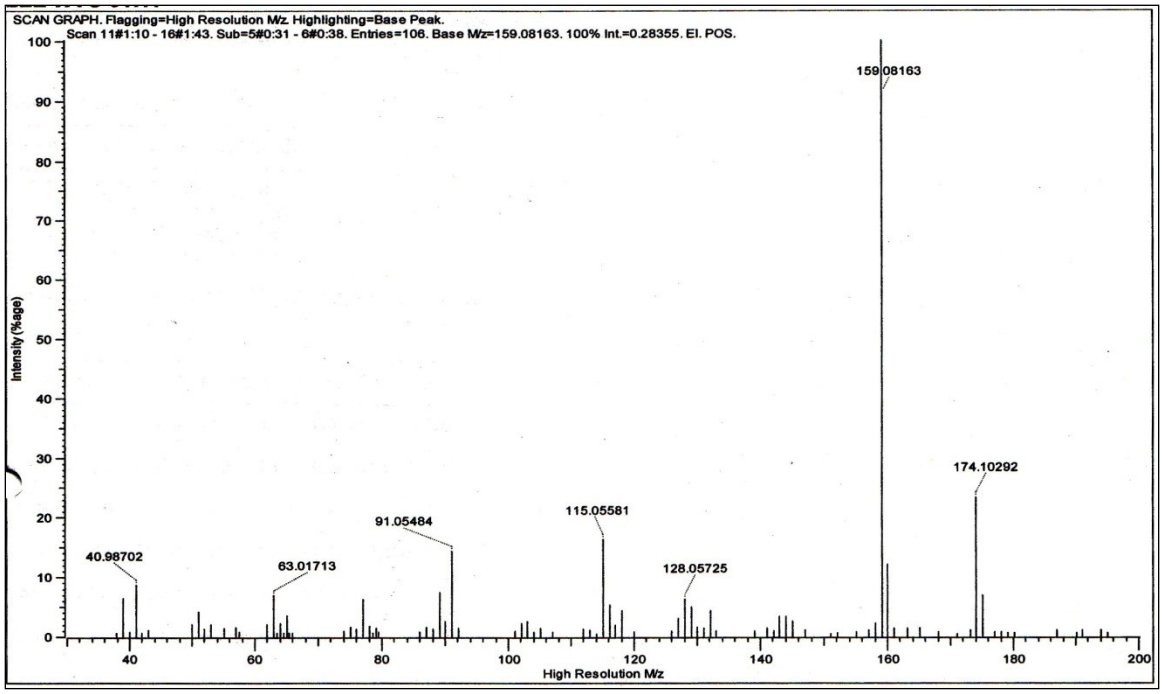

5.1.4.3 4-*tert*-butyl-2-(prop-1-en-1-yl)-1-(prop-1-en-1-yloxy)benzene 144c

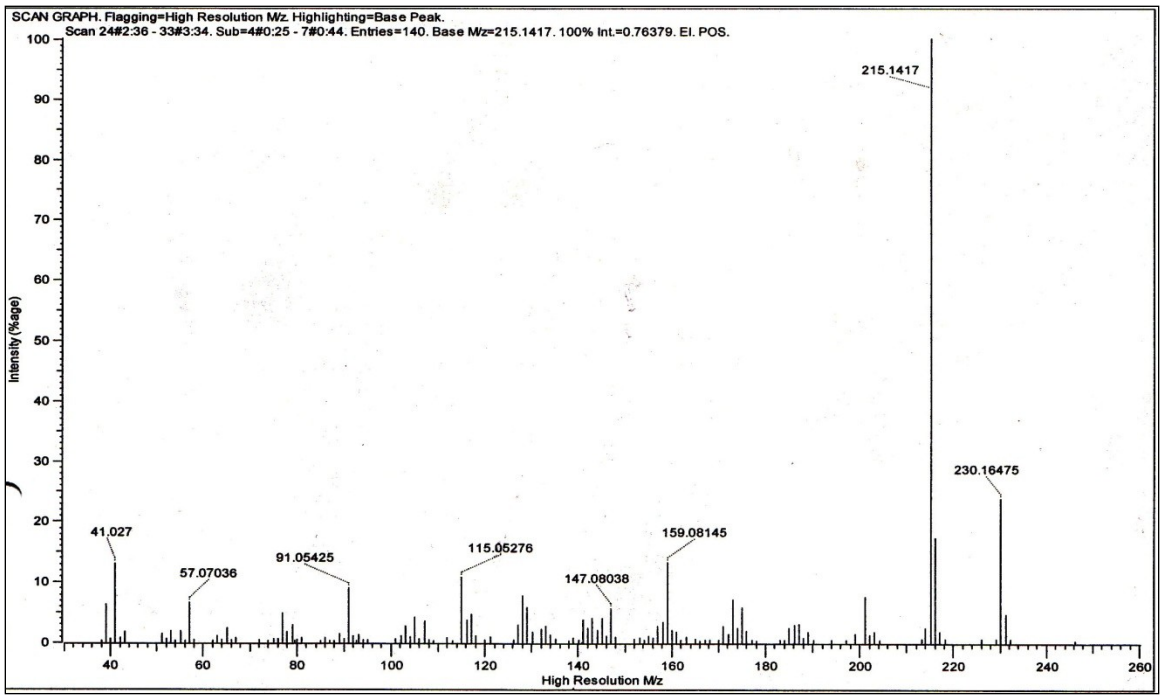

5.1.5.4 7-Phenyl-1-benzofuran 145d

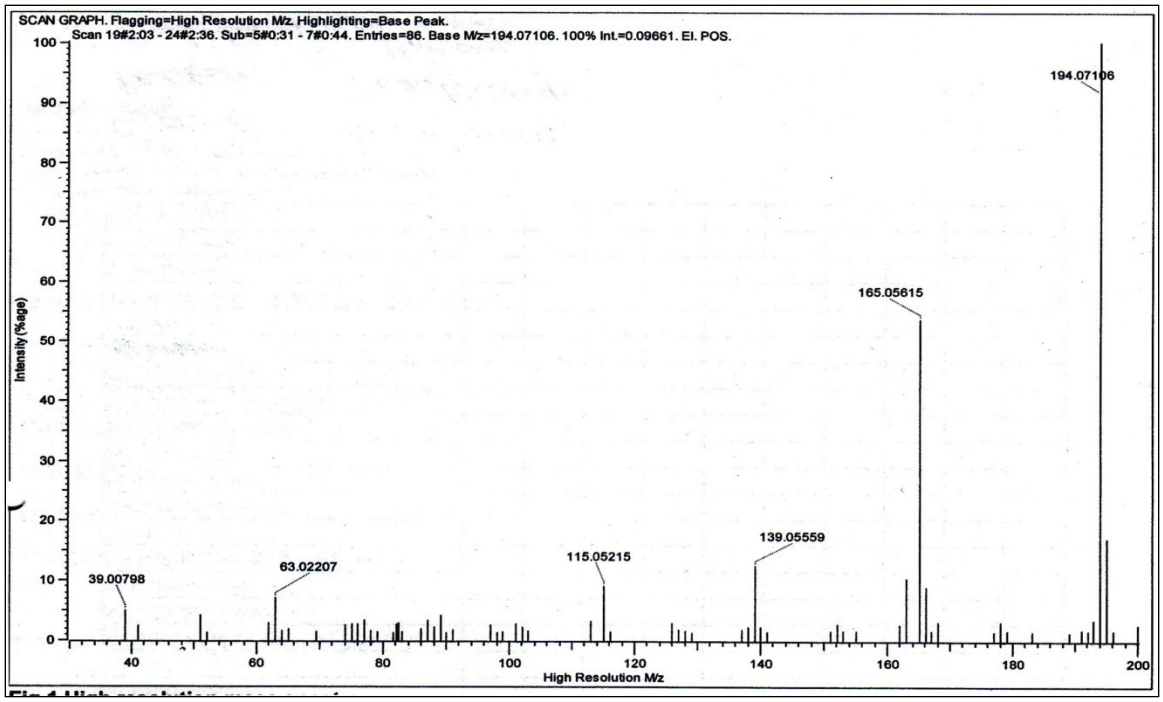

5.1.4.4 3-(Prop-1-en-1-yl)-2-(prop-1-en-1-yloxy)biphenyl 144d

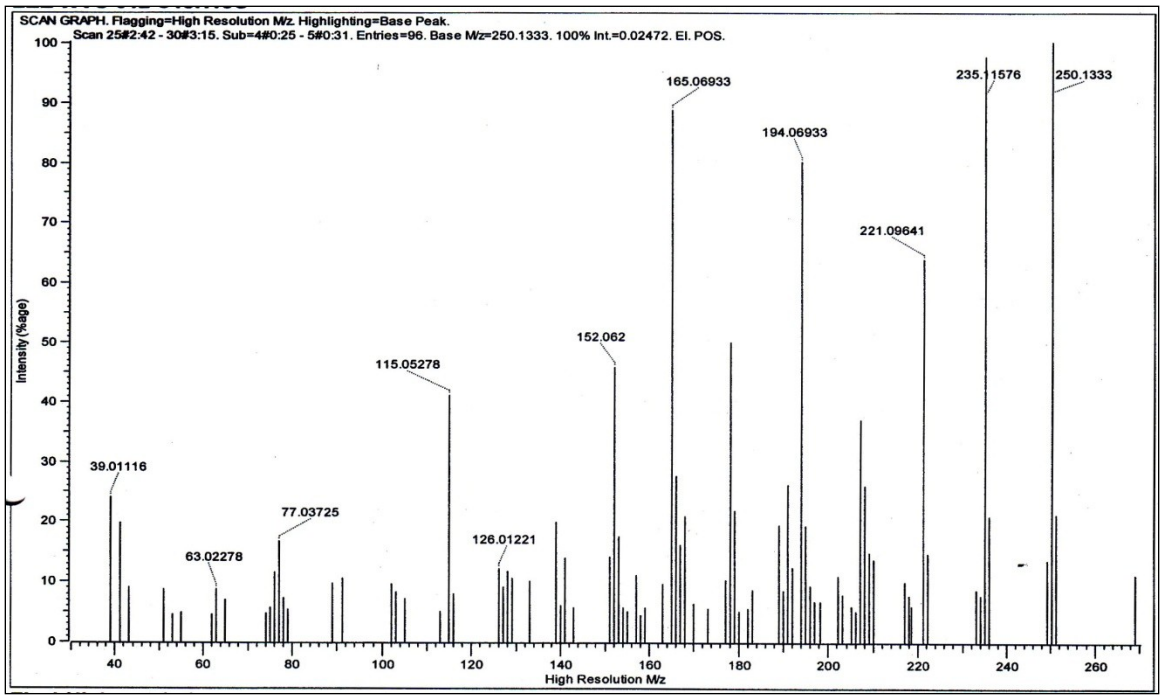

5.1.3.4 3-(Prop-2-en-1-yl)-2-(prop-2-en-1-yloxy)biphenyl 143d

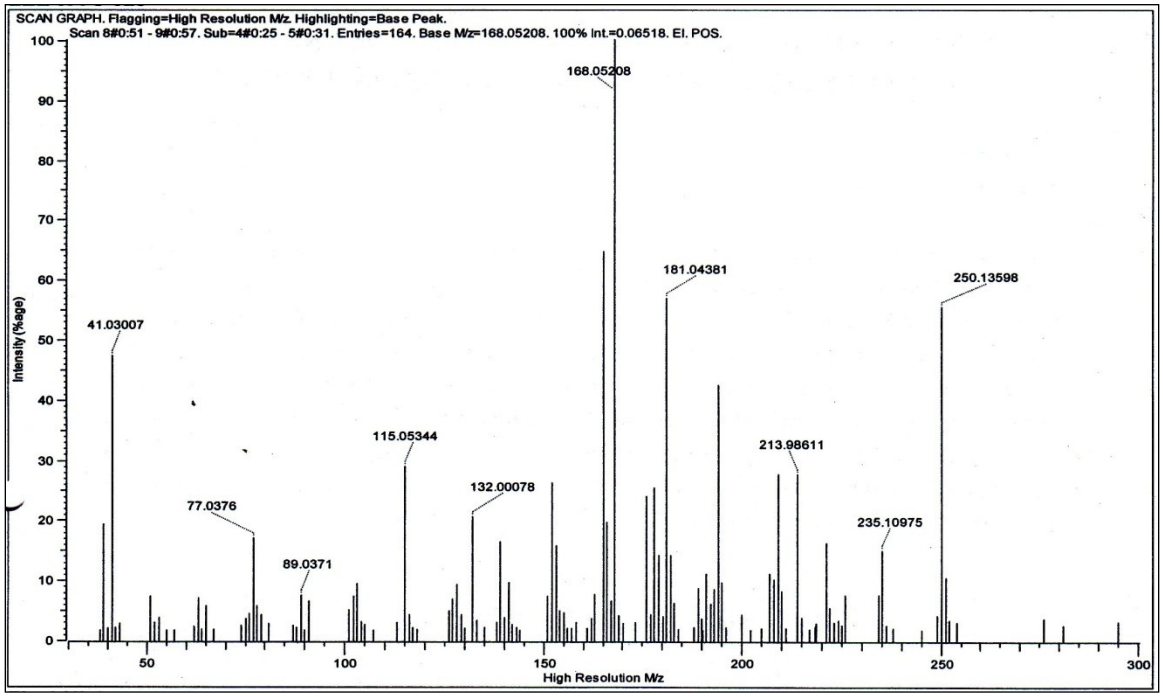

5.1.5.5 Naphtho[1,2-*b*]furan 145e

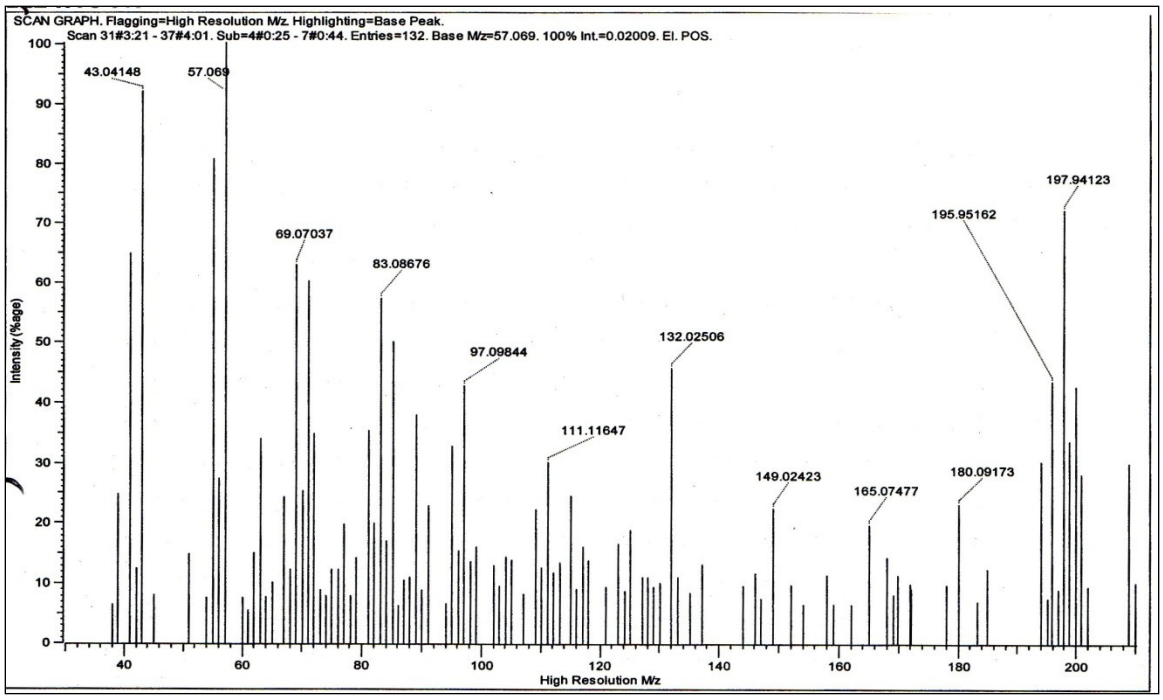

5.1.4.5 2-(Prop-1-en-1-yl)-1-(prop-1-en-1-yloxy)naphthalene 144e

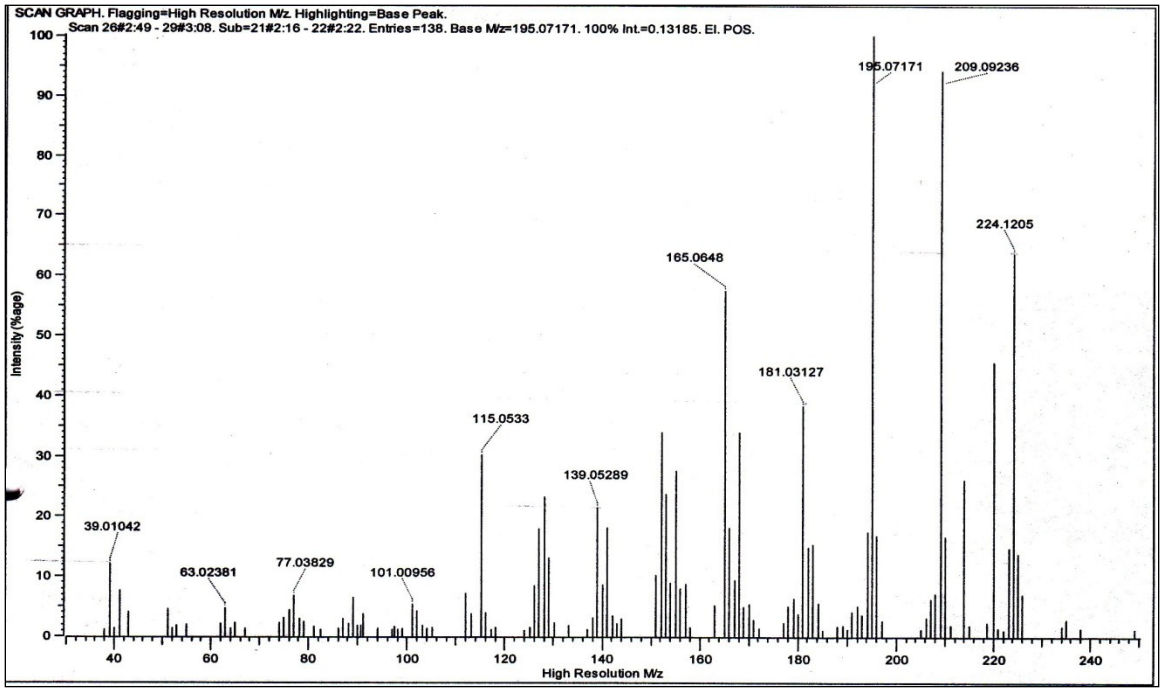

5.1.3.5 2-(Prop-2-en-1-yl)-1-(prop-2-en-1-yloxy)naphthalene 143e

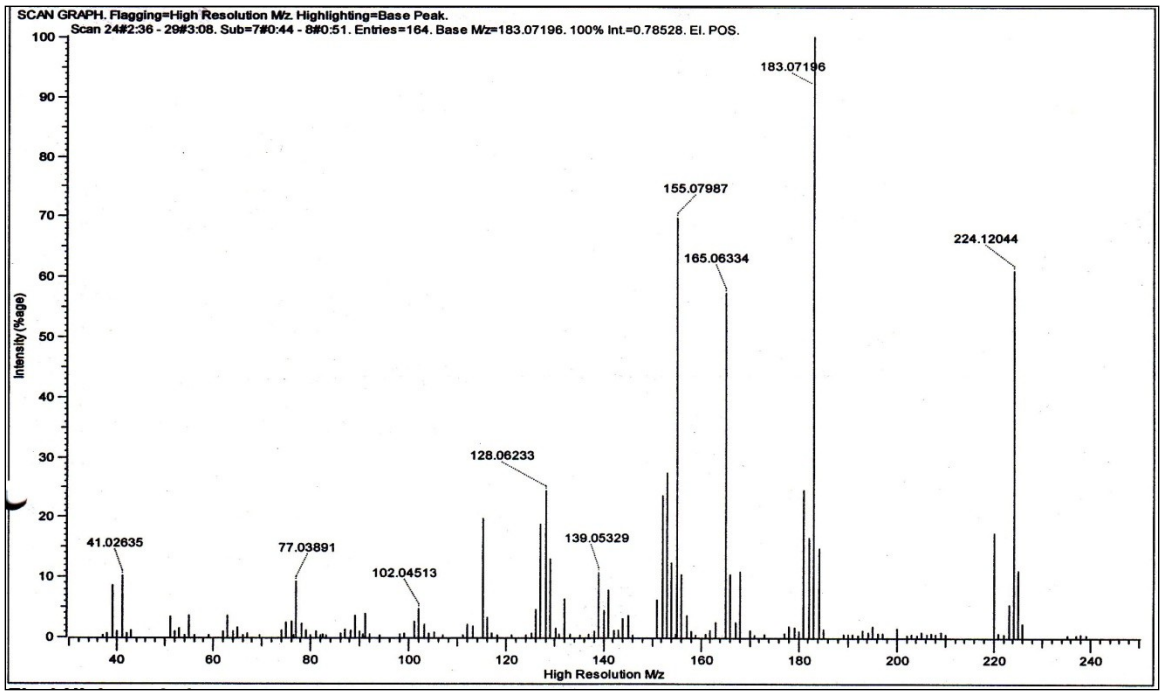

O,N-Benzo-fused heterocycles and precursors

5.2.4.2 1,5-Benzoxazepin-5(4*H*)-yl(phenyl)methanone 155

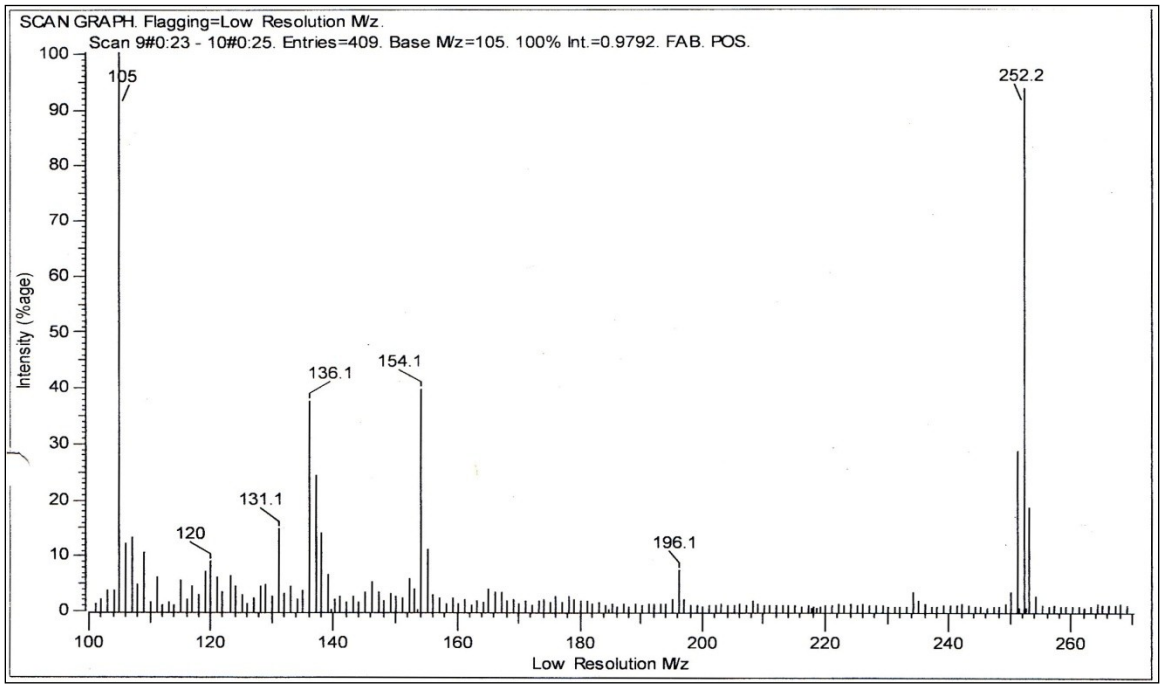

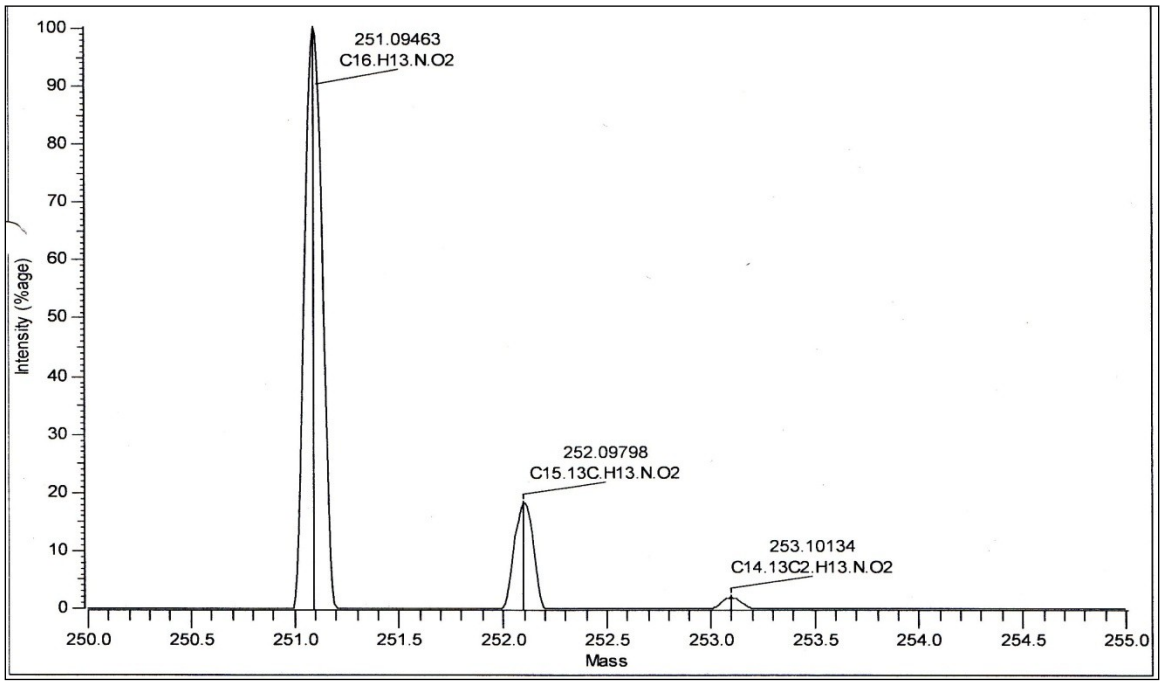

5.2.4.1 4*H*-1,4-Benzoxazin-4-yl(phenyl)methanone 152

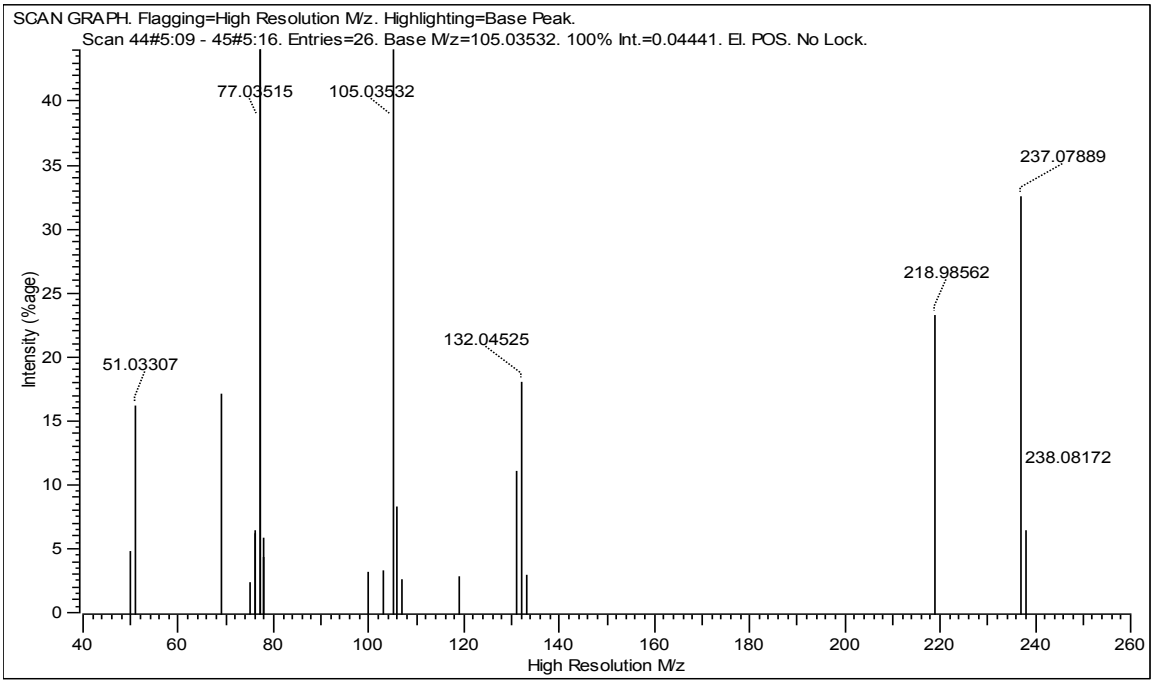

5.2.4.3 2,5-Dihydro-6*H*-1,6-benzoxazocin-6-yl(phenyl)methanone 150

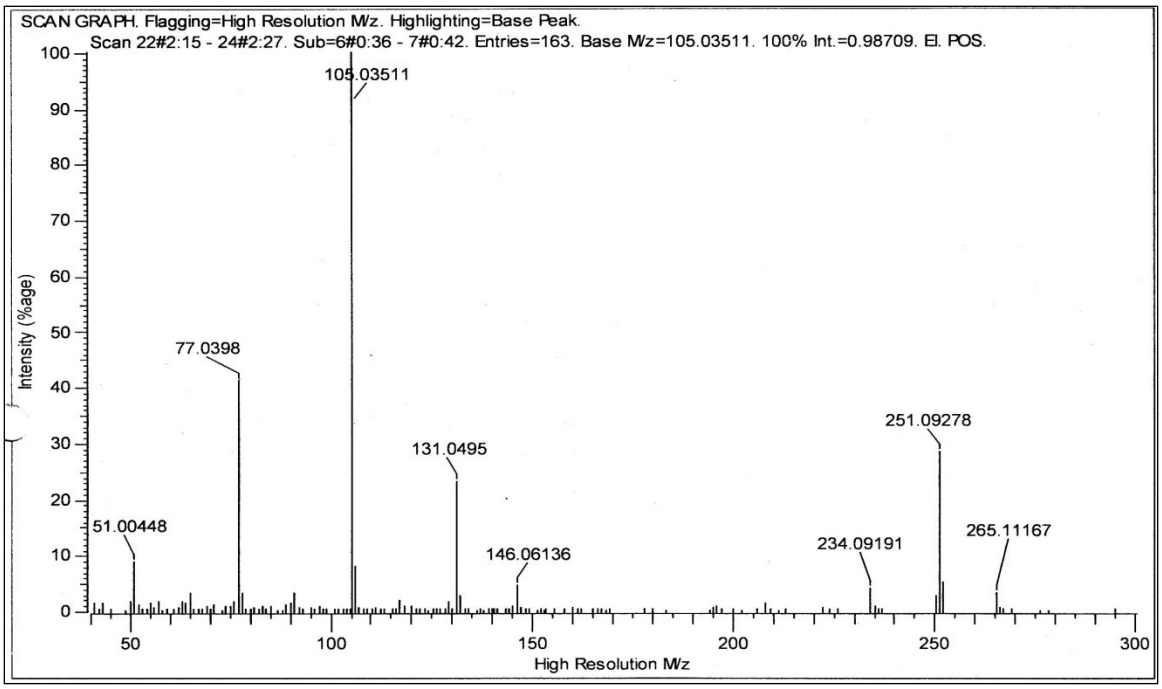

5.2.2.1 *N*-(2-(Prop-2-en-1-yloxy)phenyl)benzamide 148

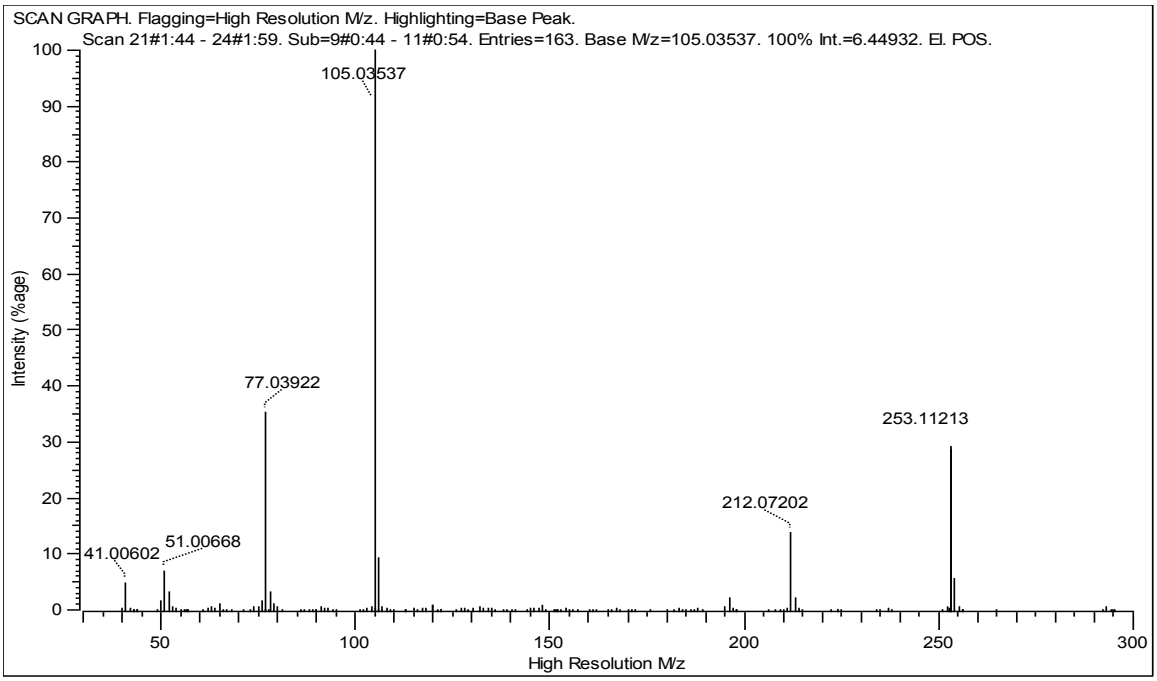

5.2.3.1 *N*-[2-(Prop-1-en-1-yloxy)phenyl]benzamide 153

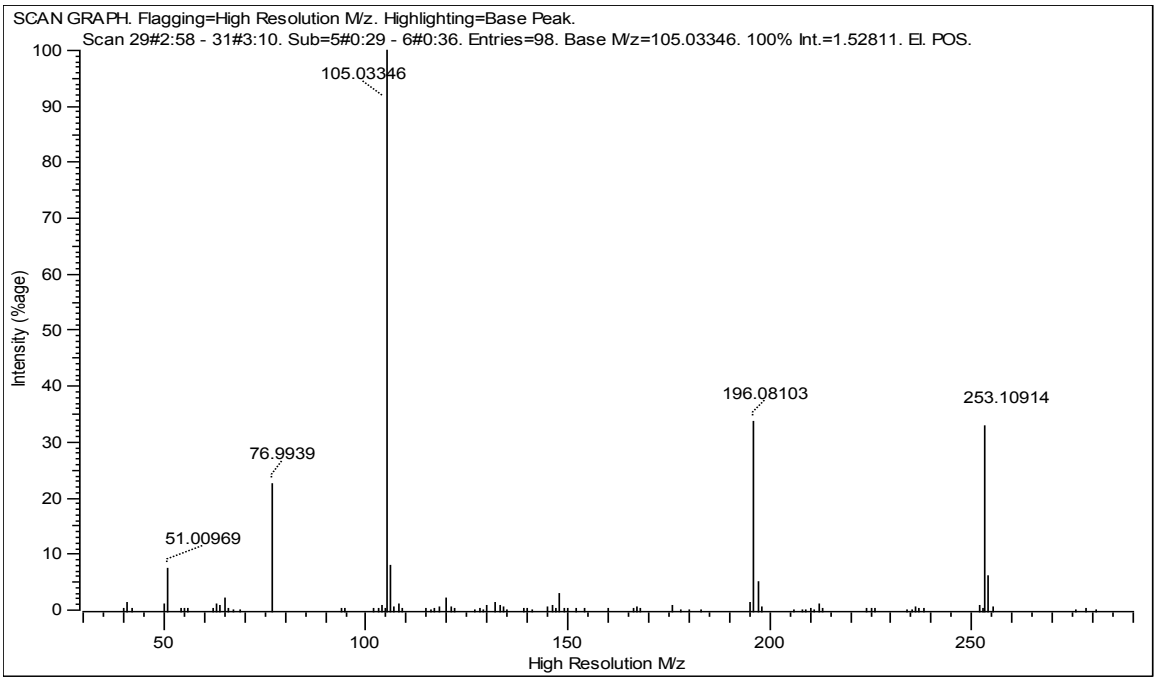

5.2.2.2 *N*-(Prop-2-en-1-yl)-*N*-[2-(prop-2-en-1-yloxy)phenyl]benzamide 149

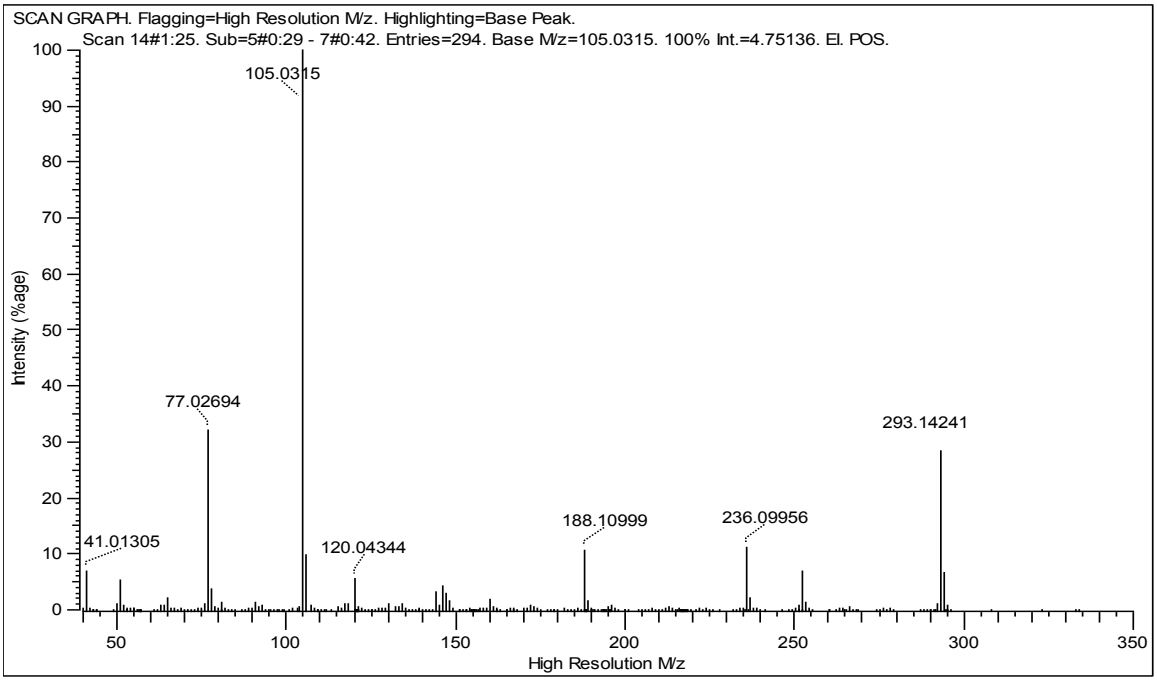

5.2.3.2 *N*-(Prop-1-en-1-yl)-*N*-(2-(prop-1-en-1-yloxy)phenyl)benzamide 151

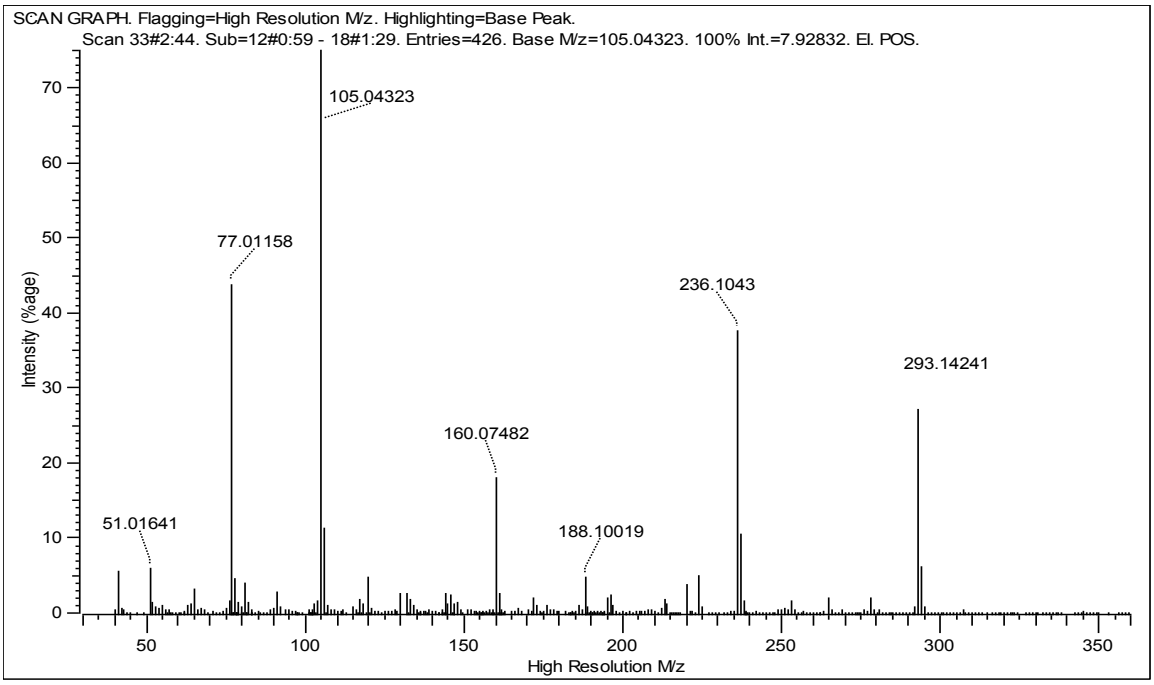

5.2.2.3 *N*-(Prop-2-en-1-yl)-*N*-(2-(prop-1-en-1-yloxy)phenyl)benzamide 154

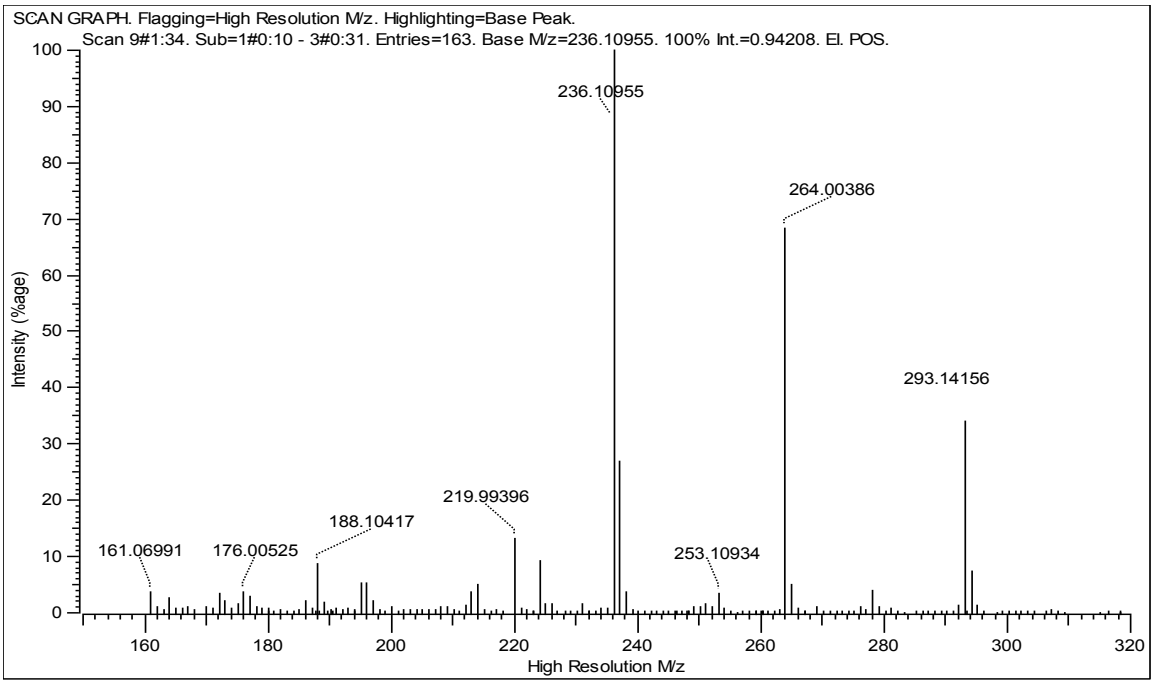

N,N-Benzo-fused heterocycles and precursors

5.3.2.1 *N*-[2-(Acetylamino)phenyl]-*N*-(prop-2-en-1-yl)acetamide 158

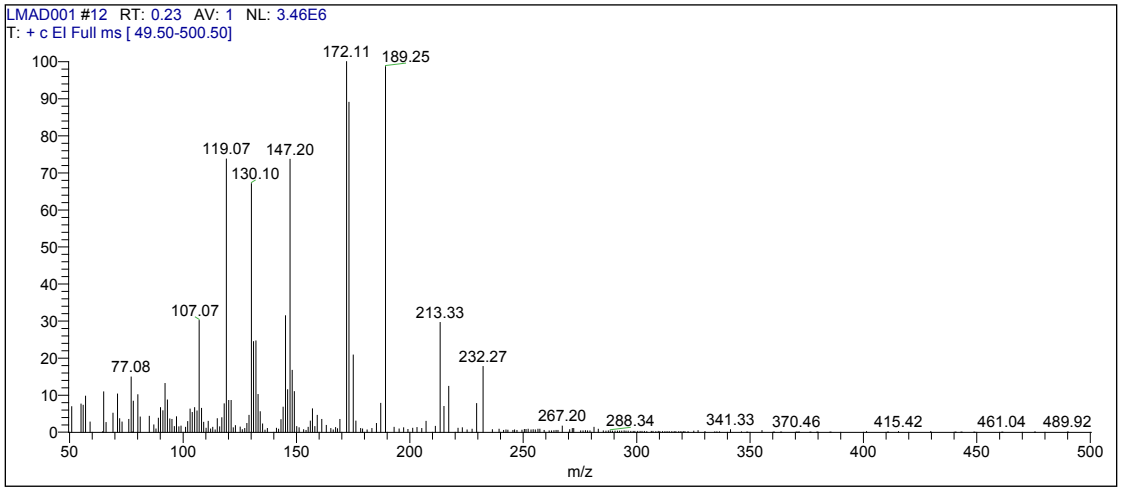

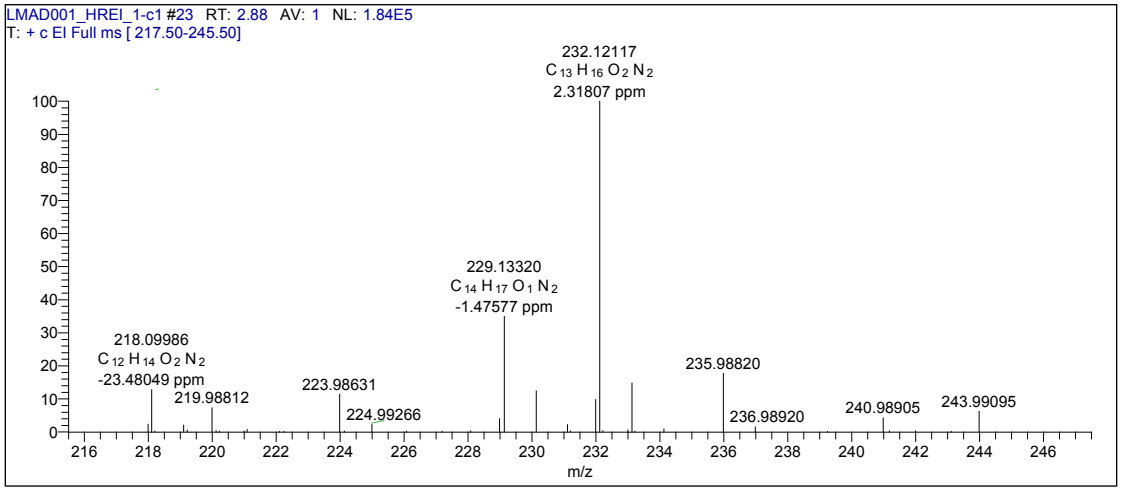

5.3.3.2 *N*-[2-(Acetylamino)phenyl]-*N*-(prop-1-en-1-yl)acetamide 163

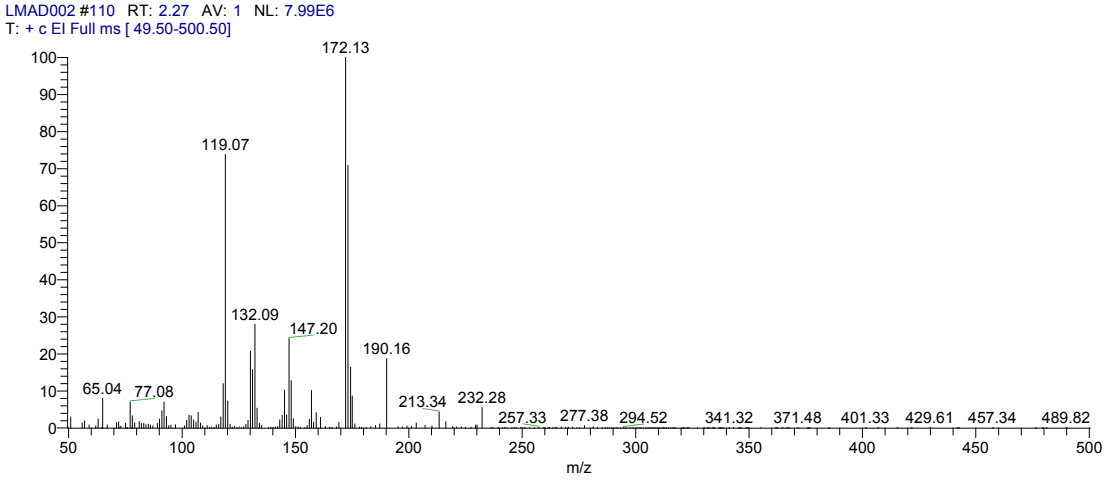

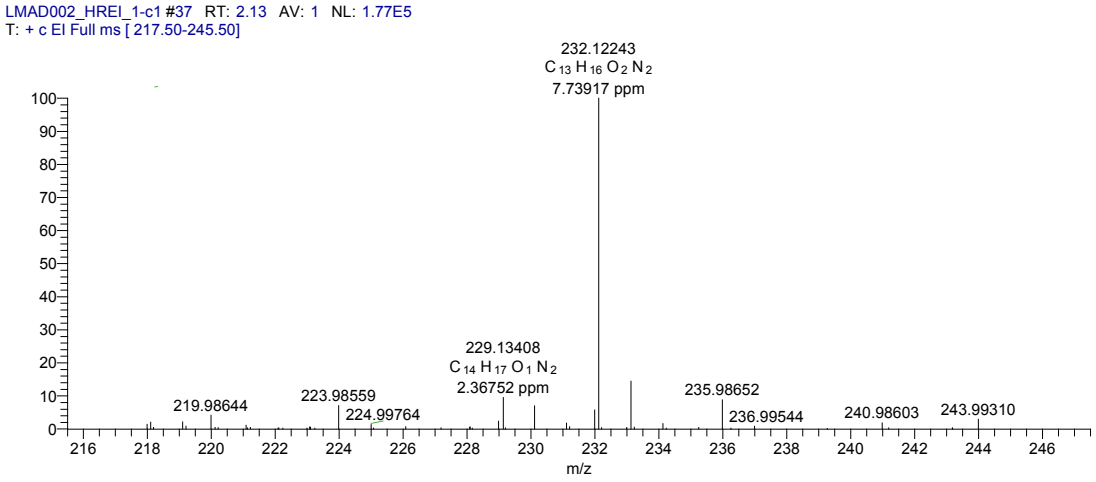

5.3.2.3 *N*-{2-[Acetyl(prop-1-en-1-yl)amino]phenyl}-*N*-(prop-2-en-1-yl)acetamide 161

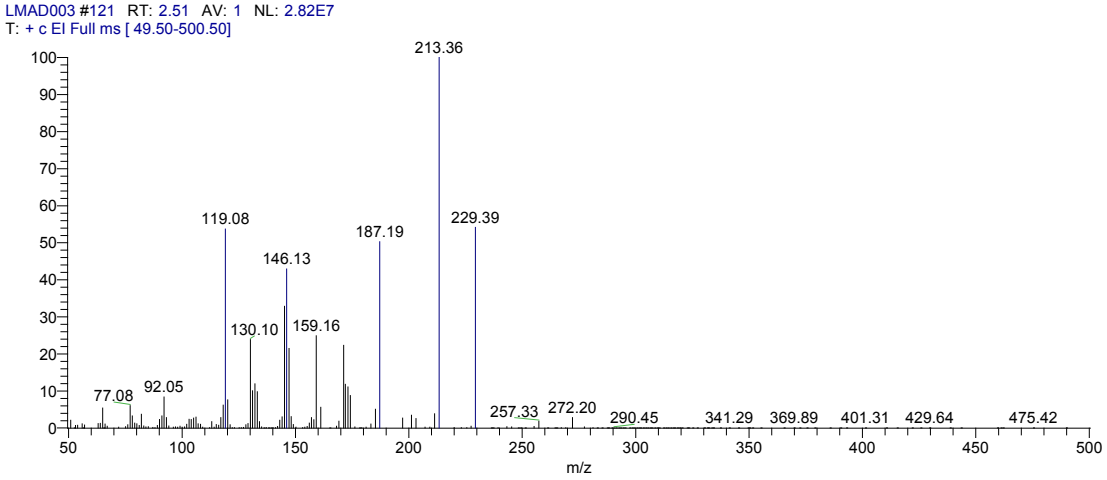

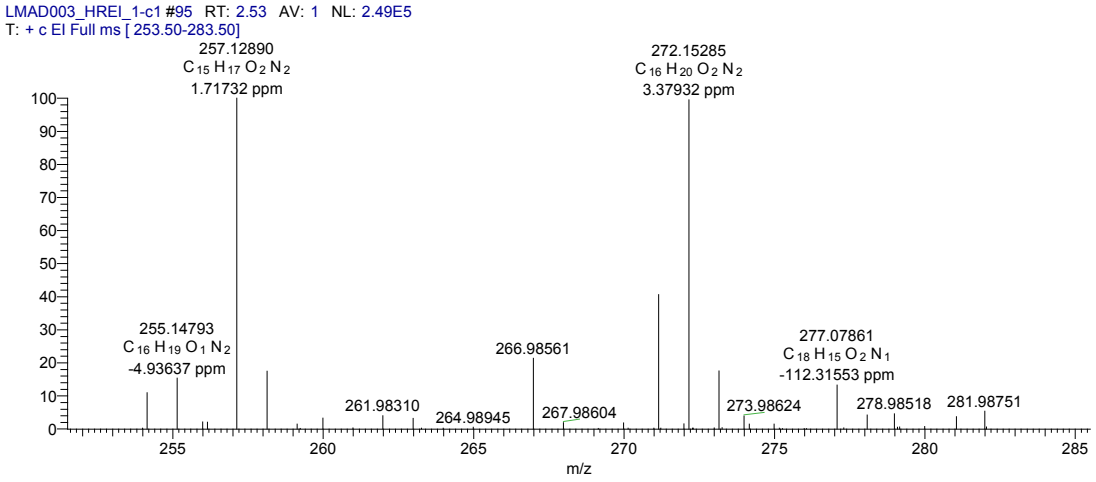

5.3.2.2 *N*,*N*'-Benzene-1,2-diyl*bis*[*N*-(prop-2-en-1-yl)acetamide] 159

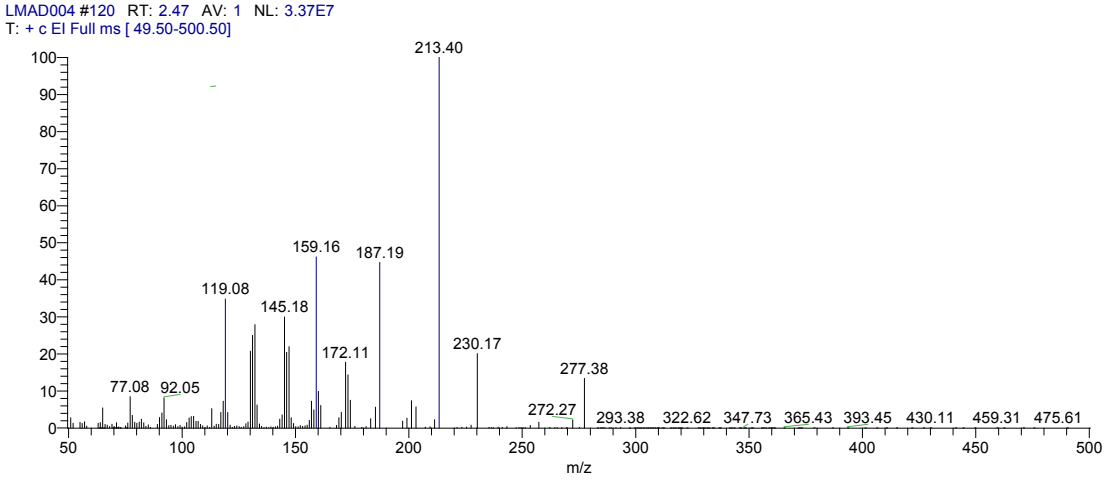

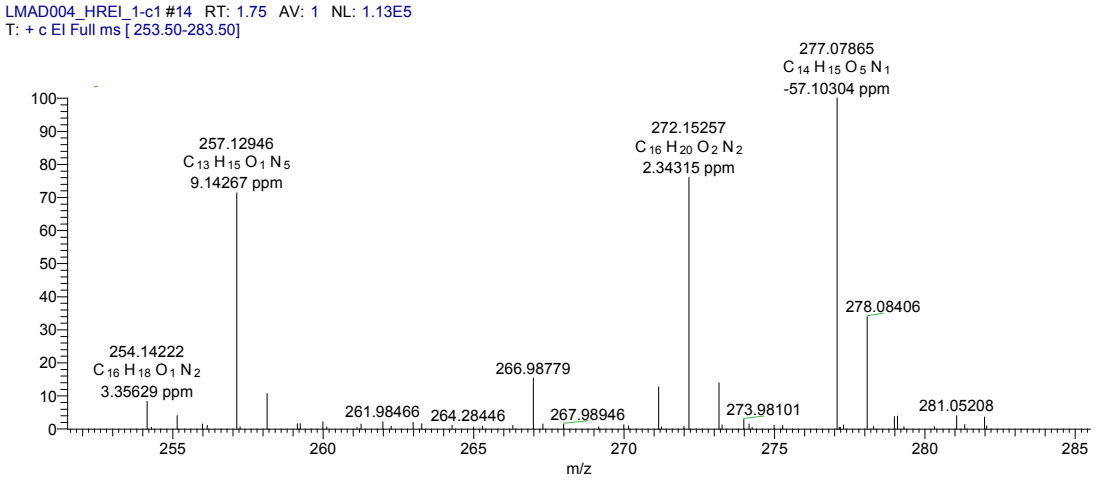

5.3.4.1 1,1'-(1*H*-1,5-Benzodiazepine-1,5(2*H*)-diyl)diethanone 165

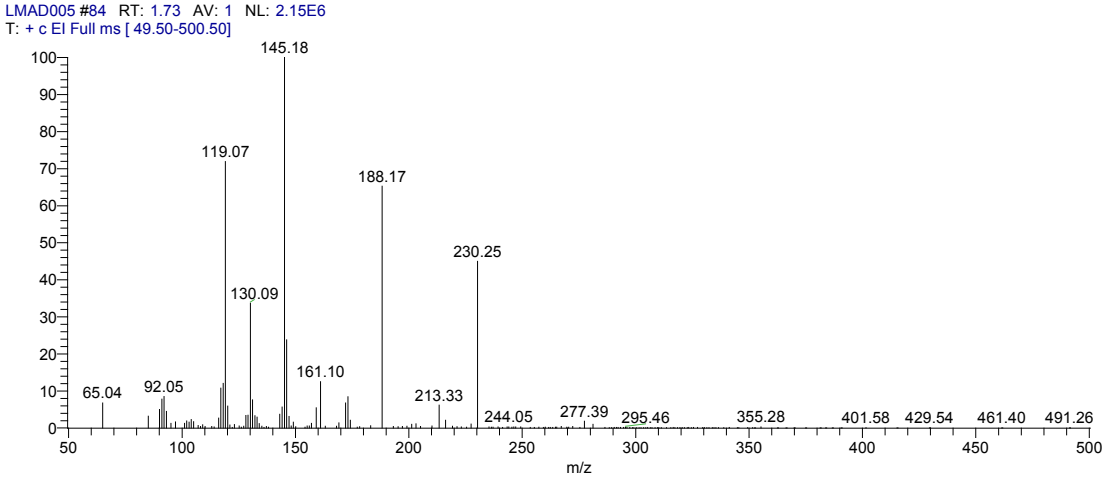

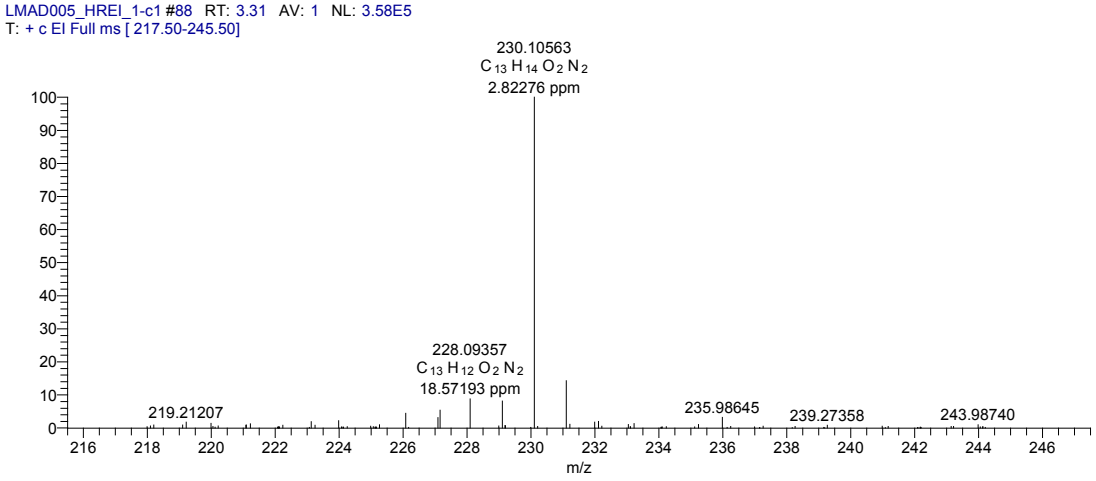

5.3.4.1 1,1'-[(3*Z*)-2,5-Dihydro-1,6-benzodiazocine-1,6-diyl]diethanone 160